The Conjugated Convection–Conduction Analysis of Heat Transfer in a Vertical Fin

Cha'o–Kuang Chen

Department of Mechanical Engineering

The Conjugated Convection – Conduction Analysis of Heat Transfer in a Vertical Fin

This thesis is submitted in accordance with the requirements of the university of Liverpool for the degree of Doctor of Philosophy

by

Cha'o - Kuang Chen

Department of Mechanical Engineering

June 1986

Statement of Originality

The work described in this thesis was carried out by the author and no part of the thesis has been submitted for a degree in any other university or place of learning.

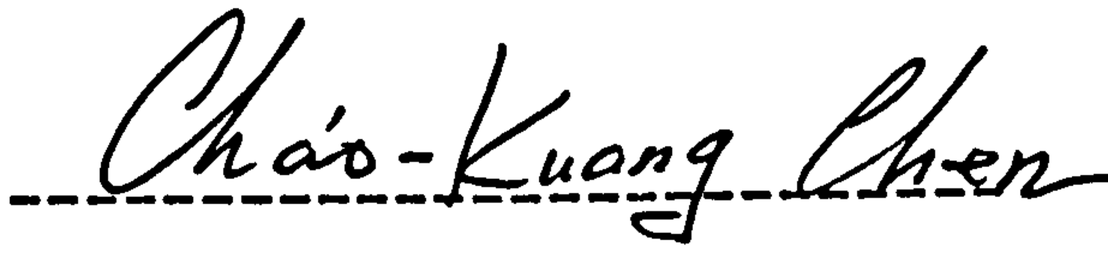

Cha'o-Kuang Chen

ACKNOWLEDGEMENT

The author wishes to express his appreciation and thanks to his advisor, Dr. J. W. cleaver, for his guidence, suggestions, encouragement and support during the course of this research. His experience and judgment were of great value in this effort.

The author is also grateful for the understanding, suggestions, criticism and supports of Dr. C. I. weng, professor and Chairman, Department of Mechanical Engineering National Cheng-Kung University R.O.C. and my colleagne , professor T.S. wang.

To my wife and father, I am indebted to their concern and patience.

TABLE OF CONTENTS

Page No.

ABSTRACT

Numerical calculations of local heat transfer coefficients are presented for steady laminar and turbulent convection flow over a vertical plate fin (or the vertical circular pin). The local heat transfer coefficient is solved simultaneously with the convective boundary layer equations of fluid and heat conduction equation of fin (or pin). In the laminar convection flow case, the radiative effect on the vertical plate fin (or pin) is considered and the optically thick limit approximation for the radiative heat flux is assumed. In the turbulent forced convection flow case, the eddy-diffusivity formulas used by Cebeci and Smith are utilized to model the Reynolds stresses.

An implicit finite difference method is employed. The results of local heat transfer coefficient and local heat flux were found to be irregular near the transition region from the laminar to turbulent flow. The overall heat transfer rate, the local heat transfer coefficient, the local heat flux and the fin temperature distribution are expressed for Pr=0.7 and various values of Nc (conjugated convection-conduction parameter). It is also found that the heat fluxes with radiative effect are higher than those without radiative effect.

LIST OF FIGURES

NOMENCLATURE

a_1, a_2	viscosity variation parameters
C_p	specific heat at constant pressure
C_T	temperature difference parameter, $T_\infty/(T_o-T_\infty)$
f	reduced stream function
g	gravitational acceleration
Gr_L	Grashof number, $g\beta(T_o-T_\infty)L^3/\nu^2$
h	local heat transfer coefficient
$\hat{h}^*$	dimensionless modified heat transfer coefficient
k	fluid thermal conductivity
k_f	fin thermal conductivity
L	fin length or pin length
N_c	convection-conduction parameter $(\frac{kL}{k_f\delta} Re_L^{\frac{1}{2}})$ for Forced Convection Plate Fin
N_c	convection-conduction parameter $(\frac{kL}{k_f\delta} Gr_L^{\frac{1}{4}})$ for Natural Convection Plate Fin
N_c	convection-conduction parameter, $2kLGr_L^{\frac{1}{4}}/(k_f r_o)$ for Natural Convection Pin
N_c	convection-conduction parameter, $2kLRe_{L_\infty}^{\frac{1}{2}}/(k_f r_o)$ for Forced convection Plate Fin
N	conduction-radiation parameter, $k\beta^*/(4\sigma(T_0-T_\infty)^3)$
Pr	Prandtl number, ν/α
P_{rt}	Turbulent Prandtl number
q^r	radiative heat flux
q	local heat flux

Q	overall heat transfer rate
r	radial coordinate
r_o	radius of the circular pin
Re_L	Reynolds number, $u_\infty L/\nu$
R_{etr}	Reynolds number at transition point
R_{et}	Reynolds number of turbulent region.
T	fluid temperature
T_o	root temperature
T_f	fin surface temperature
T_∞	ambient temperature
T_w	surface temperature
u,v	velocity component in x- and y- direction respectively
u_∞	free stream velocity
x,y	coordinates parallel and perpendicular to the fin respectively
α	thermal diffusivity
δ	half thickness of the fin
β^*	extinction coefficient
β	thermal expansion coefficient
ρ	density of fluid
σ	Stefan-Boltzmann constant
ψ	stream function
Ω	buoyancy force parameter
ε_m	eddy kinematic viscosity
ε_{mi}	inner eddy viscosity
ε_{mo}	outer eddy viscosity

ε_h eddy diffusivity

ε_{ni} inner eddy diffusivity

ε_{no} outer eddy diffusivity

ε_m^+ ratio of eddy viscosity to kinematic viscosity (ε_m/ν)

ε_h^+ ratio of eddy diffusivity to kinematic viscosity (ε_h/ν)

η pseudo-similarity variable

θ dimensionless temperature $\left(\frac{T-T_\infty}{T_o-T_\infty}\right)$

θ_f dimensionless fin temperature $\left(\frac{T_f-T_\infty}{T_o-T_\infty}\right)$

θ_w dimensionless surface temperature $\left(\frac{T_w-T_\infty}{T_o-T_\infty}\right)$

ν kinematic viscosity

ξ dimensionless streamwise coordinate (x/L)

ξ_{tr} dimensionless streamwise coordinate at the transition point

λ transverse curvature parameter ($2\sqrt{2}\ L/r_o Gr_{L_\infty}^{1/4}$) for Natural convection case

λ transverse curvature parameter ($2L/r_o Re_{L_\infty}^{1/2}$) for Forced convection case

I. INTRODUCTION

I-1 Practical Relevance

Heat-transfer generally depends on three main factors. They are heat-transfer coefficient, the area of heat-transfer and the effective temperature difference between the body and its surrounding medium. In order to improve the heat-transfer effect, detailed studies of the above three main heat-transfer factors play an important role. Experience has shown that the simplest and most effective way for increasing the heat-transfer rate is to increase the heat-transfer area.

A growing number of engineering disciplines are concerned with energy transitions requiring the rapid movement of heat. They produce an expanding demand for high-performance heat-transfer components with progressively smaller weights, volumes, costs, or accommodating shapes. Extended surface heat transfer is the study of high-performance heat-transfer components with respect to these parameters and of their behavior in a variety of thermal environments. Typical components are found in air-land-space vehicles and their power sources; chemical, refrigeration, and cryogenic processes; electric and electronic circuitry; conventional furnaces and gas turbines; process heat dissipators and waste-heat boilers; nuclear-fuel modules, direct energy conversion, and many more. Some typical examples of the equipment with extended surfaces are given in Fig.I-1.

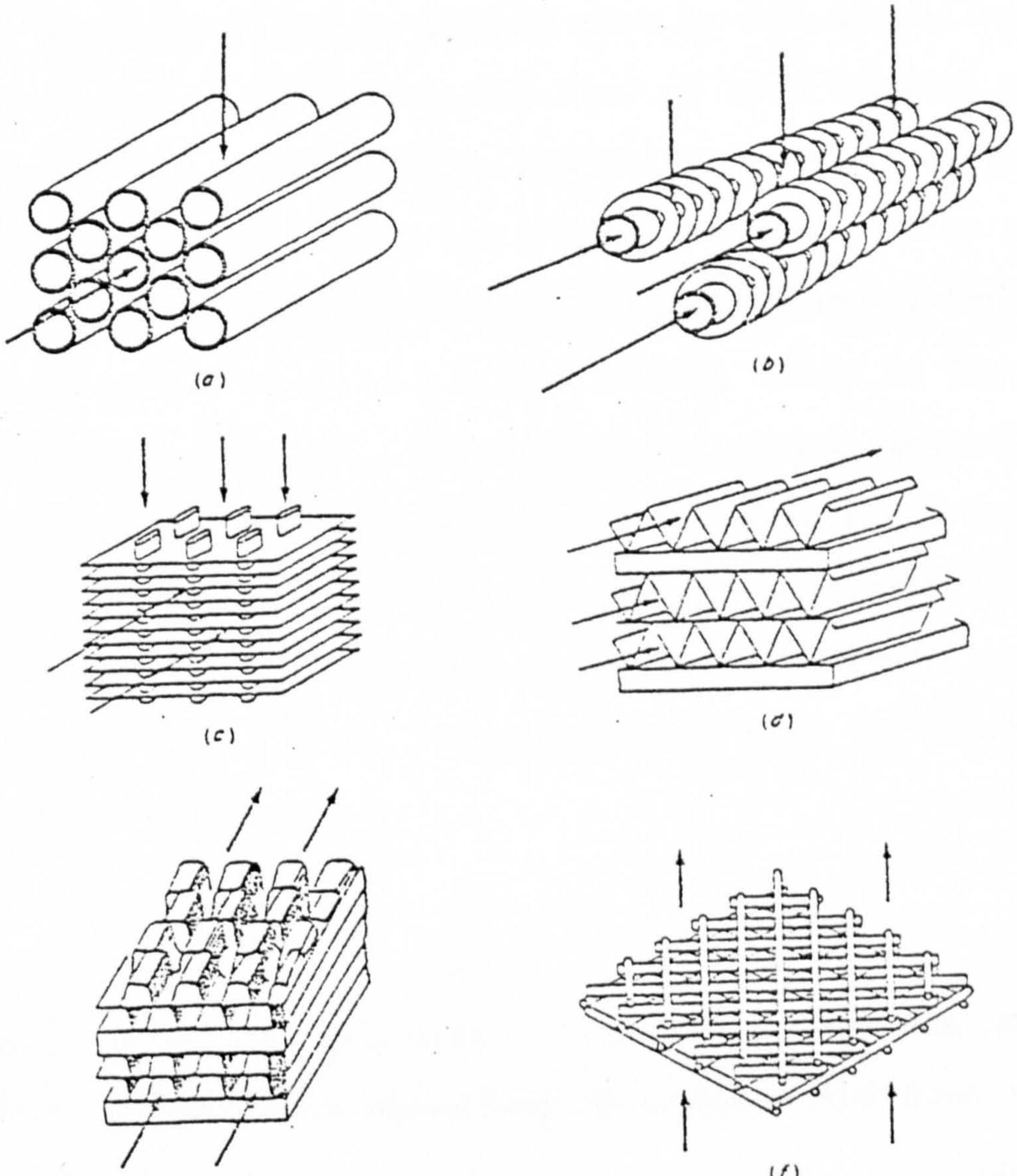

Fig. 1-1 Some typical examples of the equipment with extended surfaces

I-2 The Heat-Transfer of Extended Surfaces

In the design and construction of various types of heat-transfer equipment, simple shapes such as cylinders, bars, and plates are used to implement the flow of heat between a source and a sink. They provide heat-absorbing or heat-rejecting surfaces, and each is known as a prime surface. When a prime surface is extended by appendages intimately connected with it, such as the metal tapes and spines on the tubes in Fig.1-2. [1] the additional surface is known as an extended surface. In some disciplines, prime surfaces and their extended surfaces are known collectively as extended surfaces to distinguish them from the use of prime surfaces alone. The elements used to extend prime surfaces are referred to as fins (or pins when cylindrical in shape).

I-3 Objective of Present Work:

Studies of heat transfer in fins (or pins) can be divided into three broad areas depending on whether the heat transfer is steady, transient or periodic. Generally, the research of transient-state heat transfer analysis concentrates on the transient response of a fin to a step change in base temperature or to a step change in base heat flux. The phenomenon of the transient heat transfer of fin only exists for a very short period of time, for example, the warm-up of an internal-combustion engine or the start-up of the process heat exchanger. Periodic heat transfer analysis studies the heat transfer

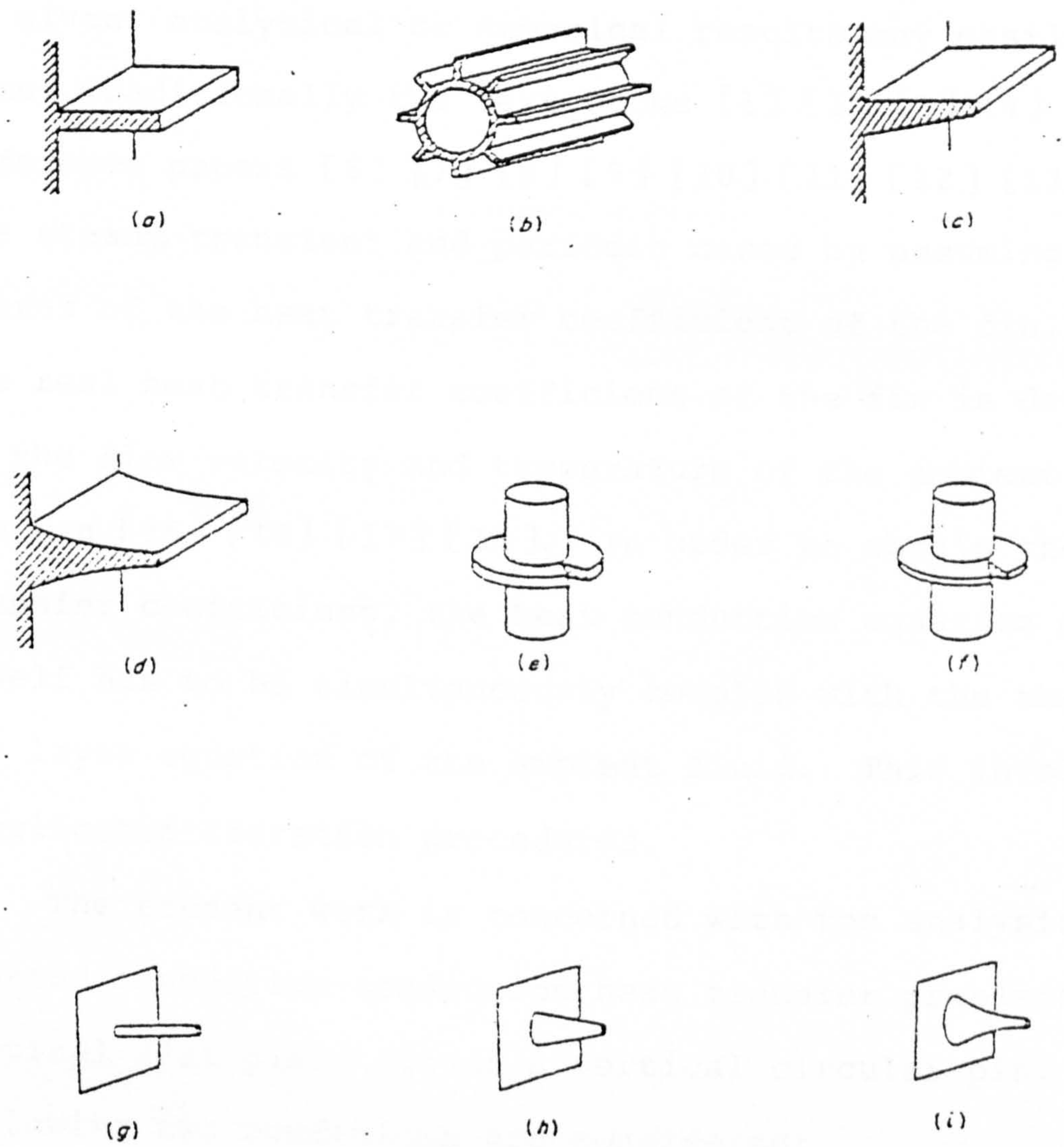

Fig. 1-2 Some typical examples of extended surface.

response of fin to a periodic function in base temperature or base heat flux. If the heat transfer coefficient of the fin is given, analytical or numerical results may easily be obtained. Thus, traditionally the text books [1] [2] [3] [4] [5] or the reference papers [6] [7] [8] [9] [10] [11] [12] [13] [14] solve the steady, transient and periodic cases by assuming given values of the heat transfer coefficient of the fin. Practically, the real heat transfer coefficient of the fin is determined by the flow velocity and temperature of the ambient fluid about the fin [15] [16] [17] [18]. In order to obtain the local heat transfer coefficient, the heat conduction equation of the fin itself has to be simultaneously coupled with the thermal boundary layer equation of the ambient fluid. This involves quite complicated iteration procedures.

The present work is concerned with the analysis of conjugated convection-conduction heat transfer problems of a vertical flat plate fin or a vertical circular pin. And the following two conditions are considered:

1) Steady conjugated laminar flow convective-conduction heat transfer in a vertical flat plate fin and a vertical circular pin.

2) Steady conjugated turbulent flow convection-conduction heat transfer in a vertical flat plate fin and a vertical circular pin.

The physical systems considered in the present work are shown in Fig1-3. The temperature outside the thermal boundary

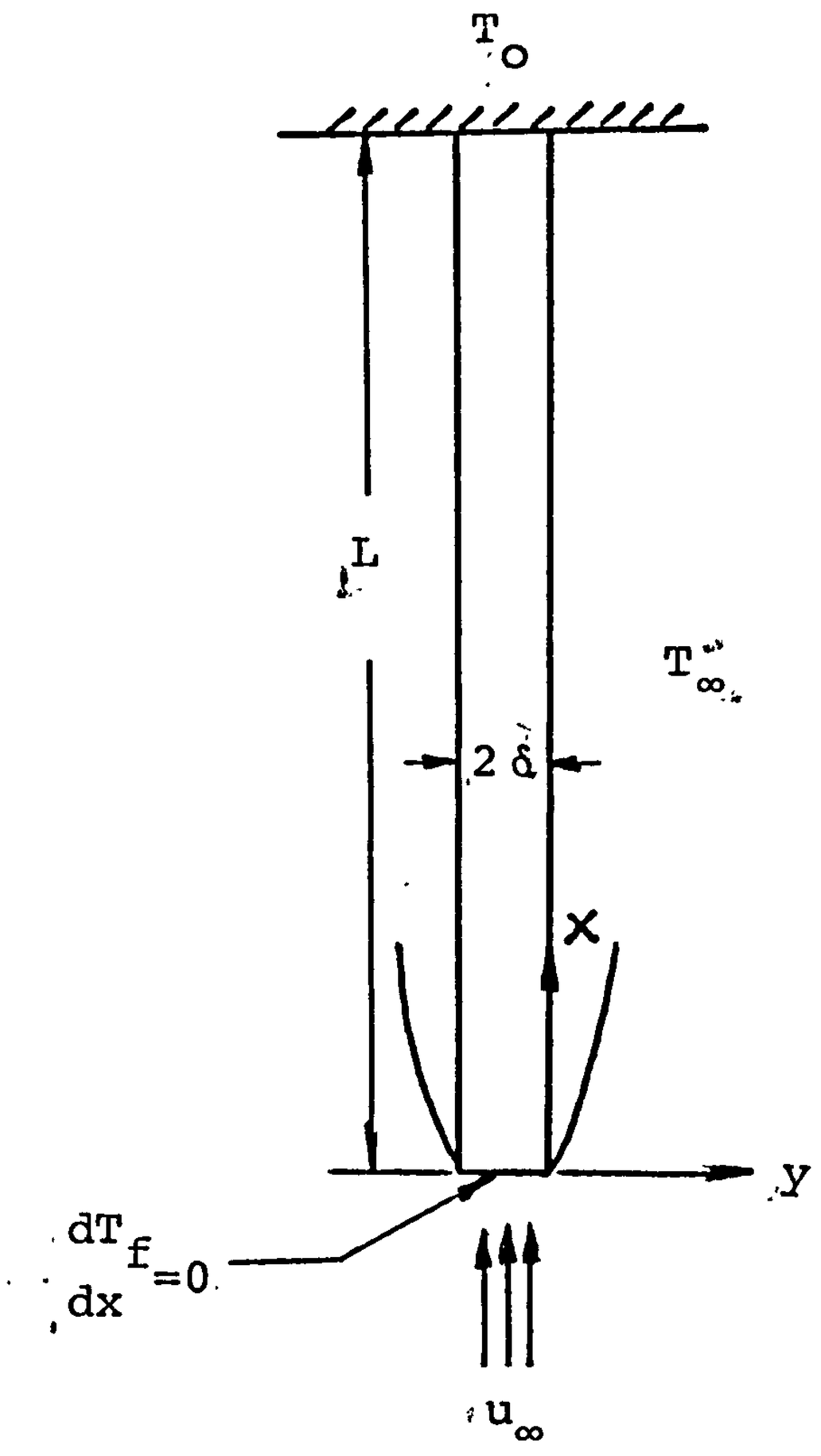

(a) Vertical Plate Fin case

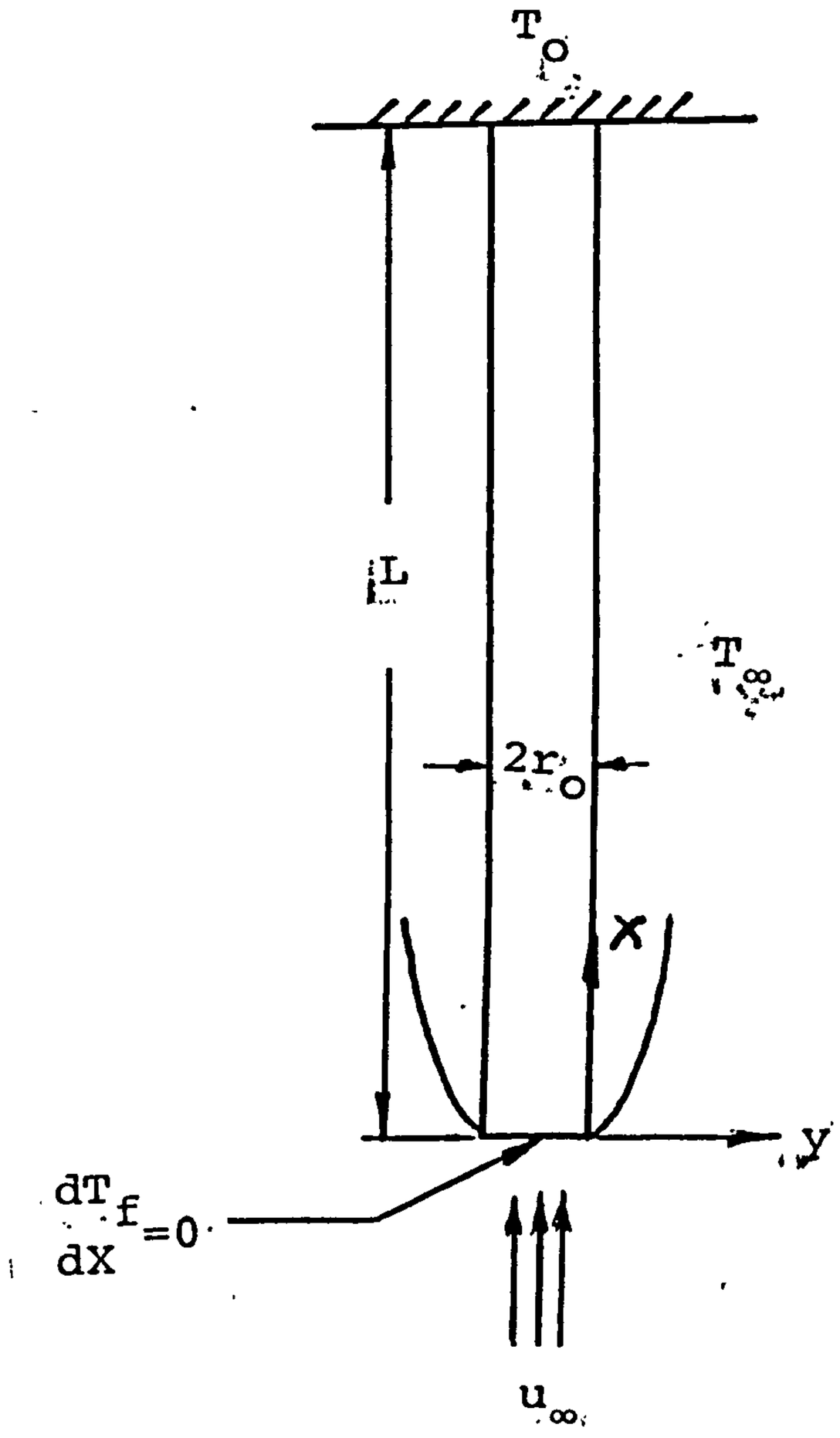

(b) Vertical Circular Pin Case

Fig. I-3 Coordinate System

layer is T_∞ , the thickness of the fin is 2δ (the radius of the circular pin is r_o.), the length of the fin (or pin) is L, and the base temperature of the fin (or pin) is T_o. The end of the fin (or pin) is insulated. It is generally assumed that the temperature of the fin (or pin) is higher than that of the ambient fluid.

The implicit finite difference method for non-similar boundary layer equations, introduced by Cebeci and Bradshaw [19], is applied in the present study. The simple inverse matrix method is used to solve the heat conduction equation of the fin. Extremely good convergence can be obtained with only 2 to 3 iterations. The method is applied to a special case dealt with by Sparrow et.al. [15] [16], (laminar flow with constant viscosity and no radiation) and good agreement is obtained with considerable savings in C.P.U. time. This arises because the present implicit finite defference method only has to use 45 mesh points to solve the problem in contrast to 1600 points used is the analysis of Sparrow [15].

I-4 Scope of Present Work

The structure of the present study is briefly shown in Fig. 1-4.

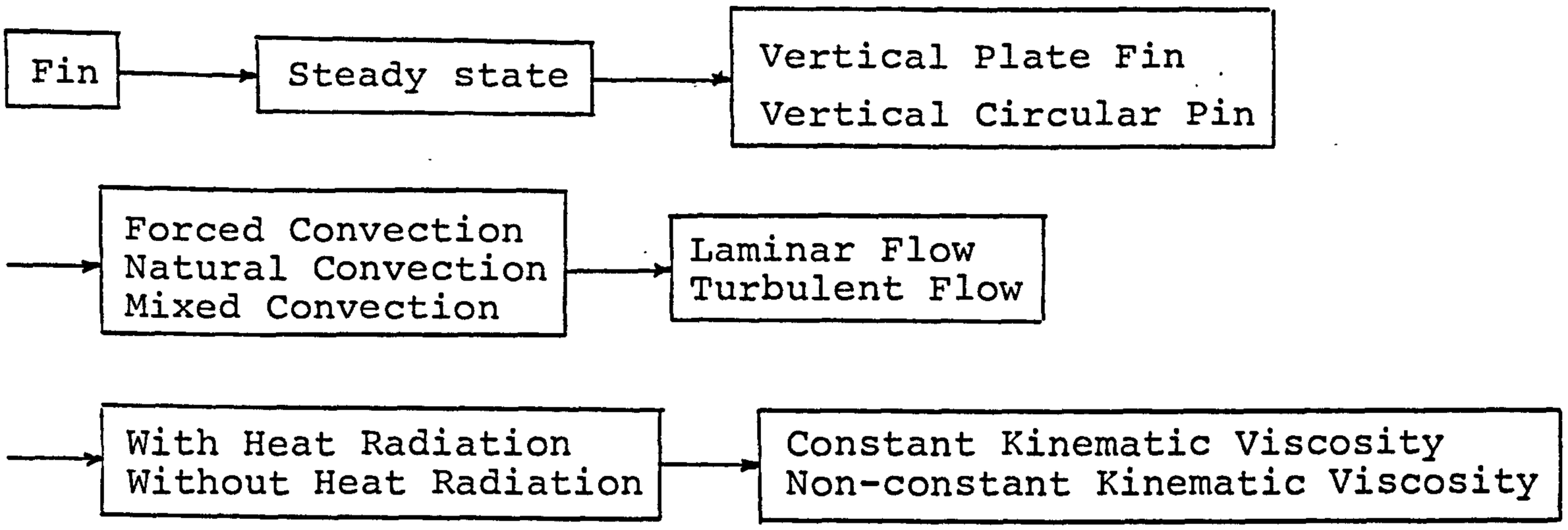

Special case in the illustrated example.

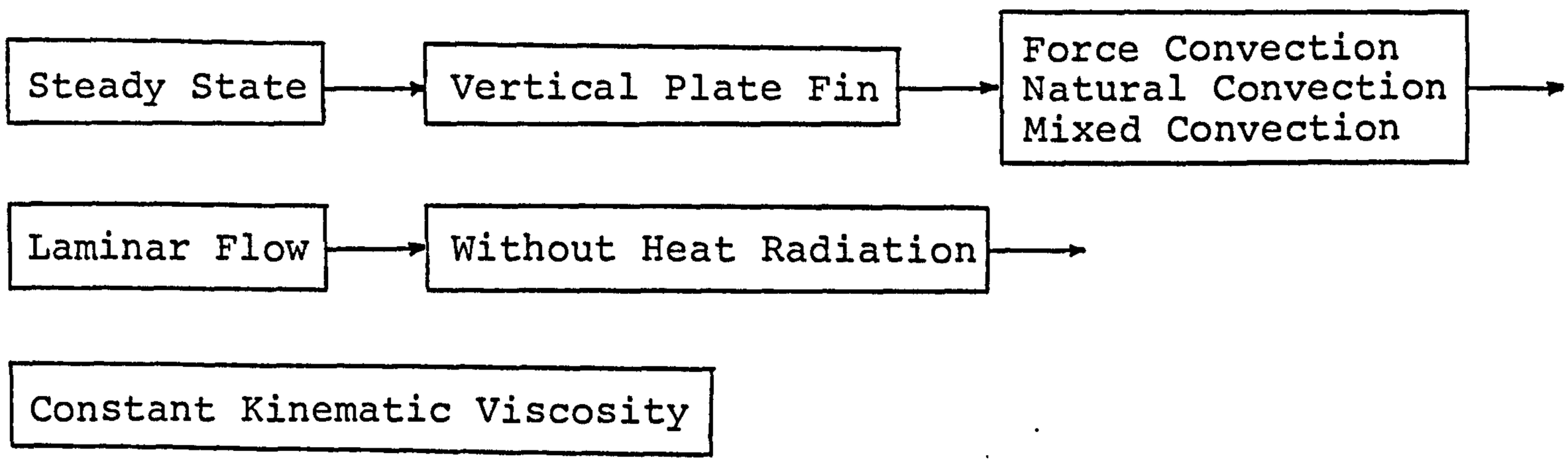

Fig.1-4 The structure of the present work.

II. REVIEW OF PREVIOUS WORKS

The fin has been applied to industrial heat transfer systems for increasing the rate of heat transfer for many years. Many scholars have theoretically studied the phenomenon of heat transfer of the fin under various boundary conditions. One of the earliest studies of steady state heat transfer rates in straight and tapered fins was made by Harper and Brown [6] in 1922. They assumed the end of the fin to be insulated and obtained theoretical results. They had to use a corrected fin length in order to obtain agreement with the practical heat transfer phenomenon of the fin. Since then Jacob [5], Gardner [7], Gates [8], Kern & Kraus [1], and Carier & Anderson [20] have presented studies of steady state heat transfer characteristics for fins with various geometrical shapes.

Gardner [7] extended the heat transfer analysis of fins to extended surfaces with cross-sectional area of arbitrary shapes. He also analyzed the phenomenon of heat transfer of a cone-pin which required the solution of the generalized Bessel equation to derive the temperature distribution of the cone-pin. The effective curves for the fins with various shapes of cross-sectional area obtained by Gardner are still applied to the practical designs extensively.

With respect to the heat transfer analysis of the fin,

it has traditionally been assumed that the heat transfer coefficient along whole length of the fin is constant. Practically, the real (local) heat transfer coefficient of the fin [21] [22] [23] depends on the flow velocity and temperature of the fluid about the fin surface. In order to obtain the practical local heat transfer coefficient of the fin, the heat conduction equation of fin itself has to be simultaneously coupled with the thermal boundary-layer equation of the ambient fluid.

For steady state conditions Sparrow et.al. [15], Karvinen [17] [18] and Huang and Chen [24] applied the above concept of coupling the heat conduction equation and thermal boundary layer equation to fins under the situation of natural convection. They found that the heat transfer coefficient differed from the traditional predictions which indicated that the heat transfer coefficient decreased gradually and monotonically. They found that the heat transfer coefficient reaches minimum value first and then increases again. The reasons for the above phenomenon are due to the non-uniform temperature distribution, the enriched buoyancy effect by the increasing flow velocity of the ambient fluid induced by the higher temperature difference between the fin base and its ambient fluid. This does not exist for the forced convection situation.

While there is a significant difference between the practical and traditional theoretical predictions of the local heat transfer rates, the total heat transfer rates are in reasonable agreement.

With respect to transient conditions, Chapman [9] first analyzed the transient heat transfer response to a step change in base temperature for the equal-thickness, one-dimensional circular pin in 1959. In 1972, Yang [11] obtained an analytical solution of the temperature distribution for analysing the longer-time heat transfer response to a periodic base temperature variation of a flat plate fin.

In 1975, Suryanarayana [12] presented a paper for discussing the transient heat transfer response to a one-dimensional flat plate fin. He divided the boundary conditions into four types. They are: 1) a step function in base temperature, 2) a cosine function in base temperature, 3) a step function in base heat flux and 4) a cosine function in base heat flux. In 1976, Chu [25] presented the transient heat transfer response to the boundary conditions of a step function in base temperature and a step change in base heat flux for two-dimensional flat plate fin. In 1975, Aziz [26] used the analytical method introduced by Yang [11] to analyse the periodic heat transfer phenomenon of annular fins. Eslinger and Chung [27] applied a finite element method and assumed the heat transfer coefficient as a constant to analyse the periodic heat transfer characteristics of the fins. In 1981, Aziz and Na[13] considered the relationship between the heat transfer coefficient and temperature to be linear and assumed the change of heat transfer coefficient to be dependent on the coordinates but independent of time for analysing the periodic heat transfer

characteristics.

During the analysis of heat transfer for a fin, the effect of heat radiation can often be an important factor.[14] It has been found that the heat radiative flux can be approximated by using the optically limit. This also proves to be convenient for handling the subsequent numerical analysis. Sparrow et.al. [16] [15] restricted the heat transfer analysis of the conjugated fin to laminar flow, but the effect of turbulent flow is also very important for the heat transfer analysis of the fin at high velocities. In the present study, the eddy viscosity model developed by Cebeci and Smith [19] [28] [29] is applied to simulate the Reynold stress produced by the turbulent flow, where as the kinematic viscosity is assumed to be a constant in previous investigations of the fin. The kinematic viscosity of the fluid is dependent on temperature when the temperature difference between the fin (or pin) and its ambient fluid is great enough. Thus, the effect of kinematic viscosity relative to the variation of temperature on heat transfer is considered in the present work.

The heat transfer analysis of a fin (or pin) for handling the heat convective problem of the vertical flat plate fin (or pin) in the present study is differs from previous studies in that temperature and heat flux may vary along the vertical flat plate fin (or pin). The temperature of the flat plate fin (or pin) will depend on the velocity and temperature of the ambient fluid. In order to obtain the temperature distri-

bution of whole the fin (or pin), we have to solve the conjugated heat conduction equation and thermal boundary layer equation simultaneously. A certain temperature distribution along the wall of the fin (or pin) is assumed as the boundary concition for the thermal boundary layer first. Then a numerical method is applied to solve the thermal boundary layer equation for obtaining the local modified heat transfer coefficient. Taking the local modified heat transfer coefficient as a given value and substituting it into the heat conduction equation, a new temperature distribution of the fin is obtained. Iterating the above calculation procedure, until the tolerance between the values of two neighboring temperature distribution is less than 10^{-3} then a convergent result is sought.

The implicit finite difference method is applied to solve the non-similar thermal boundary layer equation and the inverse matrix method is used to solve the heat conduction equation in the present study. The very good convergent results can be obtained after 2 to 3 iterations. The results of special case in the illustrated example (steady state, a flat plate fin, laminar flow, without heat radiative effect and constant kinematic viscosity) are compared with those obtained by Sparrow et.al. [15] [16]. The agreements are satisfactory. Besides, the fin is only divided into 45 points for the implicit finite different method used in the present work. Obviously, it is much simplified than the method used by Sparrow et.al. which used 1600 division points. And the C.P.U. time can be also saved.

III. TURBULENT MODEL

In 1974, Cebeci and Smith reported an algebraic viscosity formulation for use with external wall boundary layers. This has been used extensively and developed for bodies of revolution, internal flows, three-dimensional turbulent flows etc. by Cebeci and co-workers. This turbulent eddy viscosity model divides the boundary layer into inner and outer regions. The inner region is based on a Van Driest (30) approach and modified in accordance with a damped law of the wall. The outer region (31) (32) (33) is based on a velocity defect Law. The expressions are given as follows:

$$\varepsilon m = \begin{cases} \varepsilon mi = \{\{0.4y\,[1 - \exp(-Y/\bar{A})]\}^2 \left|\frac{\partial u}{\partial y}\right|\gamma_{tr}, & \text{when} \\ \qquad \varepsilon mi \leq \varepsilon m_0 \\ \varepsilon m_0 = 0.0168 \left| \int_0^{\infty} (u_\infty - u)\,dy \right| \gamma_{tr}, & \text{when} \quad \varepsilon mi \geq \varepsilon m_0 \end{cases} \tag{3-1}$$

where the damping constant $\bar{A}$ may be expressed as

$$\bar{A} = 26 \frac{\nu}{N^*} (\tau_w/\rho)^{-\frac{1}{2}} \tag{3-2}$$

For flow with no mass transfer and no pressure gradient, N*=1. [19]. The transition region intermittency factor for two-dimensional flow is defined as follows:

$$\gamma_{tr} = 1 - \exp\left[-Gx_{tr}(x-x_{tr})\left(\int_{x_{tr}}^{x} \frac{1}{u_\infty}\,dx\right)\right] \tag{3-3}$$

Where x_{tr} is the location of the onset of transition and the empirical factor G is given by

$$G = \frac{1}{1200} \frac{u_\infty^3}{\nu^2} Rx_{tr}^{-1.34} \qquad (3\text{-}4)$$

with $Rx_{tr} = u_\infty x_{tr}/\nu$

The empirical, but well-tested, nature of this formulation should be noted. Modified versions exist for particular flows and, in all cases, the empiricism implies that the expressions should not be used for configurations far from those upon which the constants are based.

The turbulent prandtl number suggested by Jischa and Rieke (34) is used in present study. It is expressed as

$$P_{rt} = \frac{\varepsilon m}{\varepsilon h} = a + b\ (Pr + 1)/\ Pr \qquad (3\text{-}5)$$

where Pr = 0.7 when the fluid is air and from experiment, a=0.825, b=0.0309.

The eddy algebraic equation (3-1) can be transformed by the following transformation formula,

$$\xi = \frac{x}{L},\ \eta = \frac{yRe_L}{L\xi^{\frac{1}{2}}},\quad f(\xi,\eta) = \frac{\psi(x,y)}{\sqrt{u_\infty \nu L \xi}}$$
$$\theta = \frac{T(x,y) - T_\infty}{T_0 - T_\infty},\qquad \theta_f = \frac{T_f(x) - T_\infty}{T_0 - T_\infty} \qquad (3\text{-}6)$$

where $Re_L = \frac{u_\infty L}{\nu}$, and ν is a constant kinematic viscosity.

The following results are obtained

$$\varepsilon m^+ = \frac{\varepsilon m}{\nu} = \begin{cases} \varepsilon m{+}i = 0.16\,[\,1-\exp(-\frac{Rex^{\frac{1}{4}}}{26} f''_w{}^{\frac{1}{2}} \eta)\,]^2 \eta^2 f'' Rex^{\frac{1}{2}} \gamma_{tr} \\ \qquad \text{when} \quad \varepsilon m^+ i \le \varepsilon m_0^+ \qquad (3\text{-}7) \\ \varepsilon m_0^+ = 0.0168 Rex^{\frac{1}{2}} [\eta_\infty - f(\eta_\infty)]\gamma_{tr},\ \text{when} \quad \varepsilon m^+ i \ge \varepsilon m_0^+ \end{cases}$$

The eddy agebraic equation (3-1) can also be transformed by the transformation formula

$$\xi = \frac{x}{L}, \quad \eta = \frac{Re_{L\infty}^{\frac{1}{2}}}{L\xi^{\frac{1}{2}}}, \qquad f(\xi,\eta) = \frac{\psi(x,y)}{\sqrt{u_\infty \nu_\infty L\xi}}$$

$$\theta = \frac{T(x,y) - T_\infty}{T_0 - T_\infty}, \qquad \theta_f = \frac{T_f(x) - T_\infty}{T_0 - T_\infty} \tag{3-8}$$

where $Re_{L\infty} = \frac{u_\infty L}{\nu_\infty}$, ν_∞ is the kinematic viscosity of the fluid outside the boundary layer.

Equation (3-1) can then be written as

$$\varepsilon m_\infty^+ = \frac{\varepsilon m}{\nu_\infty} = \begin{cases} \varepsilon m^+ i = 0.16 \quad 1\text{-}\exp\left(-\frac{Rex_\infty^{\frac{1}{4}} Ch}{26} f''_w{}^{\frac{1}{2}} \eta\right) \quad {}^2\eta^2 f'' Rex_\infty^{\frac{1}{2}} \gamma_{tr}, \\ \qquad\qquad \text{when} \quad \varepsilon m^+ i \leq \varepsilon m_0^+ \\ \varepsilon m_0^+ = 0.0168\, Rex_\infty^{\frac{1}{2}}\, \eta_\infty - f(\eta_\infty)\, \gamma_{tr}, \\ \qquad\qquad \text{when} \quad \varepsilon m^+ i \geq \varepsilon m_0^+ \end{cases} \tag{3-9}$$

where $Rex = \frac{u_\infty x}{\nu}$, $Rex_\infty = \frac{u_\infty x}{\nu_\infty}$,

$$Ch = \frac{1 + a_1\theta_w(\xi) + a_2\theta^2{}_w(\xi)^{\frac{1}{2}}}{1 + a_1\theta + a_2\theta^2}.$$

IV. Steady Laminar Flow Convection-Conduction Cases in a Vertical Plate Fin

In the conventional heat transfer analysis of fins, it is standard practice to assume that the heat transfer coefficient for convection at the fin surfaces is uniform all along the fin. There is, however, evidence in the literature [21] , [22] demonstrating that the heat transfer coefficient can experience substantial variations along the fin surfaces. These variations may be caused by nonuniformities in the temperature fields in the fiuid adjacent to the fin.

For a thin fin, the temperatures changes in the longitudinal direction can be considered to be much larger than those in the transverse direction. Hence, it may be assumed that the heat conduction equation along the fin is essentially one dimensional in nature. Consider steady state conditions and assume that the thermal conductivity is constant, and that the local heat transfer coefficient is nonuniform over the surface. Sparrow et al [15],[16] have looked at this conjugated problem for vertical plate fin. and conclude that the conventional fin model based on a uniform input value of the heat transfer coefficient yields very good predictions for the overall heat transfer rate of the fin, but the local heat predictions can be substantially in error for forced convection flow. Even for natural convection flow, the local heat transfer coefficients were found not to decrease monotonically in the flow direction, as is useal. Rather, the coefficient decreased

at first, attained a minimum, and then increased with increasing downstream distance. This behavior was attributed to an enhanced buoyancy resulting from an increase in the wall-to-fluid temperature difference along the streamwise direction. Recently, T.S. Chen et al have studied the problem of natural convection-radiation interaction in boundary layer flow over horizontal surfaces by utilizing the Rosseland approximation [35].

The analysis of the present paper is for a vertical fin with a nonuniform temperature distribution which is strongly affected by the modified heat transfer coefficient. The radiative effect on the thermal boundary layer equation is considered, and the Rosseland approximation for the radiative heat flux is assumed. This approximation is valid at points optically far from the boundary surface, and is good only for intensive absorption, that is, for an optically thick boundary layer. In spite of these shortcomings, the Rosseland approximation has been used with success in a variety of problems ranging from transport of radiation through gases at low density to the study of the effects of radiation on blast waves by nuclear explosion. Hence, in order to determine the temperature of the fin, it must be coupled with the thermal boundary layer flow.

The fin temperature distribution, which is not known a priori, serves as a boundary condition for the boundary layer equation. The solutions of the modified local heat transfer coefficient along the fin surface from the boundary layer equations is substituted into the fin energy equation as known, in order to calculate the new temperature of fin surface.

This new temperature distribution is then imposed as the surface boundary condition for the boundary layer equation, the solution of which is used to evaluate an updated h* and so on until the maximum difference of temperature between the successive cycles is less than some given small value.

IV-1 Radiative Effect on the Vertical Plate Fin in Conjugated Natural Convection-Conduction Flow

A conjugated conduction-radiation-convection analysis has been made for a vertical heated plate fin which exchange heat with its fluid environment by natural convection and radiation.

The conservation equations of the laminar boundary layer with radiative effect and the fin energy equation are first transformed into a nondimensional form and their solutions are then simultaneously solved by an implicit finite difference method. Numerical results are presented for Pr=0.7 (for carbon dioxide in the temperature range 1000-650^{o}F with corresponding Prandtl number range 0.76-0.6 , C_T=0.5 over a conjugated convection-conduction parameter of N_c=0.5,1, and 3 and a conduction to radiation parameter of N=0.1,1,5 and ∞ . It is found that the heat flux of the fin with radiative effect is higher than of the fin without radiative effect.

Analysis

Consider a vertical plate fin which is extended from a wall at temperature T_o and situated in an otherwise quiescent envi-

ronment having temperature T_∞. The coordinates parallel and normal to the fin surface are taken to be x and y respectively. The coordinate system is in Fig.(4-1-1).

By employing the Boussinesq approximation for the fluid properities, the equations expressing conservation of mass, momentum and energy are, respectively, as follows:

$$\frac{\partial u}{\partial x} + \frac{\partial v}{\partial y} = 0 \qquad (4\text{-}1\text{-}1)$$

$$u\frac{\partial u}{\partial x} + v\frac{\partial u}{\partial y} = g\beta\ (T - T_\infty) + \nu\frac{\partial^2 u}{\partial y^2} \qquad (4\text{-}1\text{-}2)$$

$$u\frac{\partial T}{\partial x} + v\frac{\partial T}{\partial y} = \alpha\frac{\partial^2 T}{\partial y^2} - \frac{1}{\rho c_p}\frac{\partial q^r}{\partial y} \qquad (4\text{-}1\text{-}3)$$

where the standard symbols are defined in the nomenclature.

In the past, several investigators [36-37] used the optically thick limit approximation to study the interaction of radiation with boundary layer heat transfer. Under the assumption of optically thick limit approximation for the radiative part, q^r may be expressed as

$$q^r = \frac{-4\sigma}{3\beta^*}\frac{\partial T^4}{\partial y} \qquad (4\text{-}1\text{-}4)$$

where σ is the Stafan-Boltzmann constant and β^* is extinction coefficient.

The system of equations (4-1-1)-(4-1-3) is subject to the following boundary conditions

$$\left.\begin{array}{llll} u=v=0, & T=Tw(x) & \text{at} & y=0 \\ u\to 0, & T\to T_\infty & \text{as} & y\to\infty \end{array}\right\} \qquad (4\text{-}1\text{-}5)$$

Equations (4-1-1)-(4-1-4) and boundary conditions (4-1-5) do not admit a similarity solution. The nonsimilarity arises from the surface temperature, Tw(x), which is undetermined. The pseudo-similarity variable η and the dimensionless streamwise coordinate ξ are introduced as follows

$$\xi = \frac{x}{L}, \quad \eta = \frac{y}{L\xi^{\frac{1}{4}}} (GrL/4)^{\frac{1}{2}} \qquad (4\text{-}1\text{-}6)$$

where L is the length of the plate fin and GrL is the Grashof number, $GrL=g\beta(To-T_\infty)L^3/\nu^2$.

The dimensionless stream function $f(\xi,\eta)$ and the dimensionless temperature $\theta(\xi,\eta)$ are defined, respectively, by

$$f(\xi, \eta) = \Psi(x, y)/(4\nu(GrL/4)^{\frac{1}{4}}\xi^{\frac{3}{4}}) \qquad (4\text{-}1\text{-}7)$$

$$\theta(\xi, \eta) = (T - T_\infty)/(T_o - T_\infty) \qquad (4\text{-}1\text{-}8)$$

where the stream function $\Psi(x,y)$ satisfies the continuity equation (4-1-1) with

$$u = \frac{\partial \Psi}{\partial y}, \qquad v = -\frac{\partial \Psi}{\partial x} \qquad (4\text{-}1\text{-}9)$$

Introducing equations (4-1-4) and (4-1-6)-(4-1-9) into equations (4-1-2), (4-1-3) and (4-1-5) gives

$$f''' + 3ff'' - 2(f')^2 + \theta = 4\xi(f'\frac{\partial f'}{\partial \xi} - f''\frac{\partial f}{\partial \xi}) \qquad (4\text{-}1\text{-}10)$$

$$Pr^{-1}\theta'' + 3f\theta' + \frac{4((\theta+c_T)^3\theta')'}{3Pr\ N} = 4\xi(f'\frac{\partial \theta}{\partial \xi} - \theta'\frac{\partial f}{\partial \xi}) \qquad (4\text{-}1\text{-}11)$$

$$\begin{aligned} &f = f' = 0, \quad \theta = \theta_w(\xi), && \text{at} \quad \eta = 0 \\ &f' = \theta = 0, && \text{as} \quad \eta \to \infty \end{aligned} \qquad (4\text{-}1\text{-}12)$$

In the foregoing equations, the primes stand for partial deriva-

tives with respect to η, Pr is the Prandtl number, $N=\frac{K\beta^*}{4\sigma(To-T_\infty)}$ and $c_T=\frac{T_\infty}{To-T_\infty}$. Assuming a one-dimensional model, the thin fin energy equation allows the temperature distribution along the longitudinal direction to be written as

$$\frac{d^2T_f}{dx^2} = \frac{h^*(x)}{kf\ \delta}(T_f - T_\infty) \qquad (4\text{-}1\text{-}13)$$

where k_f is the fin thermal conductivity, T_f is the fin temperature, and $h^*(x)$ is the modified local heat transfer coefficient which can be regarded as known from the current boundary layer solutions. The associated boundary conditions are:

$$\left.\begin{aligned} T_f &= T_o \quad \text{at} \quad x = L \\ \frac{dT_f}{dx} &= 0 \quad \text{at} \quad x = 0 \end{aligned}\right\} \qquad (4\text{-}1\text{-}14)$$

Of particular interest is the thermal coupling between the fin and the thermal boundary layer. The basic coupling is expressed by the requirement that the fin and fluid temperatures and local heat fluxes be continuous at the fin-fluid interface, at all x.

$$\left.\begin{aligned} T_f(x) &= T_w(x) \\ h^*(T_f - T_\infty) &= -k\frac{\partial T}{\partial y} + q^r \end{aligned}\right\} \quad \text{at } y = 0, \quad 0 \leq x \leq L \qquad (4\text{-}1\text{-}15)$$

Equation (4-1-13) was recast in dimensionless form by the substitutions

$$\xi = \frac{x}{L}, \qquad \theta_f = \frac{T_f - T_\infty}{T_o - T_\infty} \qquad (4\text{-}1\text{-}16)$$

and combined with equations (4-1-14) and (4-1-15), so that

$$\frac{d^2\theta_f}{d\xi^2} = Nc\ \hat{h}^*\ \theta_f \qquad (4\text{-}1\text{-}17)$$

$$\left.\begin{aligned} \theta_f &= 1 \quad , \qquad \text{at} \quad \xi = 1 \\ \frac{d\theta_f}{d\xi} &= 0 \qquad\quad \text{at} \quad \xi = 0 \end{aligned}\right\} \qquad (4\text{-}1\text{-}18)$$

and $\theta_w = \theta_f$, $h^* = k\ GrL^{\frac{1}{4}}\ \hat{h}^*/L$, at $\eta = 0$ (4-1-19)

where Nc is the conjugated convection-conduction parameter.

$$Nc = \frac{kL\ GrL^{\frac{1}{4}}}{K_f \delta} \qquad (4\text{-}1\text{-}20)$$

The quantity $\hat{h}^*$ is a dimensionless form of the modified local heat transfer coefficient. The value of $\hat{h}^*$ is obtained by substituting equations (4-1-4), (4-1-6) and (4-1-16) into equation (4-1-15).

$$\hat{h}^* = -\left(\frac{1}{4\xi}\right)^{\frac{1}{2}} \left(1+\frac{4(\theta+c_T)^3}{3N}\right)\theta'/\theta_f \qquad \text{at } \eta = 0 \quad (4\text{-}1\text{-}21)$$

Numerical Solution

The solution begins by solving the natural thermal boundary layer problem for a vertical plate fin with guessed temperature for all ξ. The dimensionless modified heat transfer coefficients $\hat{h}^*$ determined from this solution in accordance with equation (4-1-21) are then used as input to the fin heat conduction equation (4-1-17). With Nc prescribed, the differential equation (4-1-17) is then solved to yield θ_f. To begin the next cycle of the iterative procedure, the just-determined θ_f

is imposed as the thermal boundary condition for the boundary layer problem; the solution to which yields a new $\hat{h}^*$ distribution which is used as input to the fin heat conduction equation. This procedure of alternately solving the boundary problem and fin conduction problem was continued until convergence was attained. The two systems of partial differential equations (4-1-10) and (4-1-11) are coupled. In the present analysis, these equations were solved by an accurated implicit finite fifference technique [19]. To begin with, the partial differential equations (4-1-10), (4-1-11) are first converted into a system of first order equations which are then expressed in finite difference form by approximating the functions and their first derivatives in terms of centered difference and averaged at midpoints of the net segments in the (ξ,η) coordinates. The resulting non-linear finite-difference equations are then solved by Newton's iterative method. The accuracy of the order of the numerical scheme is $(\Delta\xi)^2$ and $(\Delta\eta)^2$.

The boundary layer solutions were obtained by a marching procedure starting at the leading edge ($\xi=0$), and the grids were divided into 45 points in the streamwise direction. There was a denser concentration of points near the leading edge to accommodate the initial rapid growth of the boundary layer. We use 61 grid points in the cross-stream direction.

In order to write the system in terms of a first-order system of partial differential equations, new dependent variable $\bar{u}(\xi,\eta)$, $\bar{v}(\xi,\eta)$ and $\omega(\xi,\eta)$ are introduced, so that equation

(4-1-10) and (4-1-11) can be written as

$$f' = \bar{u} \tag{4-1-22}$$

$$\bar{u}' = \bar{v} \tag{4-1-23}$$

$$\theta' = \omega \tag{4-1-24}$$

$$\bar{v}' + 3f\bar{v} - 2\bar{u}^2 + \theta = 4\xi\left(\bar{u}\frac{\partial \bar{u}}{\partial \xi} - \bar{v}\frac{\partial f}{\partial \xi}\right) \tag{4-1-25}$$

$$Pr^{-1}\omega' + 3f\omega + \frac{4\left((\theta+c_T)^3\omega\right)'}{3PrN} = 4\xi\left(\bar{u}\frac{\partial \theta}{\partial \xi} - \frac{\partial f}{\partial \xi}\right) \tag{4-1-26}$$

Consider the net rectangle shown in figure (4-1-2) and denote the net points by

$$\xi_o = 0,\ \xi_n = \xi_{n-1} + k_n,\quad n = 1, 2, \ldots N$$
$$\eta_o = 0,\ \eta_j = \eta_{j-1} + h_j \quad j = 1, 2, \ldots J \tag{4-1-27}$$
$$\eta_J = \eta_\infty$$

Approximate the quantities $(f, \bar{u}, \bar{v}, \theta, \omega)$ at points (ξ_n, η_j) of the net by net functions denoted by $(f_j, \bar{u}_j, \bar{v}_j, \theta_j, \omega_j)$ and employ the following notation for points and quantities midway between net points and for net function m_j^n

$$\xi_{n-\frac{1}{2}} \equiv \frac{1}{2}\left(\xi_n + \xi_{n-1}\right),\ m_j^{n-\frac{1}{2}} \equiv \frac{1}{2}\left(m_j^n + m_j^{n-1}\right)$$
$$\eta_{j-\frac{1}{2}} \equiv \frac{1}{2}\left(\eta_j + \eta_{j-1}\right),\ m_{j-\frac{1}{2}}^n \equiv \frac{1}{2}\left(m_j^n + m_{j-1}^n\right) \tag{4-1-28}$$

The difference equations that are to approximate (4-1-22)-(4-1-26) are now easily formulated by considering one mesh rectangle as in figure (4-1-2). Equations (4-1-22)-(4-1-24) are approximated by using centered difference quotients and averages about the midpoint $(\xi_n, \eta_{j-\frac{1}{2}})$ of the segment p_2p_4,

with the following results:

$$(f_j^n - f_{j-1}^n)h_j^{-1} = \bar{u}_{j-\frac{1}{2}}^n \qquad (4\text{-}1\text{-}29)$$

$$(\bar{u}_j^n - \bar{u}_{j-1}^n)h_j^{-1} = \bar{v}_{j-\frac{1}{2}}^n \qquad (4\text{-}1\text{-}30)$$

$$(\theta_j^n - \theta_{j-1}^n)h_j^{-1} = \omega_{j-\frac{1}{2}}^n \qquad (4\text{-}1\text{-}31)$$

Similarly, equations (4-1-25) and (4-1-26) are approximated by centering on the midpoint $(\xi_{n-\frac{1}{2}}, \eta_{j-\frac{1}{2}})$ of the rectangle $P_1P_2P_3P_4$, which gives

$$\frac{\bar{v}_j^n - \bar{v}_{j-1}^n}{h_j} + (3 + \alpha n)(f\bar{v})_{j-\frac{1}{2}}^n - (2+\alpha n)(\bar{u}^2)_{j-\frac{1}{2}}^n + \theta_{j-\frac{1}{2}}^n$$

$$- \alpha n(\bar{v}^n f^{n-1})_{j-\frac{1}{2}} + \alpha n(\bar{v}^{n-1} f^n)_{j-\frac{1}{2}} = R_{j-\frac{1}{2}}^{n-1} \qquad (4\text{-}1\text{-}32)$$

$$Pr^{-1}\frac{(\omega_j^n - \omega_{j-1}^n)}{h_j} + (3 + \alpha n)(f\omega)_{j-\frac{1}{2}}^n + \frac{4}{3\ Pr\ N}[3(\theta_{j-\frac{1}{2}}^n + c_T)^2 (\omega^2)_{j-\frac{1}{2}}^n$$

$$+ (\frac{\omega_j^n - \omega_{j-1}^n}{h_j})(\theta_{j-\frac{1}{2}}^n + c_T)^3] + \alpha n[-(\bar{u}\theta)^n - \bar{u}^{n-1}\theta^n + \bar{u}^n\theta^{n-1}$$

$$+ \omega^{n-1}f^n - \omega^n f^{n-1}]_{j-\frac{1}{2}} = Y_{j-\frac{1}{2}}^{n-1} \qquad (4\text{-}1\text{-}33)$$

where $$\alpha n = \frac{4\xi^{n-\frac{1}{2}}}{k^n} \qquad (4\text{-}1\text{-}34)$$

$$R_{j-\frac{1}{2}}^{n-1} = \alpha n[(f\bar{v})_{j-\frac{1}{2}}^{n-1}) - (\bar{u}^2)_{j-\frac{1}{2}}^{n-1}] - [(\frac{\bar{v}_j - \bar{v}_{j-1}}{h_j})^{n-1} + 3(f\bar{v})_{j-\frac{1}{2}}^{n-1}$$

$$- 2(\bar{u}^2)_{j-\frac{1}{2}}^{n-1} + \theta_{j-\frac{1}{2}}^{n-1}] \qquad (4\text{-}1\text{-}35)$$

$$Y_{j-\frac{1}{2}}^{n-1} = \alpha n[(\omega f)_{j-\frac{1}{2}}^{n-1} - (\bar{u}\theta)_{j-\frac{1}{2}}^{n-1})] - \{Pr^{-1}(\frac{\omega_j - \omega_{j-1}}{h_j})^{n-1} + 3(f\omega)_{j-\frac{1}{2}}^{n-1}$$

$$+ \frac{4}{3\ Pr\ N}[3(\theta_{j-\frac{1}{2}}^{n-1} + c_T)^2(\omega^2)_{j-\frac{1}{2}}^{n-1} + (\frac{\omega_j - \omega_{j-1}}{h_j})^{n-1}(\theta_{j-\frac{1}{2}}^{n-1} + c_T)^3] \qquad (4\text{-}1\text{-}36)$$

Equations (4-1-29)-(4-1-33) are imposed for j = 1, 2,...J. The boundary conditions (4-1-12) can be written as

$$f_o^n = 0, \quad \theta_o^n = \theta_w^n, \quad \bar{u}_o = 0, \quad \bar{u}_J^n = 0, \quad \theta_J^n = 0 \qquad (4\text{-}1\text{-}37)$$

If we assume (f_j^{n-1}, $\bar{u}_j^{n-1}$, $\bar{v}_j^{n-1}$, θ_j^{n-1}, ω_j^{n-1}) are assumed to be known for $0 \leq j \leq J$, then (4-1-29)-(4-1-33) and the boundary conditions (4-1-37) yield an implicit non-linear algebraic system of 5J+5 equations in as many unknowns (f_j^n, $\bar{u}_j^n$, $\bar{v}_j^n$, θ_j^n, ω_j^n). The system can be solved very effectively by using newton's method.

The fin conduction equation was solved by using the direct inverse matrix method. The fin equation was also divided into 45 grid points and expressed in finite difference form. To ensure high accuracy, a nonuniform grid points were employed. For small ξ , a finer ξ subdivision was also needed for the heat conduction equation.

Results and Discussion

Numerical calculations of the overall rate of heat transfer Q were obtained from the wall into the fin base at ξ=1 or from the integrating heat transfer over the fin surface. The cor-

responding Q values of these two method are found to be in agreement. They may be expressed in dimensionless from as

$$\frac{Q}{k(T_o-T_\infty)GrL^{\frac{1}{4}}} = 2\int_0^1 -\left(1+\frac{4(\theta+c_T)^3}{3N}\right)\theta'/(4\xi)^{\frac{1}{4}}d\xi, \quad \text{at} \quad \eta=0 \tag{4-1-38}$$

or

$$\frac{Q}{k(T_o-T_\infty)GrL^{\frac{1}{4}}} = \frac{2}{Nc}\left.\frac{d\theta_f}{d\xi}\right|_{\xi=1} \tag{4-1-39}$$

The results of the overall heat transfer rate Q from the fin are presented as a function of the conjugated convection-conduction parameter, Nc. The decrease of Nc indicates short fin length, L, great fin conductances, k_f δ, and low convective coefficients (low k and GrL). In Fig (4-1-3) it is found that the overall heat transfer rate of the fin with radiative effect is higher than that of the fin without radiative effect. Fig. (4-1-3) also shows that an increasing N yields a decreasing total heat transfer rate of fin for fixed Nc. The case with $N \to \infty$ corresponds to nonradiating flow, and N=1 to reasonably strong radiation effects.

Fig.(4-1-4) Fig.(4-1-5) illustrate the distributions of the modified local heat transfer coefficient for natural thermal boundary layer along the fin surface as a function of Nc and N. The modified local heat transfer coefficient can be written, in dimensionless form, as follows:

$$\hat{h}^* = h^*L/kGr_L^{\frac{1}{4}} = \frac{-1}{\sqrt{2}\xi^{\frac{1}{4}}}\left(1+\frac{4(\theta+c_T)^3}{3N}\right)\frac{\partial\theta}{\partial\eta}/\theta_f \quad , \text{at } \eta = 0 \tag{4-1-40}$$

It is shown from these two figures that the larger variations of the response of the modified local heat transfer coefficient $\hat{h}^*$ increase the streamwise variations of the fin temperature. As seen from the figures, it may be seen that $\hat{h}^*$ decreases to some minimum, and then increases steadily with ξ; the minimum approaches the tip as Nc becomes larger.

The phenomenon of this behavior is the same as the natural convective flow over a vertical plate without radiative effect [15], and is attributed to both enhanced buoyancy and radiative heat flux associated with an increase in the wall-to-fluid temperature difference along the streamwise direction for a heated fin.

Distributions of the dimensionless local heat flux at the fin surface are shown in Fig.(4-1-6)-(4-1-7), for various values of Nc and N. The local heat flux can be taken as

$$\frac{qL}{k(T_o-T_\infty)Gr_L^{\frac{1}{4}}} = \frac{-1}{\sqrt{2}\xi^{\frac{1}{4}}}\left(1+\frac{4(\theta+c_T)^3}{3N}\right)\frac{\partial\theta}{\partial\eta} \quad \text{at } \eta=0 \quad (4\text{-}1\text{-}44)$$

which composed of the conductive heat flux and the radiative heat flux. From the two figures, it is found that most of the heat fluxes transfer to the ambient fluid by natural convection and radiation near the base for higher values of Nc. Fig.(4-1-6)-(4-1-7) also show that the total heat transfer rate from the fin surface is increased as Nc decreased, which agrees with the prediction in Fig.(4-1-3)

It is observed from Fig.(4-1-4)-Fig.(4-1-7) that both of the local heat flux and modified heat transfer coefficient with

radiative effect ($N > 0$) are higher than those without radiative effect ($N \to \infty$). Fig.(4-1-7) also show that a decrease in the values of N gives rise to a larger values of modified heat transfer coefficient and local heat flux. The smaller values of N corresponds to stronger radiation effect which is due to an increase in the wall-to-fluid temperature difference.

Representative results for the fin temperature distributions are presented in Fig.(4-1-8)-(4-1-9) over a wide range of Nc and N. Fig.(4-1-8)-(4-1-9) show the expected trend whereby the fin temperature decreases monotonically from the root to the tip. The figures also confirm the assertions that larger values of Nc give rise to larger fin temperature variations. From these figures, it may be noted that the fin temperature distributions have a larger variations in the streamwise direction for smaller values of N.

Remark

The analysis of this section has yielded the results of heated vertical plate fin for natural thermal boundary layer flow with radiative effect. The optically thick limit approximation for the radiative heat flux is assumed. Although the range of the validity of the optically thick limit approximation is small in the boundary layer flow, it possesses the advantage of simplicity in the analysis because the governing energy equation can be transformed into an ordinary differential equation by the conventional similarity transformation. The

exact solutions of the fin surface temperature should lie between those for the nonradiating case and the optically thick limit approximation. The agreement of the results for special case (i.e. fin without radiation) with [15] is truely remarkable. In order to solve simultaneously the coupled fin conduction equation and the thermal boundary layer equations of fluid, a very simple and efficient "Box" scheme due to Cebeci and Bradshaw is empolyed here.

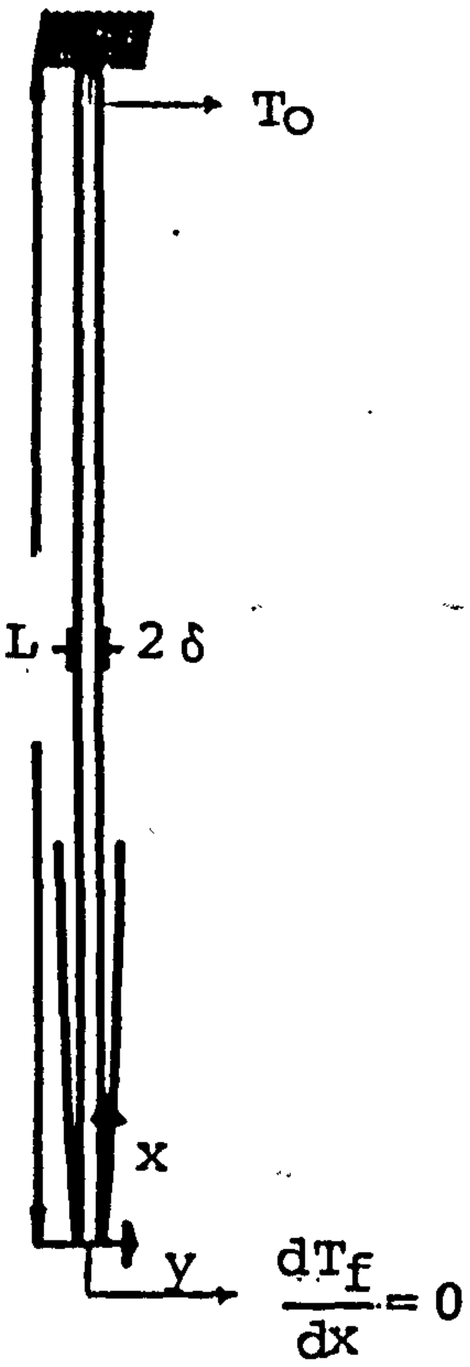

Fig.4-1-1 Physical model and coordinates system.

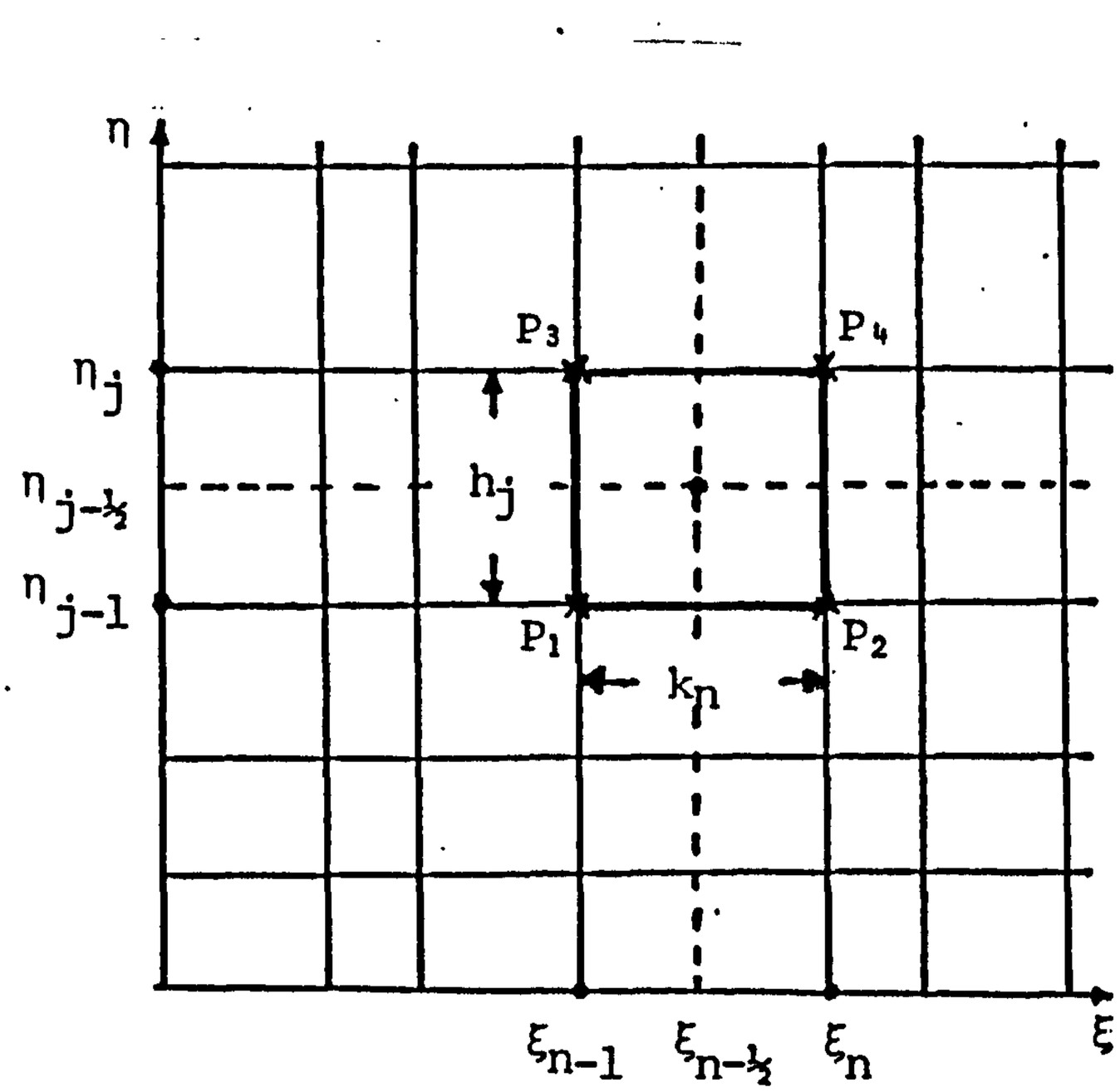

Fig.4-1-2 Net rectangle for the difference equations.

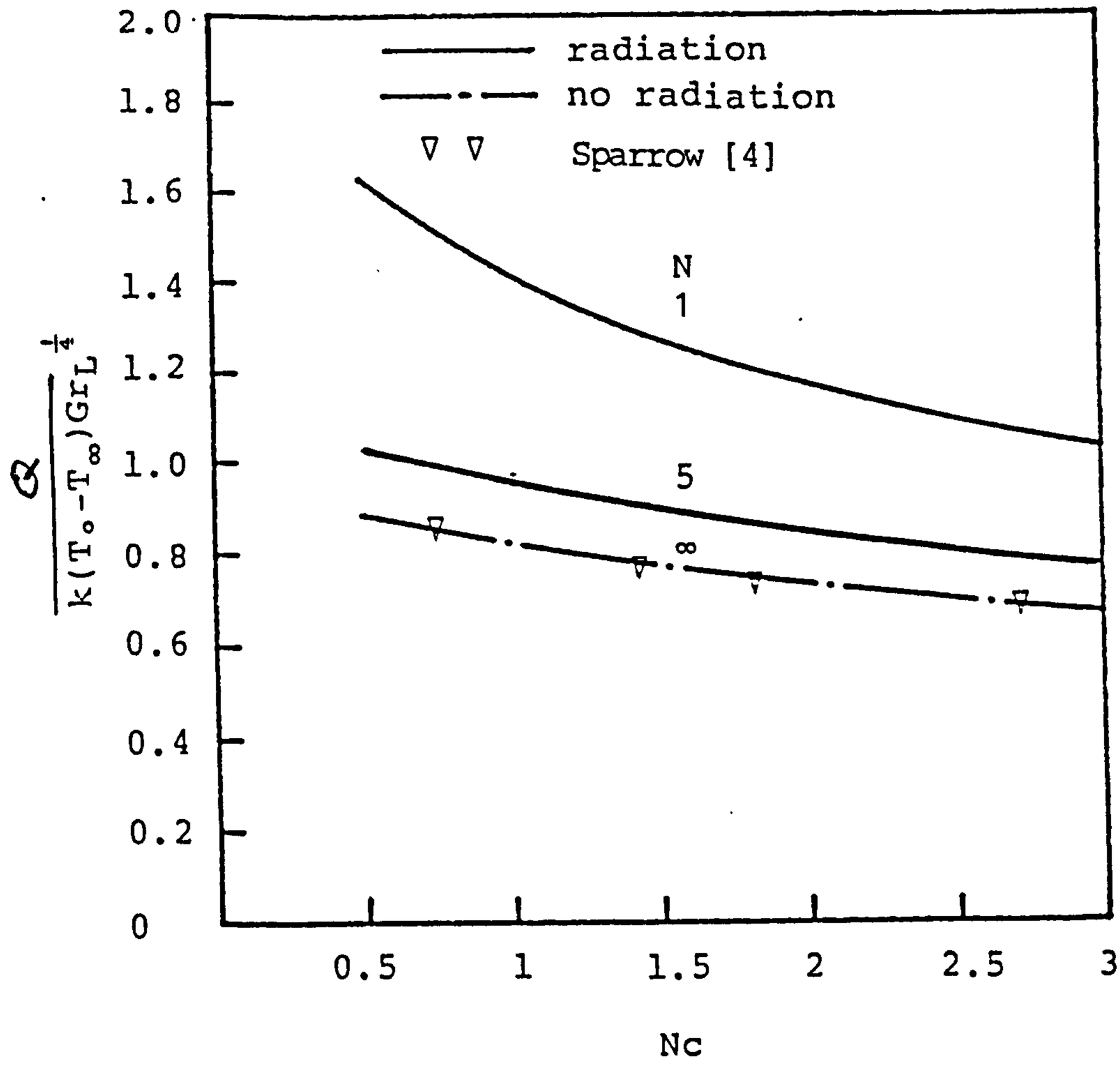

Fig.4-1-3 Total heat transfer rate for Pr=0.7, N=1, 5 , ∞ and C_T=0.5

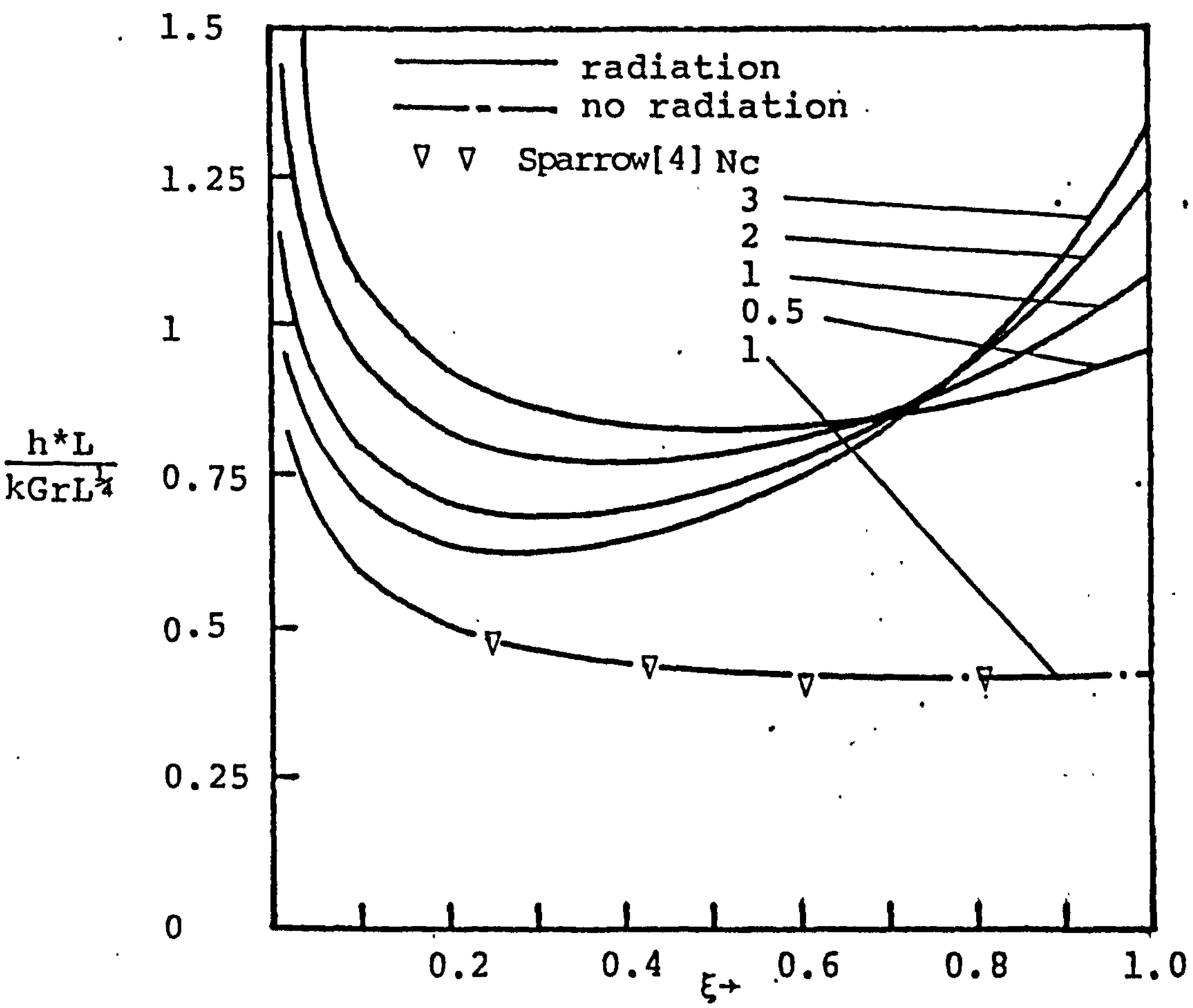

Fig.4-1-4 The modified heat transfer coefficients along the plate fin for N=1, c_T=0.5, Pr=0.7 and various values of Nc.

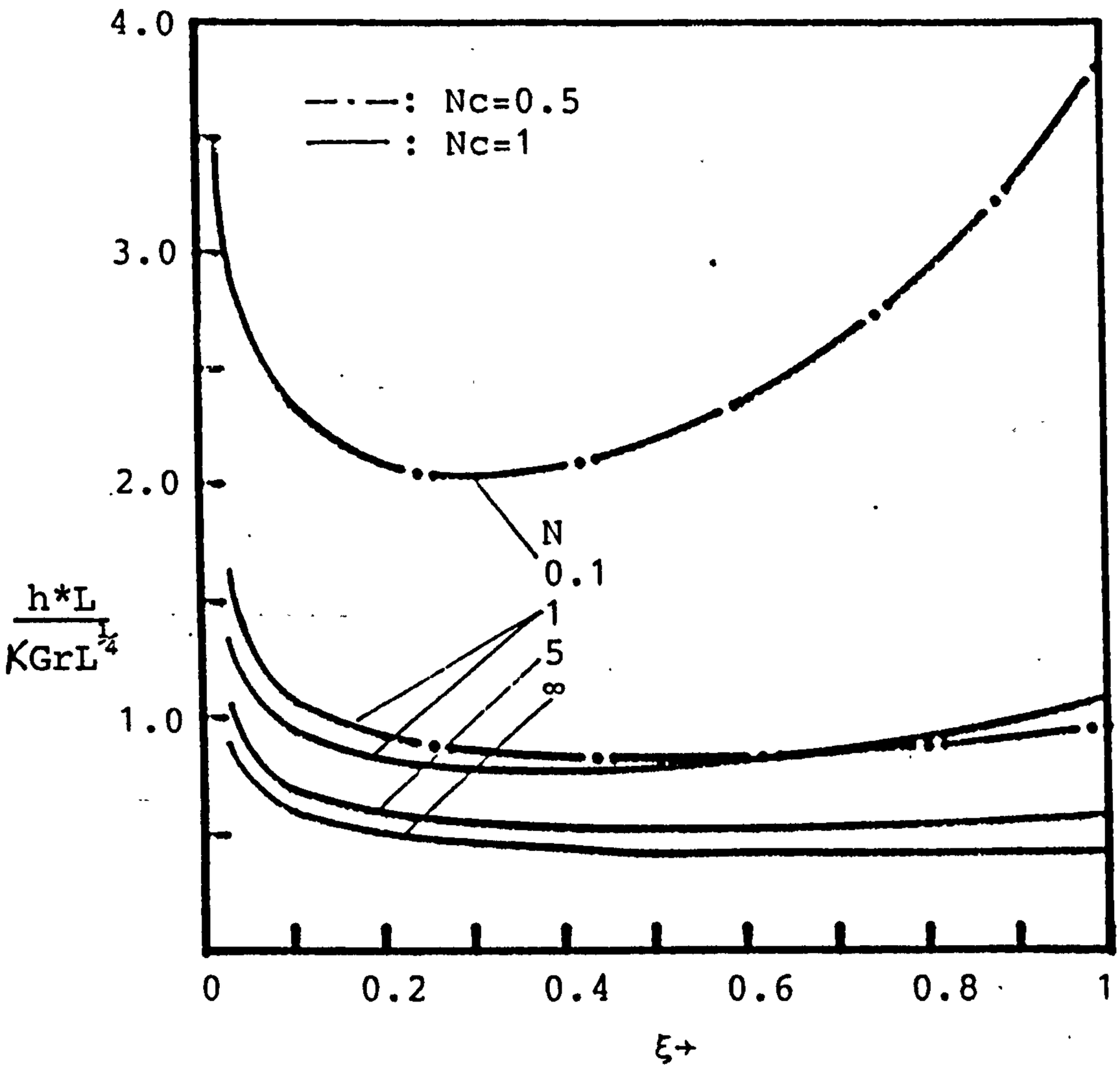

Fig.4-1-5 The modified heat transfer coefficients along the plate fin for c_T=0.5 and Pr=0.7.

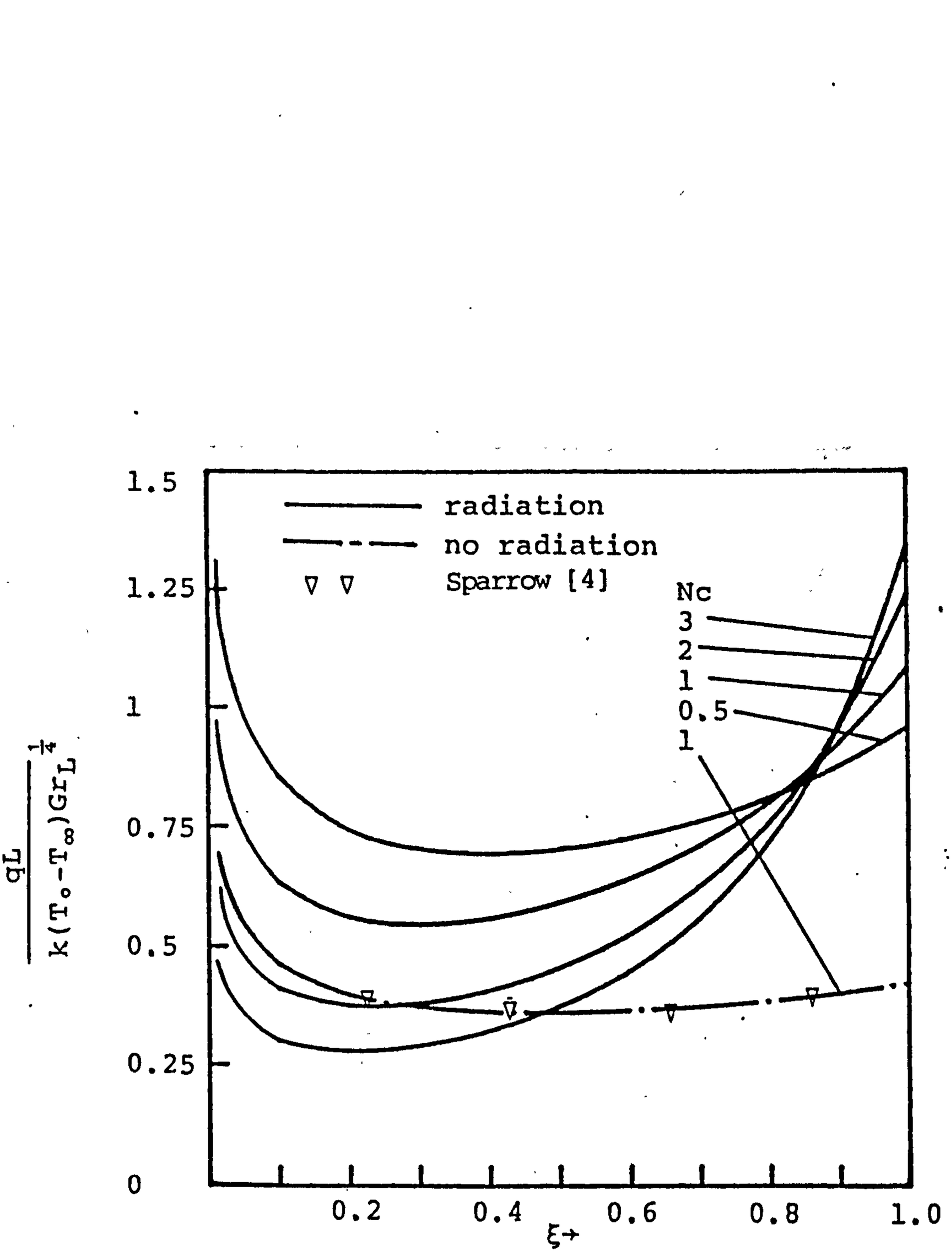

Fig.4-1-6 The local heat fluxes along the plate fin for N=1, c_T=0.5, Pr=0.7 and various values of Nc.

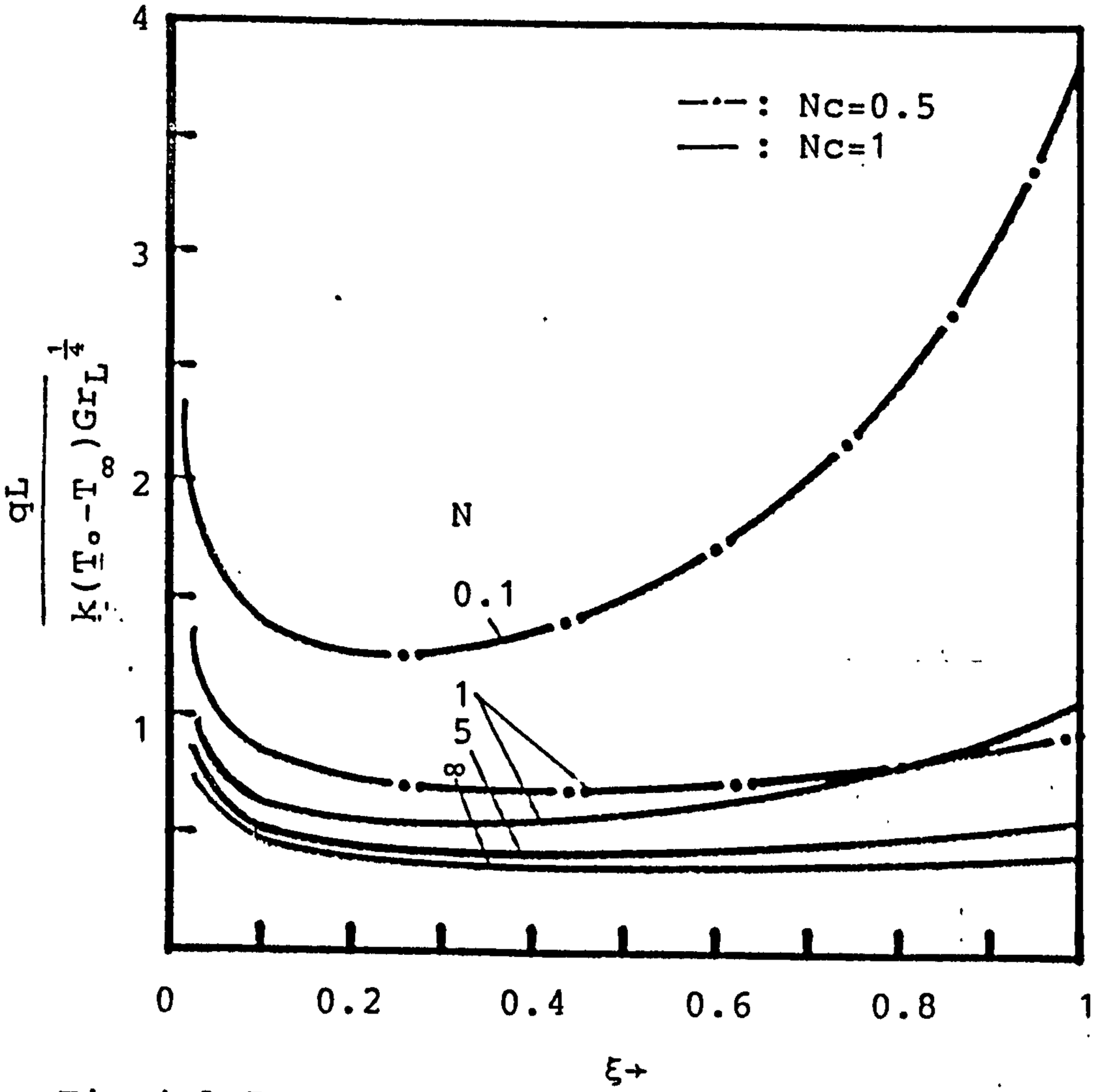

Fig.4-1-7 The local heat fluxes along the plate fin for c_T=0.5 and Pr=0.7.

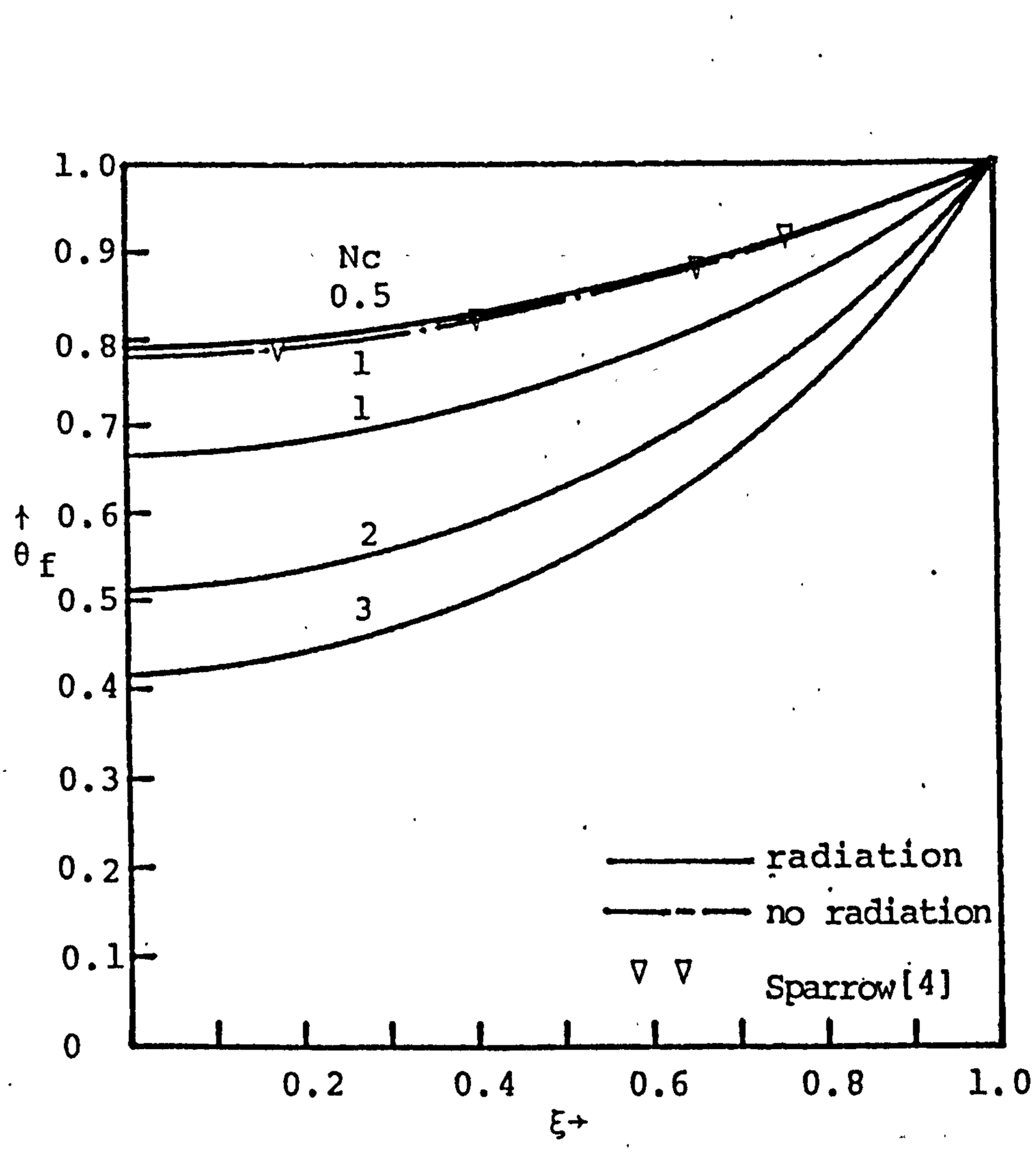

Fig.4-1-8 The temperature distributions along the plate fin for N=1, c_T=0.5, Pr=0.7 and various values of Nc.

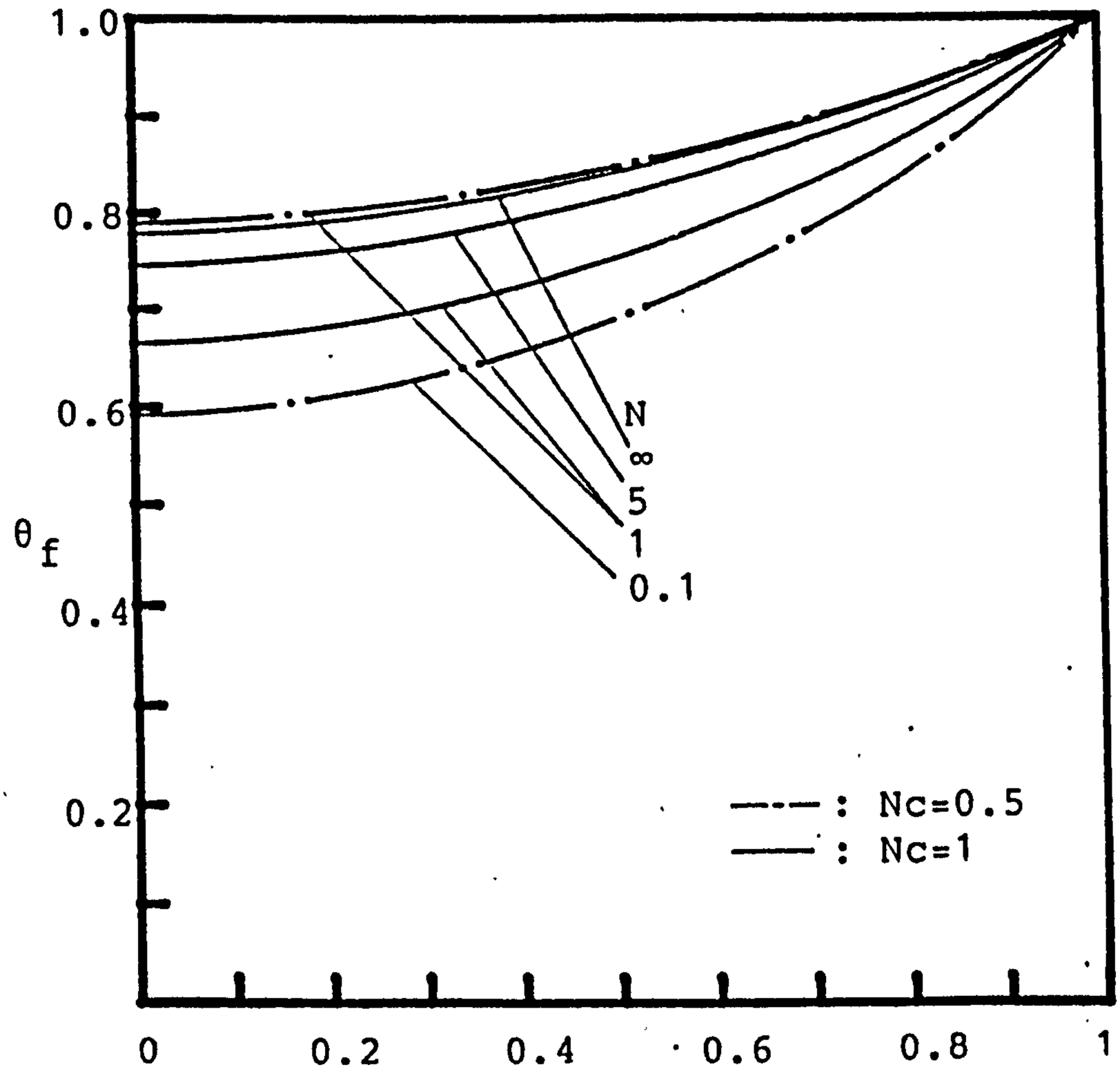

Fig.4-1-9 The temperature distributions along the plate fin for c_T=0.5 and Pr=0.7.

IV-2 Radiative Effect on the Conjugated Forced Convection-Conduction Analysis of Heat Transfer in a Plate Fin

The present section is concerned with fins which transfer heat to a surrounding fluid by forced convection and radiation. The heat transfer coefficient along the fin is not prescribed but solved in advance from the boundary layer convection flow. Therefore, the modified local heat transfer coefficient is determined by a highly coupled interaction among the fin conduction, radiation and the fluid convection flow. The fin temperature distribution has been strongly effected by the ambient fluid flow. As fin temperature distribution has been given, then the heat transfer coefficient in advance may be decided by boundary layer flow with varying temperature distribution along the fin. An implicit finite difference method is employed. The results of the overall heat transfer rate, modified local heat transfer coefficient, local heat flux and temperature distribution of the fin are given for Pr=0.7 (Prandtl number), c_T=0.5 (Temperature difference parameter), N=1 (Conduction to radiation parameter) and various value of Nc (Convection-conduction parameter).

The problem to be analyzed in this section is illustrated in Fig.(4-2-1), A vertical fin is of length L and thickness 2δ which is extended from a wall at temperature T_o and situated in a uniform free stream having temperature T_∞ and velocity u_∞. The optically thick limit approximation of radiation is assumed and the tip of the fin is insulated.

Analysis

The present study is concerned with the effects of radiation on convection along the fin surface. Consider now a vertical fin which is parallel to a uniform free stream. Let x and y denote, respectively, the streamwise and normal coordinates. The starting point of the analysis is the conservation equations for a laminar boundary layer over a vertical fin

$$\frac{\partial u}{\partial x} + \frac{\partial v}{\partial y} = 0 \qquad (4\text{-}2\text{-}1)$$

$$u \frac{\partial u}{\partial x} + v \frac{\partial u}{\partial y} = \nu \frac{\partial^2 u}{\partial y^2} \qquad (4\text{-}2\text{-}2)$$

$$u \frac{\partial T}{\partial x} + v \frac{\partial T}{\partial y} = \alpha \frac{\partial^2 T}{\partial y^2} - \frac{1}{\rho C_p} \frac{\partial q^r}{\partial y} \qquad (4\text{-}2\text{-}3)$$

where all the quantities are defined in the nomenclature.

Equations (4-2-1)-(4-2-3) are subject to the following boundary conditions:

$$\left.\begin{array}{lll} u = 0, \quad v = 0, & T = T_w(x) & \text{at } y = 0 \\ u \to u_\infty, & T \to T_\infty & \text{as } y \to \infty \end{array}\right\} \qquad (4\text{-}2\text{-}4)$$

This problem will admit similarity solutions for momentum equations. It is advantageous to introduce a pseudosimilarity variable η, a dimensionless variable ξ, with a reduced stream function $f(\xi, \eta)$ and a dimensionless temperature $\theta(\xi, \eta)$ as follows:

$$\left.\begin{aligned} \xi = \frac{x}{L}\,, \qquad \eta = \left(\frac{y}{L}\right) Re_L^{\frac{1}{2}} / \xi^{\frac{1}{2}} \\ f(\xi,\ \eta) = \psi(x,\ y)/(u_\infty \nu L \xi)^{\frac{1}{2}},\ \theta = \frac{T - T_\infty}{T_o - T_\infty} \end{aligned}\right\} \qquad (4\text{-}2\text{-}5)$$

where the stream function ψ satisfies the continuity equation with $u = \partial\psi/\partial y$ and $v = -\partial\psi/\partial x$. The motivation for employing the transformation variables (4-2-5) is that the transformed conservation equations are much less dependent on the axial coordinate than are the original conservation equations.

When the transformation is applied to equations (4-2-2) and (4-2-3), and the optically thick limit approximation for q^r is assumed, the govering system becomes

$$f''' + \frac{1}{2} ff'' = 0 \qquad (4\text{-}2\text{-}6)$$

$$P_r^{-1}\theta'' + \frac{f\theta'}{2} + \frac{4\left[(\theta+C_T)^3\theta'\right]'}{3\ P_r N} = \xi f' \frac{\partial\theta}{\partial\xi} \qquad (4\text{-}2\text{-}7)$$

subject to boundary conditions

$$\left.\begin{aligned} f = f' = 0, \quad \theta_w = \frac{T_w(x) - T_\infty}{T_o - T} \quad \text{at} \quad \eta = 0 \\ f' = 1, \qquad \theta = 0 \qquad\qquad \text{as} \quad \eta \to \infty \end{aligned}\right\} \qquad (4\text{-}2\text{-}8)$$

where C_T, N, P_r are defined in the nomenclature and the primes denote partial differentiation with respect to η .

Considering a very thin fin, it is reasonable to assume a one-dimensional model for the fin temperature along x coordinate.

The fin conservation energy equation is

$$\frac{d^2T_f}{dx^2} = \frac{h^*(x)}{k_f \delta} (T_f - T_\infty) \qquad (4\text{-}2\text{-}9)$$

where T_f is the fin temperature at any position x, k_f is the fin thermal conductivity and δ is the half thickness of the fin.

In this equation $h^*(x)$ can be regarded as known from a previous iteration cycle. Employing dimensionless variables for fin

$$\xi = \frac{x}{L} \quad , \quad \theta_f = \frac{T_f - T_\infty}{T_o - T_\infty} \qquad (4\text{-}2\text{-}10)$$

then equation (4-2-9) becomes

$$\frac{d^2\theta_f}{d\xi^2} = \frac{h^*(x)L}{k_f \delta} \theta_f \qquad (4\text{-}2\text{-}11)$$

with boundary conditions of the base root temperature T_o (at ξ=1) and adiabatic tip (at ξ=0). Coupling the fin energy and the fluid boundary layer equations, requires matching the boundary conditions that the fin and the fluid temperature are the same and the heat flux is continuous at the plate-fluid interface for all stations.

i.e. $T_w = T_f$ and $-k \frac{\partial T}{\partial y} + q^r = h^*(T_f - T_\infty)$ at $y = 0$ (4-2-12)

Substituting dimensionless variables into equation (4-2-12), then we get

$$\theta_w = \theta_f, \quad h^* = k \, Re_L^{\frac{1}{2}} \hat{h}^* / L \quad \text{at } \eta = 0 \qquad (4\text{-}2\text{-}13)$$

Thereby, equation (4-2-11) becomes

$$\frac{d^2\theta_f}{d\xi^2} = N_c \hat{h}^* \theta_f \qquad (4\text{-}2\text{-}14)$$

where N_c is the convection-conduction parameter ($N_c = \frac{kL}{k_f \delta} Re_L^{\frac{1}{2}}$). The quantity $\hat{h}^*$ is a dimensionless form of the forced convection heat transfer coefficient including radiation effects that for the current cycle of the iteration

$$\hat{h}^* = -\left(1 + \frac{4(\theta + C_T)^3}{3N}\right) \frac{\partial\theta}{\partial\eta} / (\theta_f \xi^{\frac{1}{2}}) \quad \text{at } \eta = 0 \qquad (4\text{-}2\text{-}15)$$

The method to be used here involves a succession of consecutive solutions for the fin and the boundary layer. Initially, the boundary layer equations are solved subject to an assumed fin temperature distribution which satisfies the thermal boundary conditions, and from this solution $\hat{h}^*$ is evaluated. Substituting $\hat{h}^*$ into the fin energy equation, which is solved to give new θ_f. Then this new θ_f is imposed as the fin surface boundary condition for the governing equations. This procedure of alternately solving the boundary layer problem and fin conduction problem was continued until convergence was attained.

Numerical Procedure

The solutions of the boundary layer equation were obtained by an implicit finite difference method devised by cebeci and

Bradshaw [19] . Starting from the fin tip ($\xi = 0$), step by step, to the base root ($\xi = 1$). According to this method, equations (4-2-6), (4-2-7) are first written in the first order equation by introducing new known functions. The functions and their derivatives in the first-order equations are then aproximated by centered difference quotients and averages at the mid-points of net rectangles to yield finite-difference equations. The resulting nonlinear difference equations are finally solved by using Newton's method. This gives very stable and highly accurate results. The fin conduction equation is also written in the finite difference form. For small ξ , a finner subdivision was need for the boundary layer solution. The results of the finite difference equations represent the discretized conduction equation at all fin grid points except $\xi = 0$ and $\xi = 1$. At the root, the fin temperature is equal to T_o. At the tip, the adiabatic boundary condition is applied.

The results of the special case (fin without radiation) agree with Sparrow and Chyu [16] for the forced convection fin. The present method uses 45 points in the streamise direction and {61} grid points in the cross-stream direction.

Results and Discussion

Numerical results of the overall rate of heat transfer Q

from the fin can be obtained from the heat conducted from the wall into the fin base at $\xi=1$ or by integrating the local heat flux at the fin surface. The corresponding heat flux values of these two method are found to be in agreement. They may be expressed in dimensionless form as follows:

$$\frac{Q}{k(T_o-T_\infty)Re_L^{\frac{1}{2}}} = 2\int_0^1 (-\frac{\partial\theta}{\partial\eta})\,[\,1+\frac{4(\theta+C_T)^3}{3N}\,]/\xi^{\frac{1}{2}}\,d\xi, \text{ at } \eta = 0 \qquad (4\text{-}2\text{-}16)$$

or

$$\frac{Q}{k(T_o-T_\infty)Re_L^{\frac{1}{2}}} = \frac{2}{N_c}\,\frac{d\theta_f}{d\theta}\bigg|_{\xi=1} \qquad (4\text{-}2\text{-}17)$$

The results of the overall rate of heat transfer Q from the fin are shown in Fig.4-2-2 for various values of N_c. The decrease of N_c indicates short fin length, L, great fin conductances, $k_f\delta$, and low convective coefficients (low k and Re_L). Fig. (4-2-2) also indicates that the overall heat transfer rate of the fin with radiation effect is higher than that of the fin without radiation effects. The agreement of the results from the simple model with those of [16] and the special case ($q^r=0$) in this paper is truely remarkable. This near-perfect agreement should not regarded as a validation of the simple model but only as an indication of its ability to predict overall results accurately.

The distributions of the modified local heat transfer coefficient h* for forced convection and radiation along the fin with various values of N_c are shown in Fig.(4-2-3). The modified heat transfer coefficient can be expressed as

$$\frac{h^*L}{kRe_L^{1/2}} = -\left[1+\frac{4(\theta+C_T)^3}{3N}\right]\frac{\partial\theta}{\partial\eta}/\left(\theta_f\xi^{1/2}\right) \quad \text{at } \eta = 0 \qquad (4\text{-}2\text{-}18)$$

For higher values of N_C, the fin is more nonisothermal. Thus, the more nonisothermal the fin, the greater the modified local heat transfer coefficients increase near the base root. Although the local heat transfer coefficient without radiation effects [16] monotonically decreases in the fluid flow direction, the modified local heat transfer coefficients computed in this paper with fixed radiative effect do not vary monotonically. In the direction from tip to base, those coefficients decrease at first, attain a minimum, and then increase.

The variations of the dimensionless local heat flux at the fin surface are presented in Fig.(4-2-4) for different N_C. The local heat flux can be taken as

$$\frac{qL}{k(T_o-T_\infty)Re_L^{1/2}} = -\left(1+\frac{4(\theta+C_T)^3}{3N}\right)\frac{\partial\theta}{\partial\eta}/\xi^{1/2}, \quad \text{at } \eta = 0 \qquad (4\text{-}2\text{-}19)$$

For smaller N_C, the heat flux is larger near the tip, but smaller at the near base. For higher N_C, most of the heat fluxes transfer to the ambient fluid by forced convection and radiation near the base. Fig.(4-2-3)-(4-2-4) show that the local heat transfer coefficient and local heat flux of the fin with radiation effect are always higher than those of the fin without radiation effect. The local heat transfer coefficient and local heat-flux variations presented in Fig.(4-2-3)-(4-2-4) also show a distinct difference between the results of the simple model (h* is constant

and $q^r=0$) and the special case in this paper ($q^r=0$).

Fig. (4-2-5) presents fin temperature distributions for forced convection flow with radiation effect. In the figure. It is shown that the fin temperature decreases monotonically from the root to tip. The figure also shows that the larger values of N_c give rise to larger fin temperature variations and the fin temperature without radiation effect is always higher than that of the fin with radiation. It is clear from the figure that the results of simple model predicts a smaller base-to-tip temperature variation than actually prevails.

Remark

The analysis of present paper has yielded the results of physical fin for forced convection flow with radiation effect under the optically thick limit approximation. The agreement of the results for special case (i.e. fin without radiation effect) with [16] is truly remarkable. In order to solve simultaneously the coupled fin conduction equation and the fluid convection flow with radiation effect, a very simple and efficient implicit finite difference method is employed here.

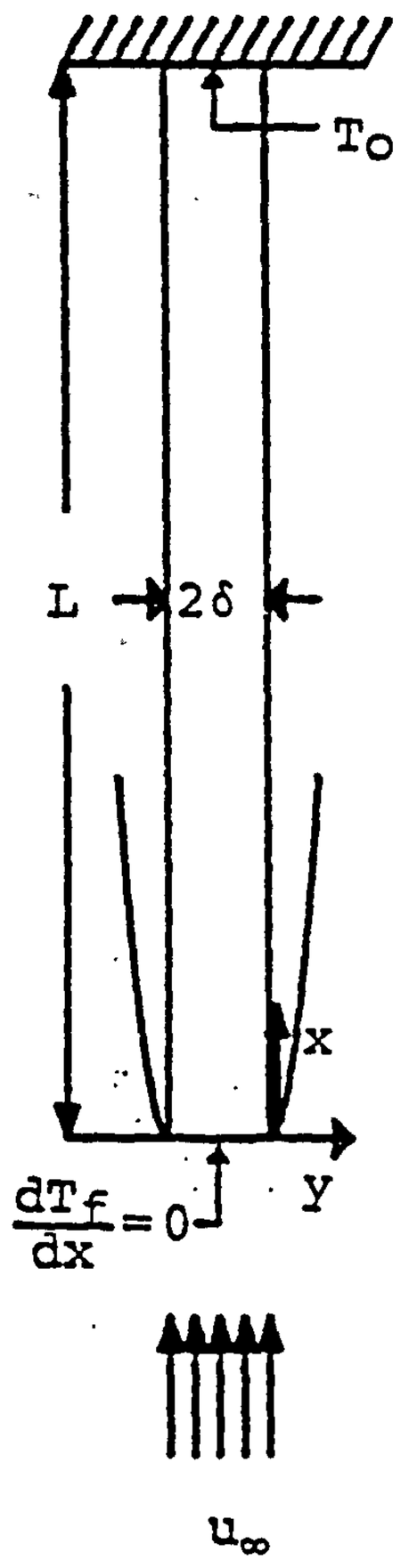

Fig.4-2-1 Physical model and coordinates of the vertical plate fin.

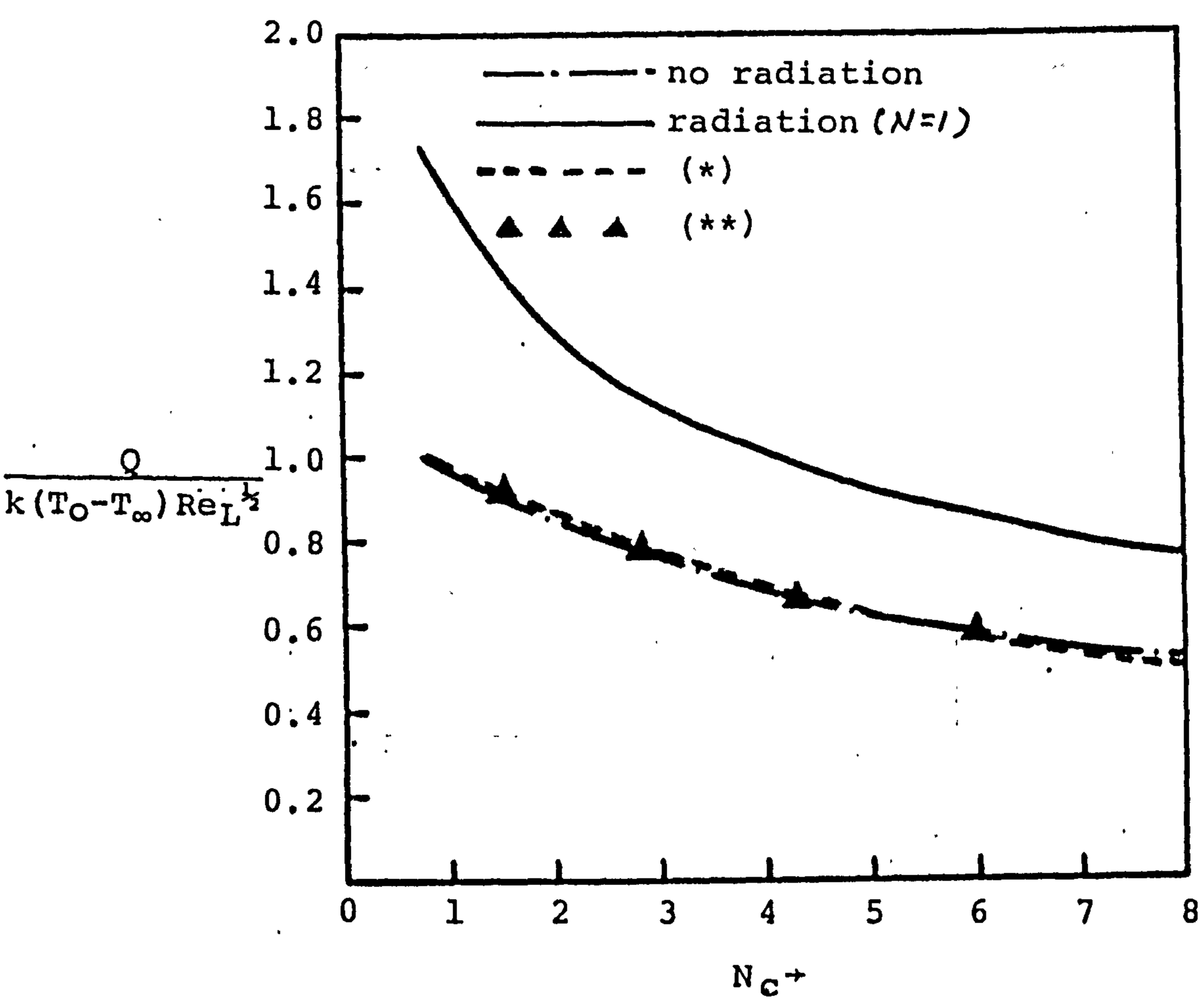

Fig.4-2-2 Total heat transfer rate.

* :simple model
**:Sparrow [16]

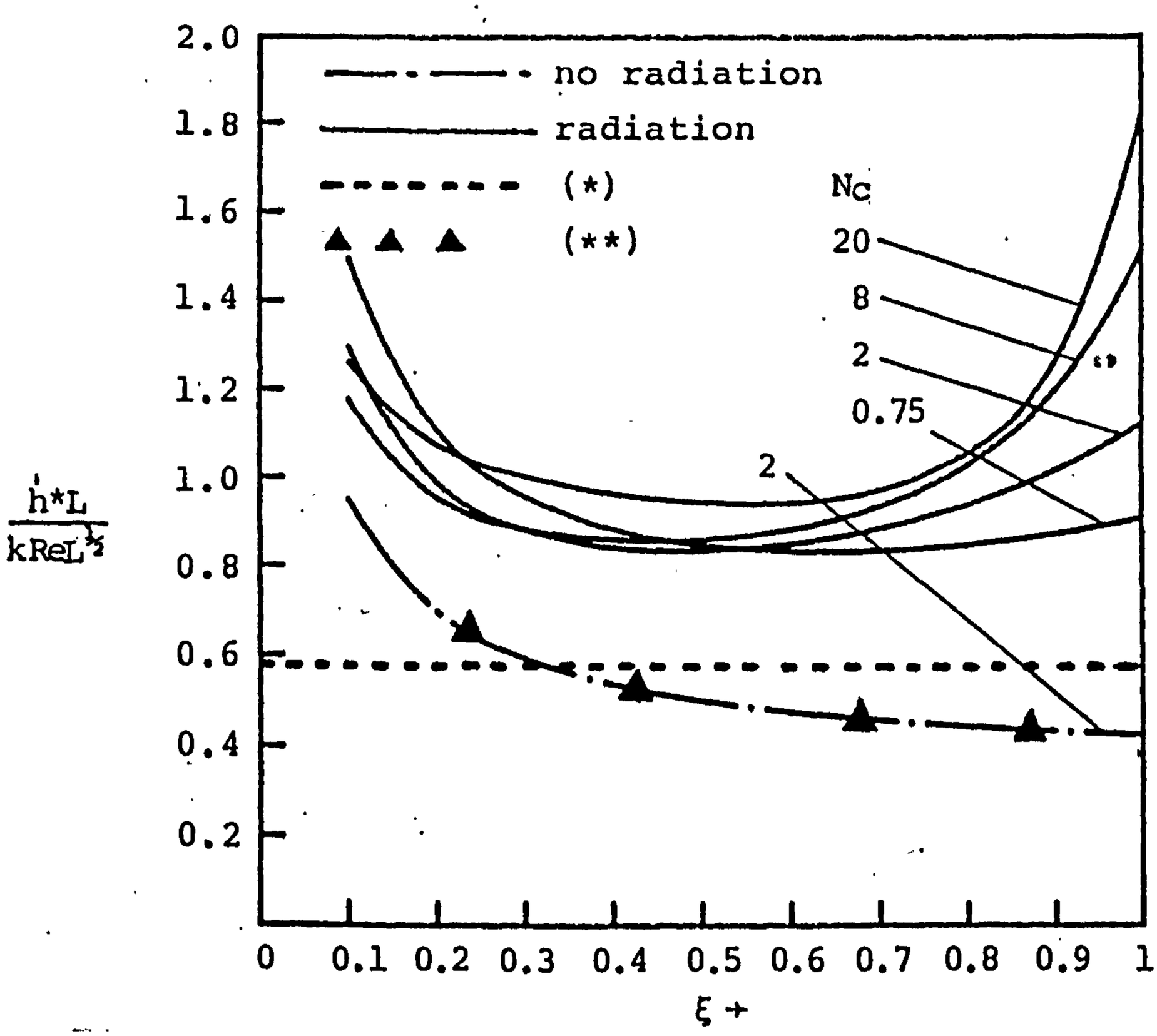

Fig.4-2-3 The modified heat transfer coefficients along the plate fin for N=1, C_T=0.5, Pr=0.7 and various values of Nc.

* :simple model
**:Sparrow [16]

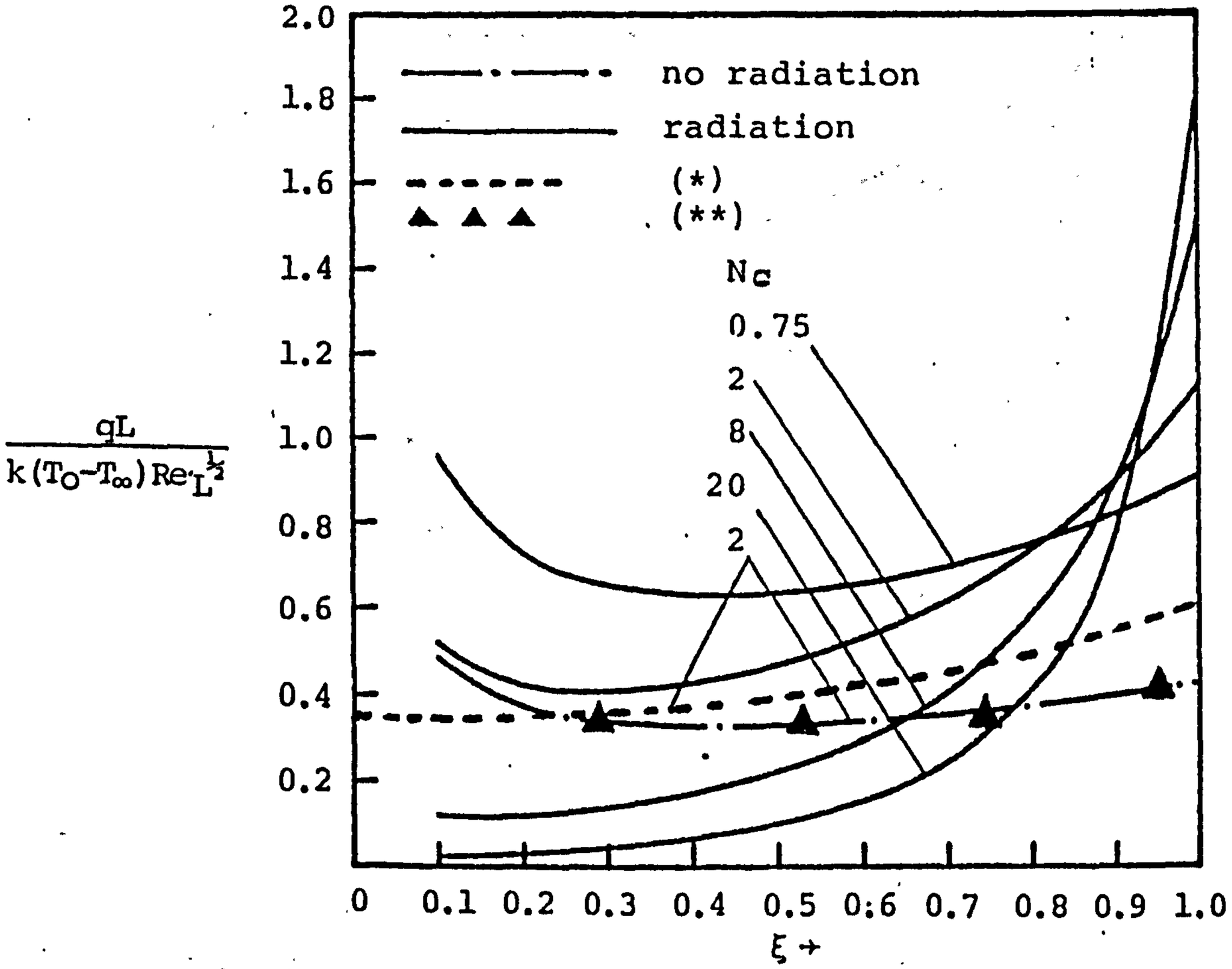

Fig.4-2-4 The local heat fluxes along the plate fin for N=1, C_T=0.5, Pr=0.7 and various values of Nc.

* :Simple model
**:Sparrow [16]

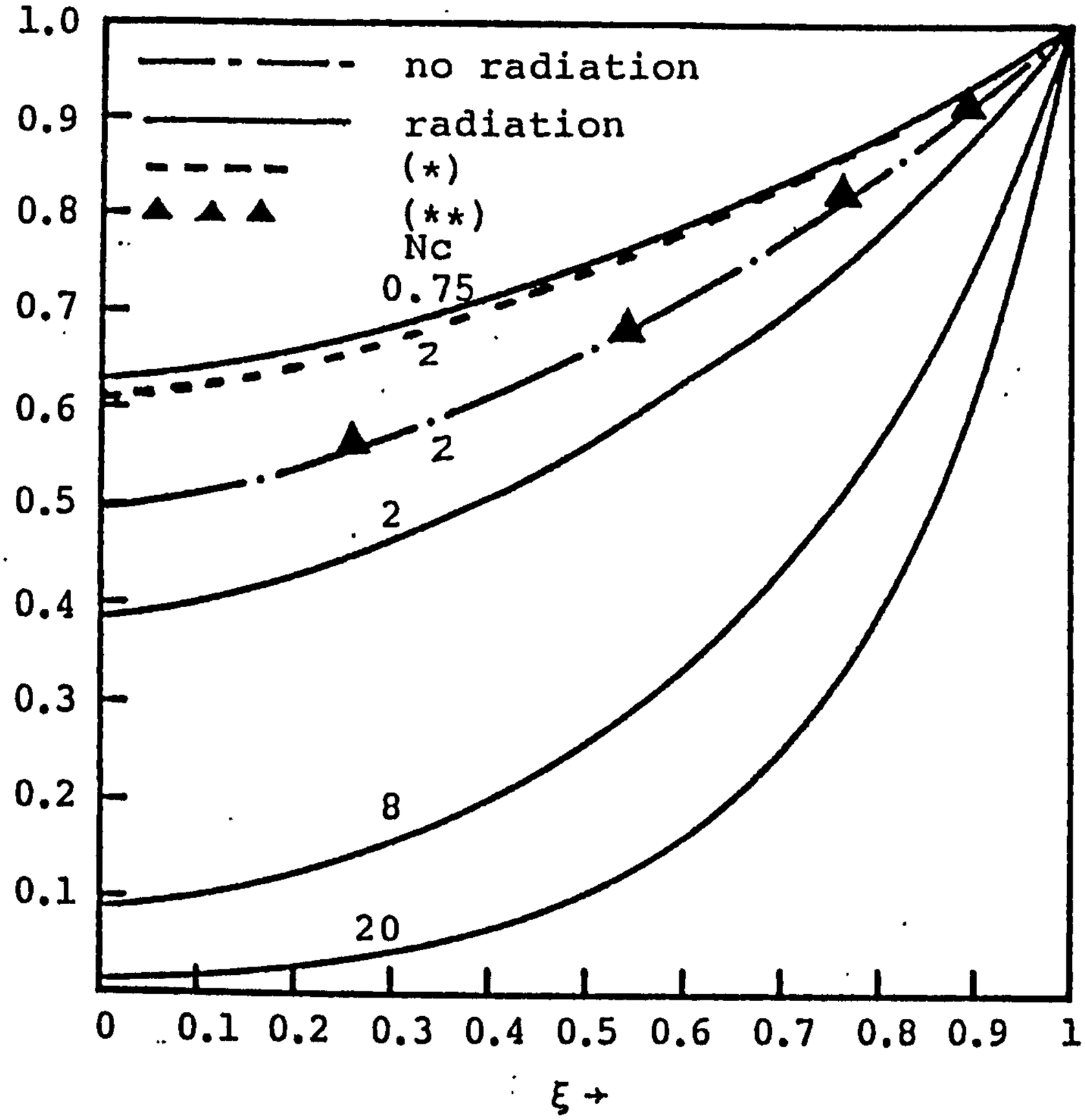

Fig.4-2-5 The temperature distributions along the plate fin for N=1, C_T=0.5 and various values of Nc.

* :Simple model

**:Sparrow [16]

IV-3 Radiative Effect on The Vertical Plate Fin in Conjugated Mixed Convection-Conduction Flow with Temperature Dependent Viscosity

In the conventional heat transfer analysis of fins, it is standard practice to assume that the heat transfer coefficient for convection at the fin surfaces is uniform all along the fin. There is, however, evidence in the literature demostrating that the heat transfer coefficient can experience substantial variations along the fin surfaces [21][22]. These variations may be caused by nonuniformities in the temperature fields in the fluid adjacent to the fin. Sparrow et al [15][16] have studied this problem for vertical plate fin, and conclude that the conventional fin model based on a uniform input value of the heat transfer coefficient yields very good predictions for the overall heat transfer rate of the fin, but the local predictions can be substantially in error for forced convection flow. Section 4-2 has looked at the problem of radiative effect on the conjugated forced convection-conduction analysis of heat transfer in a plate fin by using an implicit finite method due to Cebeci and Bradshaw, and indicates that the agreement of the special case (fin without radiation) with [16] is very remarkable. The stability problem for the natural convective boundary layer flow with temperature dependent viscosity over a vertical flat plate has been investigated by J.Y. Jang [38].

The object of this section is concerned with a plate fin with transfer heat to a surrounding fluid by mixed convection

and radiation. The present section extends the work done in section IV-2, by allowing for variations of the viscosity with temperature. The modified local heat transfer coefficient along the fin is not prescribed but is solved in advance from the boundary layer flow. Therefore, the modified local heat transfer coefficient is determined by a highly coupled interaction between the fin conduction and the fluid thermal boundary layer flow.

The fin temperature distribution, which is not known a priori, serves as a thermal boundary condition for the boundary equations. The solutions of the modified local heat transfer coefficient along the fin surface from the boundary layer equations are substituting into the fin energy equation as known, then repeatly search for the new fin surface temperature. This new temperature distribution is then imposed as the surface boundary condition for the boundary layer equations, the solution of which is used to evaluate an updated $\hat{h}^*$ and so on until the maximum difference of temperature between the successive cycles is less than 10^{-3}.

The physical model and coordinates system to be analyzed here are illustrated in Fig.(4-3-1). A vertical plate fin is of length L and thickness 2δ which is extended from a wall at temperature T_o and situated in a uniform free stream having temperature T_∞ and velocity u_∞. As radiative effect is considered, the optically thick limit approximation for the radiative heat flux is assumed and the tip of the fin is insulated.

Analysis

Consider now a vertical heated fin which is alighed parallel to a uniform free stream u_∞. Let x and y denote, respectively, the streamwise and normal coordinates. Under the assumption of Boussinesq's approximation for mixed forced and free convective flow, constant fluid properities and negligible viscous dissipation, the equations expressing conservation of mass, momentum and energy are shown as follows.

$$\frac{\partial u}{\partial x} + \frac{\partial v}{\partial y} = 0 \qquad (4\text{-}3\text{-}1)$$

$$u\frac{\partial u}{\partial x} + v\frac{\partial u}{\partial y} = \frac{\partial}{\partial y}\left(\nu\frac{\partial u}{\partial y}\right) + g\beta(T-T_\infty) \qquad (4\text{-}3\text{-}2)$$

$$u\frac{\partial T}{\partial x} + v\frac{\partial T}{\partial y} = \alpha\frac{\partial^2 T}{\partial y^2} - \frac{1}{\rho C_p}\frac{\partial q^r}{\partial y} \qquad (4\text{-}3\text{-}3)$$

subjected to the following boundary conditions:

$$\left.\begin{aligned} u = v = o, \quad T = T_w(x) \quad , \quad & \text{at} \quad y = 0 \\ u = u_\infty \quad , \quad T = T_\infty \quad , \quad & \text{as} \quad y \to \infty \end{aligned}\right\} \qquad (4\text{-}3\text{-}4)$$

where q^r is the net radiative heat flux and the other standard symbols are defined in the nomenclature.

The problem does not admit similarity solutions. The nonsimilarity arises from the variations of the surface temperature, $T_w(x)$, which is undetermined. It is advantageous to introduce pseudo-similarity variables (ξ, η) with a reduced stream function $f(\xi,\eta)$ and a dimensionless temperature $\theta(\xi,\eta)$ as follows:

$$\xi = x/L \qquad \eta = \left(\frac{y}{L}\right) Re_{L\infty}^{1/2} / \xi^{1/2}$$

$$f(\xi,\eta)=\psi(x,y)/(u_\infty L\xi\nu_\infty)^{1/2}, \qquad \theta = (T-T_\infty)/(T_o-T_\infty) \qquad \} \quad (4\text{-}3\text{-}5)$$

where the stream function satisfies the contiunity equation (4-3-1) with $u=\partial\psi/\partial y$ and $v=-\partial\psi/\partial x$. The motivation for employing the transformation variables is that the transformed conservation equations are much less dependent on the coordinate systems than are the original conservation equations.

The kinematic viscosity, ν , is assumed to vary with temperature according to a general form $\nu=\nu_\infty\, w(\theta)$, where ν_∞ is the absolute viscosity evaluated at the temperature of surrounding, and therefore $W(0)=1$. We can take the first two terms in a Taylor series expansion of $W(\theta)$ about $\theta=0$ as

$$W(\theta)= 1+\left(\frac{dW}{d\theta}\right)\Big|_{\theta=0} (\theta-0) + \left(\frac{1}{2!}\frac{d^2W}{d\theta^2}\right)\Big|_{\theta=0} (\theta-0)^2=1+a_1\theta+a_2\theta^2 \qquad (4\text{-}3\text{-}6)$$

When the transformation (4-3-5) is applied to equations (4-3-2)-(4-3-4) and (4-3-6), and the optically thick limit approximation for q^r is assumed,

i.e. $$q^r = -\frac{4\sigma}{3\beta^*}\frac{\partial T^4}{\partial y}$$

the governing system becomes:

$$(1+a_1\theta+a_2\theta^2)f''' + \frac{1}{2}ff'' + \xi\Omega\theta = \xi\left(f'\frac{\partial f'}{\partial\xi} - f''\frac{\partial f}{\partial\xi}\right) \qquad (4\text{-}3\text{-}7)$$

$$Pr_\infty^{-1}\theta'' + \frac{1}{2}f\theta' + \frac{4[(\theta+C_T)^3\theta']'}{3Pr_\infty N} = \xi\left(f'\frac{\partial\theta}{\partial\xi} - \theta'\frac{\partial f}{\partial\xi}\right) \qquad (4\text{-}3\text{-}8)$$

$$\left.\begin{aligned} f=f'=0, \quad \theta=(T_w(x)-T_\infty)/(T_o-T_\infty) &\quad , \text{ at } \eta=0 \\ f' =1, \quad \theta=0 &\quad , \text{ as } \eta\to\infty \end{aligned}\right\} \qquad (4\text{-}3\text{-}9)$$

where

$$C_T = T_\infty/(T_o-T_\infty), \qquad N = \frac{k\beta^*}{4\sigma(T_o-T\infty)^3}$$

Pr is the Prandtl number evaluated at the temperature of surrounding, σ is the Stefan-Boltzmann constant, β^* is the extinction coefficient, the primes denote partial differentiation with respect to η and Ω is the buoyancy force parameter defined as

$$\Omega = Gr_{L\infty}/Re^2_{L\infty} \qquad (4\text{-}3\text{-}10)$$

in which

$$Gr_{L\infty} = g\beta(T_o-T_\infty)L^3/\nu^2_\infty$$

and

$$Re_{L\infty} = u_\infty L/\nu_\infty$$

The formulation of the present analysis for the vertical fin in conjugated mixed convection-conduction flow involves the energy conservation equation for the fin and the boundary layer equations for the fluid. Considering the very thin fin, it is reasonable to assumed a one-dimensional model for the fin temperature distributions along the x-direction. The fin conservation energy equation can be written as

$$\frac{d^2T_f}{dx^2} = \frac{h^*(x)}{k_f\delta}\ (T_f-T_\infty) \qquad (4\text{-}3\text{-}11)$$

where T_f is the fin temperature, k_f is the fin thermal conductivity and δ is the half thickness of the fin. In this equation $h^*(x)$ can be regarded as known for previous iteration cycle. Employing dimensionless variables for the fin

$$\xi = x/L, \quad \theta_f = (T_f-T_\infty)/(T_o-T_\infty) \qquad (4\text{-}3\text{-}12)$$

with boundary conditions of the base root temperature T_o (at ξ =1) and adiabatic tip (at ξ=0). Of particular interest is the thermal coupling between the fin and the thermal boundary layer of fluid. The basic coupling is expressed by the requirement that the fin and fluid temperatures and local heat fluxes be continuous at the plate-fluid interface at all x-positions.

$$\text{i.e.} \qquad T_w = T_f, \quad -k\frac{\partial T}{\partial y} + q^r = h^*(T_f - T_\infty), \quad \text{at } y = 0 \qquad (4\text{-}3\text{-}13)$$

Substituting dimensionless variables into equation (4-3-13), we get

$$\theta_w = \theta_f, \quad h^* = kRe_{L\infty}^{\frac{1}{2}}\,\hat{h}^*/L\,, \quad \text{at } \eta = 0 \qquad (4\text{-}3\text{-}14)$$

The dimensionless heat conduction equation can be obtained by substituting equation (4-3-12) into equation (4-3-11)

$$\frac{d^2\theta_f}{d\xi^2} = N_c\hat{h}^*\theta_f \qquad (4\text{-}3\text{-}15)$$

where N_c is the conjugated convection-conduction parameter (N_c=$kLRe_{L\infty}^{\frac{1}{2}}/k_f\delta$). The quantity $\hat{h}^*$ is a dimensionless form of the mixed convective heat transfer coefficient with radiative effect that is current at a given cycle of the iteration.

$$\hat{h}^* = -(1+\frac{4(\theta+C_T)^3}{3N})\frac{\partial\theta}{\partial\eta}/(\theta_f\,\xi^{\frac{1}{2}}) \quad , \quad \text{at} \quad \eta = 0 \quad (4\text{-}3\text{-}16)$$

Numerical Procedure

The solution begins by solving the mixed convective boundary layer problem for a vertical plate fin with guessed tempe-

rature along the fin surface. The dimensionless heat transfer coefficient $\hat{h}^*$ determined from equation (4-3-16) are then used as input to the fin heat conduction equation (4-3-15). With Nc prescribed, the differential equation (4-3-15) is then solved to yield θ_f. To begin the next cycle of the iterative procedure, the just-determined θ_f is imposed as the thermal boundary condition for the mixed convective boundary layer equations of Newtonian fluid; the solution to which is used as input to the fin heat conduction equation. This procedure of alternatively solving the boundary layer problem and the fin conduction problem was continued until convergence was attained.

The two systems of partial differential equations (4-3-7) -(4-3-8) are coupled. In the present study, these equations were solved by an accurate implicit finite-difference technique due to Cebeci and Bradshaw [19]. To begin with, the partial differential equations (4-3-7)-(4-3-8) are first converted into a system of first order equations which are then expressed in finite-difference form by approximating the functions and their first derivatives in terms of centered difference and averaged at midpoints of the net segment in the (ξ,η) coordinates. The resulting nonlinear finite-difference equations are then solved by Newton's iterative method.

The boundary layer solutions were obtained by a marching procedure, starting at the leading edge and the grids were divided into 45 points in the streamwise direction. There was a denser concentration of points near the leading edge to

accommodate the initial rapid growth of the boundary layer. We use 61 grid points in the cross-stream direction.

The conduction equation was solved by using the direct inverse matrix method. The Fin equation was also divided into 45 grid points and expressed in finite-difference form. To ensure high accuracy, a nonuniform grid points were employed. For small ξ , a finer ξ subdivision was needed for the boundary layer solution.

Results and Discussion

Numerical calculations for a vertical plate fin in the fluid having Pr_∞=0.7 are performed for the following case: heated plate fin with T_o=900°K and T_∞=300°K. By curve-fitting procedure, we can obtain a_1=3, a_2=2 (viscosity variation parameters) from experimental data.

The overall rate of heat transfer from the fin can be obtained from the wall into the fin base or from the integrating heat transfer over the fin surface. The corresponding overall heat transfer rate of these two methods are found to be in agreement. They can be expressed in dimensionless form as follows.

$$\frac{Q}{k(T_o-T\infty)Re_{L\infty}^{1/2}} = 2\int_0^1 (-\frac{\partial\theta}{\partial\eta})\left[1+\frac{4(\theta+C_T)^3}{3N}\right]/\xi^{1/2}\, d\xi \ , \text{ at } \eta = 0 \qquad (4\text{-}3\text{-}17)$$

or

$$\frac{Q}{k(T_o-T_\infty)Re_{L\infty}^{1/2}} = \frac{2d\theta_f}{N_c d\xi}\bigg|_{\xi=1} \qquad (4\text{-}3\text{-}18)$$

The results of the overall rate of heat transfer from the fin are shown in Fig.(4-3-2) over the values of buoyancy force parameters Ω =0,1,3 and conjugated convection-conduction parameters N_c=0.25, 0.75,2 and 3. The decrease of N_c indicates short fin length, L, great fin conductance, $k_f\delta$, and low convctive coefficients (low k and $Re_{L\infty}$). In Fig.(4-3-2) shows that the overall heat transfer rate of the heated fin in a Newtonian fluid with temperature dependent viscosity is lower than that with constant viscosity (ν_∞). Fig.(4-3-2) also shows that an increase in the values of N_c yields a decrease in the values of the overall heat transfer rate of the fin, and an increasing Ω give rise to an increasing overall heat transfer rate of fin.

The distributions of the modified local heat transfer coefficient $\hat{h}^*$ for mixed convection and radiation along the fin with different N_c and fixed Ω are shown in Fig.(4-3-3)-(4-3-4). The modified heat transfer coefficient can be expressed as follow:

$$\hat{h}^* = -\left[1+\frac{4(\theta+C_T)^3}{3N}\right]\frac{\partial\theta}{\partial\eta}/(\theta_f\xi^{1/2}), \quad \text{at } \eta=0 \qquad (4\text{-}3\text{-}19)$$

Although the $\hat{h}^*$ without radiative effect [16] decreased monotonically in the streamwise direction, but the $\hat{h}^*$ computed in this paper did not always decrease monotonically in the streamwise direction when the radiative parameters are fixed. The coefficient decreased at first, attained a minimum, and then increased with increasing downstream distance. The phenomenon of this behavior is attributed to an enhanced radiative heat flux and buoyancy force associated with an increase in the

wall-to-fluid temperature difference along the streamwise direction.

The distributions of the dimensionless local heat flux at the fin surface are presented in Fig.(4-3-5)-(4-3-6) for different N_c and fixed buoyancy force parameter. The local heat flux can be taken as

$$\frac{qL}{k(T_o-T_\infty)Re_{L\infty}^{1/2}} = -\left[1+\frac{4(\theta+C_T)^3}{3N}\right]\frac{\partial\theta}{\partial\eta}/\xi^{1/2}, \quad \text{at } \eta = 0 \qquad (4\text{-}3\text{-}20)$$

In those figures, we find that for fixed buoyancy force parameter the total heat transfer rate from the fin surface is increased as N_c decreased, which agrees with the prediction in Fig.(4-3-2)

Fig.(4-3-3)-(4-3-6) show the values of the local flux and modified heat transfer coefficient increased with increasing Ω. It is observed from Fig.(4-3-3)-(4-3-6) that the local heat transfer coefficient and the local heat flux of the heated fin in the fluid with temperature dependent viscosity are lower than those in the fluid with constant viscosity (ν_∞).

Fig.(4-3-7)-(4-3-8) present the temperature distributions along the fin surface. In these figures, we find that the larger values of N_c and Ω give rise to greater fin temperature variations. The two figures also show that the temperature distributions of the heated fin in the fluid with temperature dependent viscosity has a smaller variations along the streamwise direction than that in the fluid with constant viscosity (ν_∞).

Remark

The analysis of this paper has yielded the results of physical fin for mixed convection flow with temperature dependent viscosity. The radiative effect on the fin is considered and the optically thick limit approximation for the radiative heat flux q^r is assumed. In order to solve the conjugated mixed convection-conduction problem, a very simple and efficient "Box" scheme is employed here.

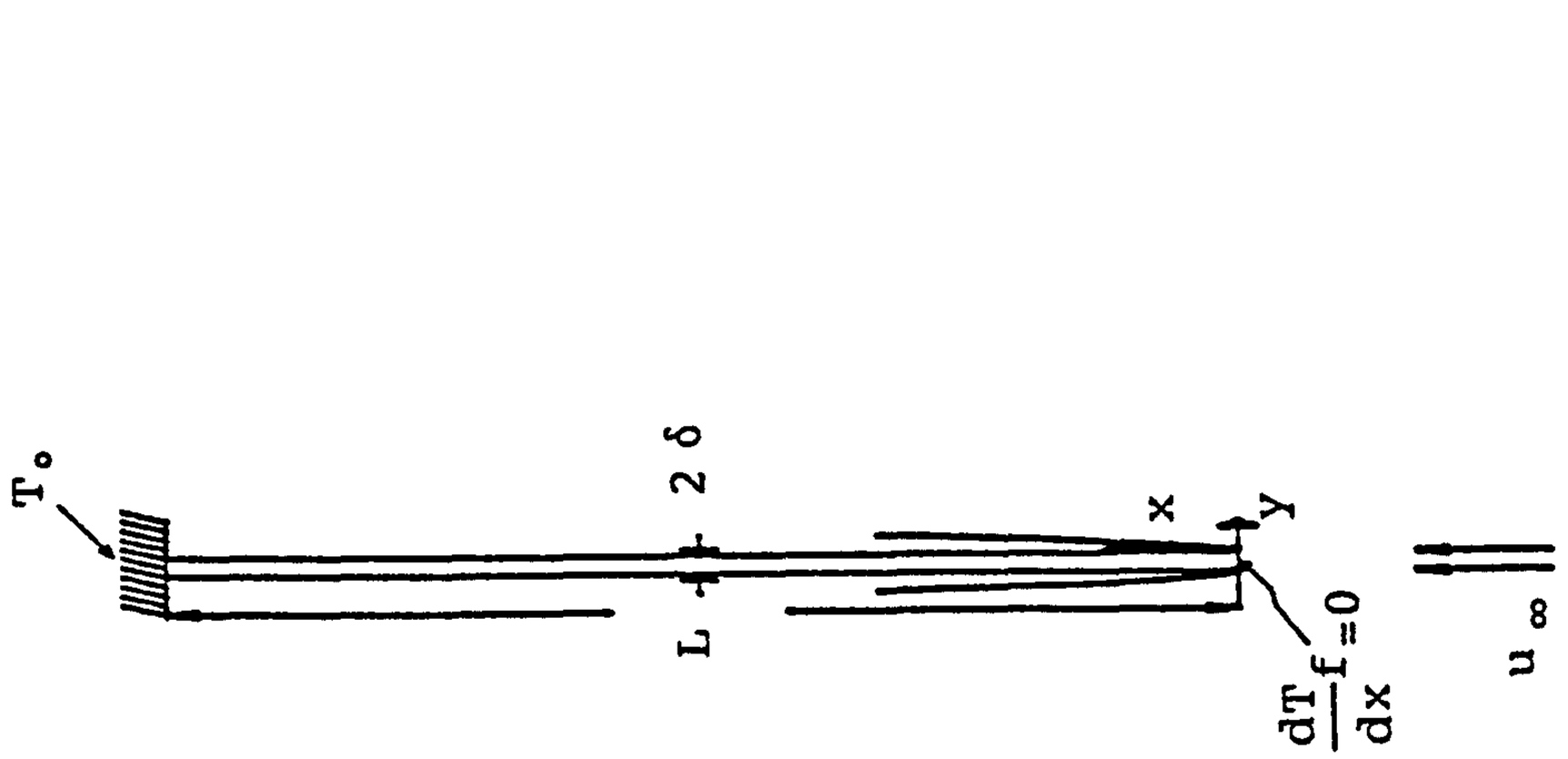

Fig.4-3-1 Coordinate system.

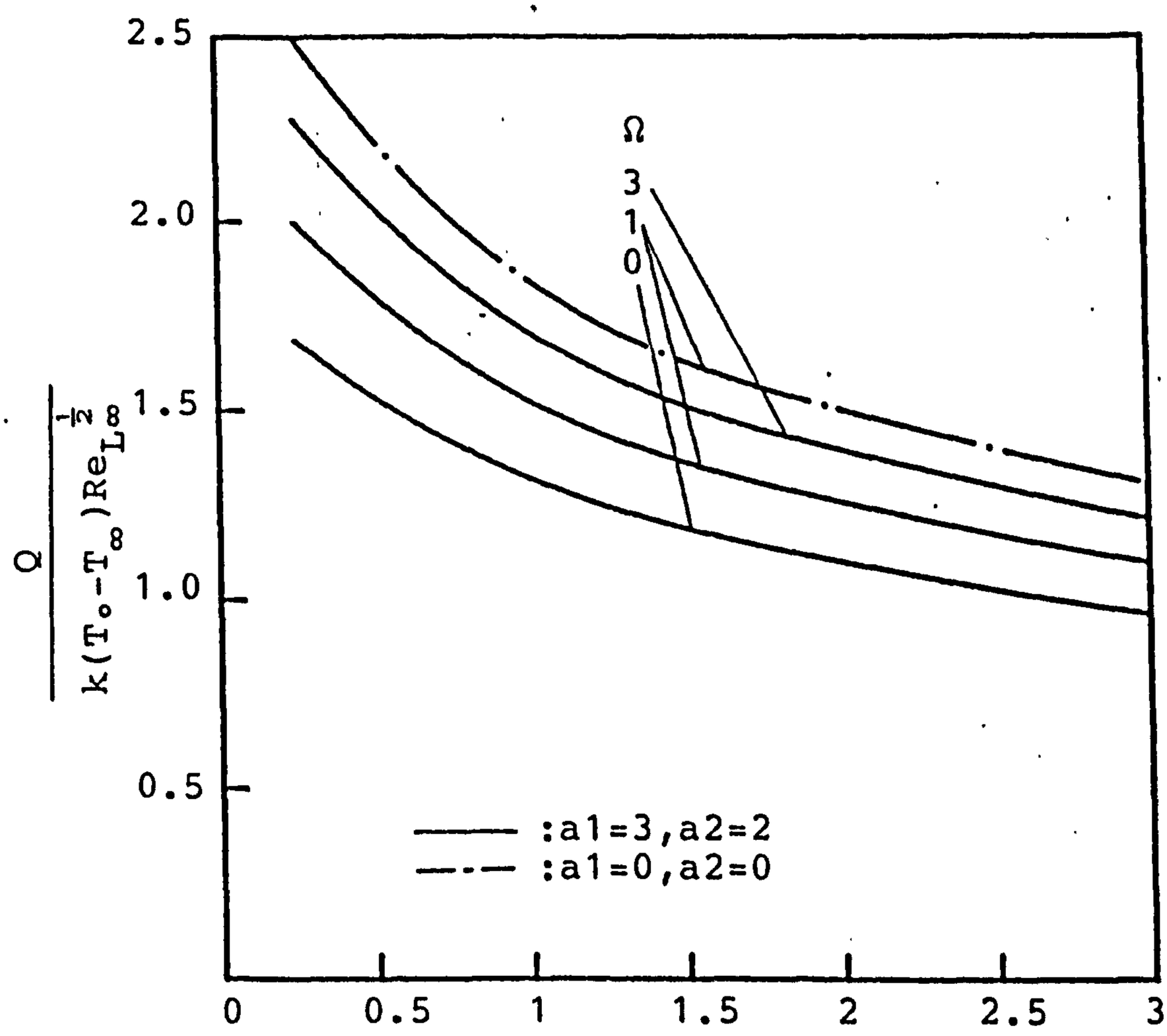

Fig.4-3-2 Total heat transfer rate of the fin for Pr_∞=0.7,N=1 and C_T=0.5

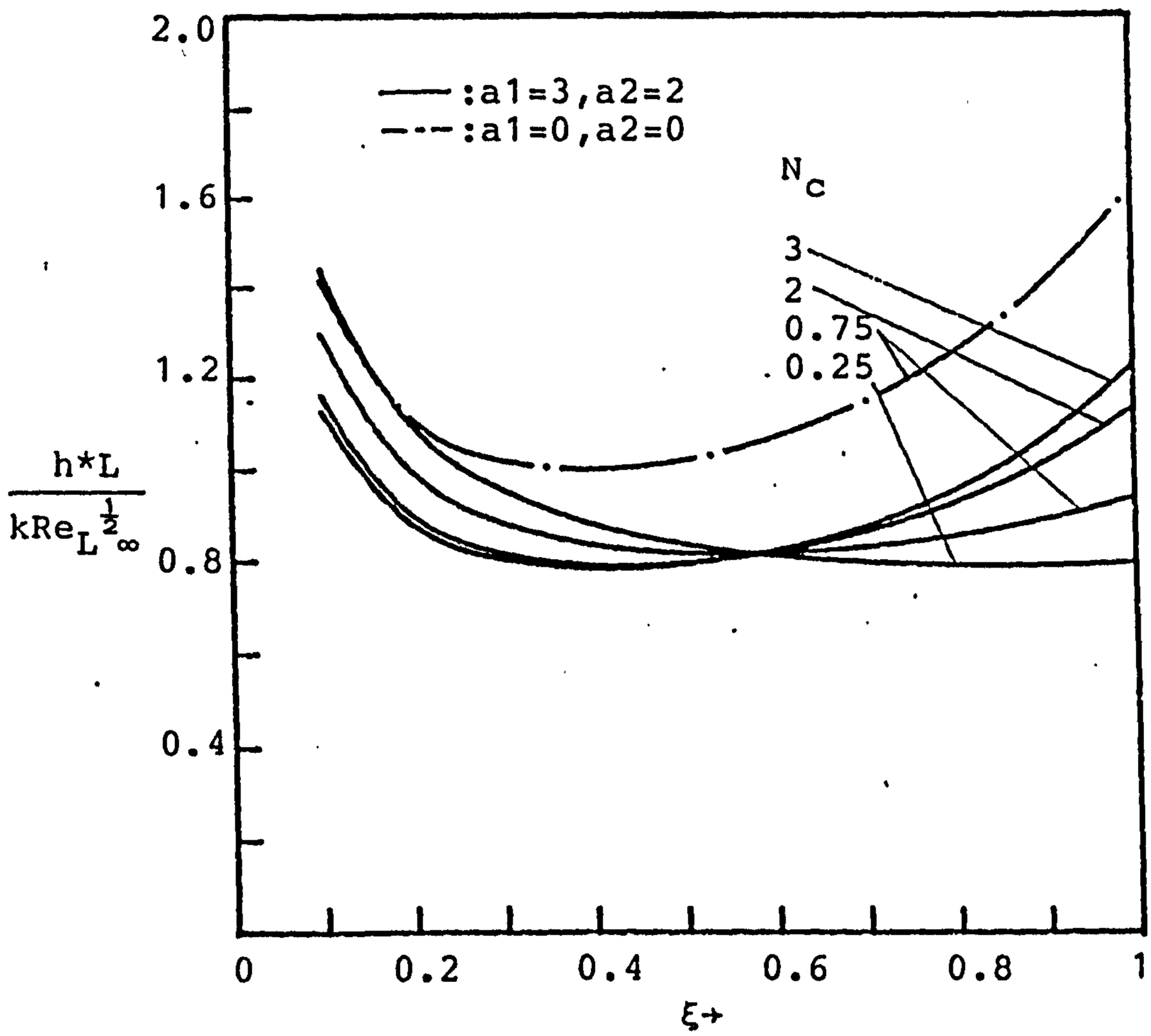

Fig.4-3-3 The modified local heat transfer coefficients of the fin for Pr_∞=0.7,N=1 ,C_T=0.5 and Ω=1.

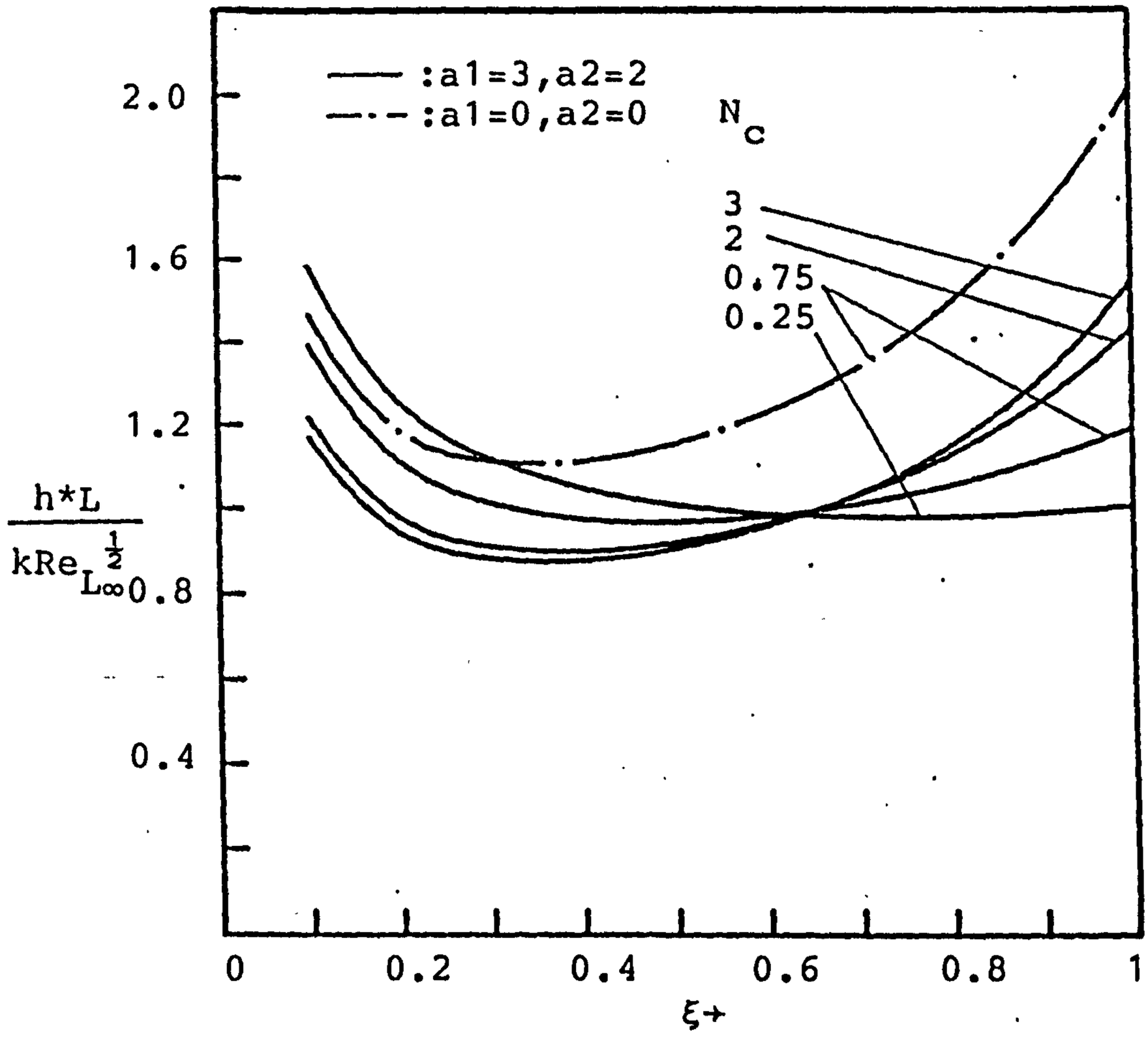

Fig.4-3-4 The modified local heat transfer coefficients of the fin for Pr_∞=0.7,N=1 ,C_T=0.5 and Ω=3.

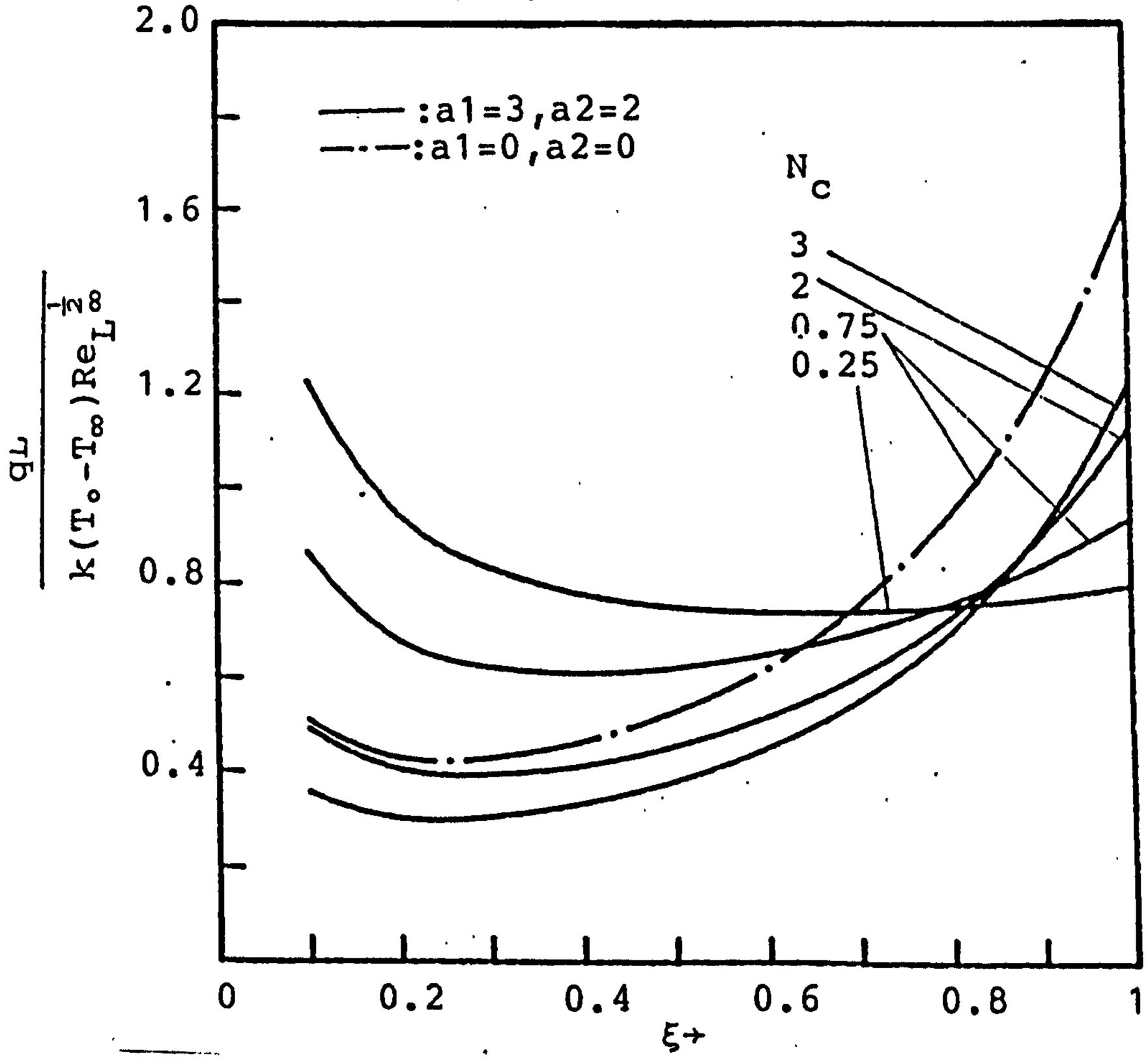

Fig.4-3-5 The local heat flux of the fin for $Pr_\infty=0.7, N=1, C_T=0.5$ and $\Omega=1$.

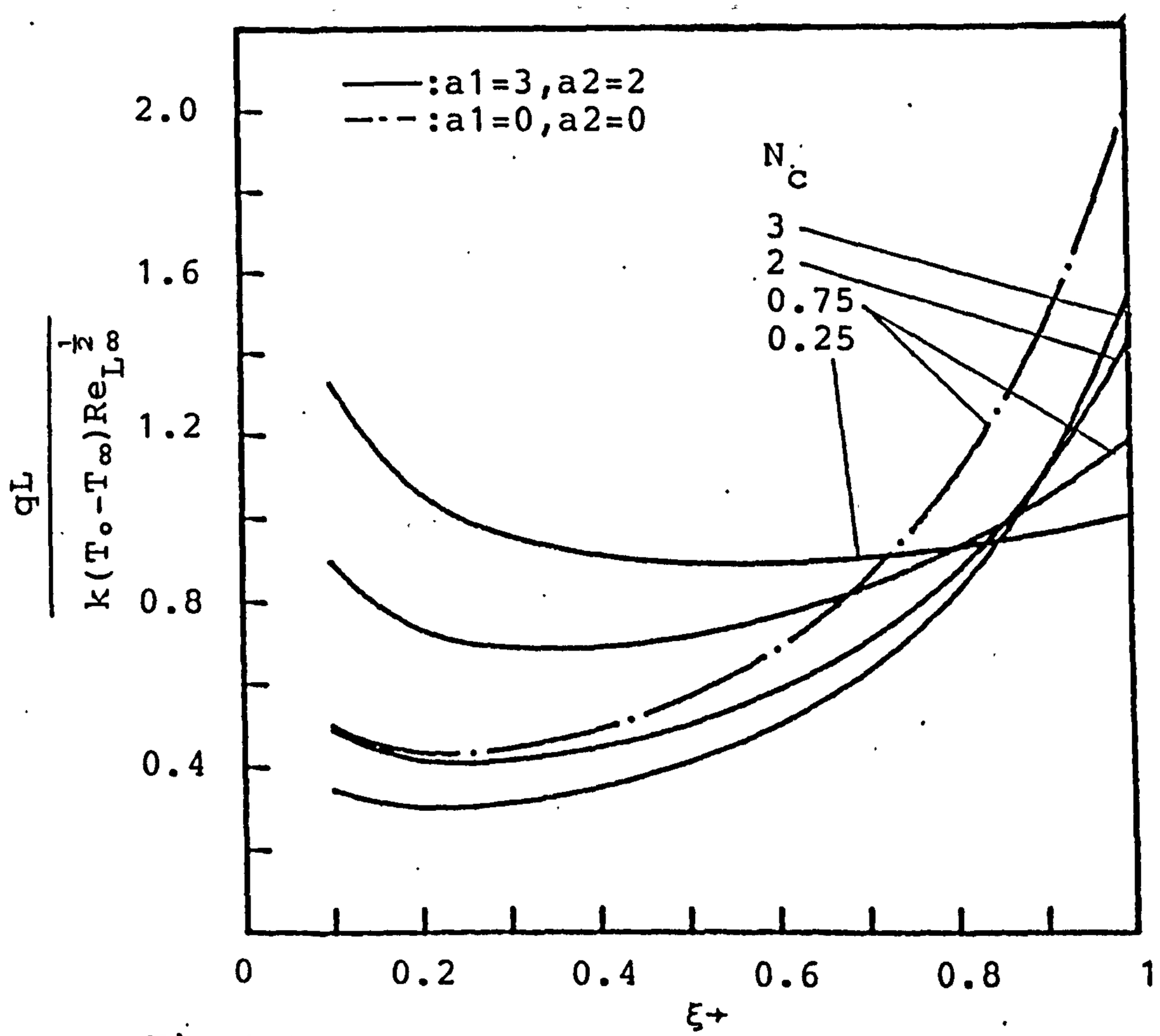

Fig.4-3-6 The local heat flux of the fin for $Pr_\infty=0.7, N=1, C_T=0.5$ and $\Omega=3$.

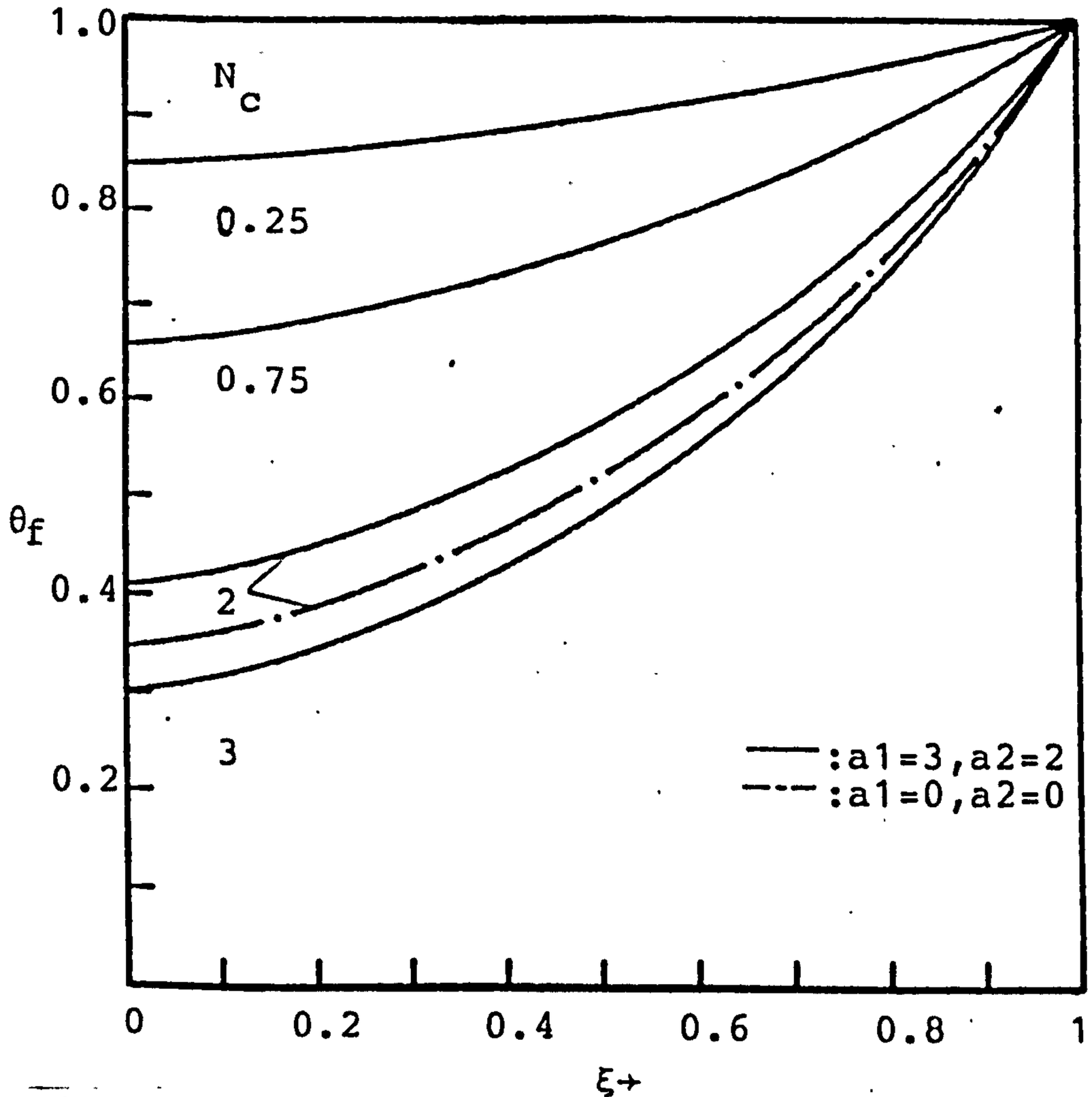

Fig.4-3-7 The temperature distributions of the fin for Pr_∞=0.7,N=1,C_T=0.5 and Ω=1.

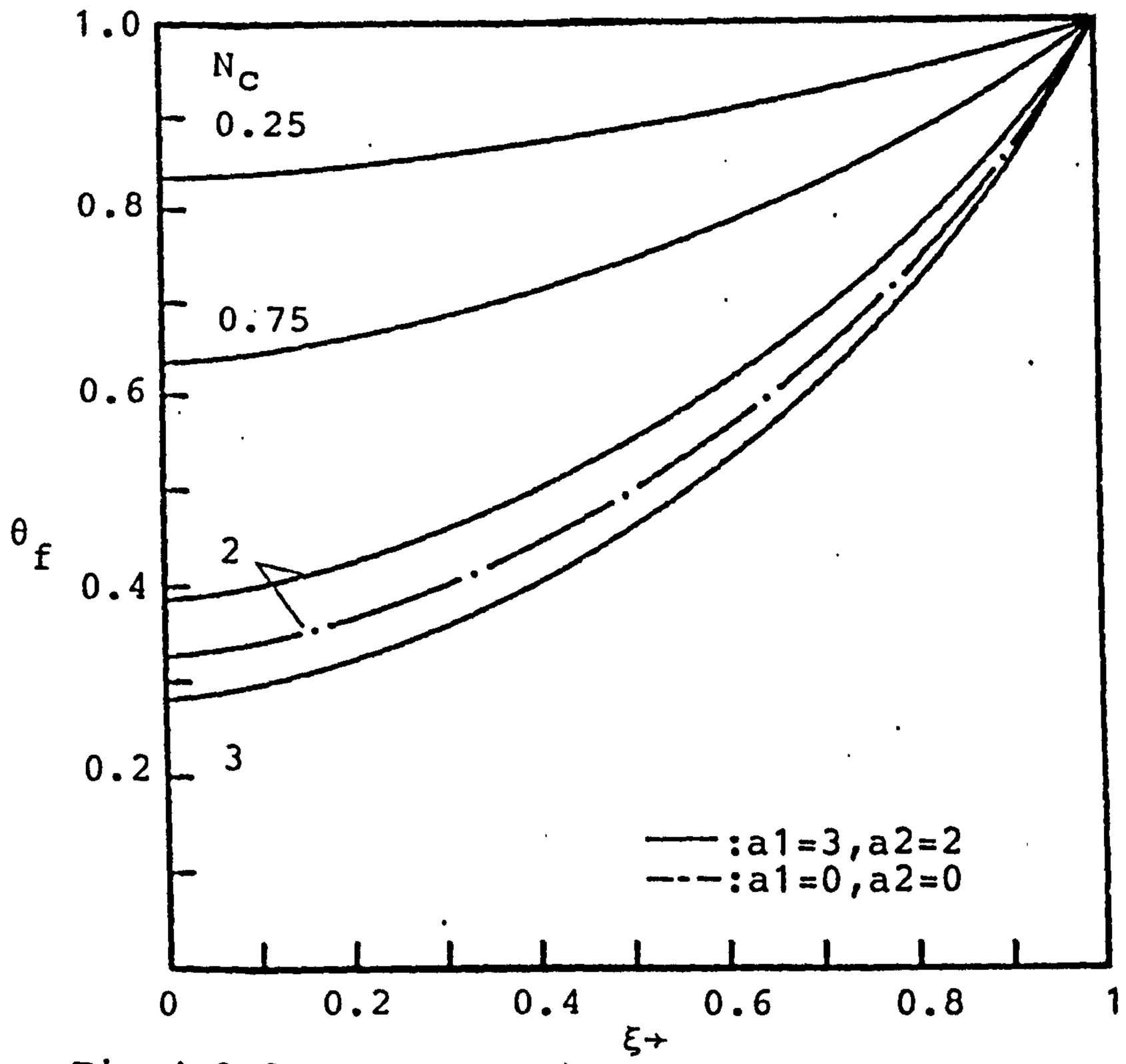

Fig.4-3-8 The temperature distributions of the fin for Pr_∞=0.7,N=1,C_T=0.5 and Ω=3.

V. STEADY LAMINAR FLOW CONVECTION-CONDUCTION CASES IN A VERTICAL CIRCULAR PIN

Extension of the surface in the form of a pin is commonly used to enhance the heat transfer rate between a solid surface and an adjoining fluid. The temperature gradients within the pin sustains heat transfer not only by internal heat conduction but also through energy transfer by convection from the surface. For a thin pin, the temperature changing in the longitudinal direction can be considered to be much larger than those in the transverse direction. Hence, it is reasonable to assume a one-dimensional model for the heat conduction equation.

In the conventional heat transfer analysis of fins, it is standard practice to assume that the heat transfer coefficient for convection at the fin surfaces is uniform all along the fin. However, the heat transfer coefficient can experience substantial variations along the fin surfaces. These variations may be caused by nonuniformities in the temperature field in the fluid adjacent to the fin. Sparrow et al [15][16] have looked at this problem for vertical plate fin, and conclude that the conventional fin model based on a uniform input value of the heat transfer coefficient yields very good predictions for the overall heat transfer rate of the fin, but the local predictions can be substantially in error for forced convection flow.

Recently, M. J. Huang and C. K. Chen [39,42] have studied the problem of vertical circular pin with conjugated forced and mixed convection-conduction flow and concluded, based on their

numerical analysis, that the overall heat transfer rate increased with decreasing radius of the cylinder pin.

The analysis of this chapter is for a vertical cylinder pin with a nonuniform temperature distribution which is strongly affected by the heat transfer coefficient, the heat transfer coefficient is decided to the ambient fluid flow. The radiative effect on the cylinder pin is considered and the optically thick limit approximation for the radiative heat flux is assumed. Besides, the Newtonian fluid adjacent to the cylinder pin is extended to include the variation of viscosity with temperature. Hence, in order to determine the temperature distributions of the pin, it must be coupled with the thermal boundary layer flow.

The pin temperature distribution, which is not known a priori, serves as a thermal boundary condition for the boundary layer equations. The solutions of the modified local heat transfer coefficient along the pin surface from the boundary layer equations are resubstituting into the pin energy equation as known, then repeatly search for the new pin surface temperature. This new temperature distribution is then imposed as the surface boundary condition for the boundary layer equations, the solution of which is used to evaluate an updated $\hat{h}^*$ and so on until the maximum difference of temperature between the successive cycles is less than 10^{-3}.

V-1 Radiative Effect on The Vertical Circular Pin in Conjugated Natural Convection-Conduction Flow With Temperature Dependent Viscosity

The analysis of this section is for a vertical cylinder pin with a nonuniform temperature distribution which is strongly affected by the heat transfer coefficient, the heat transfer coefficient is decided to the ambient fluid flow.

The radiative effect on the conjugated natural convection-conduction flow is considered and the kinematic viscosity of the fluid is temperature dependent. The conservation equation of the laminar boundary layer and the energy equation of the pin are first transformed into a nondimensional form and their solutions are then simultaneously solved by an efficient implicit finite difference method. To get a physical insight of the problem, the results are computed for Pr_∞=0.7 (air), a_1=3, a_2=2 (viscosity variation parameters), N=1 (conduction to radiation parameter), C_T=0.5 (temperature difference parameter) over a conjugated convection-conduction parameter of N_c=0.5, 1, 2 and 3 and a transverse curvature parameter of λ=1 and 2.

Analysis

Consider a vertical cylinder pin of radius r_o which is extended from a wall at temperature T_o and situated in an otherwise quiescent environment having temperature T_∞. The axial and radial coordinates are taken to be x and r, with x measuring the

distance along the centerline of the cylinder from its tip end and r measuring normal to the cylinder. The coordinate system is in Fig.(5-1-1) .

By employing the boussinesq approximation for the fluid property, the natural convective boundary layer equations with radiative effect are

$$\frac{\partial (ru)}{\partial x} + \frac{\partial (rv)}{\partial r} = 0 \qquad (5\text{-}1\text{-}1)$$

$$u\frac{\partial u}{\partial x} + v\frac{\partial u}{\partial r} = g\beta(T-T_\infty) + \frac{1}{r}\frac{\partial}{\partial r}(r\nu\frac{\partial u}{\partial r}) \qquad (5\text{-}1\text{-}2)$$

$$u\frac{\partial T}{\partial x} + v\frac{\partial T}{\partial r} = \frac{\alpha}{r}\frac{\partial}{\partial r}(r\frac{\partial T}{\partial r}) - \frac{1}{\rho C_p r}\frac{\partial}{\partial r}(rq^r) \qquad (5\text{-}1\text{-}3)$$

where u, v are streamwise and radial velocity components, respectively, T is the temperature of the fluid, α is the thermal diffusivity , g is the gravitational acceleration, ν is the kinematic viscosity, β is the thermal expansion coefficient, ρ is the density, C_p is the fluid specific heat and q^r is the radiative heat flux. The system of equations (5-1-1)-(5-1-3) is subject to the following boundary conditions

$$\begin{aligned} &u = v = 0 , \quad T = T_w(x), \quad \text{at } r = r_o \\ &u \to 0 \quad , \quad T \to T_\infty \quad , \quad \text{at } r \to \infty \\ &u = 0 \quad , \quad T \to T_\infty \quad , \quad \text{at } x = 0,\ r \geq r_o \end{aligned} \qquad (5\text{-}1\text{-}4)$$

Equations (5-1-1)-(5-1-3) and boundary condition do not admit a similarity solution. The nonsimilarity arises from the surface curvature of the cylinder and the surface temperature, Tw(x), which is undetermined. The pseudo-similarity variable η and the dimensionless axial coordinate ξ are introduced as follows

$$\xi = \frac{x}{L} \quad , \qquad \eta = \frac{r^2 - r_o^2}{2Lr_o} \left[GrL_\infty / (4\xi) \right]^{\frac{1}{4}} \tag{5-1-5}$$

where L is the length of the circular cylinder and GrL_∞ is the Grashof number evaluated at the temperature of surrounding, $GrL_\infty = g\beta(To - T_\infty)L_\infty^3/\nu_\infty^2$. The dimensionless stream function $f(\xi,\eta)$ and the dimensionless temperature $\theta(\xi,\eta)$ are defined, respectively, by

$$f(\xi,\eta) = \psi(x,r)/(2\sqrt{2}\ \nu_\infty r_o\ GrL_\infty^{\frac{1}{4}} \xi^{\frac{3}{4}}) \tag{5-1-6}$$

$$\theta(\xi,\eta) = (T - T_\infty)/(T_o - T_\infty) \tag{5-1-7}$$

where the stream function $\psi(x,r)$ satisfies the continuity equation (5-1-1) with

$$ru = \frac{\partial \psi}{\partial r} \quad , \qquad rv = -\frac{\partial \psi}{\partial x} \tag{5-1-8}$$

Under the assumption of the optically thick limit approximation, the radiative heat flux q^r can be expressed as follows

$$q^r = -\frac{4\sigma}{3\beta^*} \frac{\partial T^4}{\partial r} \tag{5-1-9}$$

where σ is the Stefan-Boltzmann constant and β^* is the extinction coefficient.

The kinematic viscosity, ν , is assumed to vary with temperature according to a general functional form $\nu = \nu_\infty w(\theta)$, where ν_∞ is the absolute viscosity at the temperature of surrounding, T_∞, and therefore $w(0)=1$. We can take the first two terms in a Taylor series expansion of w about $\theta = 0$ as follows:

$$w(\theta) = 1 + \left.\frac{dw}{d\theta}\right|_{\theta=0} (\theta - 0) + \frac{1}{2!}\left.\frac{d^2w}{d\theta^2}\right|_{\theta=0} (\theta - 0)$$

$$= 1 + a_1\theta + a_2\theta \qquad (5\text{-}1\text{-}10)$$

By introducting equations (5-1-5)-(5-1-10) into equations (5-1-2)-(5-1-4) the momentum and energy equations become:

$$(1+\lambda\eta\xi^{\frac{1}{4}})\ \{(1+a_1\theta+a_2\theta^2)f''\}'-2(f')^2+\theta$$

$$+\{\lambda\xi^{\frac{1}{4}}(1+a_1\theta+a_2\theta^2) + 3f\}f'' = 4\xi(f'\frac{\partial f'}{\partial\xi} - f''\frac{\partial f}{\partial\xi}) \qquad (5\text{-}1\text{-}11)$$

$$Pr_\infty^{-1}(1+\lambda\eta\xi^{\frac{1}{4}})\theta'' + [Pr_\infty^{-1}\lambda\xi^{\frac{1}{4}} + 3f)\theta'] + \frac{4}{3NPr_\infty}\cdot$$

$$\cdot\{(1+\lambda\xi^{\frac{1}{4}}\eta)[\theta'(\theta+C_T)^3]' + \lambda\xi^{\frac{1}{4}}\theta'(\theta+C_T)^3\} = 4\xi(f'\frac{\partial\theta}{\partial\xi} - \theta'\frac{\partial f}{\partial\xi})$$

(5-1-12)

The boundary condition (5-1-4) are transformed to

$$\left.\begin{array}{ll} f = f' = 0, \quad \theta = \theta_w & \text{at} \quad \eta = 0 \\ f' = \theta = 0 & \text{as} \quad \eta \to \infty \end{array}\right\} \qquad (5\text{-}1\text{-}13)$$

In the foregoing equations, the primes stand for partial derivatives with respect to η , Pr_∞ is the Prandtl number evaluated at the temperature of surrpunding $N=k\beta^*/4\sigma(T_o-T_\infty)^3$, $C_T=T_\infty/T_o-T_\infty$ and λ is the transverse curvature parameter, defined as

$$\lambda = 2\sqrt{2}\ L/r_o\ GrL_\infty^{\frac{1}{4}} \qquad (5\text{-}1\text{-}14)$$

Assuming a one-dimensional model the thin pin energy equation allows the temperature distribution along the longitudinal direction to be written as

$$\frac{d^2T_f}{dx^2} = \frac{2h^*(x)}{k_f r_o}\ (T_f - T_\infty) \qquad (5\text{-}1\text{-}15)$$

where k_f is the pin thermal conductivity, T_f is the pin temper-

ature, and h*(x) is the local heat transfer coefficient with radiative effect which can be regarded as known from the current boundary layer solution. The associated boundaryconditions are

$$\left.\begin{aligned} T_f &= T_o \qquad \text{at} \qquad x = L \\ \frac{dT_f}{dx} &= 0 \qquad \text{at} \qquad x = 0 \end{aligned}\right\} \tag{5-1-16}$$

Of particular interest is the thermal coupling between the pin and the boundary layer equations. The basic coupling is expressed by the requirement that the pin and fluid temperatures and heat fluxes be continuous at the pin-fluid interface, at all x.

$$T_f = T_w$$

$$h^*(T_f - T_\infty) = -k\frac{\partial T}{\partial r} + q^r \qquad \text{at } r = r_o,\ 0 \leq x \leq L \tag{5-1-17}$$

Equation (5-1-15) was recast in dimensionless form by the substitutions.

$$\xi = \frac{x}{L'} \qquad \theta_f = \frac{T_f - T_\infty}{T_o - T_\infty} \tag{5-1-18}$$

and combined with (5-1-16) and (5-1-17), so that

$$\frac{d^2\theta_f}{d\xi^2} = Nc\ \hat{h}^*\ \theta_f \tag{5-1-19}$$

$$\theta_f = 1, \qquad \text{at } \xi = 1$$

$$\frac{d\theta_f}{d\xi} = 0, \qquad \text{at } \xi = 0 \tag{5-1-20}$$

and $\theta_w = \theta_f$, and $h^* = \hat{h}^*\ k\ GrL_\infty^{1/4}/L$ at $\eta = 0$ (5-1-21)

where Nc is the conjugated convection-conduction paramenter,

$$Nc = \frac{2\ kL\ GrL_{\infty}^{\frac{1}{4}}}{k_f\ r_o} \qquad (5\text{-}1\text{-}22)$$

The quantity $\hat{h}^*$ is a dimensionless form of the local heat transfer coefficient with radiative effect. The value of $\hat{h}^*$ is obtained by substituting equations (5-1-5), (5-1-9) and (5-1-18) into equation (5-1-17).

$$\hat{h}^* = \frac{-1}{\sqrt{2}\ \xi^{\frac{1}{4}}} \left(1 + \frac{4(\theta+C_T)^3}{3N} \right) \frac{\partial\theta}{\partial\eta}/\theta_f \ , \quad \text{at } \eta = 0 \qquad (5\text{-}1\text{-}23)$$

Numerical Procedure

The solution begins by solving the natural convective boundary layer problem for a vertical circular pin with guessed temperature for all ξ . The dimensionless heat transfer coefficients h* determined from this solution in accordance with equation (5-1-23) are then used as input to the pin heat conduction equation (5-1-19). With Nc prescribed, the differential equation (5-1-19) is then solved to yield θ_f. To begin the next cycle of the iterative procedure, the just-determined θ_f is imposed as the thermal boundary condition for the natural convective boundary layer problem; the solution to which yields a new $\hat{h}^*$ distribution which is used as input to the pin heat conduction equation. This procedure of alternately solving the boundary layer problem and pin heat conduction problem was continued until convergence was attained.

The two systems of partial differential equations (5-1-11), (5-1-12) are coupled. In the present study, these equations

were solved by an accurate implicit finite-difference technique [19] . To begin with, the partial differential equations (5-1-11), (5-1-12) are first converted into system of first order equations which are then expressed in finite-difference form by approximating the functions and their first derivatives in terms of centered difference and averaged at midpoints of the net segments in the (ξ,η) coordinates. The resulting nonlinear finite difference equations are then solved by Newton's iterative method.

The boundary layer solutions were obtained by a marching procedure, starting at the leading edge ($\xi=0$) and the grids were divided into 45 points in the streamwise direction. There was a denser concentration of points near the leading edge to accommodate the initial rapid growth of the boundary layer. In order to write the system in terms of a first order system of partial differential equations, new dependent variables $\bar{u}(\xi,\eta)$, $\bar{v}(\xi,\eta)$ and$\omega(\xi,\eta)$, are introduced so that Equations (5-1-11), (5-1-12) can be written as

$$f' = \bar{u} \qquad (5\text{-}1\text{-}24)$$

$$\bar{u}' = \bar{v} \qquad (5\text{-}1\text{-}25)$$

$$\theta' = \omega \qquad (5\text{-}1\text{-}26)$$

$$(1+\lambda\eta\xi^{\frac{1}{4}})((1+a_1\theta+a_2\theta^2)\bar{v})'-2(\bar{u})^2+\theta$$

$$+(\lambda\xi^{\frac{1}{4}}(1+a_1\theta+a_2\theta^2)+3f)\bar{v}=4\xi(\bar{u}\frac{\partial\bar{u}}{\partial\xi}-\bar{v}\frac{\partial f}{\partial\xi}) \qquad (5\text{-}1\text{-}27)$$

$$Pr_\infty^{-1}(1+\lambda\eta\xi^{\frac{1}{4}})\omega' + (Pr_\infty^{-1}\lambda\xi^{\frac{1}{4}}+3f)\omega + \frac{4}{3NPr_\infty}$$

$$\{(1+\lambda\eta\xi^{\frac{1}{4}})(\omega(\theta+C_T)^3)' + \lambda\xi^{\frac{1}{4}}\omega(\theta+C_T)^3\}=4\xi(\bar{u}\frac{\partial\theta}{\partial\xi}-\omega\frac{\partial f}{\partial\xi}) \qquad (5\text{-}1\text{-}28)$$

Consider next the net rectangle shown in figure (5-1-2). and denote the net points by

$$\left.\begin{aligned} &\xi_o=0, \quad \xi_n=\xi_{n-1}+k_n, \quad n=1,2,3,\ldots N \\ &\eta_o=0, \quad \eta_j=\eta_{j-1}+h_j, \quad j=1,2,3,\ldots J \\ &\eta_J=\eta_\infty \end{aligned}\right\} \qquad (5\text{-}1\text{-}29)$$

Approximate the quanities $(f,\bar{u},\bar{v},\theta,\omega)$ at points (ξ_n,η_j) of the net by net functions denoted by $(f_j^n,\ u_j^n,\ v_j^n,\ \theta_j^n,\ \omega_j^n)$ employ the notation, for points and quantities midway between net points and for any net function m_j^n;

$$\xi_{n-\frac{1}{2}}=\frac{1}{2}(\xi_n+\xi_{n-1}), \quad \eta_{j-\frac{1}{2}}=\frac{1}{2}(\eta_j+\eta_{j-1}) \qquad (5\text{-}1\text{-}30)$$

$$m_j^{n-\frac{1}{2}}=\frac{1}{2}(m_j^n+m_j^{n-1}), \quad m_{j-\frac{1}{2}}^n=\frac{1}{2}(m_j^n+m_{j-1}^n)$$

The difference equations that are to approximate (5-1-24)-(5-1-28) are now easily formulated by considering one mesh rectangles as in figure (5-1-2). Equations (5-1-24)-(5-1-28) are approximated by centered difference quotients and average about the midpoint $(\xi_n,\eta_{j-\frac{1}{2}})$ of the segment P_2P_4, with the following results:

$$(f_j^n - f_{j-1}^n)h_j^{-1} = \bar{u}_{j-\frac{1}{2}}^n \qquad (5\text{-}1\text{-}31)$$

$$(\bar{u}_j^n - \bar{u}_{j-1}^n)h_j^{-1} = \bar{v}_{j-\frac{1}{2}}^n \qquad (5\text{-}1\text{-}32)$$

$$(\theta_j^n - \theta_{j-1}^n)h_j^{-1} = \omega_{j-\frac{1}{2}}^n \qquad (5\text{-}1\text{-}33)$$

Similarly (5-1-27) and (5-1-28) are approximated by contering on the midpoint $(\xi_{n-\frac{1}{2}},\eta_{j-\frac{1}{2}})$ of the rectangle $P_1P_2P_3P_4$, which gives

$$(1+\lambda\eta_{j-\frac{1}{2}}(\xi^n)^{\frac{1}{4}})\{(\frac{\bar{v}_j^n - \bar{v}_{j-1}^n}{h_j})(1+a_1\theta_{j-\frac{1}{2}}^n+a_2(\theta^2)_{j-\frac{1}{2}}^n)$$

$$+ (a_1\omega_{j-\frac{1}{2}}^n+2a_2\theta_{j-\frac{1}{2}}^n\omega_{j-\frac{1}{2}}^n)\bar{v}_{j-\frac{1}{2}}^n\}+ \lambda(\xi^n)^{\frac{1}{4}} (1+a_1\theta_{j-\frac{1}{2}}^n+a_2(\theta^2)_{j-\frac{1}{2}}^n)\bar{v}_{j-\frac{1}{2}}^n$$

$$+ (3+\alpha_n)(f\bar{v})_{j-\frac{1}{2}}^n- (2+\alpha_n)(\bar{u}^2)_{j-\frac{1}{2}}^n+\theta_{j-\frac{1}{2}}^n + \alpha_n(\bar{v}_{j-\frac{1}{2}}^{n-1} f_{j-\frac{1}{2}}^n -$$

$$f_{j-\frac{1}{2}}^{n-1} \bar{v}_{j-\frac{1}{2}}^n) = R_{j-\frac{1}{2}}^{n-1} \qquad (5\text{-}1\text{-}34)$$

$$(1+\lambda\eta_{j-\frac{1}{2}}(\xi^n)^{\frac{1}{4}})Pr_\infty^{-1}(\frac{\omega_j^n-\omega_{j-1}^n}{h_j})+Pr_\infty^{-1}\lambda(\theta^n)^{\frac{1}{4}}\omega_{j-\frac{1}{2}}^n+(3+\alpha_n)(f\omega)_{j-\frac{1}{2}}^n$$

$$+\frac{4}{3Pr_\infty N}\{(1+\lambda\eta_{j-\frac{1}{2}}(\xi^n)^{\frac{1}{4}})((\theta_{j-\frac{1}{2}}^n+C_T)^3(\frac{\omega_j-\omega_{j-1}}{h_j})^n$$

$$+3(\theta_{j-\frac{1}{2}}^n+C_T)^2 (\omega^2)_{j-\frac{1}{2}}^n)+\lambda(\xi^n)^{\frac{1}{4}}(\theta_{j-\frac{1}{2}}^n+C_T)^3 +\alpha_n(-(\bar{u}\theta)^n-u^{n-1}\theta^n$$

$$+\bar{u}^n\theta^{n-1}+\omega^{n-1}f^n-\omega^n f^{n-1})_{j-\frac{1}{2}}= Y_{j-\frac{1}{2}}^{n-1} \qquad (5\text{-}1\text{-}35)$$

where

$$\alpha_n = 4\ \xi^{n-\frac{1}{2}} / kn \qquad (5\text{-}1\text{-}36)$$

$$R_{j-\frac{1}{2}}^{n-1} = \alpha_n((f\bar{v})_{j-\frac{1}{2}}^{n-1}-(\bar{u}^2)_{j-\frac{1}{2}}^{n-1})-\{((1+\lambda\eta_{j-\frac{1}{2}})(\xi^{n-1})^{\frac{1}{4}})$$

$$((\frac{\bar{v}_j-\bar{v}_{j-1}}{h_j})^{n-1}(1+a_1\theta_{j-\frac{1}{2}}^{n-1}+a_2(\theta^2)_{j-\frac{1}{2}}^{n-1}+(a_1\omega_{j-\frac{1}{2}}^{n-1}+2a_2\theta_{j-\frac{1}{2}}^{n-1}\omega_{j-\frac{1}{2}}^{n-1})$$

$$\bar{v}_{j-\frac{1}{2}}^{n-1})-2(\bar{u}^2)_{j-\frac{1}{2}}^{n-1} + \theta_{j-\frac{1}{2}}^{n-1} + 3(f\bar{v})_{j-\frac{1}{2}}^{n-1}+\lambda(\xi^{n-1})^{\frac{1}{4}}\bar{v}_{j-\frac{1}{2}}^{n-1}(1+$$

$$a_1{}_{j-\frac{1}{2}}^{n-1}+a_2(\theta^2)_{j-\frac{1}{2}}^{n-1})\} \qquad (5\text{-}1\text{-}37)$$

$$Y_{j-\frac{1}{2}}^{n-1} = \alpha_n((\omega f)_{j-\frac{1}{2}}^{n-1}-(\bar{u}\theta)_{j-\frac{1}{2}}^{n-1})- Pr_\infty^{-1}(1+\lambda\eta_{j-\frac{1}{2}}(\xi^{n-1})^{\frac{1}{4}})$$

$$\left(\frac{\omega_j-\omega_{j-1}}{h_j}\right)^{n-1}+Pr_\infty^{-1}\lambda\left(\xi^{n-1}\right)^{\frac{1}{4}}\ \omega_{j-\frac{1}{2}}^{n-1}+3\left(f\omega\right)_{j-\frac{1}{2}}^{n-1}$$

$$+\frac{4}{3Pr_\infty N}\left\{\left(1+\lambda\eta_{j-\frac{1}{2}}\left(\xi^{n-1}\right)^{\frac{1}{4}}\right)\ \left(\left(\theta_{j-\frac{1}{2}}^{n-1}+C_T\right)^3\left(\frac{\omega_j-\omega_{j-1}}{h_j}\right)^{n-1}\right.\right.$$

$$\left.+\ 3\left(\theta_{j-\frac{1}{2}}^{n-1}+C_T\right)^2\ \left(\omega^2\right)_{j-\frac{1}{2}}^{n-1}\right)+\lambda\left(\xi^{n-1}\right)^{\frac{1}{4}}\left(\theta_{j-\frac{1}{2}}^{n-1}+C_T\right)^3\Big\} \qquad (5\text{-}1\text{-}38)$$

Equations (5-1-31)-(5-1-35) are imposed for j=1,2,3...J. The boundary conditions (5-1-13) can be written as

$$f_o^n = 0,\quad \theta_0^n = \theta_w^n,\quad \bar{u}_o^n = 0$$
$$\bar{u}_J^n = 0,\quad \theta_J^n = 0 \qquad (5\text{-}1\text{-}39)$$

If it is assumed that $(f_j^{n-1},\ \bar{u}_j^{n-1},\ \bar{v}_j^{n-1},\ \theta_j^{n-1},\ \omega_j^{n-1})$ are known for $0\leq j\leq J$, then (5-1-31)-(5-1-35) and boundary conditions (5-1-39) yield an implicit nonlinear algebraic system of 5J+5 equations in as many unknown $(f_j^n,\ \bar{u}_j^n,\ \bar{v}_j^n,\ \theta_j^n,\ \omega_j^n)$. The system can be solved very efficiently by using Newton's method. The important observations are that the linearized equations obtained by applying Newton's method to (5-1-31)-(5-1-35) and (5-1-39) form a block tridiagonal system (with 5 x 5 blocks) and that system can be solved very efficiently by the procedure discussed in refs. [19].

For most laminar flows the transformed boundary layer thickness is essentially constant. However, in flows in which the transverse-curvature effect is important, the transformed boundary layer thickness (η_∞) varies with increasing ξ. To

maintain the computation accuracy, it is necessary to use a variable grid, rather than a uniform grid, normal to the flow.

The net in the η-direction reported here is a geometric progression having the properity that the ratio of lengths of any two adjacent itervals is a constant; that is $h_j = M\ h_{j-1}$. The distance to the j-th line is given by the following formula:

$$\eta_j = h_1 \frac{M^j - 1}{M - 1}, \quad j=1,\ 2,\ 3,\ldots J, \quad M > 1 \tag{5-1-40}$$

There are two parameters: h_1, the length of the first $\Delta\eta$-step, and M, the ratio of two successive steps. The total number of points J can calculated by the following formula:

$$J = \frac{\ln(1+(M-1)\eta_\infty/h_1)}{\ln M} \tag{5-1-41}$$

In the calculations we select the parameters h_1 and M and calculate the η_∞. Here they were taken as 0.01 and 1.1, respectively.

The pin conduction equation was solved by using the direct inverse matrix method. The pin conduction equation was also divided into 45 grid points and expressed in finite defference form. To ensure high accuracy, a nonuniform grid points were employed. For small ξ, a finer ξ subdivision was also needed for the heat conduction equation.

Results and Discussion

Numerical results of the overall rate of heat transfer Q from the pin can be obtained from the heat conducted from the

wall into the pin base at ξ =1 or from the integrating heat convection over the pin surface. The corresponding Q values of these two methods are found to be in agreement. They may be expressed as

$$Q = k_f \pi r_o^2 \left.\frac{dT_f}{dx}\right|_{x=L} \tag{5-1-42}$$

or

$$Q = 2\pi r_o \int_o^L q\, dx \tag{5-1-43}$$

in dimensionless form

$$\frac{Q}{r_o k (T_o - T_\infty) Gr L_\infty^{1/4}} = \frac{2\pi}{Nc} \left.\frac{d\theta_f}{d\xi}\right|_{\xi=1} \tag{5-1-44}$$

or

$$\frac{Q}{r_o K (T_o - T_\infty) Gr L_\infty^{1/4}} = 2\pi \int_0^1 \frac{-1}{\sqrt{2}\xi^{1/4}} \left(1 + \frac{4(\theta+CT)^3}{3N}\right) \frac{\partial\theta}{\partial\eta}\, d\xi$$

$$\text{at } \eta = 0 \tag{5-1-45}$$

The results of the overall rate of heat transfer Q from the pin are presented as a function of the conjugated convection-conduction parameter Nc for two values of the transverse curvature parameter λ in Fig.(5-1-3). Because r_o and GrL_∞ appear in the ordinate, obscissa and transverse curvature parameter groups, the down-sloping trend of the curve indicates that, as expected, the pin heat transfer increases as the pin conductance k_f increases.

The ordinate and obscissa coordinates are replaced by the group

$$\frac{Q}{r_o k(T_o-T_\infty)GrL_\infty^{\frac{1}{4}}}/\lambda = \frac{Q}{2\sqrt{2}L\ k(T_o-T_\infty)} \qquad (5\text{-}1\text{-}46)$$

and

$$\frac{2k\ L\ GrL_\infty^{\frac{1}{4}}}{k_f r_o}/\lambda = \frac{k\ GrL_\infty^{\frac{1}{4}}}{\sqrt{2}\ k_f} \qquad (5\text{-}1\text{-}47)$$

Since both groups are independent of r_o, it follows that the actual total heat transfer is a function of the transverse curvature. It is observed from Fig.(5-1-3) that the smaller transverse curvature of the pin has the smaller total heat transfer rate. The viscosity variation parameters a_1, a_2 are calculated by the procedure of curve fitting which gives $a_1=3$, $a_2=2$ for the case $T_o=900^oK$, $T_\infty=300^ok$ and $Pr_\infty=0.7$. For a heated vertical pin, the viscosity of fluid near the pin surface is higher than the viscosity of surrounding. In consequance it is found that the overall heat transfer rate of the pin in the fluid with temperature dependent viscosity is lower than that of the pin in the fluid with constant viscosity ν_∞. Fig.(5-1-3) also shows that the overall heat transfer rate of the pin with radiative effect is higher than that of the pin without radiative effect.

Fig.(5-1-4)-(5-1-5) illustrate, respectively, the distribution of the modified local heat transfer coefficient along the pin surface as a function of Nc for fixed $\lambda=1$ and 2. The modified local heat transfer coefficient can be written as in dimensionless form

$$\hat{h}^* = \frac{-1}{\sqrt{2}\ \xi^{\frac{1}{4}}} \left(1 + \frac{4(\theta+CT)^3}{3N}\right) \frac{\partial\theta}{\partial\eta} / \theta_f \quad \text{at } \eta = 0 \qquad (5\text{-}1\text{-}48)$$

The increasing values of Nc are indicative of smaller pin conductance. It is shown from Fig.(5-1-4)-(5-1-5) that the larger variations of the response of the modified local heat transfer coefficient increase streamwise variations of the pin temperature for a given transverse curvature of cylinder. The distribution of the modified local heat transfer coefficient first decreases to some minimum; and then increases steadily with ξ for larger value of Nc. The phenomenon of this behavior is attributed to enhanced buoyancy and radiative heat flux associated with an increase in the wall-to-fluid temperature difference along the streamise direction. Similarly, as the transverse curvature of the pin increase, the local heat transfer coefficient also increases.

Distributions of the dimensionless local heat flux at the pin surface are shown in Fig.(5-1-6)-(5-1-7) as a function of Nc for fixed transverse parameters. The local heat flux can be taken as

$$\frac{qL}{k(T_o-T_\infty)GrL_\infty^{\frac{1}{4}}} = \frac{--1}{\sqrt{2}\ \xi^{\frac{1}{4}}} \left(1 + \frac{(\theta+CT)^3}{3N}\right) \frac{\partial\theta}{\partial\eta} \quad \text{at } \eta = 0 \qquad (5\text{-}1\text{-}49)$$

Fig.(5-1-6)-(5-1-7) show that most of the local heat fluxes at the pin surface increase as Nc decreases for a given transverse curvature.

From Fig.(5-1-3)-(5-1-7), it is found that the local heat transfer coefficient and local heat flux of the pin with radi-

ative effect are higher than those of the pin without radiative effect. Fig.(5-1-3)-(5-1-7) also show that the local heat transfer coefficient and local heat flux of the pin in the fluid with temperature dependent viscosity are lower than those of the pin in the fluid with constant viscosity ν_∞.

Representative results for the pin temperature distribution are presented in Fig.(5-1-8)-(5-1-9) for two different transverse curvature case. Fig.(5-1-8)-(5-1-9) confirm the assertions that larger values fo Nc give rise to larger pin temperature variations. From the figures it can be seen that the temperature distribution of the pin with radiative effect is lower than that of the pin without radiative effect. The figures also show that the temperature distribution of the pin in the fluid with temperature dependent viscosity is higher than that of the pin in the fluid with constant viscosity ν_∞.

Remark

The present analysis of the laminar free convective flow with radiative effect over a vertical cylinder pin has been studied. The modified local heat transfer coefficient along the pin is simultaneously solved for the laminar free convective boundary layer equations of the fluid and the heat conduction equation of the pin.

An efficient implicit finite difference technique is employed. The results showed that the modified local heat transfer coefficient along the streamwise direction does not monotonically

decrease but decreases at first to a minimum and then increases. This phenomenon is more obvious when the variations of the pin temperature are more nonuniform.

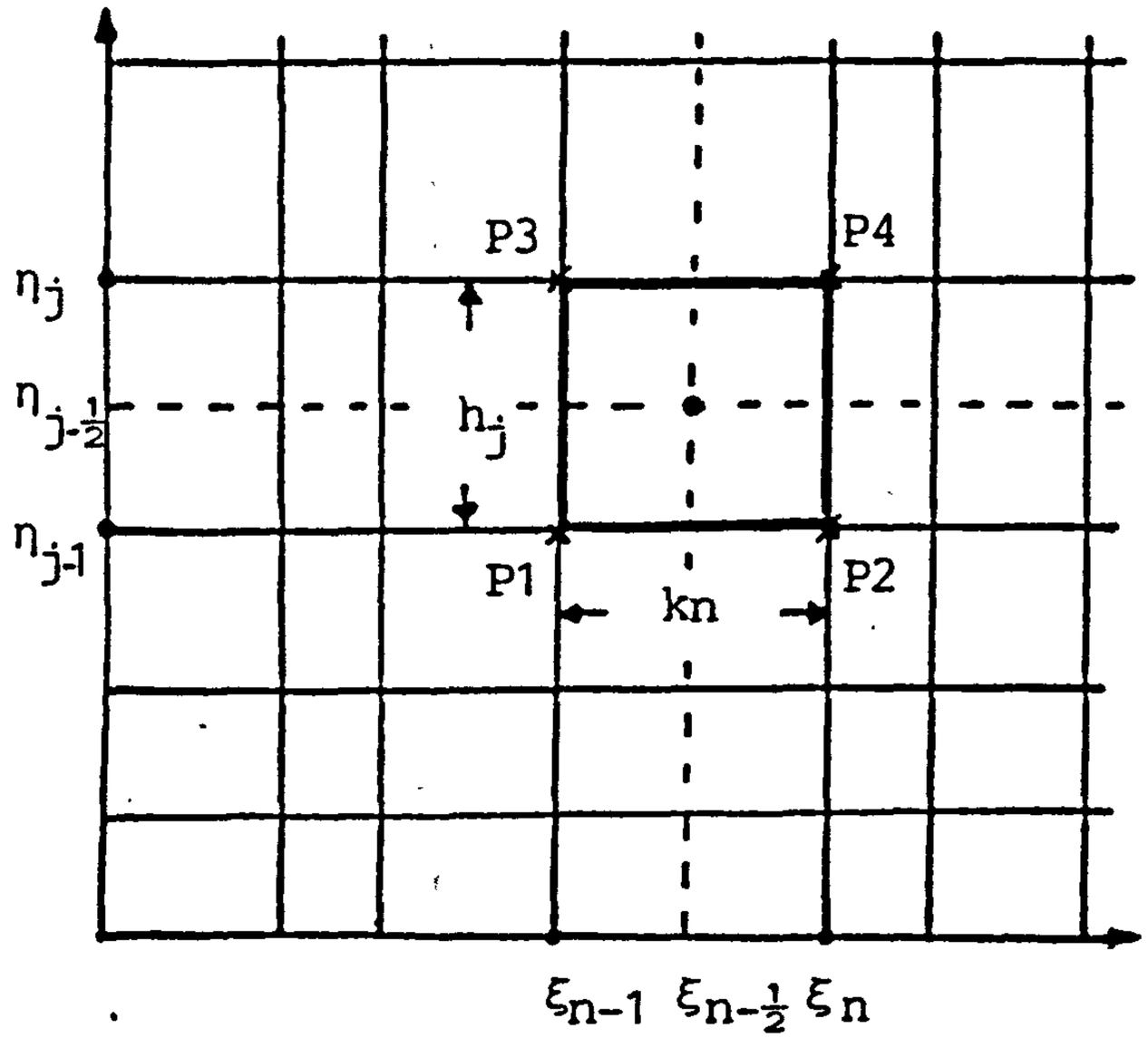

Fig.5-1-2 Net rectangle for the difference equations.

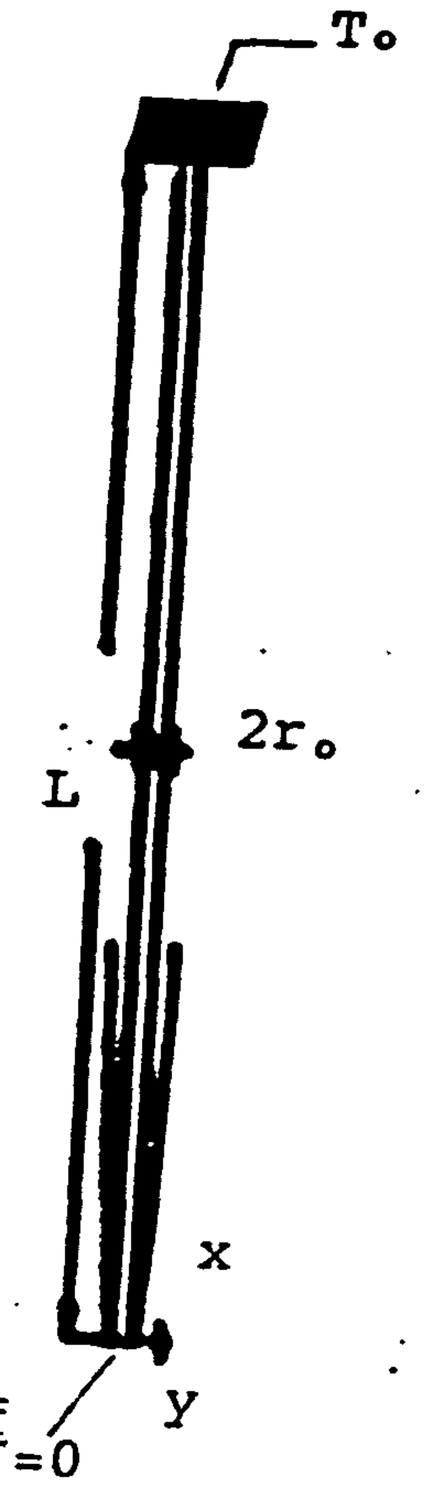

Fig.5-1-1 coordinate system.

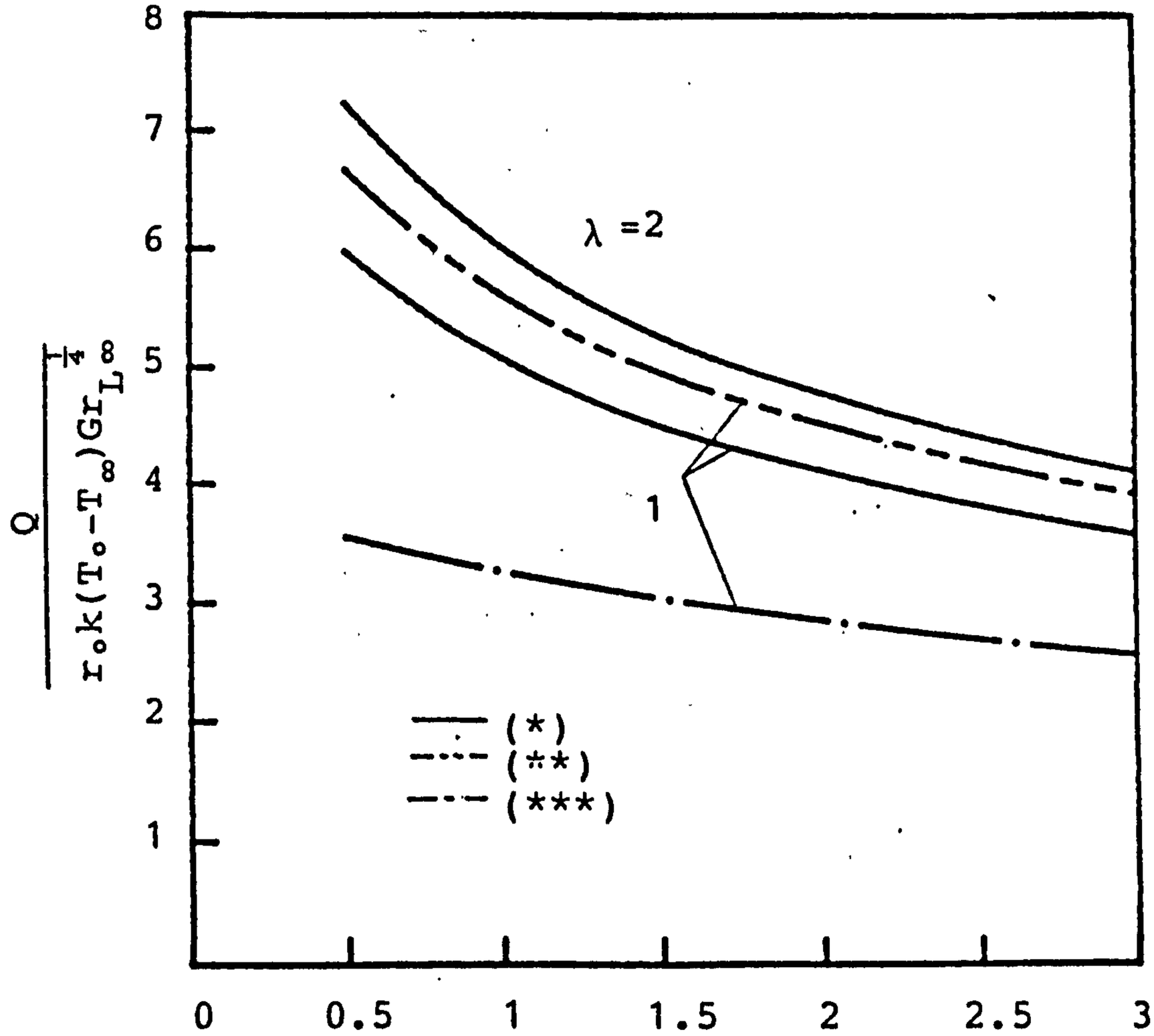

Fig.5-1-3 The total heat transfer rate of the circular pin for Pr_∞=0.7.

* :a1=3,a2=2,N=1,C_T=0.5

** :a1=0,a2=0,N=1,C_T=0.5

*** :a1=0,a2=0,N → ∞

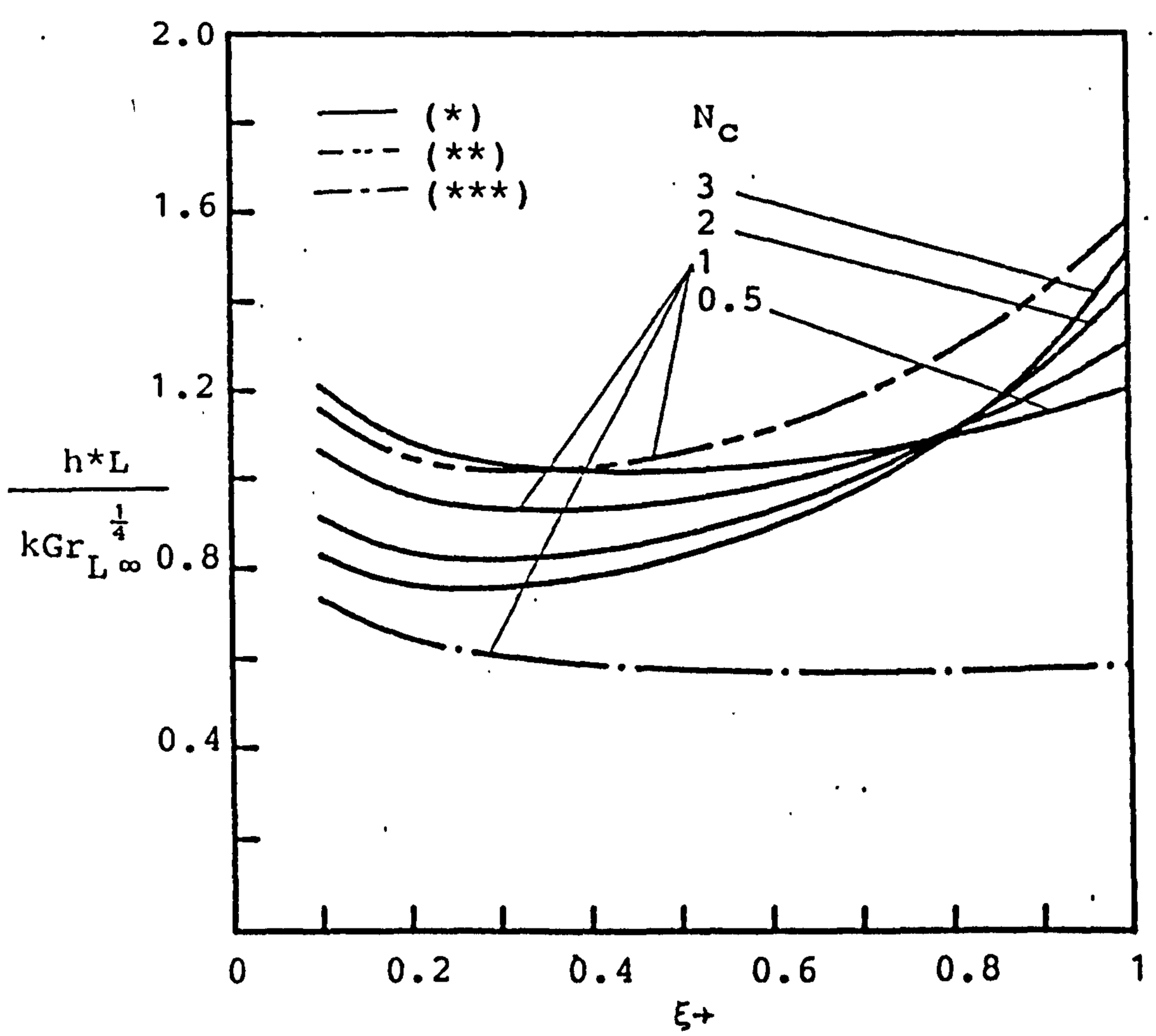

Fig.5-1-4 The modified local heat transfer coefficient of the circular pin for Pr_∞=0.7 and λ=1.

* :a1=3,a2=2,N=1,C_T=0.5

** :a1=0,a2=0,N=1,C_T=0.5

*** :a1=0,a2=0,N→∞

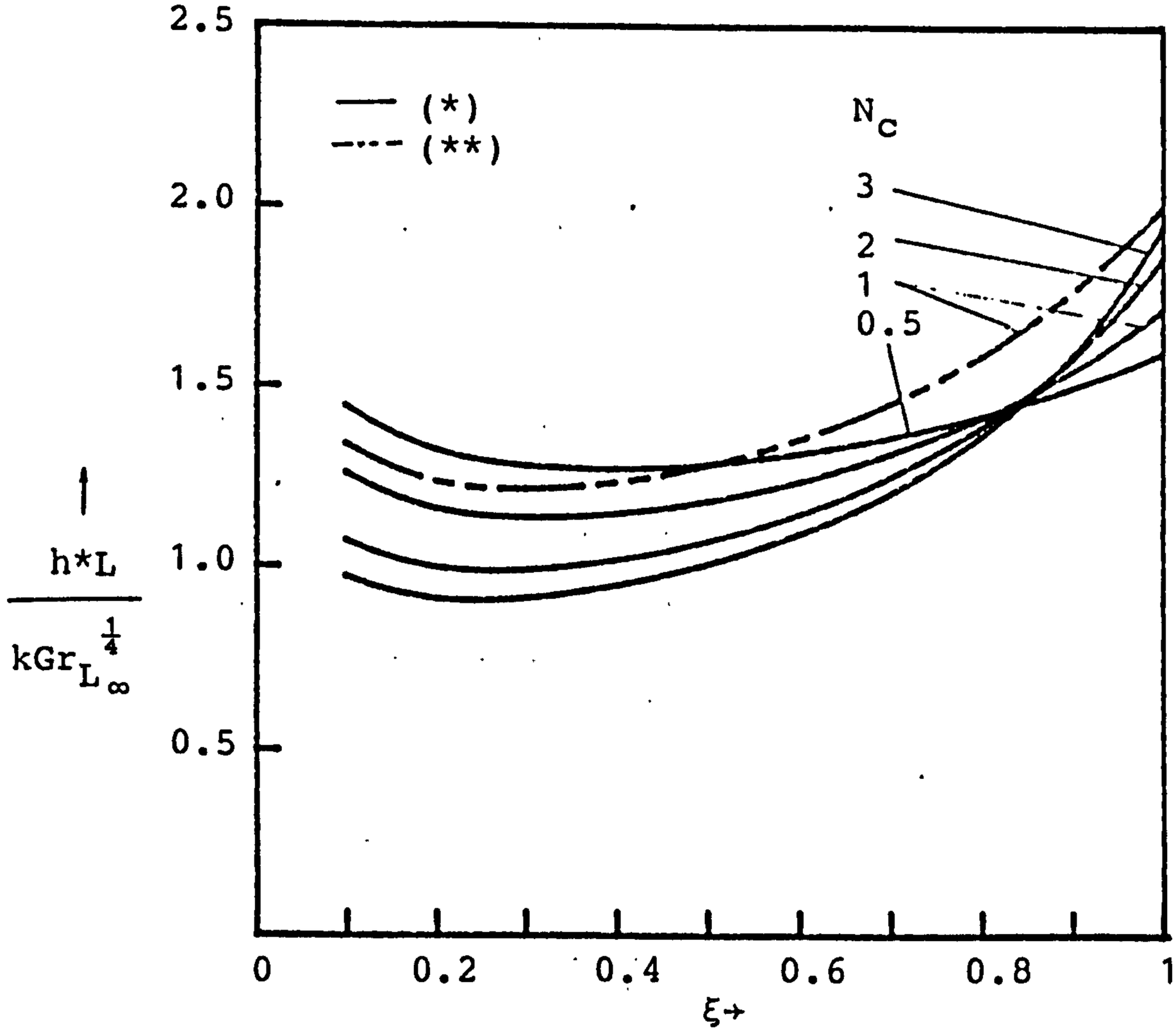

Fig.5-1-5 The modified local heat transfer coefficient of the circular pin for Pr_∞=0.7 ,N=1,C_T=0.5 and λ=2.

* :a1=3,a2=2

** :a1=0,a2=0

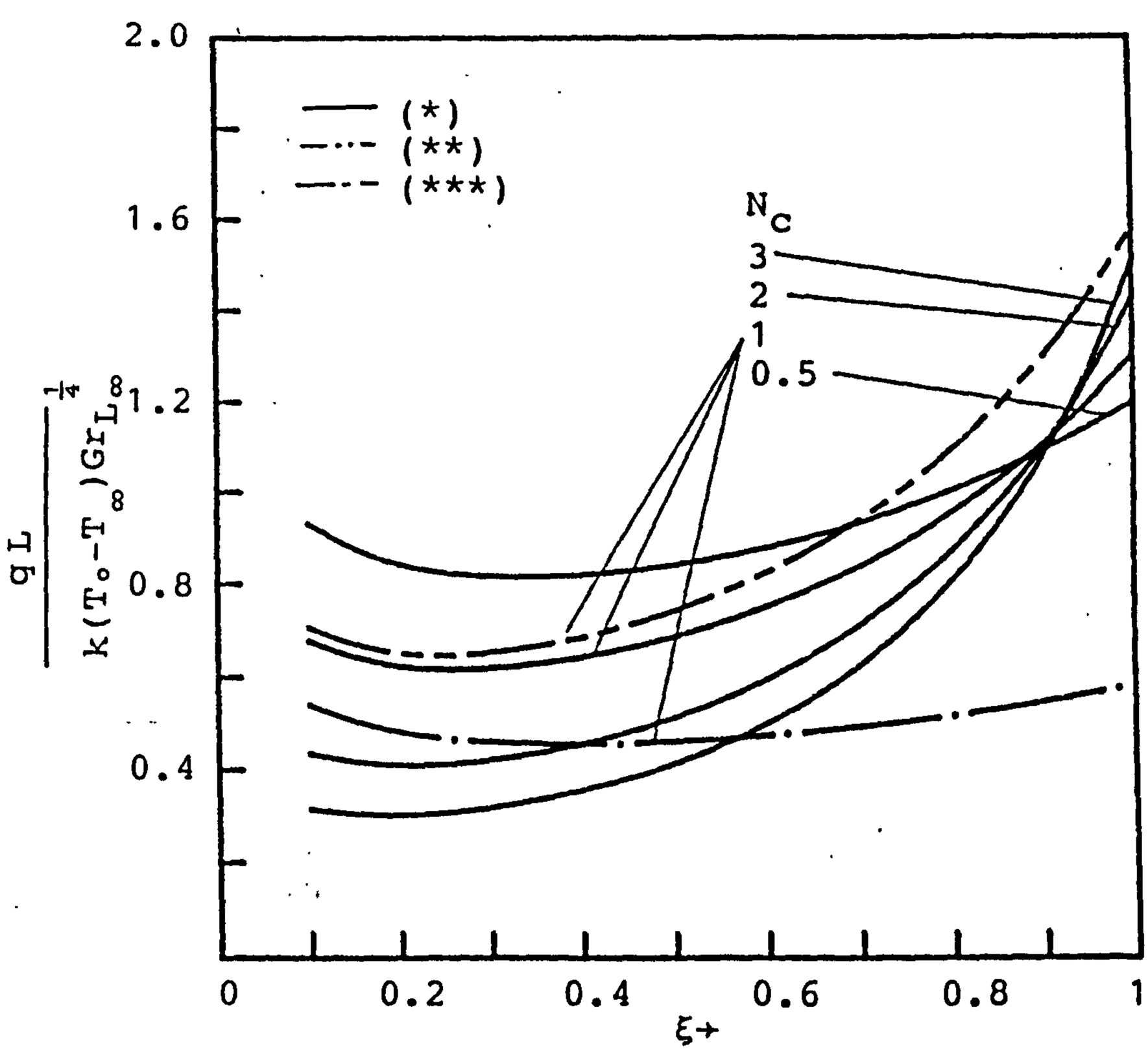

Fig.5-1-6 The local heat flux of the circular pin for $Pr_\infty=0.7$ and $\lambda=1$.

*　:a1=3,a2=2,N=1,C_T=0.5

**　:a1=0,a2=0,N=1,C_T=0.5

*** :a1=0,a2=0,N → ∞

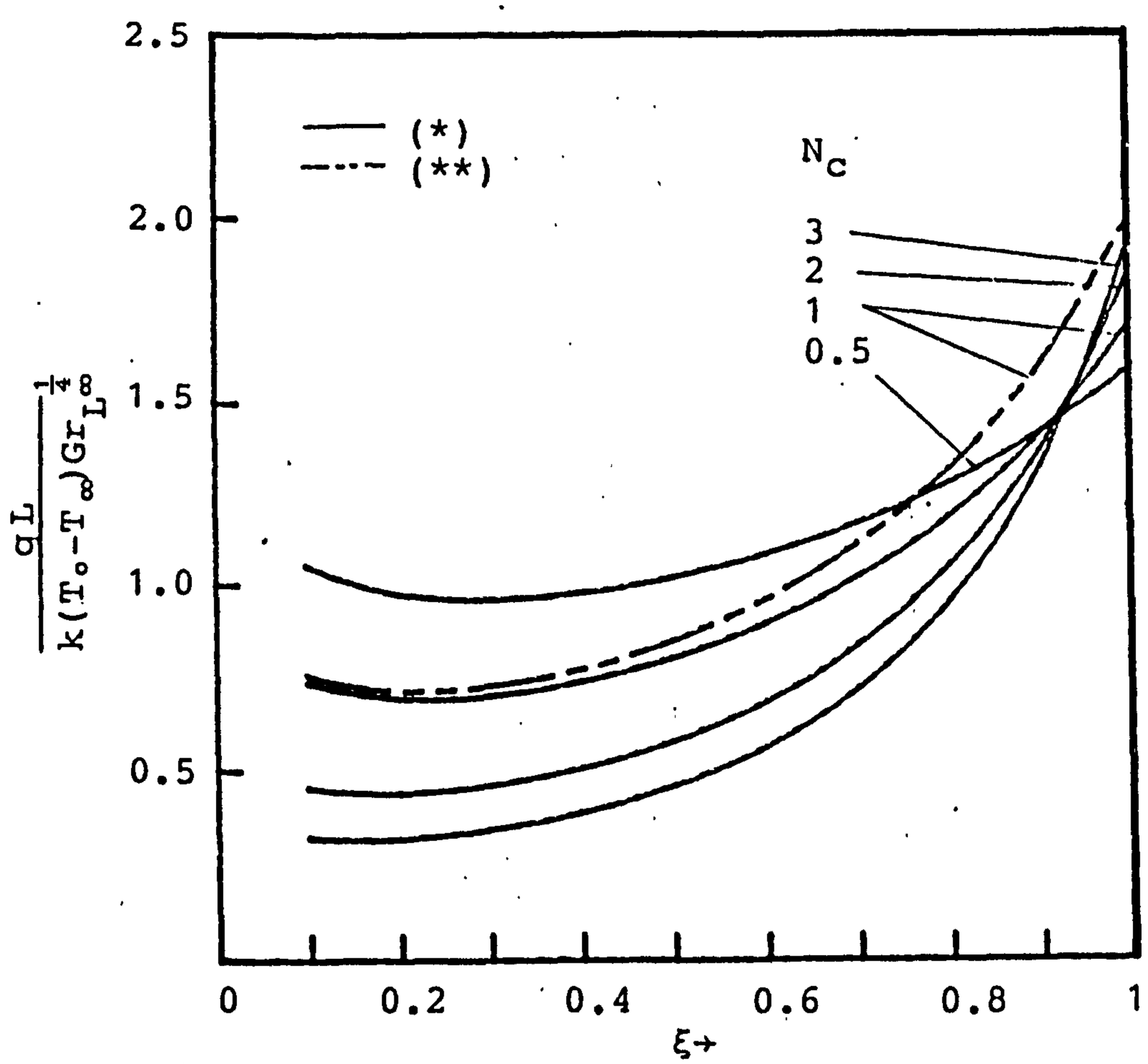

Fig.5-1-7 The local heat flux of the circular pin for Pr_∞=0.7,N=1,C_T=0.5 and λ=2.

* :a1=3,a2=2

** :a1=0,a2=0

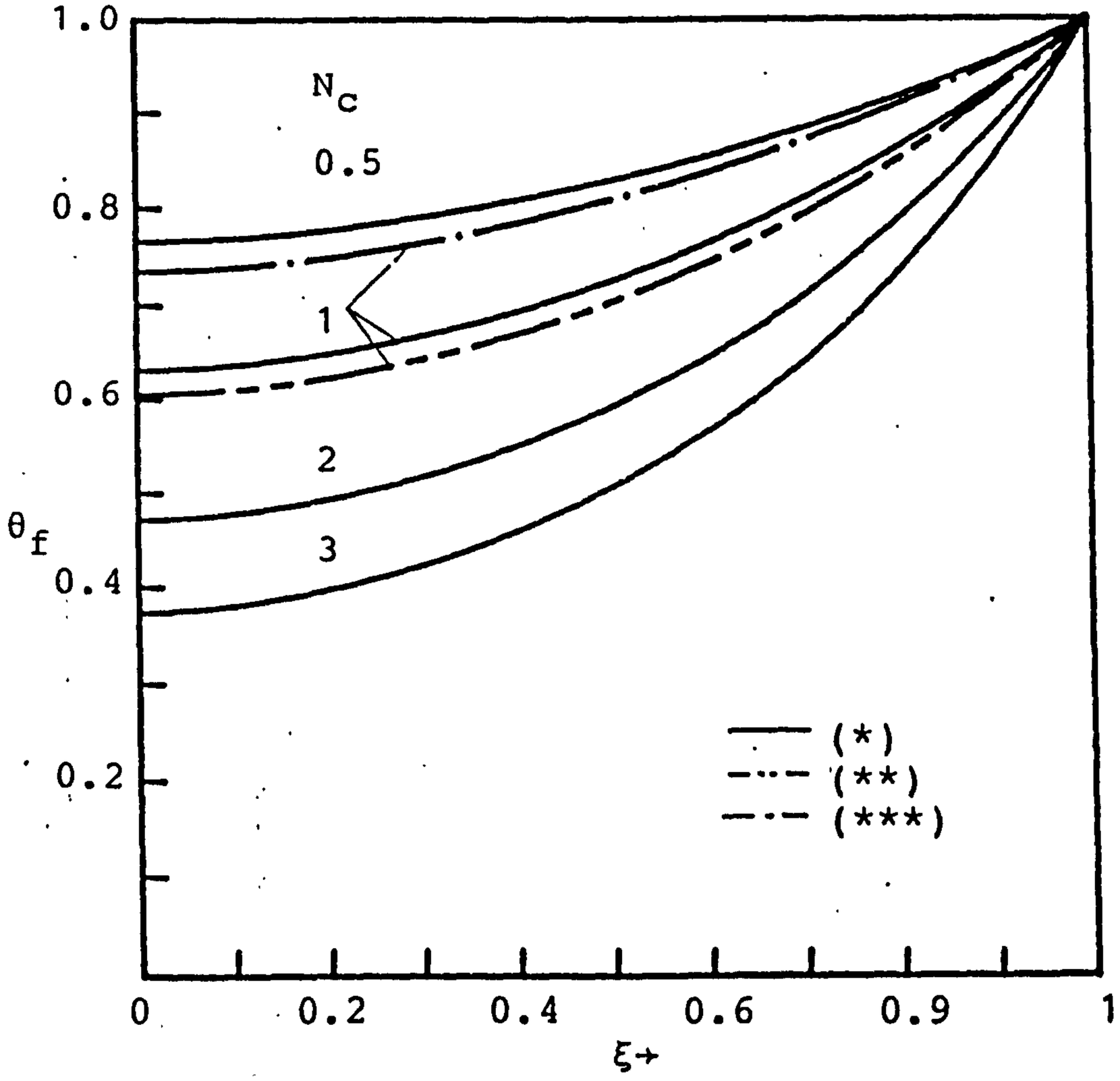

Fig.5-1-8 The temperature distribution of the circular pin for Pr_∞=0.7 and λ=1.

* :a1=3,a2=2,N=1,C_T=0.5

** :a1=0,a2=0,N=1,C_T=0.5

*** :a1=0,a2=0,N → ∞

V-2 Radiative Effect on The Vertical Circular Pin In Conjugated Forced Convection-Conduction Flow With Temperature Dependent Viscosity

In this section, a conjugated convection-radiation-conduction analysis has been made for a vertical circular pin which exchanges heat with its fluid environment by forced convection and radiation. The fluid with temperature dependent viscosity is considered.

Numerical results for a vertical circular pin in the gas having Pr_∞=0.7 with temperature dependent viscosity are performed for the following case: heated wall with T_o=900^oK and T =300^oK for N_c=0.25, 0.75, 2 and 3.

Analysis

Consider a vertical circular pin which is extended from a wall at temperature T_o and situated in a Newtonian flow field with undisturbed oncoming free stream velocity u_∞ and temperature T_∞. The coordinates parallel and normal to the pin surface are taken to be x and r, respectively. The coordinates system is in Fig.(5-2-1).

Under the assumption of constant C_p, k,ρ along with the application of the boundary layer approximations and negligible viscous dissipation, motion pressure, and volumetric energy generation, the equations expressing conservation of mass, momentum and energy for the physical model are, respectively,

as follows:

$$\frac{\partial(ru)}{\partial x} + \frac{\partial(rv)}{\partial r} = 0 \qquad (5\text{-}2\text{-}1)$$

$$u\frac{\partial u}{\partial x} + v\frac{\partial u}{\partial r} = \frac{1}{r}\frac{\partial}{\partial r}\left(r\nu\frac{\partial u}{\partial r}\right) \qquad (5\text{-}2\text{-}2)$$

$$u\frac{\partial T}{\partial x} + v\frac{\partial T}{\partial r} = \frac{\alpha}{r}\frac{\partial}{\partial r}\left(r\frac{\partial T}{\partial r}\right) - \frac{1}{\rho C_p r}\frac{\partial(rq^r)}{\partial r} \qquad (5\text{-}2\text{-}3)$$

where q^r is the net radiative heat flux and the other standard symbols are defined in the nomenclature. The system of equations (5-2-1)-(5-2-3) is subject to the following conditions:

$$\begin{aligned} &u=v=0, \quad T=T_w(x), \quad \text{at} \quad r = r \\ &u=u_\infty, \quad T=T_\infty, \quad \text{as} \quad r \to \infty \\ &u=u_\infty, \quad T=T_\infty, \quad \text{at} \quad x=0,\ r \geq r \end{aligned} \qquad (5\text{-}2\text{-}4)$$

Equations (5-2-1)-(5-2-3) and boundary conditions (5-2-4) do not admit a similarity solution. The nonsimilarity arises from the surface curvature of the cylinder pin and the surface temperature, $T_w(x)$, which is undetermined. The pseudo-similarity variable η and the dimensionless streamwise coordinate ξ are introduced as follows:

$$\xi = x/L, \qquad \eta = \frac{r^2 - r_o^2}{2r_o L}\left(Re_{L\infty}/\xi\right)^{1/2} \qquad (5\text{-}2\text{-}5)$$

where L is the length of the cylinder pin and $Re_{L\infty}$ is the Reynolds number evaluated at the temperature of surrounding, $Re_{L\infty} = u_\infty L/\nu_\infty$.

The dimensionless stream function $f(\xi, \eta)$ and the dimensionless temperature $\theta(\xi, \eta)$ are defined, respectively, by

$$f(\xi,\eta) = \psi(x,r)/[\, r_o(u_\infty L\xi\nu_\infty)^{\frac{1}{2}}\,] \qquad (5\text{-}2\text{-}6)$$

$$\theta(\xi,\eta) = (T-T_\infty)/(T - T_\infty) \qquad (5\text{-}2\text{-}7)$$

where the stream function $\psi(x,r)$ satisfies the continuity equation (5-2-1) with

$$ru = \partial\psi/\partial r, \qquad rv = -\partial\psi/\partial x \qquad (5\text{-}2\text{-}8)$$

The kinematic viscosity, ν, is assumed to very with temperature according to a general functional form $\nu=\nu_\infty W(\theta)$, where ν_∞ is the absolute viscosity at the temperature of surr-ounding, T_∞ , and therefore $w(0)=1$. The first two terms in a Taylor series expansion of $W(\theta)$ about $\theta=0$ are taken as

$$W(\theta) = 1 + \left(\frac{dW}{d\theta}\Big|_{\theta=0}\right)\theta + \left(\frac{1}{2!}\,\frac{d^2W}{d\theta^2}\Big|_{\theta=0}\right)\theta^2$$

$$= 1 + a_1\theta + a_2\theta^2 \qquad (5\text{-}2\text{-}9)$$

where a_1, a_2 are the viscosity variation parameters.

By introducing equations (5-2-5)-(5-2-9) into equations (5-2-2) -(5-2-4) and invoking the optically thick limit approximation for the net radiative heat flus q^r,

i.e.

$$q^r = -\frac{4\sigma}{3\beta^*}\,\frac{\partial T^4}{\partial r} \qquad (5\text{-}2\text{-}10)$$

the momentum and energy equations becomes:

$$[\,(1+a_1\theta+a_2\theta^2)(1+\lambda\eta\xi^{\frac{1}{2}})f"]' + \frac{1}{2}ff" = \xi\left(f'\frac{\partial f'}{\partial\xi} - f"\frac{\partial f}{\partial\xi}\right) \qquad (5\text{-}2\text{-}11)$$

$$Pr_\infty^{-1}[\,(1+\lambda\eta\xi^{\frac{1}{2}})\theta']' + \frac{1}{2}f\theta' + \frac{[\,4\,(\theta+C_T)^3\theta'(1+\lambda\eta\xi^{\frac{1}{2}})]'}{3Pr_\infty N}$$

$$= \xi\left(f'\,\frac{\partial\theta}{\partial\xi} - \theta'\,\frac{\partial f}{\partial\xi}\right) \qquad (5\text{-}2\text{-}12)$$

$$f = f' = 0,\ \theta = \theta_w, \qquad \text{at } \eta = 0$$

$$f' = 1,\ \theta = 0, \qquad \text{as } \eta \to \infty \qquad (5\text{-}2\text{-}13)$$

In the foregoing equations, the primes stand for partial derivations with respect to η, Pr_∞ is the Prandtl number evaluated at the temperature of surrounding,

$$N = \frac{k\beta^*}{4\sigma(T_o - T_\infty)^3} \qquad C_T = T_\infty/(T_o - T_\infty),$$

σ is the Stefan-Boltzmann constant, β^* is the extiction coefficient and λ is the transverse curvature parameter defined as

$$\lambda = \frac{2L}{r_o Re_{L\infty}^{1/2}} \qquad (5\text{-}2\text{-}14)$$

Assuming a one-dimensional model, the thin pin energy equation allows the temperature distribution along the longitudinal direction to be written as

$$\frac{d^2T_f}{dx^2} = \frac{2h^*(x)}{k_f r_o}(T_f - T_\infty) \qquad (5\text{-}2\text{-}15)$$

where k_f is the pin thermal conductivity, T_f is the pin temperature, and $h^*(x)$ is the modified local heat transfer coefficient with radiative effect which can be regarded as known from the current boundary layer solution. The associated boundary conditions are:

$$T_f = T_o \quad , \text{ at } \quad x = L$$

$$\frac{dT_f}{dx} = 0 \quad , \text{ at } \quad x = 0 \qquad (5\text{-}2\text{-}16)$$

Of particular interest is the thermal coupling between the

pin and the thermal boundary layer. The basic coupling is expressed by the requirement that the pin and fluid temperatures and local heat flux be continuous at the pin-fluid interface, at all x-positions.

$$T_f(x)=T_w(x)$$

$$h^*(T_f-T_\infty)=-k\frac{\partial T_w}{\partial r} + q^r \qquad \text{at } r=r_o,\ 0 \leq x \leq L \qquad (5\text{-}2\text{-}17)$$

Equation (5-2-15) was recast in dimensionless form by the substitutions

$$\xi = x/L \quad , \qquad \theta_f = (T_f-T_\infty)/(T_o-T_\infty) \qquad (5\text{-}2\text{-}18)$$

and combined with equations (5-2-16)-(5-2-17), so that

$$\frac{d^2\theta}{d\xi^2}_f = N_c\hat{h}^*\theta_f \qquad (5\text{-}2\text{-}19)$$

$$\theta_f = 1, \quad \text{at } \xi = 1 \ , \quad \frac{d\theta_f}{d\xi} = 0, \quad \text{at } \xi = 0 \qquad (5\text{-}2\text{-}20)$$

$$\text{and} \qquad \theta_w = \theta_f \quad , \quad h^* = kRe_{L\infty}^{\frac{1}{2}}\ \hat{h}^*/L \ , \quad \text{at } \eta = 0 \qquad (5\text{-}2\text{-}21)$$

where N_c is the conjugated convection-conduction parameter

$$N_c = \frac{2kL}{k_f r_o}\ Re_{L\infty}^{\frac{1}{2}} \qquad (5\text{-}2\text{-}22)$$

The quantity $\hat{h}^*$ is a dimensionless form of the local forced convective heat transfer coefficient with radiative effect. The value of $\hat{h}^*$ can be obtained by substituting equations (5-2-5), (5-2-10) and (5-2-18) into equation (5-2-17)

$$\hat{h}^* = -\left(1+\frac{4(\theta+C_T)^3}{3N}\right)\frac{\partial\theta}{\partial\eta}/(\theta_f\xi^{\frac{1}{2}}), \quad \text{at} \quad \eta = 0 \qquad (5\text{-}2\text{-}23)$$

Numerical Procedure

The solution begins by solving the forced convective boundary layer problem for a vertical cylinder pin with guessed temperature along the pin surface. The dimensionless heat transfer coefficient $\hat{h}^*$ determined from equation (5-2-23) are then used as input to the pin heat conduction equation (5-2-19). With N_c prescribed, the differential equation (5-2-19) is then solved to yield θ_f. To begin the next cycle of the iterative procedure, the just-determined θ_f is imposed as the thermal boundary condition for the forced convective boundary layer equations of Newtonian fluid the solution to which is used as input to the pin heat conduction equation. This procedure of alternatively solving the boundary layer problem and the pin conduction problem was continued until convergence was attained.

The two systems of partial differential equations (5-2-11) -(5-2-12) are coupled. In the present study, these equations were solved by an accurate implicit finite-difference technique due to Cebeci and Bradshaw [19]. To begin with, the partial differential equations (5-2-11)-(5-2-12) are first converted into a system of first order equations which are then expressed in finite-difference form by approximating the functions and their first derivatives in terms of centered difference and averaged at midpoints of the net segment in the (ξ,η) coordinates. The resulting nonlinear finite-difference equations are then solved by Newton's iterative method.

The boundary layer solutions were obtained by a marching procedure, starting at the leading edge and the grids were divided into 45 points in the streamwise direction. There was a denser concentration of points near the leading edge to accommodate the initial rapid growth of the boundary layer. Owing to the transverse curvature effect, the transformed boundary layer thickness (η_∞) varies with λ . It is therefore necessary to use a variable grid, rather a uniform grid, normal to the flow.

The conduction equation was solved by using the direct inverse matrix method. The pin equation was also divided into 45 grid points and expressed in finite-difference form. To ensure high accuracy, a nonuniform grid points were employed. For small ξ , a finer ξ subdivision was needed for the boundary layer solution.

Results and Discussion

Numerical results of the overall rate of heat transfer were obtained from the wall into the pin base at ξ =1 or from the integrating heat transfer over the pin surface. The corr-esponding overall heat transfer rate of these two methods are found to be in agreement. They may be expressed in dimensionless form as:

$$\frac{Q}{r_o k\ (T_o-T_\infty) Re_{L\infty}^{\frac{1}{2}}} = 2\pi \int_0^1 (-\frac{\partial\theta}{\partial\eta})\,(1+\frac{4(\theta+C_T)^3}{3N})/\xi^{\frac{1}{2}}\ d\xi \qquad (5\text{-}2\text{-}24)$$

$$\frac{Q}{r_o k (T_o-T_\infty) Re_{L\infty}^{\frac{1}{2}}} = \frac{2\pi}{N_c}\ \left.\frac{d\theta_f}{d\xi}\right|_{\xi=1} \qquad (5\text{-}2\text{-}25)$$

The results of the overall rate of heat transfer from the pin are presented as a function of the conjugated convection-conduction parameter N_c. The decrease of N_c indicates short pin length, L, great pin conductances, $k_f r_o$ and lower convective coefficient (low k and $Re_{L\infty}$).

The ordinate and abscissa coordinates are replaced by the groups

$$\frac{Q}{r_o k(T_o-T_\infty) Re_{L\infty}^{\frac{1}{4}}} / \lambda = \frac{Q}{2Lk(T_o-T_\infty)} \qquad (5\text{-}2\text{-}26)$$

and

$$\frac{2kLRe_{L\infty}^{\frac{1}{2}}}{k_f r_o} / \lambda = kRe_{L\infty} / k_f \qquad (5\text{-}2\text{-}27)$$

Since both groups are independent of r_o, it follows that the actual heat transfer is a function of the transverse curvature. In this figure, we may find that the smaller radius of the pin has the greater total heat transfer rate. Fig.(5-2-2) illustrates that the overall heat transfer rate of the pin with radiative effect is always higher than that without radiative effect. Fig.(5-2-2) also shows that the overall heat transfer rate of the heated pin in the fluid (Pr_∞=0.7) with constant viscosity (ν_∞) is higher than that in the fluid with temperature dependent viscosity when the other parameters are fixed.

Fig.(5-2-3)-(5-2-4) illustrate the distributions of the local forced convective heat transfer coefficient with radiative effect along the pin surface as a function of N_c for two values

of the transverse curvature parameter λ . The modified local heat transfer coefficient can be written in dimensionless form, as follows

$$\frac{h^*L}{kRe_{L\infty}^{\frac{1}{2}}} = -\left[1 + \frac{4(\theta+C_T)^3}{3N}\right] \frac{\partial\theta}{\partial\eta}/(\theta_f\xi^{\frac{1}{2}}), \quad \text{at } \eta = 0 \qquad (5\text{-}2\text{-}28)$$

It is found that the larger variations of the response of the modified local heat transfer coefficient $\hat{h}^*$ give rise to larger streamwise variations of the pin temperature. In this figure, it is found that the $\hat{h}^*$ decreases to some minimum, and then increases steadily with ξ ; the phenomenon of this behavior is attributed to an enhanced radiative heat flux associated with an increase in the wall-to-fluid temperature difference along the streamwise direction.

The variations of the dimensionless local heat flux at the pin surface are presented in Fig.(5-2-5)-(5-2-6) for different N_C and fixed transverse curvature parameter. The local heat flux ca be taken as

$$\frac{qL}{k(T_o-T_\infty)Re_{L\infty}^{\frac{1}{2}}} = -\left[1 + \frac{4(\theta+C_T)^3}{3N}\right] \frac{\partial\theta}{\partial\eta}/\xi^{\frac{1}{2}}, \quad \text{at}\eta = 0 \qquad (5\text{-}2\text{-}29)$$

The heat fluxes for lower N_C are higher near the tip, but smaller near the base than those for higher N_C. Those figures also show that the total heat transfer rate from the pin surface is increased as N_C decreased, which agrees with the predictions in Fig.(5-2-2).

It is observed from Fig.(5-2-3)-(5-2-6) that the local heat

transfer coefficient and local heat flux with radiative effect are always higher than those without radiative effect. Fig. (5-2-3)-(5-2-6) illustrate that the modified local heat transfer coefficient and local heat flux of the heated pin in the fluid with constant viscosity (ν_∞) are higher than those in the fluid with temperature dependent viscosity. Fig.(5-2-3)-(5-2-6) also show that the local heat transfer coefficient and local heat flux from the pin are increased as λ increased.

Representative results for the pin temperature distributions are presented in Fig.(5-2-7)-(5-2-8). In these figures, it is shown that the larger values of N_c and λ give rise to larger pin temperature variations, and the pin temperature without radiative effect is higher than that with radiative effect. These figures also show that the temperature distribution of the heated pin in the fluid with constant viscosity (ν_∞) give a larger variation in the streamwise direction than that of the same pin in the fluid with temperature dependent viscosity when the other parameters are fixed.

Remark

The analysis of present paper has yielded the results of the heated vertical circular pin in forced thermal boundary layer flow with temperature dependent viscosity. The viscosity varistion parameters a_1, a_2 are determined by the procedure of curve-fitting technique for the case of heates wall with T_o= 900^oK and T_∞=300^oK. The radiative effect on the boundary layer

problem is also considered and the optically thick limit approximation for the radiative part is assumed. In order to solve the simultaneously the coupled pin conduction equation and the fluid thermal boundary layer equation, a very simple and efficient "Box" scheme is employed here. The results show that the local heat transfer coefficient along the streamwise direction do not monotonically decrease but decreases at first to a minimum and then increases.

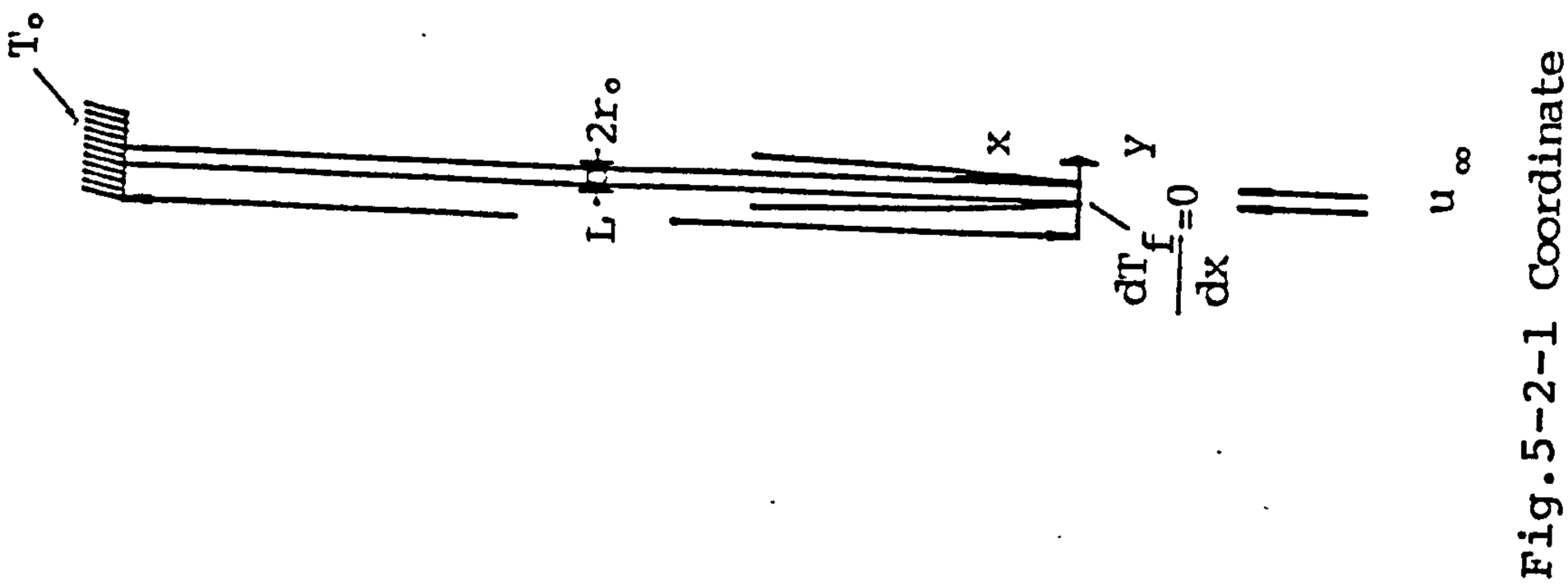

Fig.5-2-1 Coordinate system.

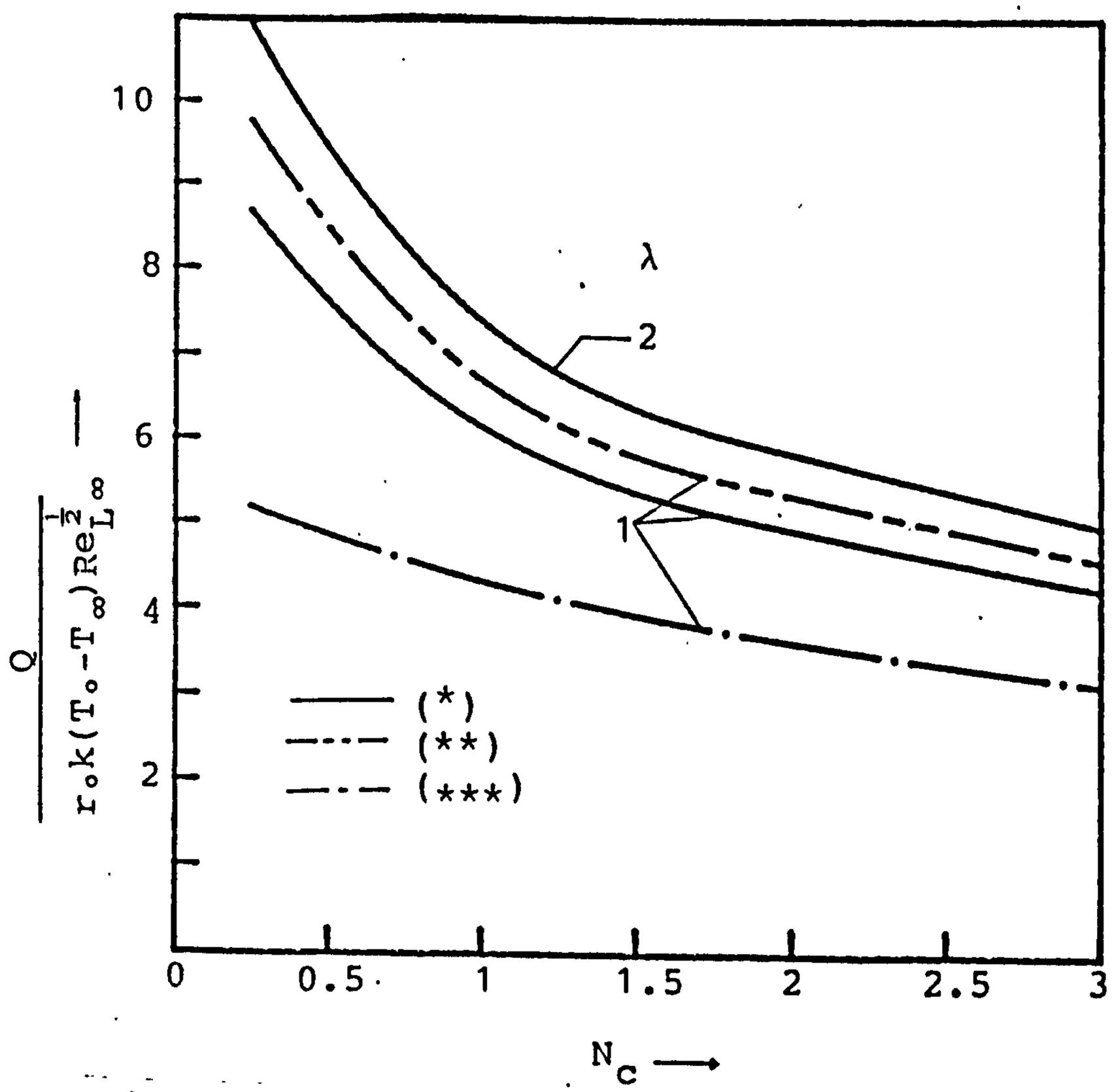

Fig.5-2-2 The total heat transfer rate of the circular pin for Pr=0.7

* : a1=3 ,a2=2 ,N=1 ,C_T=0.5

** : a1=0 ,a2=0 ,N=1 ,C_T=0.5

*** : a1=0 ,a2=0 ,N$\longrightarrow\infty$

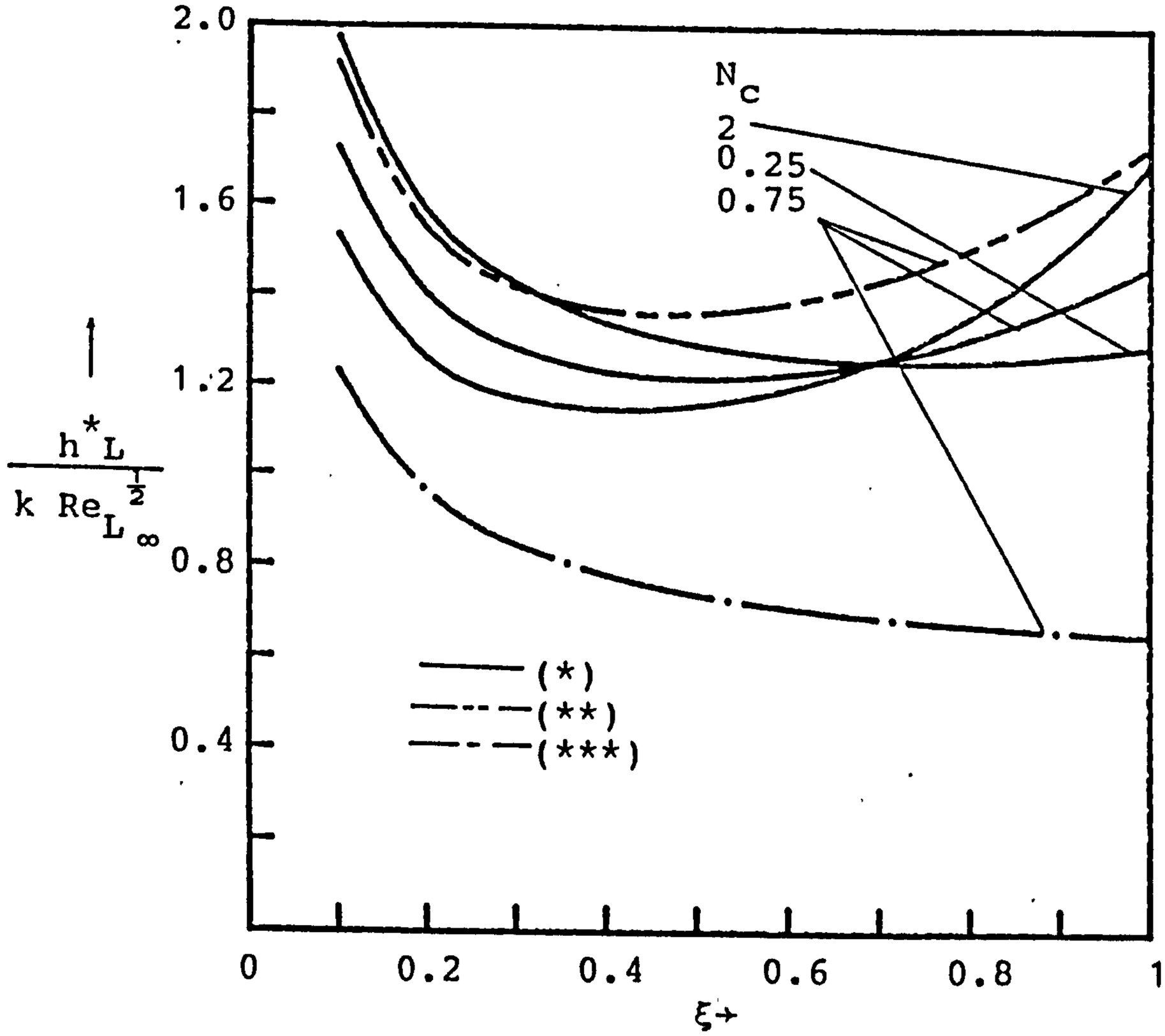

Fig.5-2-3 The modified local heat transfer coefficient of the pin for Pr=0.7, λ=1, and various values of N_c.

* : a1=3 ,a2=2 ,N=1 ,C_T=0.5
** : a1=0 ,a2=0 ,N=1 ,C_T=0.5
*** : a1=0 ,a2=0 ,N$\longrightarrow_\infty$

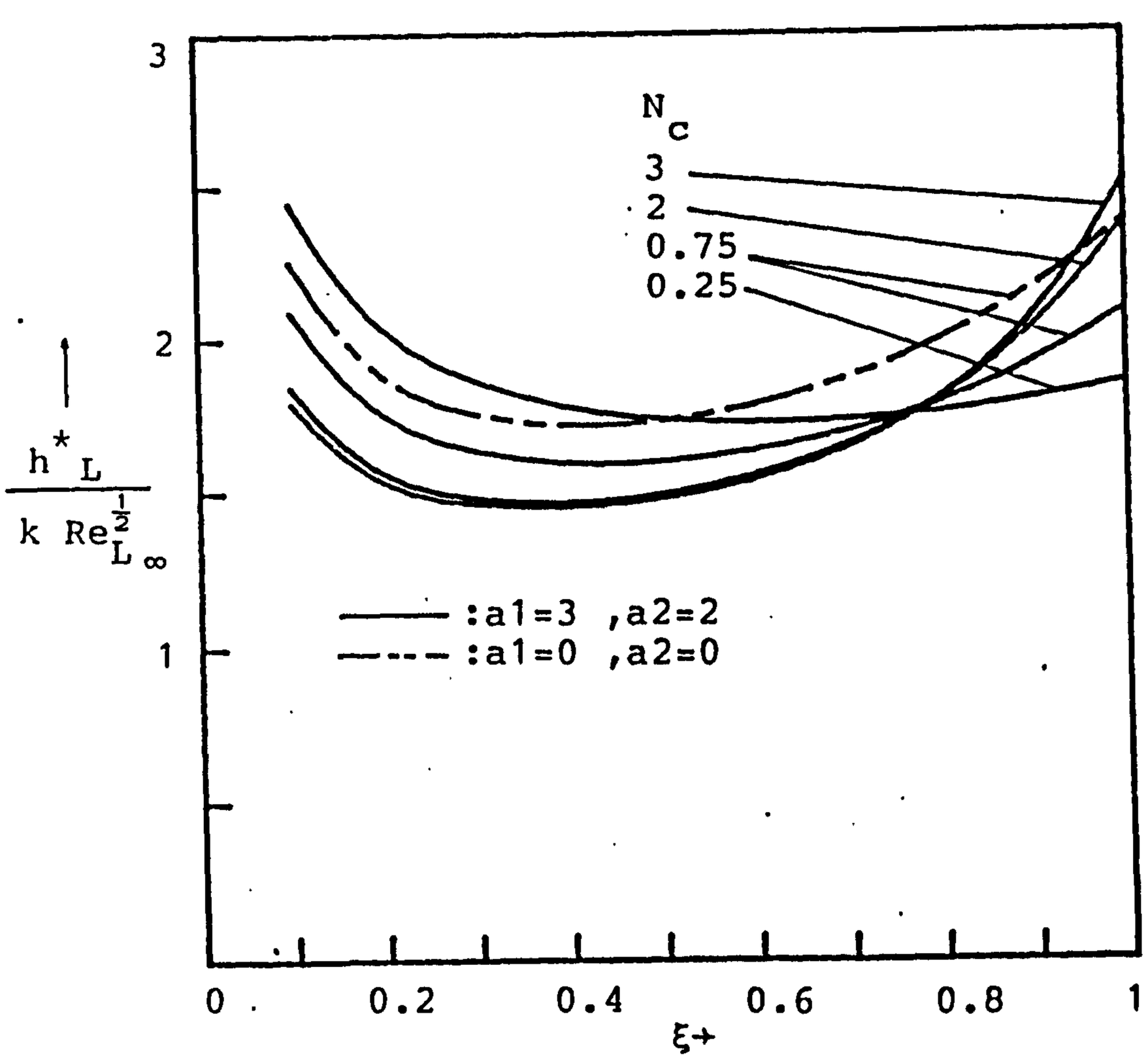

Fig.5-2-4 The modified local heat transfer coefficient of the circular pin for Pr=0.7,N=1,C_T=0.5,λ=2 and various values of N_c.

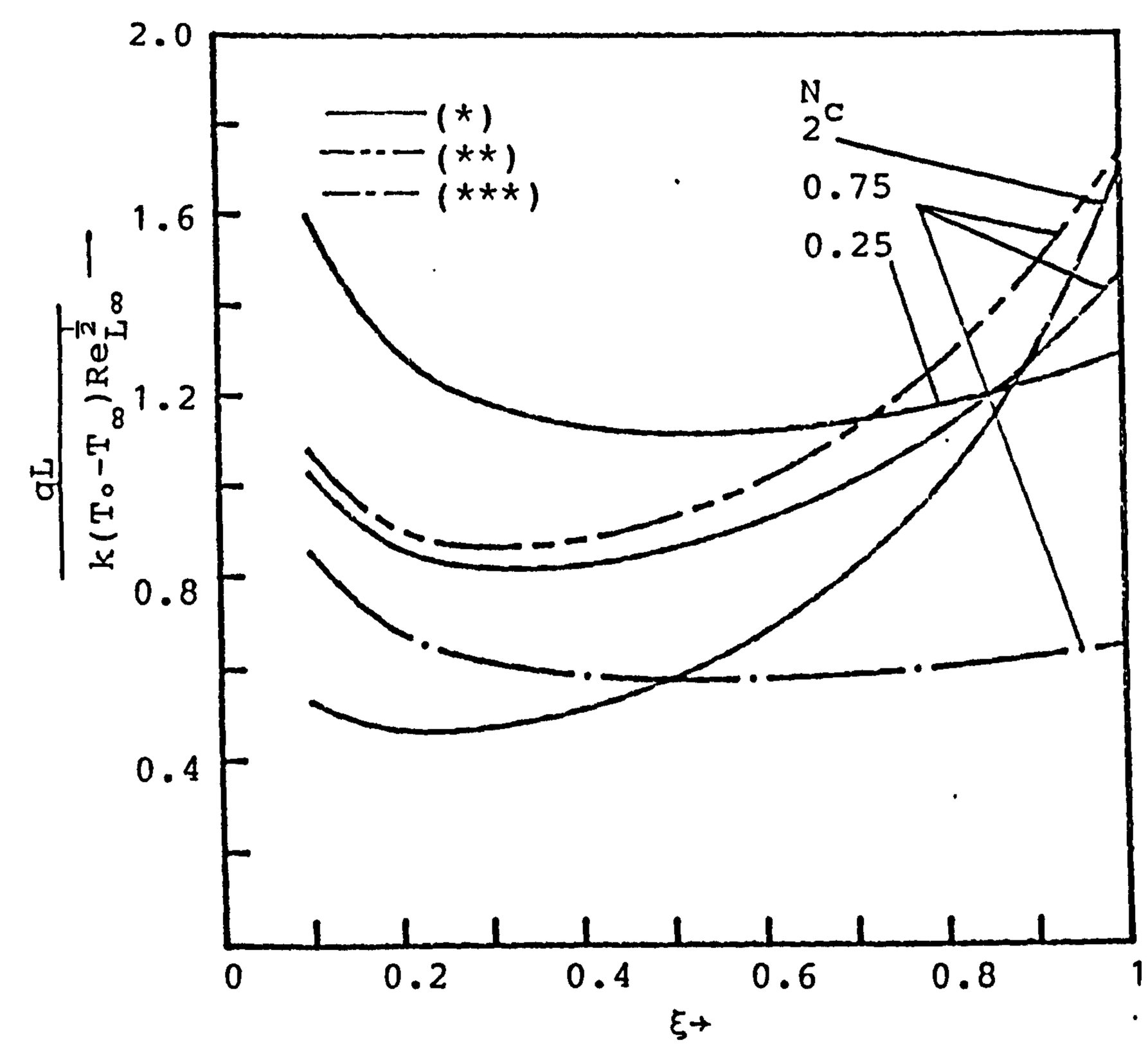

Fig.5-2-5 The local heat flux of the circular pin for Pr=0.7, λ=1 and various values of N_C.

* : a1=3 , a2=2 , N=1 , C_T=0.5

** : a1=0 , a2=0 , N=1 , C_T=0.5

*** : a1=0 , a2=0 , N $\longrightarrow \infty$

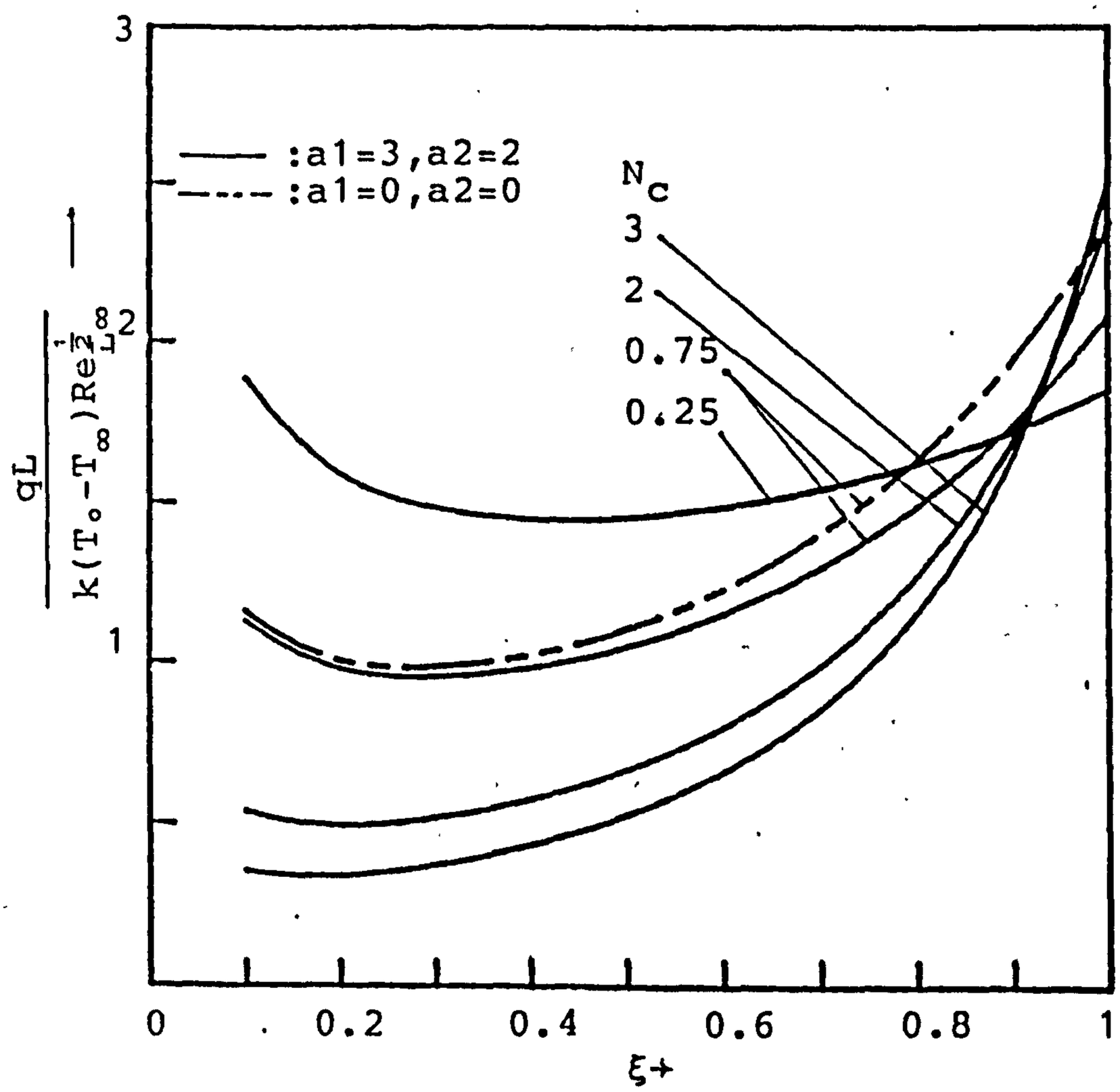

Fig.5-2-6 The local heat flux of the circular pin for Pr=0.7,N=1,C_T=0.5,λ=2 and various values of N_c.

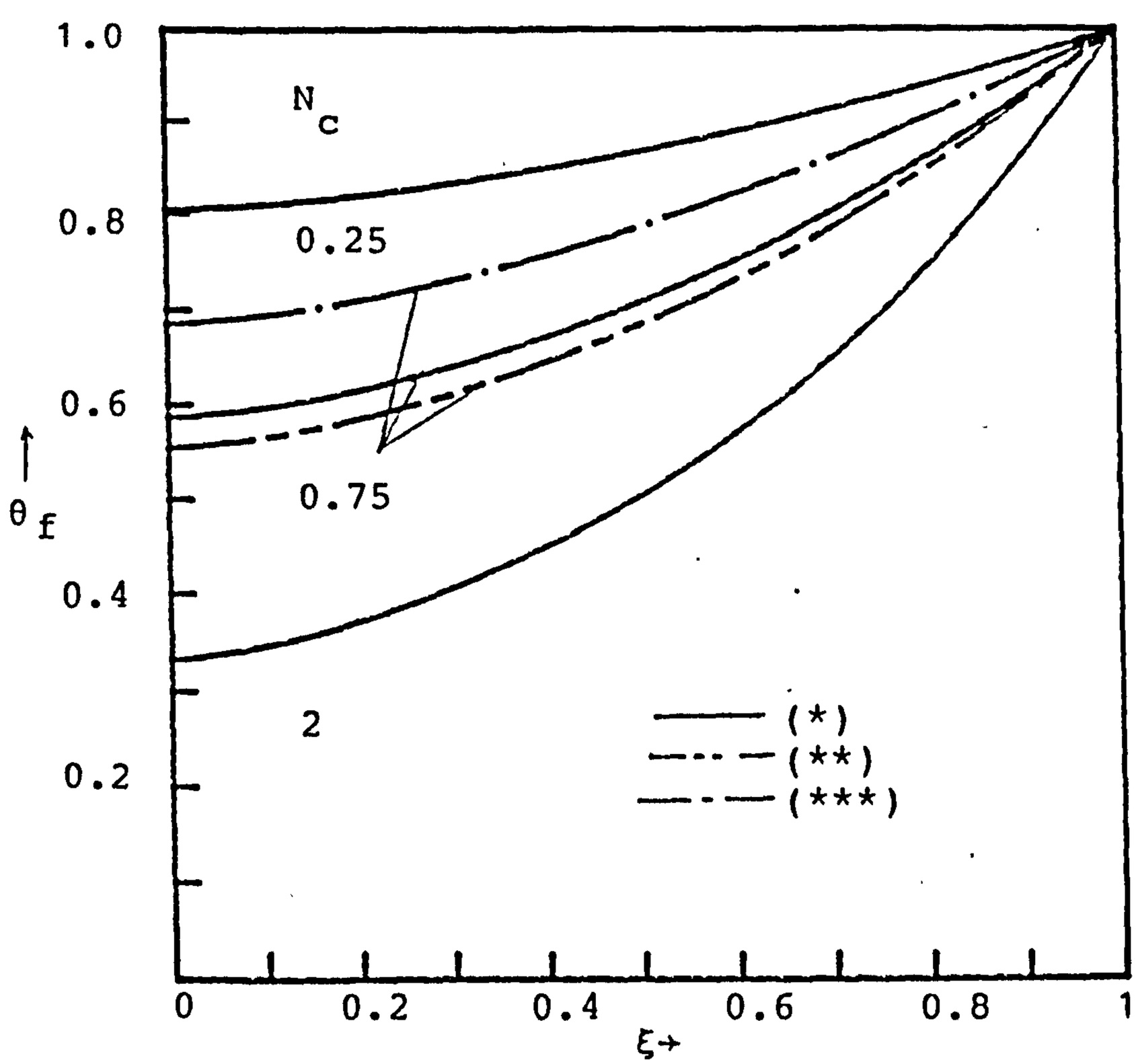

Fig.5-2-7 The temperature distributions of the circular pin for Pr=0.7, λ=1 and various values of N_c.

* : a1=3 ,a2=2 ,N=1 ,C_T=0.5

** : a1=0 ,a2=0 ,N=1 ,C_T=0.5

*** : a1=0 ,a2=0 ,N ⟶ ∞

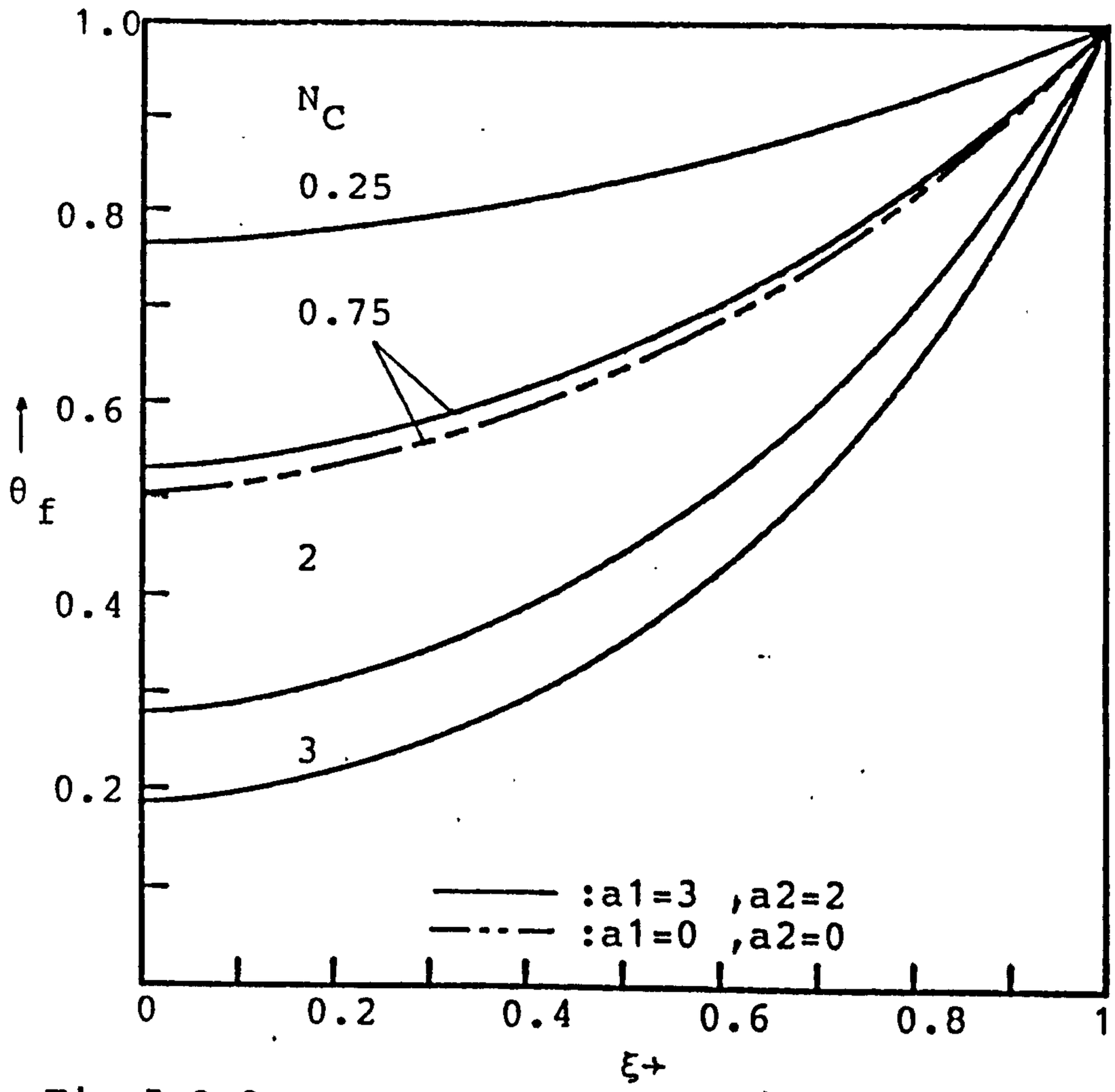

Fig.5-2-8 The temperature distributions of the circular pin for Pr=0.7,N=1,C_T=0.5 λ=2 and various values of N_C.

V-3 Radiative Effect on The Vertical Circular Pin in Conjugated Mixed Convection-Conduction Flow With Temperature Dependent Viscosity

The object of this section is concerned with the vertical circular pin which transfer heat to a surrounding fluid by mixed convection and radiation. The present paper is an extension to the work done in [38] and [43]. Besides, the Newtonian fluid adjacent to the pin is extended to include the variation of the viscosity with temperature.

The conservation equation of the laminar boundary layer and the energy equation of the pin are first transformed into a nondimensional form and their solutions are then simultaneously solved by an efficient finite difference scheme. Numerical results for a vertical pin in the gas having Pr_∞=0.7 with temperature dependent viscosity are performed for the following case: heated wall with To=900^{o}K and T_∞=300^{o}K over a wide range of conjugated convection-conduction parameter N_c=0.25, 0.75, 2 and 3, transverse curvature parameter λ =1 and 2 and buoyancy force parameter Ω =0,1 and 3.

Analysis

Conside a vertical circular pin which is extended from a wall at temperature T_o and situated in a Newtonian flow field with undisturbed oncoming free stream velocity u_∞ and temperature T_∞ . The coordinates parallel and normal to the pin surface are taken to be x and r, respectively. The coordinates system

is in Fig. (5-3-1)

Under the assumption of constant C_p, α, ρ and negligible viscous dissipation, motion pressure and volumetric energy generation along with the application of the boundary layer approximation and Boussinesq approximation, the equations expressing conservation of mass, momentum and energy for the physical model are, respectively, as follows:

$$\frac{\partial(ru)}{\partial x} + \frac{\partial(rv)}{\partial r} = 0 \qquad (5\text{-}3\text{-}1)$$

$$u\frac{\partial u}{\partial x} + v\frac{\partial u}{\partial r} = \frac{1}{r}\frac{\partial}{r}(r\nu\frac{\partial u}{\partial r}) + g\beta(T-T_\infty) \qquad (5\text{-}3\text{-}2)$$

$$u\frac{\partial T}{\partial x} + v\frac{\partial T}{\partial r} = \frac{\alpha}{r}\frac{\partial}{\partial r}(r\frac{\partial T}{\partial r}) - \frac{1}{\rho C_p r}\frac{\partial(r\,q^r)}{\partial r} \qquad (5\text{-}3\text{-}3)$$

where q^r is the net radiative heat flux and the other standard symbols are defined in the nomenclature. The system of equations (5-3-1)-(5-3-3) is subject to the following conditions:

$$\begin{aligned} &u = v = 0, \quad T = T_w(x), \quad &&\text{at} \quad r = r_o \\ &u = u_\infty \quad , \quad T = T_\infty \quad , \quad &&\text{as} \quad r \to \infty \\ &u = u_\infty \quad , \quad T = T_\infty \quad , \quad &&\text{at} \quad x = 0, \; r \geq r_o \end{aligned} \qquad (5\text{-}3\text{-}4)$$

Equations (5-3-1)-(5-3-3) and boundary conditions (5-3-4) do not admit a similarity solution. The nonsimilarity arises from the surface curvature of the cylinder pin and the surface temperature $T_w(x)$, which is undetermined. The pseudo-similarity variable η and the dimensionless streamwise coordinate ξ are introduced as follows:

$$\xi = x/L \ , \qquad \eta = \frac{r^2 - r_o^2}{2r_o L}(Re_{L\infty}/\xi)^{\frac{1}{2}} \tag{5-3-5}$$

where L is the length of the cylinder pin and $Re_{L\infty}$ is the Reynolds number evaluated at the temperature of surrounding, $Re_{L\infty} = u_\infty L/\nu_\infty$.

The dimensionless stream function $f(\xi,\eta)$ and the dimensionless temperature $\theta(\xi,\eta)$ are defined, respectively, by

$$f(\xi,\eta) = \psi(x,r)/\left[r_o(u_\infty L\xi\nu_\infty)^{\frac{1}{2}}\right] \tag{5-3-6}$$

$$\theta(\xi,\eta) = (T-T_\infty)/(T_o-T_\infty) \tag{5-3-7}$$

where the stream function $\psi(x,r)$ satisfies the continuity equation (5-3-1) with

$$ru = \partial\psi/\partial r \ , \qquad rv = -\partial\psi/\partial x \tag{5-3-8}$$

The kinematic viscosity, ν , is assumed to vary with temperature according to a general functional form $\nu = \nu_\infty W(\theta)$, where ν_∞ is the absolute viscosity at the temperature of surrcanding, T_∞ , and therefore $W(0)=1$. The first two terms in a Taylor series expansion of $W(\theta)$ about $\theta = 0$ are taken as

$$W(\theta) = 1 + \left(\frac{dW}{d\theta}\right)\Big|_{\theta=0} + \left(\frac{1}{2!}\frac{d^2W}{d\theta^2}\Big|_{\theta=0}\right)\theta^2$$

$$= 1+a_1\theta + a_2\theta^2 \tag{5-3-9}$$

where a_1, a_2 are the viscosity variation parameters.

By introducing equations (5-3-5)-(5-3-9) into equations (5-3-2)-(5-3-4) and invoking the optically thick limit approximation for the net radiative heat flux q^r,

i.e. $$q^r = -\frac{4\sigma}{3\beta^*}\frac{\partial T^4}{\partial r} \tag{5-3-10}$$

the momentum and energy equations become:

$$[(1+a_1\theta+a_2\theta^2)(1+\lambda\eta\xi^{\frac{1}{2}})f'']' + \frac{1}{2}ff'' + \xi\Omega\theta$$

$$= \xi(f'\frac{\partial f'}{\partial \xi} - f''\frac{\partial f}{\partial \xi}) \qquad (5\text{-}3\text{-}11)$$

$$Pr_\infty^{-1}[(1+\lambda\eta\xi^{\frac{1}{2}})\theta']' + \frac{1}{2}f\theta' + \frac{4[(\theta+C_T)^3\theta'(1+\lambda\eta\xi^{\frac{1}{2}})]'}{3Pr_\infty N}$$

$$= \xi(f'\frac{\partial \theta}{\partial \xi} - \theta'\frac{\partial f}{\partial \xi}) \qquad (5\text{-}3\text{-}12)$$

$$f = f' = 0, \quad \theta = \theta_w \qquad \text{at } \eta = 0 \qquad (5\text{-}3\text{-}13)$$

$$f'=1, \qquad \theta = 0 \qquad \text{as } \eta \to \infty$$

In the foregoing equations, the primes stand for partial deri vatives with respect to η , Pr_∞ is the Prandtl number evaluated at the temperature of surrounding,

$$N = \frac{k\ \beta^*}{4\ \sigma(T_o-T_\infty)^3}, \quad C_T = T_\infty/(T_o-T_\infty),$$

σ is the Stefan-Boltzmann constant, β^* is the extinction coef-ficient, λ is the transverse curvature parameter ($\lambda = 2L/[r_o Re_{L\infty}^{\frac{1}{2}}]$) and Ω is the buoyancy force parameter defined as

$$\Omega = Gr_{L\infty}/Re_{L\infty}^2 \qquad (5\text{-}3\text{-}14)$$

in which $Gr_{L\infty}$ is the Grashof number evaluated at the tempera-ture of surrounding, $Gr_{L\infty} = g\beta(T_o-T_\infty)L^3/\nu_\infty^2$.

Assuming a one-diensional model, the thin pin energy equation allows the temperature distribution along the longi-tudinal direction to be written as

$$\frac{d^2T_f}{dx^2} = \frac{2h^*(x)}{k_f r_o}(T_f-T_\infty) \qquad (5\text{-}3\text{-}15)$$

where k_f is the pin thermal conductivity, T_f is the pin temperature, and h*(x) is the modified local heat transfer coefficient with radiative effect which can be regarded as known from the current boundary layer solution. The associated boundary conditions are:

$$\left.\begin{aligned} T_f &= T_o \quad , \quad \text{at} \quad x = L \\ \frac{dT_f}{dx} &= 0 \quad , \quad \text{at} \quad x = 0 \end{aligned}\right\} \qquad (5\text{-}3\text{-}16)$$

Of particular interest is the thermal coupling between the pin and the thermal boundary layer. The basic coupling is expressed by the requirement that the pin and fluid temperatures and local heat flux be continuous at the pin-fluid interface, at all x-positions.

$$\left.\begin{aligned} t_f(x) &= T_w(x) \\ h^*(T_f - T_\infty) &= -k \frac{\partial T_w}{\partial r} + q^r \end{aligned}\right\} \quad \text{at} \quad r = r_o, \quad 0 \leq x \leq L \qquad (5\text{-}3\text{-}17)$$

Equation (5-3-15) was recast in dimensionless form by the substitutions

$$\xi = x/L \quad , \qquad \theta_f = (T_f - T_\infty)/(T_o - T_\infty) \qquad (5\text{-}3\text{-}18)$$

and combined with equations (5-3-16)-(5-3-17), so that

$$\frac{d^2\theta_f}{d\xi^2} = N_c \hat{h}^* \theta_f \qquad (5\text{-}3\text{-}19)$$

$$\theta_f = 1, \quad \text{at } \xi = 1 \ , \qquad \frac{d\theta_f}{d\xi} = 0, \quad \text{at } \xi = 0 \qquad (5\text{-}3\text{-}20)$$

$$\text{and} \qquad \theta_w = \theta_f \quad , \ h^* = kRe_{L\infty}^{\frac{1}{2}} \hat{h}^*/L, \quad \text{at } \eta = 0 \qquad (5\text{-}3\text{-}21)$$

where N_c is the conjugated convection-conduction parameter

$$N_c = \frac{2kL}{k_f r_o} Re_{L_\infty}^{\frac{1}{2}} \qquad (5\text{-}3\text{-}22)$$

The quantity $\hat{h}^*$ is a dimensionless form of the local mixed convective heat transfer coefficient with radiative effect. The value of $\hat{h}^*$ can be obtained by substituting equations (5-3-5) (5-3-10) and (5-3-18) into equation (5-3-17).

$$\hat{h}^* = -(1+\frac{4(\theta+C_T)^3}{3N})\frac{\partial\theta}{\partial\eta} / (\theta_f \xi^{\frac{1}{2}}), \quad \text{at } \eta = 0 \qquad (5\text{-}3\text{-}23)$$

Numerical Procedure

The solution begins by solving the mixed convective boundary layer problem for a vertical cylinder pin with guessed temperature along the pin surface. The dimensionless heat transfer coefficient $\hat{h}^*$ determined from equation (5-3-23) are than used as input to the pin heat conduction equation (5-3-19). With N_c prescribed, the differential equation (5-3-19) is then solved to yield θ_f. To begin the next cycle of the iterative procedure, the just--determined θ_f is imposed as the thermal boundary condition for the mixed convective boundary layer equations of Newtonian fluid; the solution to which is used as input to the pin heat conduction equation. This procedure of alternatively solving the boundary layer problem and the pin conduction problem was continued until convergence was attained.

The two systems of partial differential equations (5-3-11) -(5-3-12) are coupled. In the present study, these equations were solved by an accurate implicit finite-difference technique

due to Cebeci and Bradshaw [19]. To begin with, the partial differential equations (5-3-11)-(5-3-12) are first converted into a system of first order equations which are then expressed in finite-difference form with the order of $(\Delta\xi)^2$ and $(\Delta\eta)^2$ by approximating the functions and their first derivatives in terms of centered difference and averaged at midpoints of the net segment in the (ξ,η) coordinates. The resulting nonlinear finite-difference equations are then solved by Newton's iterative method.

The boundary layer solutions were obtained by a marching procedure, starting at the leading edge and the grids were divided into 45 points in the streamwise direction and 61 grid points in the cross-stream direction. There was a denser concentration of points near the leading edge to accommodate the initial rapid growth of the boundary layer. Owing to the transverse curvature effect, the transformed boundary layer thickness (η_∞) varies with λ . It is therefore necessary to use a variable grid, rather a uniform grid, normal to the flow.

The conduction equation was solved by using the direct inverse matrix method. The pin equation was also divided into 45 grid points and expressed in finite-difference form. To ensure high accuracy, a nonuniform grid points were employed. For small ξ , a finer ξ subdivision was needed for the boundary layer solution.

Results and Discussion

Numerical results of the overall rate of heat transfer were obtained from the wall into the pin base at ξ =1 or from the integrating heat transfer over the pin surface. The corresponding overall heat transfer rate of these two methods are found to be in agreement. They may be expressed in dimensionless form as:

$$\frac{Q}{r_o k(T_o-T_\infty)Re_{L\infty}^{\frac{1}{2}}} = 2\pi \int_0^1 (-\frac{\partial\theta}{\partial\eta}) [\ 1+\frac{4(\theta+C_T)^3}{3N}]/\xi^{\frac{1}{2}}\ d\xi \quad (5\text{-}3\text{-}24)$$

$$\frac{Q}{r_o k(T_o-T_\infty)Re_{L\infty}^{\frac{1}{2}}} = \frac{2\pi}{N_c} \left.\frac{d\theta_f}{d\xi}\right|_{\xi=1} \quad (5\text{-}3\text{-}25)$$

The results of the overall rate of heat transfer from the pin are presented as a function of the conjugated convection-conduation parameter N_c. The decrease of N_c indicates short pin length, L, great pin conductances, $k_f r_o$ and lower convective coefficient (low k and $Re_{L\infty}$).

The ordinate and abscissa coordinates are replaced by the groups.

$$\frac{Q}{r_o k(T_o-T_\infty)Re_{L\infty}^{\frac{1}{2}}}/\ \lambda = \frac{Q}{2Lk(T_o-T_\infty)} \quad (5\text{-}3\text{-}26)$$

and

$$\frac{2kLRe_{L\infty}^{\frac{1}{2}}}{k_f r_o}/\lambda = kRe_{L\infty}/k_f \quad (5\text{-}3\text{-}27)$$

Since both groups are independent of r_o, it follows that the actual total heat transfer is a function of the transverse curvature. It is observed from Fig.(5-3-3) that an increasing λ gives rise to a larger value of overall heat transfer rate. As the viscosity of fluid is temperature dependent, the viscosity variation parameters a_1, a_2 can be calculated by the procedure of curve fitting and obtain the results that $a_1=3$, $a_2=2$ for the case of $T_o=900^oK$, $T_\infty=300^oK$ and $Pr_\infty=0.7$. For a heated pin, the viscosity of fluid near the pin surface is higher than that of surrounding. So we may find that the total heat transfer rate of the pin in the fluid with temperature dependent viscosity is lower than that in the fluid with constant viscosity (ν_∞). Fig.(5-3-2)-(5-3-3) also show that an increase in Ω or a decrease in N yields an increasing total heat transfer rate Q when the other parameters are fixed. The case with $N \to \infty$ corresponds to nonradiating flow, and N=1 to reasonably strong radiation effects.

Fig.(5-3-2)-(5-3-5) illustrate, respectively, the distribution of the modified local heat transfer coefficient along the pin surface as a function of Nc, a_1, a_2 and Ω for fixed transverse curvature parameters of λ =1 and 2. The modified local heat transfer coefficient can be written, in dimensionless form as

$$\frac{h^*L}{kRe_{L\infty}^{1/2}} = -\left[1+\frac{4(\theta+C_T)^3}{3N}\right]\frac{\partial\theta}{\partial\eta}\Big/(\theta_f\xi^{1/2}) \quad , \quad \text{at } \eta = 0 \qquad (5\text{-}3\text{-}28)$$

It is found that the larger variations of the response of the

modified local heat transfer coefficient $\hat{h}^*$ give rise to larger streamwise variations of the pin surface temperature. In these two figures, it is found that the local heat transfer coefficient do not decrease monotonically in the flow direction, as is usual. Rather, the coefficient decreases at first, attains a minimum, and then increases with increasing downstream distance. This behavior is attributed to an enhanced buoyancy and radiative heat flux resulting from an increase in the wall-to-fluid temperature difference along the stream direction.

The variations of the dimensionless local heat flux at the pin surface are presented in Fig.(5-3-6)-(5-3-7) for different N_c, a_1, a_2, and fixed transverse curvature parameter λ. The local heat flux can be expressed, in dimensionless form, as

$$\frac{qL}{k(T_o-T_\infty)Re_{L\infty}^{\frac{1}{2}}} = -\left[1+\frac{4(\theta+C_T)^3}{3N}\right]\frac{\partial\theta}{\partial\eta}/\xi^{\frac{1}{2}}, \quad \text{at } \eta = 0 \quad (5\text{-}3\text{-}29)$$

Fig.(5-3-6)-(5-3-7) show that for a given transverse curvature the total heat transfer rate from the pin surface is increased as N_c decreased, which agrees with the prediction in Fig.(5-3-2)-(5-3-3)

It is shown in Fig.(5-3-4)-(5-3-7) that the modified local heat transfer coefficient and local heat flux increase with increasing buoyancy force parameter Ω or transverse curvature parameter λ when the other parameters are fixed. Fig.(5-3-4)-(5-3-7) also illustrate that the modified local heat transfer coefficient and local heat flux of the heated pin in the fluid with temperature dependent viscosity are lower than those in the fluid with constant fluid viscosity of surrounding.

Representative results for the pin temperature distribution are presented in Fig.(5-3-8)-(5-3-9) for two different transverse curvature cases. Each case contains the pin temperature distribution as a function of N_c, a_1, a_2 and Ω. Fig. (5-3-8)-(5-3-9) shown the expected trend whereby the pin temperature decreases monotonically from the root to the tip. The two figures also confirms the assertions that larger values of N_c,λ and Ω give rise to larger pin timperature varitations. It is observed from Fig.(5-3-8)-(5-3-9) that the surface temperature of heated pin in the fluid with constant viscosity (ν_∞) give a larger variation in the streamwise direction than that of the same pin in the fluid with temperature dependent viscosity when the other parameters are fixed.

Remark

The analysis of present paper has yielded the results of heated vertical circular pin for mixed forced and free convective boundary layer flow with radiative effect. The optically thick limit approximation for the radiative heat flux is assumed. Although the range of the validity of the optically thick limit approximation is small in the boundary layer flow, it possesses the advantage of simiplicity in the analysis because the governing energy equation can be transformed into an ordinary differential equation by the conventional similarity transformation. The exact solutions of the pin surface temperature should lie between those for the nonradiating case and the optically thick limit approximation. In order to solve simultaneously the coupled

pin conduction equation and the thermal boundary layer equations of fluid, a very efficient "Box" scheme is employed here. From the numerical results we may find that the overall heat transfer rate increasing with decreasing radius of the cylinder pin, which agrees with behavior in [39] and [43].

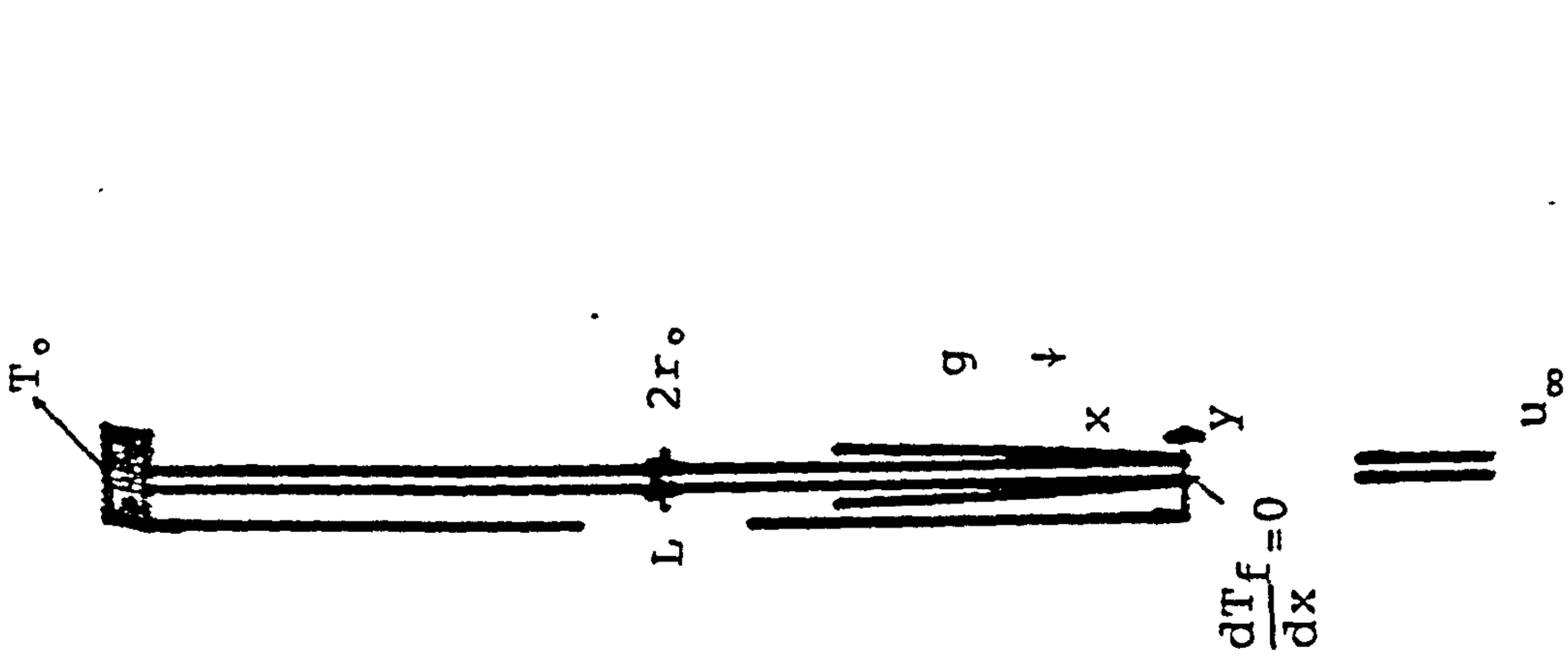

Fig.5-3-1 Coordinate system.

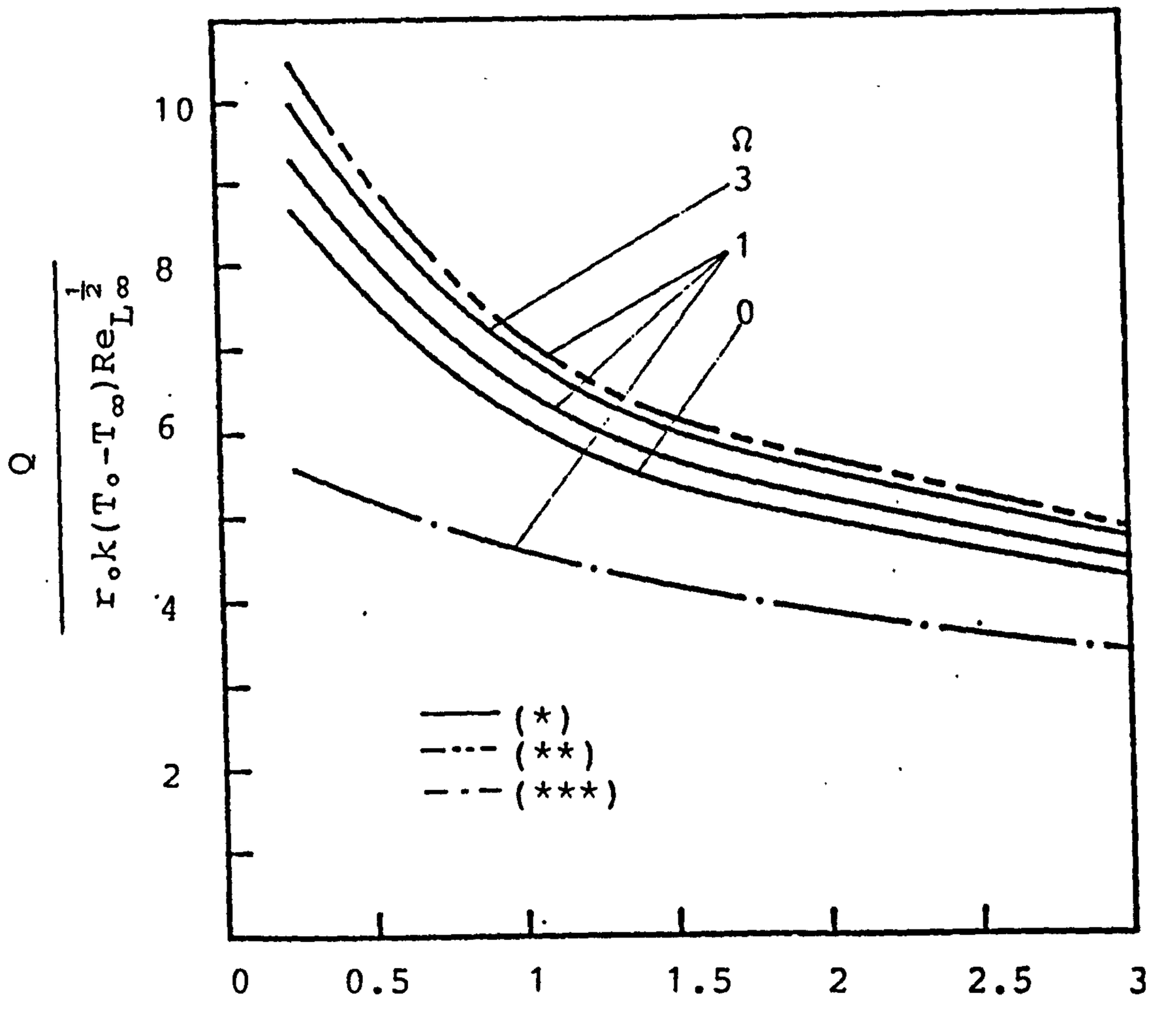

Fig.5-3-2 The total heat transfer rate of the circular cylinder for $P_{r\infty}$=0.7 and λ =1.

* :a1=3,a2=2,N=1,C_T=0.5

** :a1=0,a2=0,N=1,C_T=0.5

*** :a1=0,a2=0,N → ∞

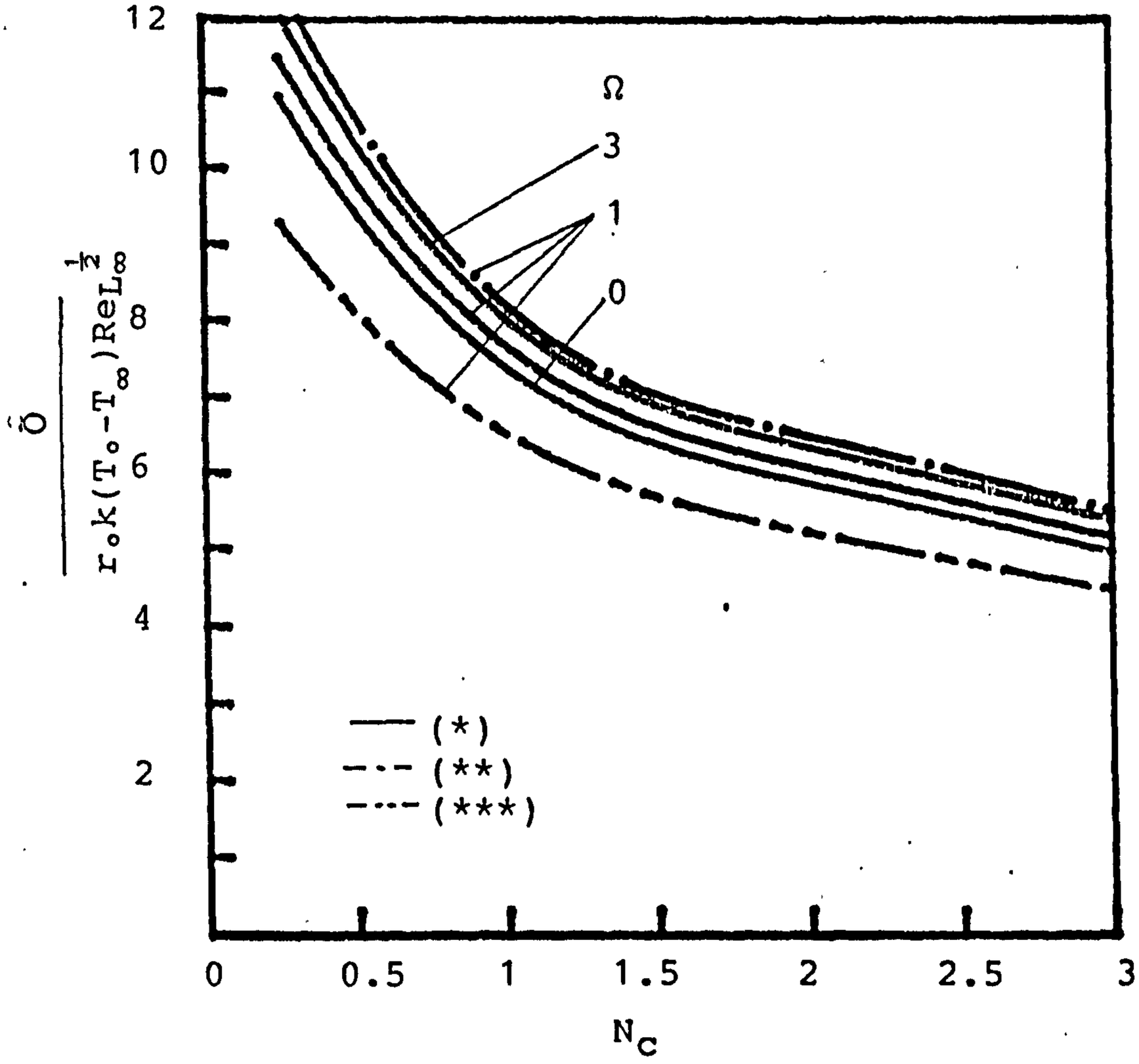

Fig.5-3-3 The total heat transfer rate of the circular cylinder for Pr_∞=0.7, C_T=0.5 and N=1.

* :a1=3, a2=2, λ=2

** :a1=0, a2=0, λ=2

*** :a1=3, a2=2, λ=1

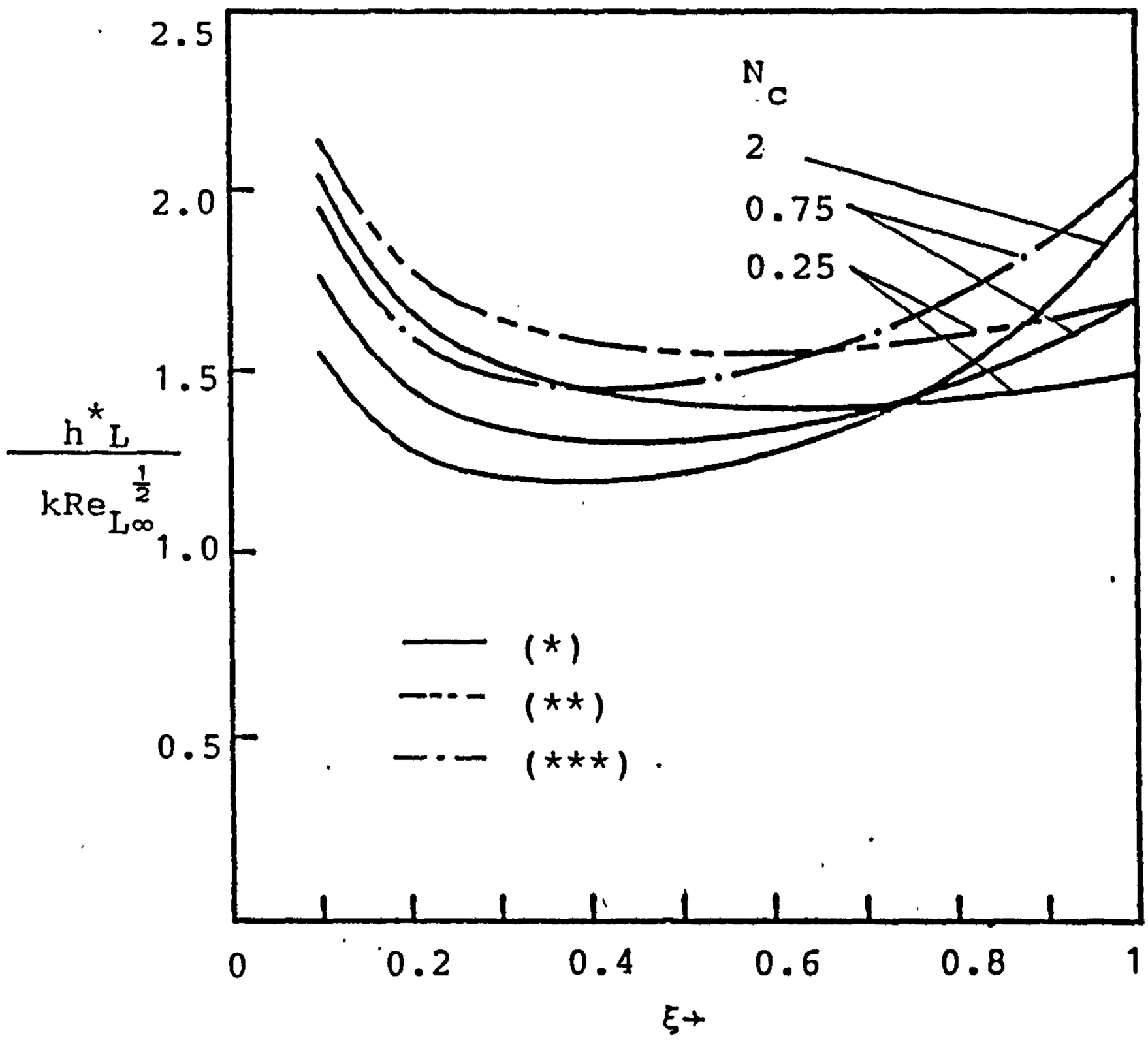

Fig.5-3-4 The modified local heat transfer coefficients of the circular cylinder for Pr_∞=0.7, λ=1, N=1 and C_T=0.5.

* :a1=3, a2=2, Ω=1.

** :a1=3, a2=2, Ω=3.

*** :a1=0, a2=0, Ω=1.

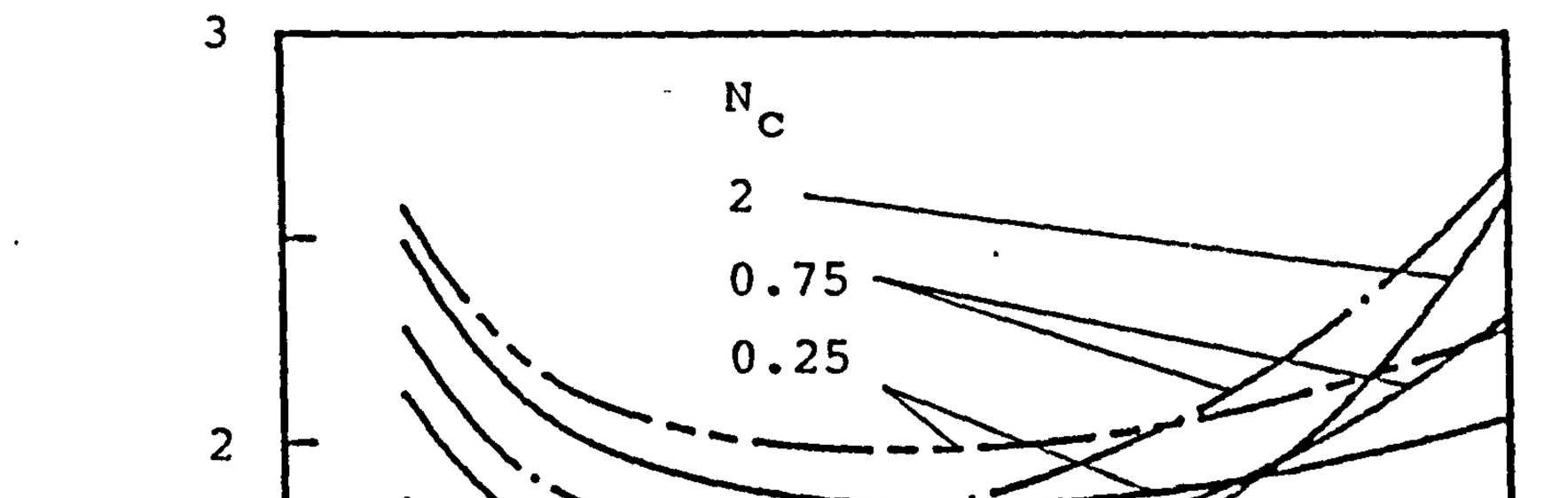

Fig.5-3-5 The modified local heat transfer coefficients of the circular cylinder for Pr_∞=0.7, λ=2, N=1 and C_T=0.5.

* :a1=3, a2=2, Ω=1.

** :a1=3, a2=2, Ω=3.

*** :a1=0, a2=0, Ω=1.

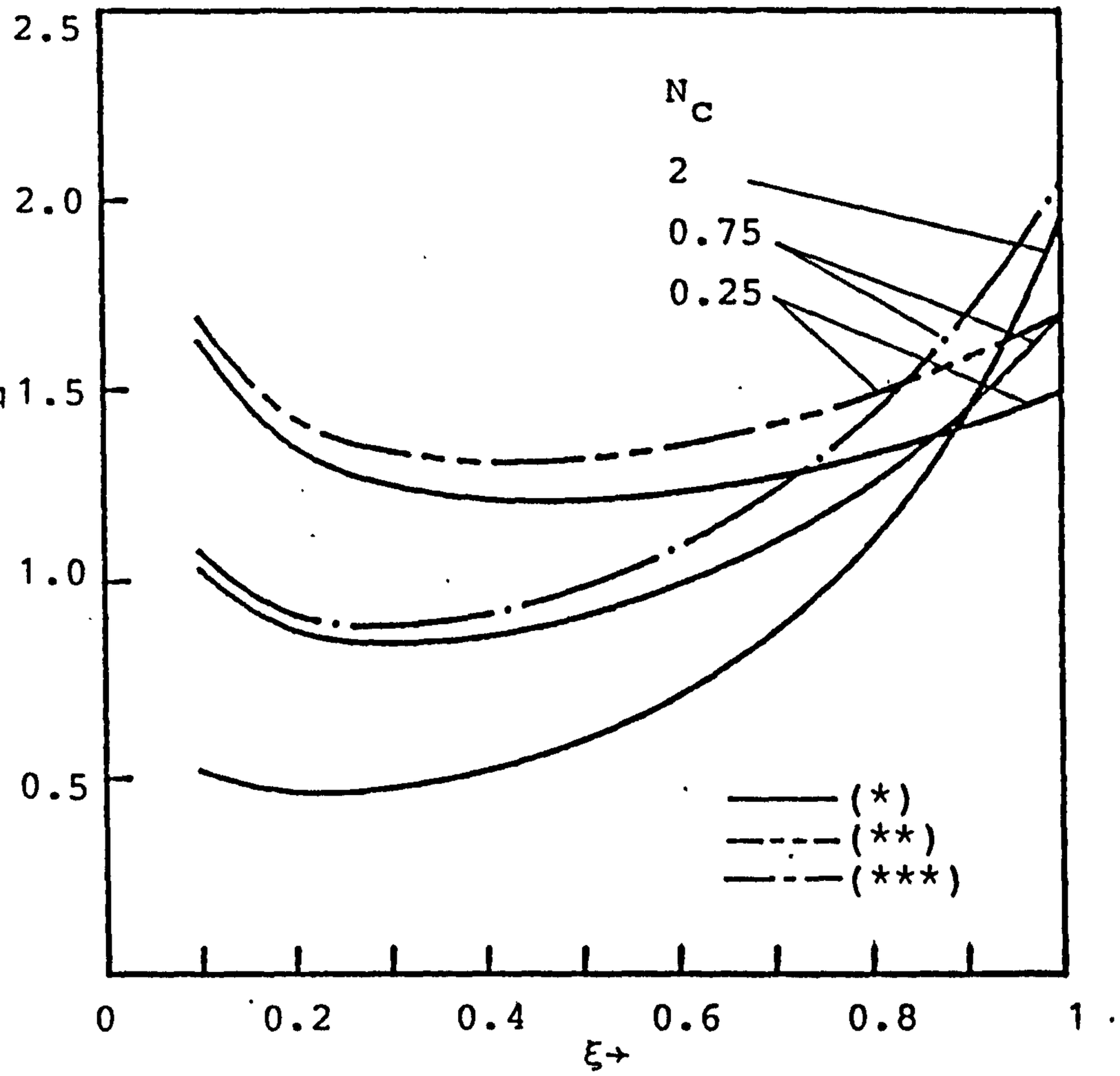

Fig.5-3-6 The local heat flux of the circular cylinder for Pr_∞=0.7, λ=1, N=1 and C_T=0.5.

* :a1=3, a2=2, Ω=1.

** :a1=3, a2=2, Ω=3.

*** :a1=0, a2=0, Ω=1.

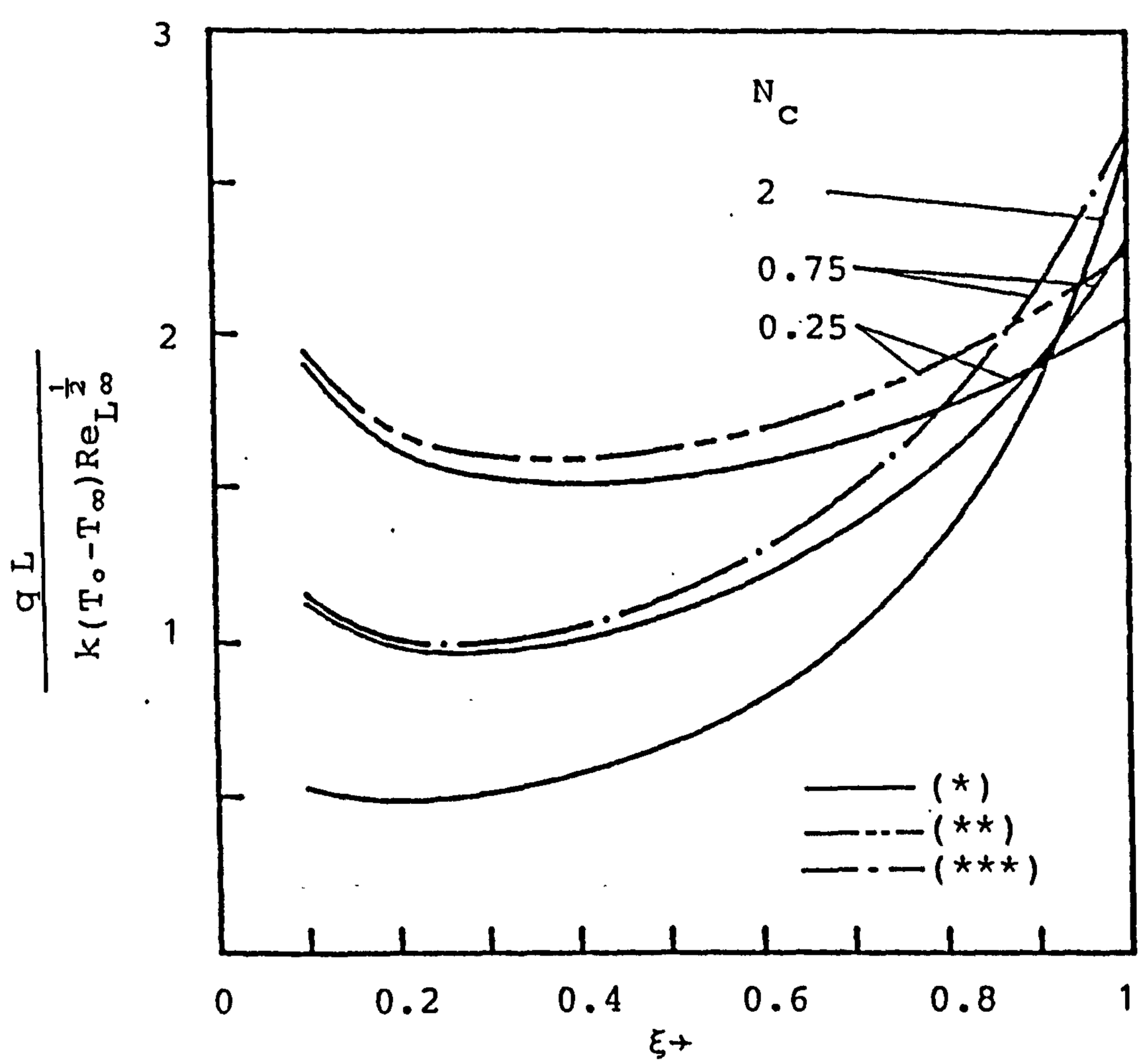

Fig.5-3-7 The local heat flux of the circular cylinder for Pr_∞=0.7, λ=2,N=1 and C_T=0.5.

* :a1=3,a2=2,Ω=1.

** :a1=3,a2=2,Ω=3.

*** :a1=0,a2=0,Ω=1.

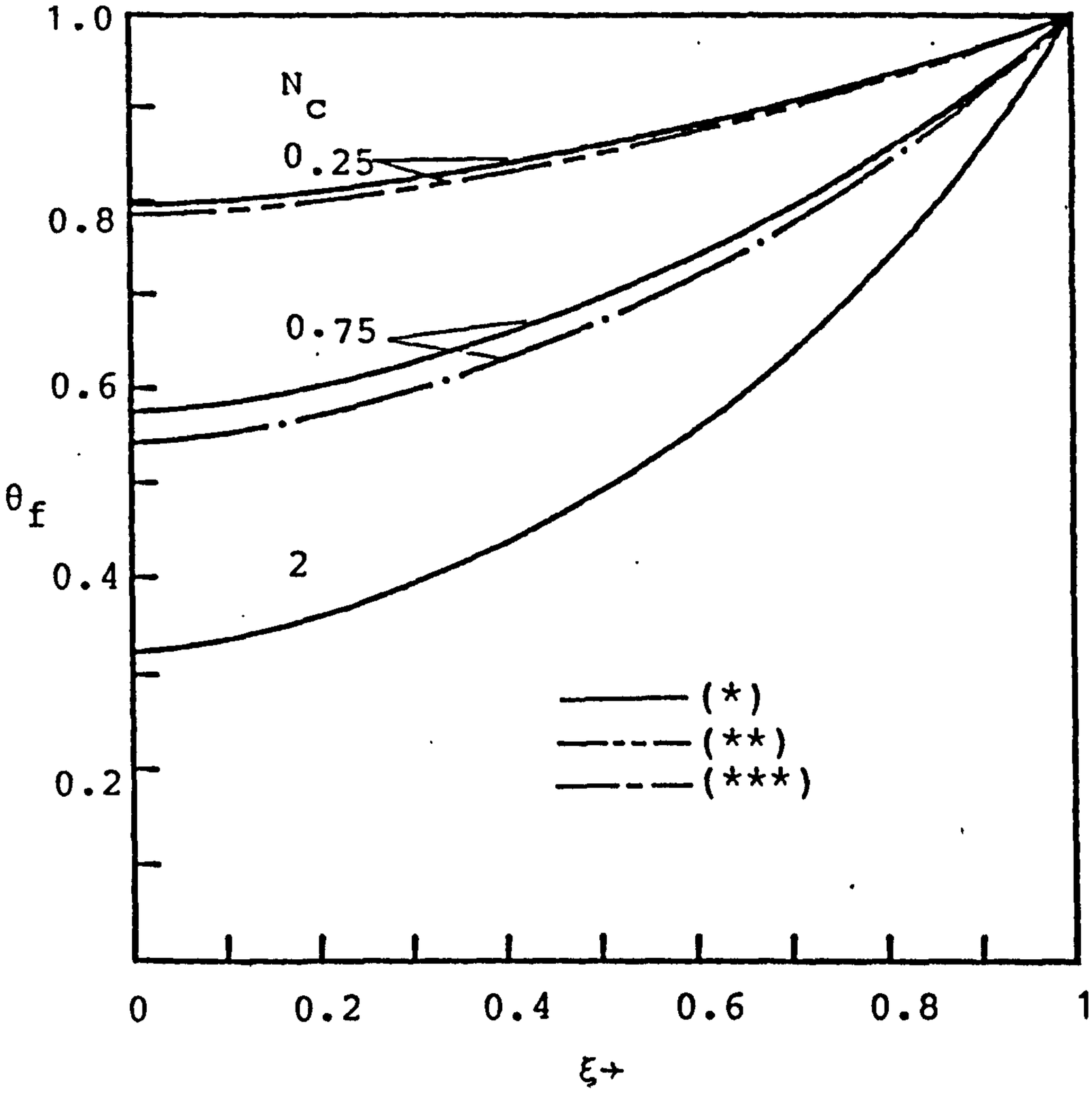

Fig.5-3-8 The temperature distributions of the circular cylinder for Pr_∞=0.7, λ=1, N=1 and C_T=0.5.

* :a1=3,a2=2,Ω=1.

** :a1=3,a2=2,Ω=3.

*** :a1=0,a2=0,Ω=1.

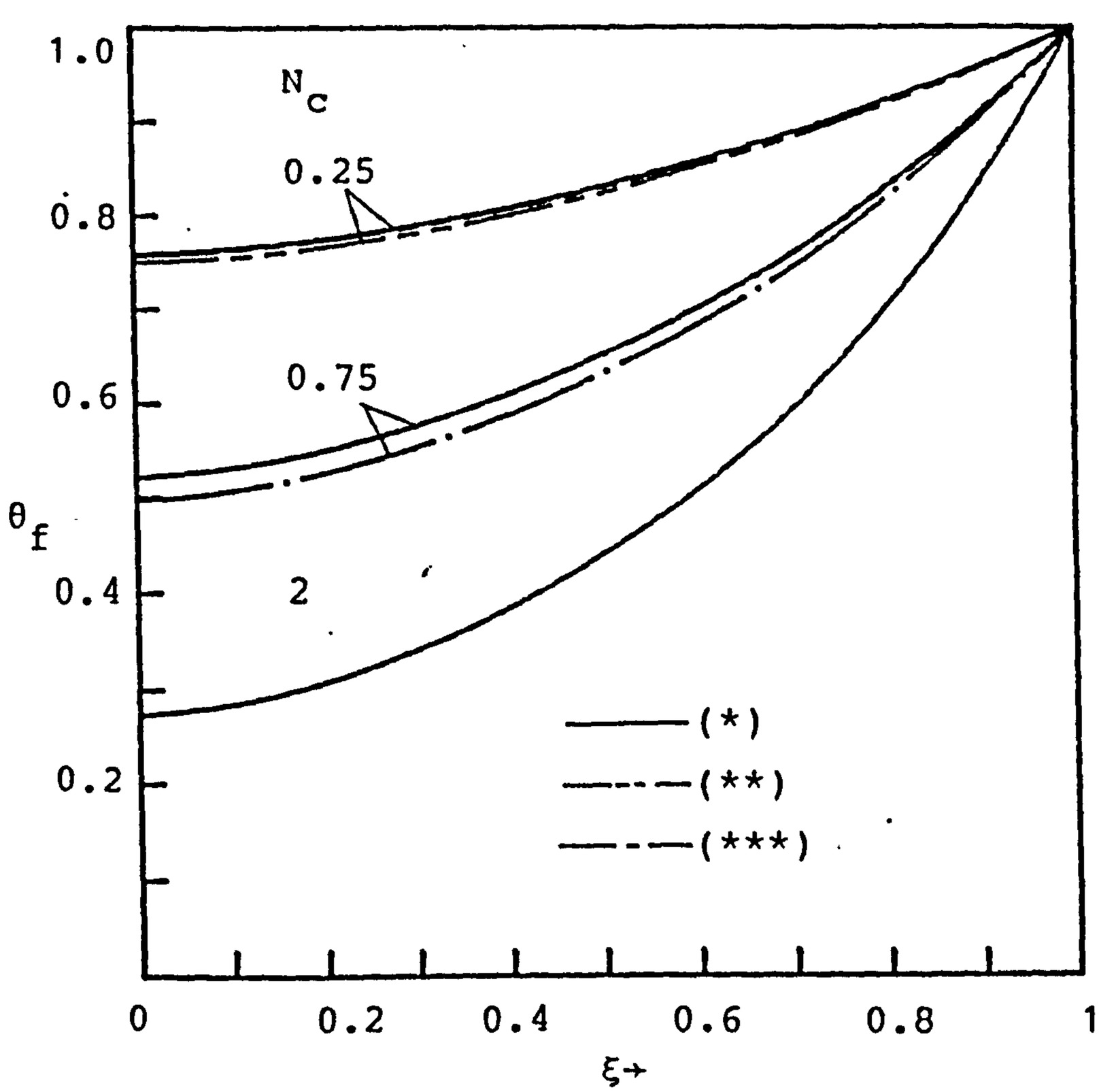

Fig.5-3-9 The temperature distributions of the circular cylinder for Pr_∞=0.7, λ=2, N=1 and C_T=0.5.

* :a1=3,a2=2,Ω=1.

** :a1=3,a2=2,Ω=3.

*** :a1=0,a2=0,Ω=1.

VI. STEADY TURBULENT FLOW CONVECTION-CONDUCTION CASES IN A VERTICAL EXTENDED SURFACE

In the conventional method to deal with the characteristics of vertical plate fin, the constant convective heat transfer coefficient is assumed along the fin surface. However, there is substantial variations along the fin which has been proved by Sparrow and Acharya [15] for laminar natural convection and Sparrow and Chyu [16] for laminar forced convection.

The analysis of present chapter is for a vertical plate fin (or, vertical circular pin) with a nonuniform temperature distribution which is strongly affected by the heat transfer coefficient, the heat transfer coefficient is decided by the ambient turbulent flow. The transition point was assumed at $R_{xtr}=5x10^5$. Hence, in order to determine the temperature distribution of the plate fin (or pin) it must be coupled with the convective boundary layer flow. It becomes more complicated.

The conservation equation of the turbulent boundary layer and the energy equation of the fin are first transformed into a nondimensional form and their solutions are then simultaneously solved by an efficient implicit finite difference method. In this study we use the eddy viscosity formulation for forced convection flow developed by Cebeci and Smith [29].

The fin temperature distribution, which is not known a priori, serves as a boundary condition for the boundary layer

equation. The solutions of the local heat transfer coefficient along the fin surface from the boundary layer equation is re-substituting into the fin energy equation as known, then repeatly searched for the new temperature distribution of the fin surface. This new temperature distribution is then imposed as the surface boundary condition for the boundary layer equation, the solution of which is used to evaluate an updated h and so on until the maximum difference of temperature between the successive cycles is less than some given small value.

VI-1 Vertical Plate Fin with Conjugated Forced Convection-Conduction Turbulent Flow

Numerical calculations of local heat transfer coefficients are presented in this section for steady turbulent forced convection flow over a vertical plate fin. The local heat transfer coefficient is solved simultaneously with the convective boundary layer equations of fluid and the heat conduction equation of fin. The eddy-diffusivity formulas used by Cebeci and Smith are utilized to model the Reynolds stresses. An implicit finite difference method is employed. The physical model of this problem is illustrated in Fig.(6-1-1). A vertical fin is of length L and thickness 2δ which is extended from a wall at temperature To and situated in a uniform free stream having temperature T_∞ and velocity u_∞. Numerical results are presented for Pr=0.7, Prt=0.9, U = 150m/s, $\nu=9.5\ 10^{-6}\ m^2/s$, L=0.05m and $R_{xtr}=5\times10^5$ over a conjugated convection-conduction parameters of Nc=0.75, 2, 8 and 20.

Analysis

The present study is concerned with the turbulent eddy effect on convection along the fin surface. Consider now a vertical fin which is alighed parallel to a uniform free stream. Let x and y denote, respectively, the streamwise and normal coordinates. The conservation equations for turbulent boundary layer over a vertical fin are given as follows

$$\frac{\partial u}{\partial x} + \frac{\partial v}{\partial y} = 0 \qquad (6\text{-}1\text{-}1)$$

$$u\frac{\partial u}{\partial x} + v\frac{\partial u}{\partial y} = \frac{\partial}{\partial y}\left((\nu+\varepsilon_m)\ \frac{\partial u}{y}\right) \qquad (6\text{-}1\text{-}2)$$

$$u\frac{\partial T}{\partial x} + v\frac{\partial T}{\partial y} = \frac{\partial}{\partial y}\left((\ \alpha+\varepsilon_h)\ \frac{\partial T}{\partial y}\right) \qquad (6\text{-}1\text{-}3)$$

where u and v are the streamwise and normal velocity components, respectively, T is the temperature of the fluid, α is the thermal diffusivity, ν is the kinematic viscosity, ε_m is the eddy viscosity and ε_h is the eddy diffusivity..

The system of equations (6-1-1)-(6-1-3) is subject to the following boundary conditions

$$\left.\begin{array}{llll} u = v = 0, & T = T_w(x) & \text{at} & y = 0 \\ u = u_\infty\ , & T = T_\infty & \text{as} & y \to \infty \end{array}\right\} \qquad (6\text{-}1\text{-}4)$$

Equations (6-1-1)-(6-1-3) and boundary conditions (6-1-4) do not admit a simiarity solution. The nonsimilarity arises from the eddy viscosity, eddy diffusivity and the surface temperature, $T_w(x)$, which is undetermined. The pseudo-similarity variable η and the dimensionless streamwise coordinate ξ are introduced as follows:

$$\xi = \frac{x}{L}, \qquad \eta = \left(\frac{y}{L}\right)\ ReL^{1/2}/\xi^{1/2} \qquad (6\text{-}1\text{-}5)$$

where L is the fin length and ReL is the Reynold number, $\frac{u_\infty L}{\nu}$.

The dimensionless stream function $f(\xi,\eta)$ and the dimensionless temperature $\theta(\xi,\eta)$ are defined, respectively, by

$$f(\xi,\eta) = \psi(x,y)/(u_\infty \nu L \xi)^{\frac{1}{2}} \qquad (6\text{-}1\text{-}6)$$

$$\theta(\xi,\eta) = (T - T_\infty)/(T_o - T_\infty) \qquad (6\text{-}1\text{-}7)$$

where the stream function $\psi(x,y)$ satisfies the continuity equation (6-1-1) with

$$u = \frac{\partial \psi}{\partial y} \quad \text{and} \quad v = -\frac{\partial \psi}{\partial x} \qquad (6\text{-}1\text{-}8)$$

Introducing equations (6-1-5)-(6-1-8) into equations (6-1-2)-(6-1-4) gives

$$(f''(1+\varepsilon_m^+))' + \frac{1}{2} f f'' = \xi\left(f' \frac{\partial f'}{\partial \xi} - f'' \frac{\partial f}{\partial \xi}\right) \qquad (6\text{-}1\text{-}9)$$

$$(\theta'(Pr^{-1} + \varepsilon_h^+))' + \frac{1}{2} f \theta' = \xi\left(f' \frac{\partial \theta}{\partial \xi} - \theta' \frac{\partial f}{\partial \xi}\right) \qquad (6\text{-}1\text{-}10)$$

$$\left.\begin{aligned} f = f' = 0, \quad \theta = \theta_w(\xi) \quad & \text{at } \eta = 0 \\ f' = 1, \quad \theta = 0 \quad & \text{as } \eta \to \infty \end{aligned}\right\} \qquad (6\text{-}1\text{-}11)$$

In the foregoing equations, the primes stand for partial derivatives with respect to η, Pr is the prandtl number, ε_m^+ is the ratio of eddy viscosity to kinematic viscosity and ε_h^+ is the ratio of eddy conductivity to kinematic viscosity.

Assuming a one-dimensional model, the thin fin energy equation allows the temperature distribution along the longitudinal direction to be written as

$$\frac{d^2 Tf}{dx^2} = \frac{h(x)}{k_f \delta} (T_f - T_\infty) \qquad (6\text{-}1\text{-}12)$$

where k_f is the fin thermal conductivity, T_f is the fin temperature, and h(x) is the local heat transfer coefficient which

can be regarded as known from the current boundary layer solution. The associated boundary conditions are

$$\left.\begin{aligned} T_f &= T_o \quad \text{at} \quad x = L \\ \frac{dT_f}{dx} &= 0 \quad \text{at} \quad x = 0 \end{aligned}\right\} \tag{6-1-13}$$

of particular interest is the thermal coupling between the fin and the convective boundary layer. The basic coupling is expressed by the requirement that the fin and fluid temperatures and heat fluxes be continuous at the fin-fluid interface at all ξ.

$$T_f = T_w \quad \text{and} \quad -k\frac{\partial T}{\partial y} = h(T_f - T_\infty), \text{ at } y = 0 \tag{6-1-14}$$

Equation (6-1-12) was recast in dimensionless form by the substitutions.

$$\xi = \frac{x}{L}, \qquad \theta_f = \frac{T_f - T_\infty}{T_o - T_\infty} \tag{6-1-15}$$

and combined with equations (6-1-13) and (6-1-14) so that

$$\frac{d^2\theta_f}{d\xi^2} = Nc\ \hat{h}\ \theta_f \tag{6-1-16}$$

$$\left.\begin{aligned} \theta_f &= 1 \quad \text{at} \quad \xi = 1 \\ \frac{d\theta_f}{d\xi} &= 0 \quad \text{at} \quad \xi = 0 \end{aligned}\right\} \tag{6-1-17}$$

$$\text{and} \qquad \theta_w = \theta_f, \qquad h = k\ ReL^{\frac{1}{2}}\ \hat{h}/L \tag{6-1-18}$$

where Nc is the conjugated convection-conduction parameter

$$Nc = \frac{kL}{k_f\ \delta}\ ReL^{\frac{1}{2}} \tag{6-1-19}$$

The quantity $\hat{h}$ is a dimensionless form of the local forced convective heat transfer coefficient. The value of h is obtained by substituting equation (6-1-5) and (6-1-15) into equation (6-1-14).

$$\hat{h} = -\frac{\partial\theta}{\partial\eta} / (\theta_f \xi^{\frac{1}{2}}), \qquad \text{at } \eta = 0 \tag{6-1-20}$$

Eddy Diffusivity Formulas

Cebeci and Smith (1974) [29]reported an algebraic viscosity formulation for use with external wall boundary layers. It is based on a Van Driest approach to the inner region, with a damped law of the wall, and on a velocity defect approach to the outer region.

$$\varepsilon_m = \begin{cases} \varepsilon_{mi} = \{ 0.4y(1-\exp(-y/\bar{A})) \}^2 \left|\frac{\partial u}{\partial y}\right| \gamma_{tr} & \varepsilon_{mi} \leq \varepsilon_{mo} \\ \varepsilon_{mo} = 0.0168 \left| \int_0^\infty (u_\infty - u)\, dy \right| \gamma_{tr} & \varepsilon_{mi} \geq \varepsilon_{mo} \end{cases} \tag{6-1-21}$$

where $\bar{A} = 26\nu(\tau_w/\rho)^{-\frac{1}{2}}$, $\gamma_{tr} = 1-\exp(-G(x-X_{tr}) \int_{X_{tr}}^{x} \frac{dx}{u_\infty})$

and $G = \frac{1}{1200} \frac{u\infty^3}{\nu^2} Rx_{tr}^{-1.34}$

we choose the turbulent Prandtl expression of Jischa and Rieke [34], which is

$$P_{rt} = \frac{\varepsilon m}{\varepsilon_h} = a + b(Pr + 1)/ Pr \tag{6-1-22}$$

with experiment giving a=0.825 and b=0.0309, a result fitting data for air (Pr=0.7) quite well.

Numerical Solution

The solution begins by solving the forced convective boundary layer problem for a vertical plate with guessed temperature for all ξ . The dimensionless heat transfer coefficients $\hat{h}$ determined from this solution in accordance with equation (6-1-20) are then used as input to the fin heat conduction equation (6-1-16). With Nc prescribed, the differential equation (6-1-16) is then solved to yield θ_f. To begin the next cycle of the iterative procedure, the just determined θ_f is imposed as the thermal boundary condition for the forced convective boundary layer problem. The solutions of the boundary layer problem yield a new $\hat{h}$ distribution which is used as input to the fin heat conduction equation. This procedure of alternately solving the boundary layer problem and the fin conduction problem was continued until convergence was attained.

The two systems of partial differential equations (6-1-9), (6-1-10) are solved by an accurate implicit finite difference technique [19]. To begin with, the partial differential equations (6-1-9), (6-1-10) are first converted into a system of first order equations which are then expressed in finite difference form by approximating the functions and their first derivatives in terms of centred difference and averaged at midpoint of the net segments in the (ξ,η) coordinates. The resulting nonlinear finite difference equations are then solved by Newton's iterative method. The boundary layer so-

lutions were obtained by a marching procedure, starting at the leading edge ($\xi=0$) and the grids were divided into 45 points in the streamwise direction. There was a denser concentration of points near the leading edge to accommodate the initial rapid growth of the boundary layer.

In order to write the system in terms of a first order system of partial differential equations, we introduce new dependent variables $\bar{u}(\xi,\eta)$, $\bar{v}(\xi,\eta)$ and $\omega(\xi,\eta)$ are introduced, so that equation (6-1-9) and (6-1-10) can be written

$$f' = \bar{u} \tag{6-1-23}$$

$$\bar{u}' = \bar{v} \tag{6-1-24}$$

$$\theta' = \omega \tag{6-1-25}$$

$$(b\bar{v})' + \frac{1}{2}f\bar{v} = \xi(\bar{u}\frac{\partial u}{\partial \xi} - \bar{v}\frac{\partial f}{\partial \xi}) \tag{6-1-26}$$

$$(Pr^{-1} - Prt^{-1})\omega' + Prt^{-1}(b\omega)' + \frac{1}{2}f\omega = \xi(\bar{u}\frac{\partial \theta}{\partial \xi} - \omega\frac{\partial f}{\partial \xi}) \tag{6-1-27}$$

where $b = (1 + \varepsilon_m^+)$

Next consider the net rectangle shown in Fig.(6-1-2) and denote the net points by

$$\begin{aligned} \xi_o &= 0, \quad \xi_n = \xi_{n-1} + k_n, \quad n = 1, 2, 3, \ldots N \\ \eta_o &= 0, \quad \eta_i = \eta_{j-1} + h_j, \quad j = 1, 2, 3, \ldots J \\ \eta_J &\equiv \eta_\infty \end{aligned} \tag{6-1-28}$$

Approximate the Quantities (f, $\bar{u}$, $\bar{v}$, θ, ω) at points (ξ_n, η_j) of the net by net functions denoted by (f_j^n, $\bar{u}_j^n$, $\bar{v}_j^n$, θ_j^n, ω_j^n) and employ the following notation, for points and quantities midway between net points and for net function m_j^n;

$$\xi_{n-\frac{1}{2}} \equiv \frac{1}{2}\,(\xi_n + \xi_{n-1}), \qquad \eta_{j-\frac{1}{2}} \equiv \frac{1}{2}\,(\eta_j + \eta_{j-1})$$

$$m_j^{n-\frac{1}{2}} \equiv \frac{1}{2}\,(m_j^n + m_j^{n-1}), \qquad m_{j-\frac{1}{2}}^n \equiv \frac{1}{2}\,(m_j^n + m_{j-1}^n) \tag{6-1-29}$$

The difference equations that are to approximate (6-1-23)-(6-1-27) are now easily formulated by considering one mesh rectangle as in figure (6-1-2). We approximate (6-1-23) to (6-1-25) using centered difference quotients and average about the midpoint $(\xi_n, \eta_{j-\frac{1}{2}})$ of the segment P_2P_4, with the following results:

$$(f_j^n - f_{j-1}^n)\, h_j^{-1} = \bar{u}_{j-\frac{1}{2}}^n \tag{6-1-30}$$

$$(\bar{u}_j^n - \bar{u}_{j-1}^n)\, h_j^{-1} = \bar{v}_{j-\frac{1}{2}}^n \tag{6-1-31}$$

$$(\theta_j^n - \theta_{j-1}^n)\, h_j^{-1} = \omega_{j-\frac{1}{2}}^n \tag{6-1-32}$$

Similarly (6-1-26) and (6-1-27) are approximated by centering on the midpoint $(\xi_{n-\frac{1}{2}}, \eta_{j-\frac{1}{2}})$ of the rectangle $P_1P_2P_3P_4$, which gives

$$\frac{b_j^{n-n}\bar{v}_j^n - b_{j-1}^n \bar{v}_{j-1}^n}{h_j} + \frac{1}{2}(f\bar{v})_{j-\frac{1}{2}}^n + \alpha_n(\bar{v}^n f^n - \bar{v}^n f^{n-1} + \bar{v}^{n-1} f^n - (\bar{u}^2)^n)_{j-\frac{1}{2}}$$
$$= R_{j-\frac{1}{2}}^{n-1} \tag{6-1-33}$$

$$(Pr^{-1} - Prt^{-1})\frac{\omega_j^n - \omega_{j-1}^n}{h_j} + P_{rt}^{-1}\left(\frac{b_j^n \omega_j^n - b_{j-1}^n \omega_{j-1}^n}{h_j}\right) + \left(\frac{1}{2} + \alpha_n\right)$$

$$(f\omega)_{j-\frac{1}{2}}^n + \alpha_n(-(\bar{u}\theta)^n - \bar{u}^{n-1}\theta^n + \bar{u}^n\theta^{n-1} + \omega^{n-1}f^n - \omega^n f^{n-1})_{j-\frac{1}{2}}$$

$$= Y_{j-\frac{1}{2}}^{n-1} \tag{6-1-34}$$

where

$$\alpha_n = \frac{\xi^{n-\frac{1}{2}}}{kn}$$

$$R_{j-\frac{1}{2}}^{n-1} = \alpha_n \left((\bar{fv})_{j-\frac{1}{2}}^{n-1} - (\bar{u}^2)_{j-\frac{1}{2}}^{n-1} \right) - \left(\frac{b_j \bar{v}_j - b_{j-1} \bar{v}_{j-1}}{h_j} + \frac{1}{2} (\bar{fv})_{j-\frac{1}{2}} \right)^{n-1}$$

$$Y_{j-\frac{1}{2}}^{n-1} = \alpha_n \left((\omega f)_{j-\frac{1}{2}}^{n-1} - (\bar{u}\theta)_{j-\frac{1}{2}}^{n-1} \right) - \left((Pr^{-1} - P_{rt}^{-1}) \left(\frac{\omega_j - \omega_{j-1}}{h_j} \right) + \right.$$

$$\left. P_{rt}^{-1} \left(\frac{b_j \omega_j - b_{j-1} \omega_{j-1}}{h_j} \right) + \frac{1}{2} (f\omega)_{j-\frac{1}{2}} \right)^{n-1} \qquad (6\text{-}1\text{-}35)$$

Equations (6-1-30)-(6-1-34) are imposed for j=1,2,3...J. The boundary conditions (6-1-11) can be written as

$$f_o^n = 0, \quad \theta_o^n = \theta_w^n, \quad \bar{u}_o^n = 0, \quad \bar{u}_J^n = 1, \quad \theta_J^n = 0 \qquad (6\text{-}1\text{-}36)$$

If it is assumed that $(f_j^{n-1}, \bar{u}_j^{n-1}, \bar{v}_j^{n-1}, \theta_j^{n-1}, \omega_j^{n-1})$ are known for $0 \leq j \leq J$, then (6-1-30)-(6-1-34) and boundary conditions (6-1-36) yield an implicit nonlinear algebraic system of 5J+5 equations in as many unknown $(f_j^n, \bar{u}_j^n, \bar{v}_j^n, \theta_j^n, \omega_j^n)$. The system can be solved very efficiently by using Newton's method. The important observations are that the linearized equations obtained by applying Newton's method to (6-1-30)-(6-1-34) and (6-1-36) form a block tridiagonal system (with 5x5 blocks) and that system can be solved very efficiently by the procedure discussed in refs. [19]

For most laminar flows the transformed boundary layer thick-

ness is essentially constant. However, in turbulent flow in which the eddy effect is important, the transformed boundary-layer thickness (η_∞) varies with increasing ξ. To maintain the computation accuracy, it is necessary to use a variable grid, rather than a uniform grid, normal to the flow.

The net in the η-direction reported here is a geometric progression having the properity that the ratio of lengths of any two adjacent intervals is a constant; that is $h_j = Mh_{j-1}$. The distance to the j-th line is given by the following formula:

$$\eta_j = h_1 \frac{M^j - 1}{M-1}, \quad j + 1, 2, \ldots J, \qquad M > 1 \qquad (6\text{-}1\text{-}36)$$

There are two parameters: h_1, the length of the first $\Delta\eta$-step, and M, the ratio of two successive steps. The total number of points J can be calculated by the following formula:

$$J = \frac{\ln[1+(M-1)(\eta_\infty/h_1)]}{\ln M} \qquad (6\text{-}1\text{-}37)$$

In the calculations we select the parameters h_1 and M and calculate the η_∞. Here they were takne as 0.01 and 1.1, respectively.

The fin conduction equation was solved by using the direct inverse matrix method. The fin conduction equation was also divided into 45 grid points and expressed in finite difference form. To ensure high accuracy, a nonuniform grid points were employed. For small ξ , a finer ξ subdivision was also needed for the heat conduction equation.

Results and Discussion

Numerical results of the overall rate of heat transfer Q from the fin can be obtained from the wall into the fin base at $\xi=1$ or from the integrating heat convection over the fin surface. The corresponding Q values of these two methods are found to be in agreement. They may be expressed in dimensionless form as

$$\frac{Q}{k(T_o-T_\infty)ReL^{\frac{1}{2}}} = 2\int_0^1 (-\frac{\partial\theta}{\partial\eta})/\xi^{\frac{1}{2}}d\xi \ , \quad \text{at} \quad \eta = 0 \qquad (6\text{-}1\text{-}38)$$

or

$$\frac{Q}{k(T_o-T_\infty)ReL^{\frac{1}{2}}} = \frac{2}{Nc}\left.\frac{d\theta_f}{d\xi}\right|_{\xi=1} \qquad (6\text{-}1\text{-}39)$$

The results of the overall rate of heat transfer Q from the fin are presented as a function of the conjugated convection-conduction parameter Nc in Fig.(6-1-3). The decrease of Nc indicates short fin length, L, great fin conductances, k_f, and low convective coefficints (low k and ReL). It is observed from Fig.(6-1-3) that an increase in Nc yields a decrease in the corresponding Q. Fig. (6-1-3) also show that the overall heat transfer rate of the fin in the turbulent flow is higher than that of the fin in the laminar flow when the parameters Nc and Pr are fixed.

Fig.(6-1-4) illustrates the distribution of the local heat transfer coefficient along the fin surface for various values of Nc. The local heat transfer coefficient can be written as,

in dimensionless form

$$\frac{hL}{kReL^{\frac{1}{2}}} = -\frac{\partial\theta}{\partial\eta} \Big/ (\theta f \xi^{\frac{1}{2}}), \qquad \text{at} \quad \eta = 0 \quad (6\text{-}1\text{-}40)$$

As seen from the figure, the distribution of local heat transfer coefficient decreases monotonically before the transition zone along the streamwise direction, but the local heat transfer coefficient $\hat{h}$ in the transition zone becomes irregular. This figure also shows that the larger values of Nc give rise to larger values of $\hat{h}$.

The distributions of the dimensionless local heat flux along the fin surface are presented in Fig.(6-1-4) for different Nc. The local heat flux can be taken as

$$\frac{qL}{k(T_o - T_\infty)ReL^{\frac{1}{2}}} = -\frac{\partial\theta}{\partial\eta} \Big/ \xi^{\frac{1}{2}} \qquad \text{at} \quad \eta = 0 \qquad (6\text{-}1\text{-}41)$$

For smaller Nc, the local heat flux of the fin is larger near the tip but smaller near the base root than that of the fin for larger Nc. Most of the heat fluxes transfer to the ambient fluid by forced convection near the base for higher Nc. The local heat flux becomes irregular near the transition point ξ_{tr}. Fig. (6-1-4)-(6-1-5) also show that the local heat transfer coefficient and local heat flux of the fin in the turbulent flow are always higher than those of the fin in the laminar flow when the parameters Nc and Pr are fixed.

Fig.(6-1-6) presents fin temperature distributions for turbulent forced convective flow. In this figure, it is shown

that the fin temperature decreases monotonically in the direction from the root to tip. The figure also shows that the lower values of Nc give rise to higher values of fin temperature distributions and the temperature distributions of the fin in the turbulent flow are always lower that of the fin in the laminar flow when the parameters Nc and Pr are fixed.

Remark

The present analysis of the turbulent forced convective flow over a vertical plate fin has been studied. The local heat transfer coefficient along the fin is similtaneously solved for the turbulent forced convective boundary layer equations of the fluid and the conduction equation of the fin.

An efficient implicit finite difference technique is employed. The agreement of the results for special case (i.e. fin in the laminar flow) with [16] is truly remarkable.

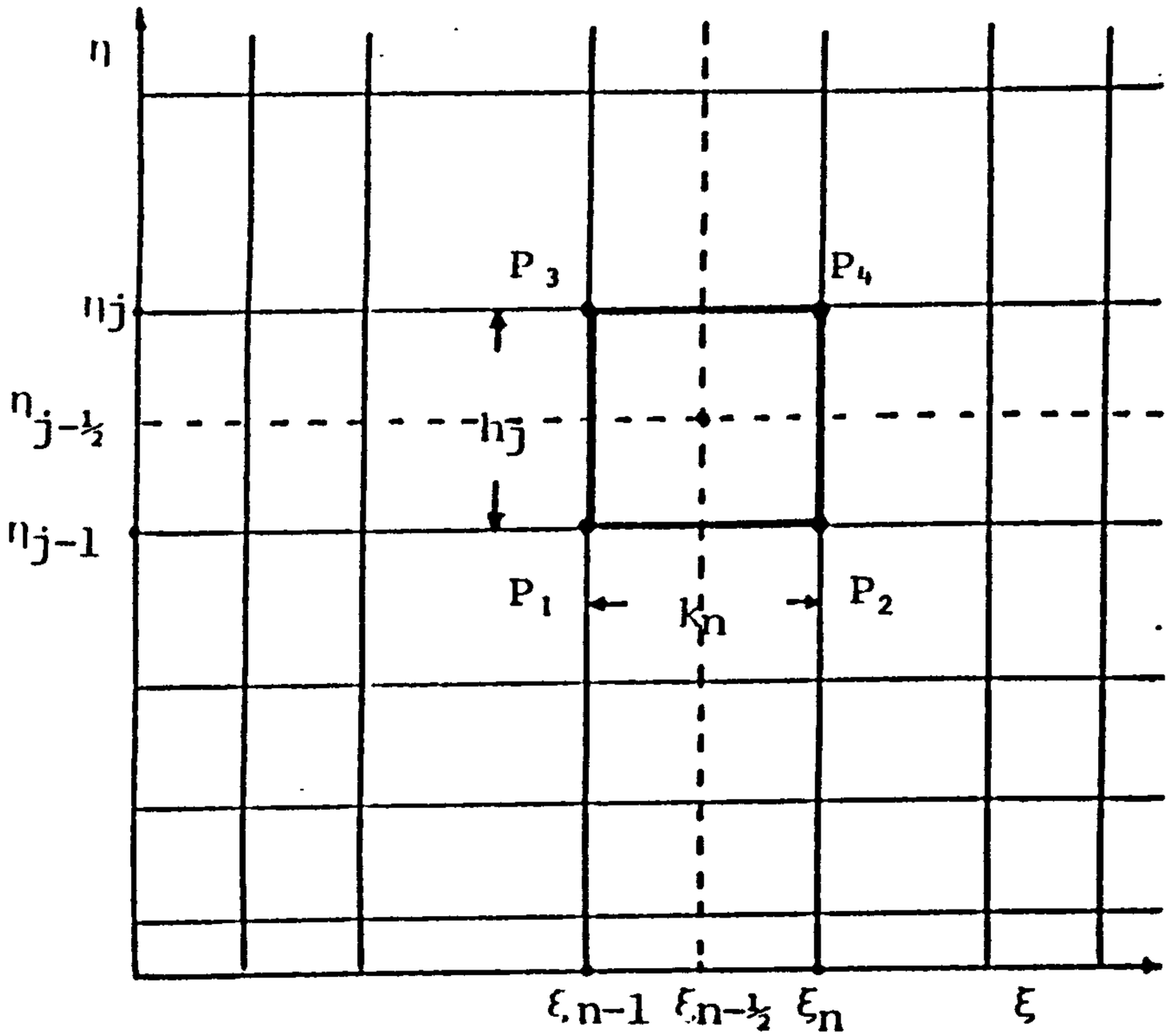

Fig.6-1-2 Net rectangle for the difference equations.

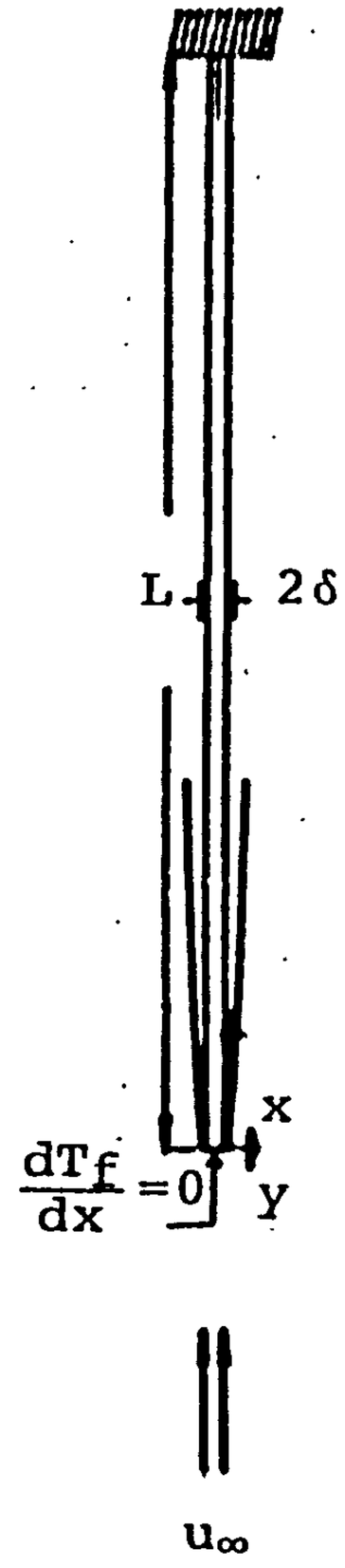

Fig.6-1-1 Physical model and coordinates of the vertical plate fin.

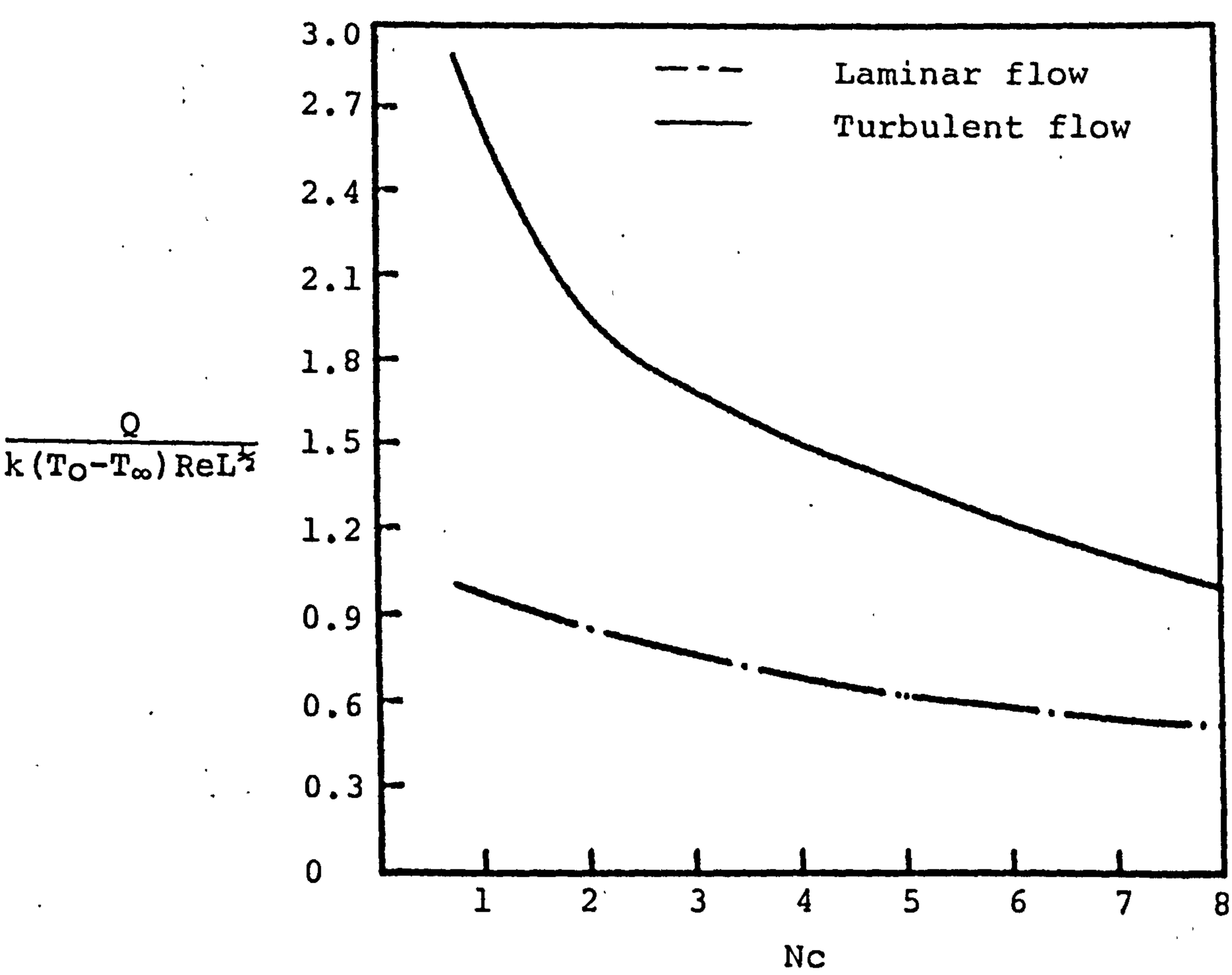

Fig.6-1-3 Total heat transfer rate for Pr=0.7, Prt=0.9 and ξ_{tr}=0.633.

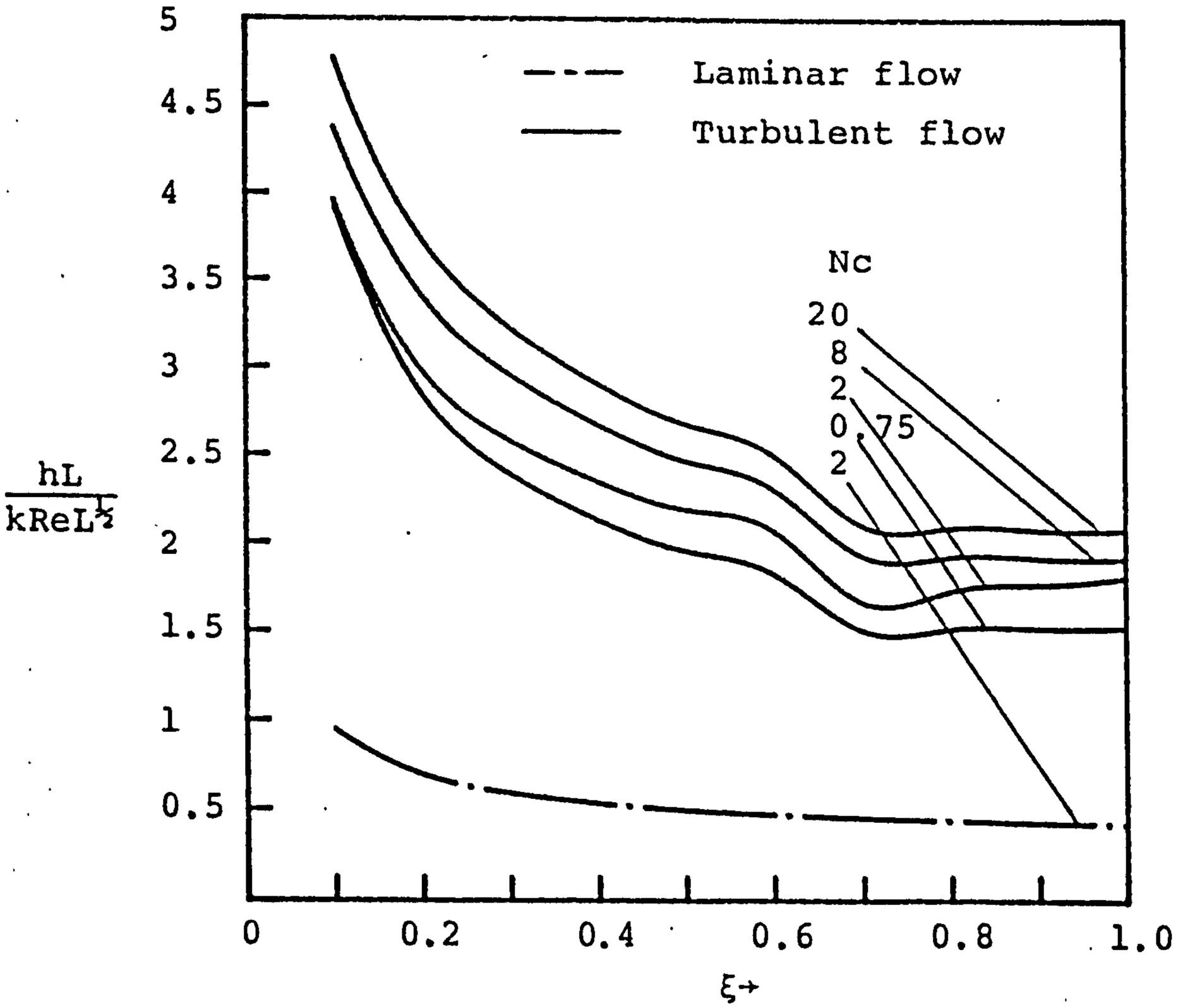

Fig.6-1-4 The local heat transfer coefficients along the plate fin for Pr=0.7, Prt=0.9, ξ_{tr}=0.633 and various values of Nc.

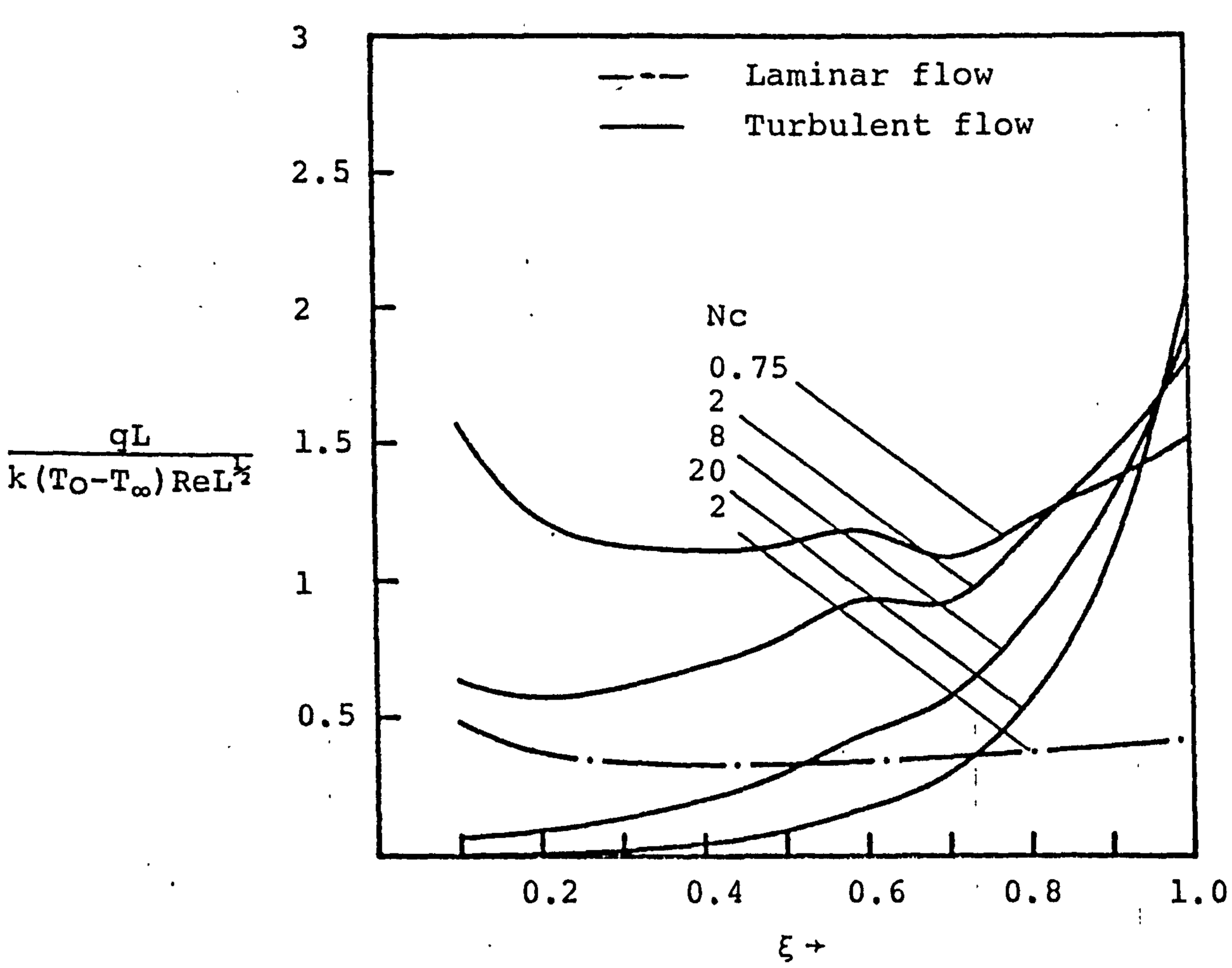

Fig.6-1-5 The local heat fluxes along the plate fin for Pr=0.7, Prt=0.9, ξ_{tr}=0.633 and various values of Nc.

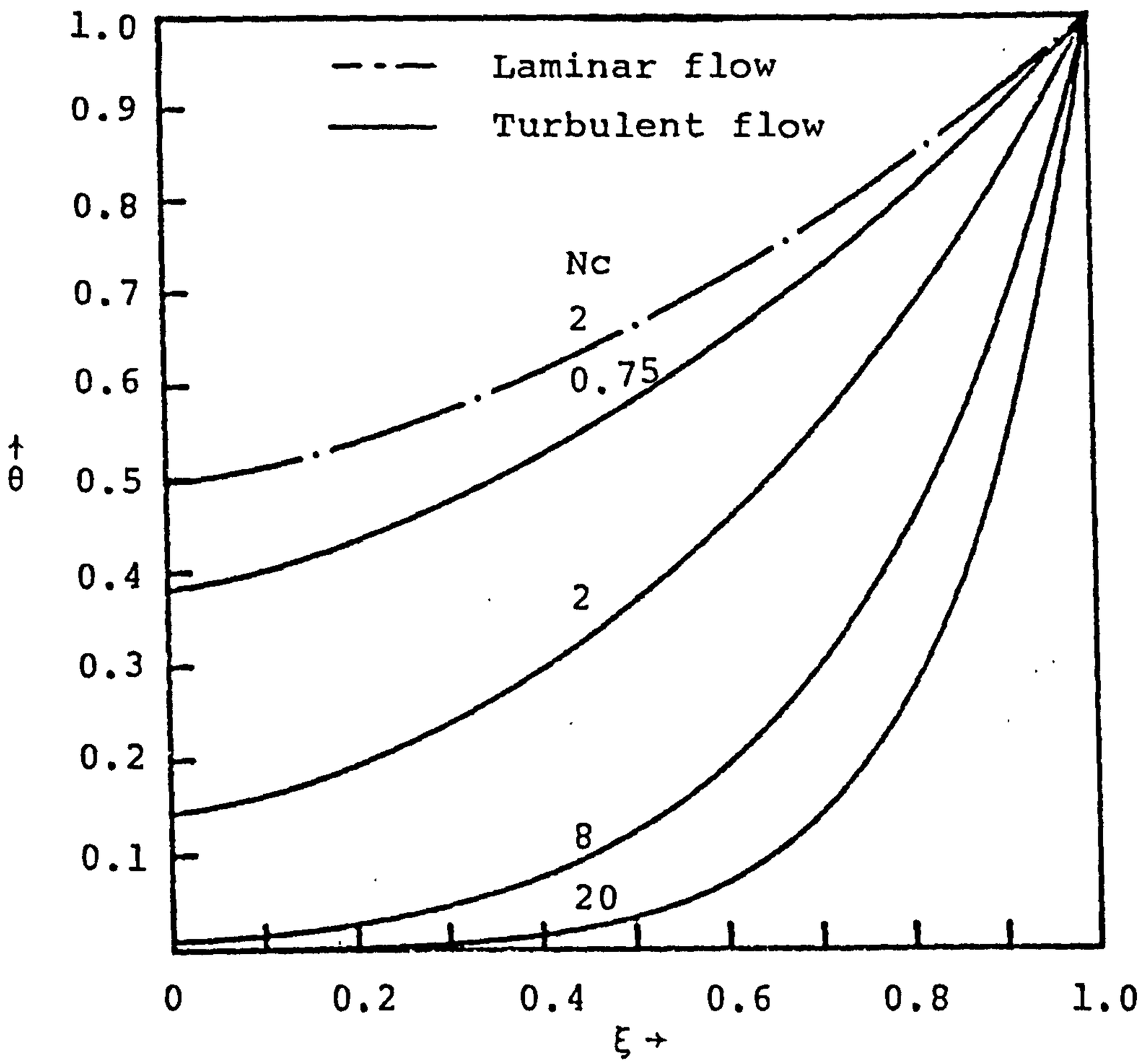

Fig.6-1-6 The temperature distributions along the plate fin for Pr=0.7, Prt=0.9, ξ_{tr}=0.633 and various values of Nc.

VI-2 Vertical Circular Pin with Cinjugated Forced Convection-Conduction Turbulent flow

In the conventional heat transfer analysis of a fin, it is standard practice to assume that the heat transfer coefficient for convection at the fin surface is uniform all over the fin. This approach is generally inadeguate, since the heat transfer coefficient varies along the fin surface. Recently, Huang and Chen [39], [42] have studied the problem of a vertical circular pin with conjugated forced and mixed convection-conduction flow and concluded, based on their numerical analysis, that the overall heat transfer rate increase with decreasing radius of the cylindrical pin.

Although the above investigations have been extensively carried out for the case of laminar Newtonian fluid, there exist relatively fewer works concerning turbulent fluid. To the best knowledge of the author, the only such studies for the problem of vertical plate fin with conjugated forced convection-conduction turbulent flow which have been reported are the numerical work of Lien, Chen and Cleaver [43].

The present analysis is a numerical study of heat transfer due to turbulent flow along a vertical circular pin. The transition position was assumed to occur at $R_{etr}=5x10^5$. In this study the eddy viscosity formulation is used for forced convection flow developed by Cebeci and Smith [29]. Numerical results are presented for Pr=0.7, Prt=0.9, u_∞=100 m/s, ν=1.5×

10^{-5} m^2/s, L=0.1m and r_o=0.5 cm over a conjugated convection-conduction parameter of N_c=0.25, 0.75, 2 and 3.

Analysis

Consider a vertical circular pin which is extended from a wall at temperature T_o and situated in a turbulent flow field with undisturbed oncoming free stream velocity u_∞ and temperature T_∞. The coordinate system is given in Fig.(6-2-1). The boundary layer equations and their boundary conditions are expressed, respectively, as follows:

$$\frac{\partial(ru)}{\partial x} + \frac{\partial(rv)}{\partial r} = 0 \qquad (6\text{-}2\text{-}1)$$

$$u\frac{\partial u}{\partial x} + v\frac{\partial u}{\partial r} = \frac{1}{r}\frac{\partial}{\partial r}\left[r\frac{\partial u}{\partial r}(\varepsilon_m+\nu)\right] \qquad (6\text{-}2\text{-}2)$$

$$u\frac{\partial T}{\partial x} + v\frac{\partial T}{\partial r} = \frac{1}{r}\frac{\partial}{\partial r}\left[r\frac{\partial T}{\partial r}(\varepsilon_h+\alpha)\right] \qquad (6\text{-}2\text{-}3)$$

$$\left.\begin{aligned} &u=v=0,\ T=T_w(x), && \text{at } r=r_o \\ &u=u_\infty,\ T=T_\infty, && \text{as } r\to\infty \\ &u=u_\infty,\ T=T_\infty, && \text{at } x=0,\ r\geq r_o \end{aligned}\right\} \qquad (6\text{-}2\text{-}4)$$

where ε_m and ε_h are the eddy viscosity and the eddy conduction y

The pseudo-similarity variables (ξ,η), dimensionless stream function $f(\xi,\eta)$ and dimensionless temperature $\theta(\xi,\eta)$ are introduced as follows:

$$\xi = x/L \quad , \quad \eta = \frac{r^2 - r_o^2}{2r_oL}(Re_L/\xi)^{\frac{1}{2}} \qquad (6\text{-}2\text{-}5)$$

$$f(\xi,\eta) = \psi(x,r)/\left[r_o (u_\infty L\xi\nu)^{\frac{1}{2}} \right] \qquad (6\text{-}2\text{-}6)$$

$$\theta(\xi,\eta) = (T-T_\infty)/(T_o-T_\infty) \qquad (6\text{-}2\text{-}7)$$

where L is the length of the cylinder pin and Re_L is the Reynolds number, $Re_L=u_\infty L/\nu$ and the stream function $\psi(x,r)$ satisfies the continuity equation (6-2-1) with

$$ru=\partial\psi/\partial r, \qquad rv= -\partial\psi/\partial x \qquad (6\text{-}2\text{-}8)$$

Substituting equations (6-2-5)-(6-2-7) into (6-2-2)-(6-2-4), gives momentum equation

$$(1+\lambda\eta\xi^{\frac{1}{2}})\{(1+\varepsilon m^+)f''\}' + \{\lambda\xi^{\frac{1}{2}}(1+\varepsilon m^+)+\frac{f}{2}\} f''$$

$$= \xi(f' \frac{\partial f'}{\partial \xi} - f'' \frac{\partial f}{\partial \xi}) \qquad (6\text{-}2\text{-}9)$$

energy equation

$$(1+\lambda\eta\xi^{\frac{1}{2}}) \{(Pr^{-1}+\varepsilon_h^+)\theta'\}' +\{\lambda\xi^{\frac{1}{2}}(Pr^{-1}+\varepsilon_h^+)+ \frac{f}{2}\}\theta'$$

$$=\xi (f'\frac{\partial\theta}{\partial\xi} - \theta' \frac{\partial f}{\partial\xi}) \qquad (6\text{-}2\text{-}10)$$

$$\left.\begin{array}{lll} f = f' = 0, & \theta = \theta_w(\xi), & \text{at } \eta = 0 \\ f' \to 1 \quad , & \theta \to 0 & \text{as } \eta \to \infty \end{array}\right\} \qquad (6\text{-}2\text{-}11)$$

In the foregoing equations, the primes stand for partial derivatives with respect to η, Pr is the Prandtl number and λ is the transverse curvature parameter defined as:

$$\lambda = 2L/(Re_L^{\frac{1}{2}} r_o).$$

The thin pin energy equation, associated boundary condi-

tions and basic thermal coupling conditions are the same as those in Ref. [39]. Then the the dimensionless heat-conduction equation and its boundary conditions are:

$$\frac{d^2\theta}{d\xi^2 f} = N_c \hat{h}\, \theta_f \qquad (6\text{-}2\text{-}12)$$

and $\theta_f=1$, at $\xi = 1$, $d\theta_f/d\xi = 0$, at $\xi = 0$ (6-2-13)

where N_c is the conjugated convection-conduction parameter

$$N_c = 2kLRe_L^{1/2}/k_f r_o \qquad (6\text{-}2\text{-}14)$$

The quantity $\hat{h}$ is a dimensionless form of the local heat transfer coefficient which can be obtained by equation (6-2-5) and the thermal coupling condition in Ref.[39]

$$\hat{h} = -(\partial\theta/\partial\eta)/(\theta_f \xi^{1/2}), \quad \text{at} \quad \eta = 0 \qquad (6\text{-}2\text{-}15)$$

Eddy Diffusivity Formulas

Cebeci and Smith [29]reported an algebraic eddy viscosity formulation which is simple and effective for external wall boundary layer. According to this formulation, ε_m is defined by two separate formulas given by

$$\varepsilon_m = \begin{cases} \varepsilon_{mi} = L^2 (r/r_o) \left|\frac{\partial u}{\partial r}\right| \gamma_{tr} & , \quad \varepsilon_{mi} \leq \varepsilon_{mo} \\ \varepsilon_{mo} = 0.0168 \left| \int_{r_o}^{\infty} (u_\infty - u)\, dr \right| \gamma_{tr}, & \varepsilon_{mi} \geq \varepsilon_{mo} \end{cases} \qquad (6\text{-}2\text{-}16)$$

where $L = 0.4\, r_o \ln(r/r_o)\{ 1-\exp [- \frac{r_o}{A} \ln(r/r_o) \}$ (6-2-17)

and $\bar{A} = 26\ \nu(\tau_w/\rho)^{-\frac{1}{2}}$, (6-2-18)

In equation (6-2-16), γ_{tr} is an intermittency factor that accounts for the transitional region that exists between a laminar and turbulent flow.

$$\gamma_{tr} = 1 - \exp\left[-G\, r_o(x_{tr})\ \left(\int_{x_{tr}}^{x} \frac{dx}{r_o}\right)\ \int_{x_{tr}}^{x} \frac{dx}{u_\infty}\right] \qquad (6\text{-}2\text{-}19)$$

where x_{tr} is the location of the start of the transition and the empirical factor, G is given by

$$G = u_\infty^3\ Rx_{tr}^{-1.34}/(1200\ \nu^2) \qquad (6\text{-}2\text{-}20)$$

In terms of transformed variables, ε_m can be written as

$$\varepsilon_m = \begin{cases} \varepsilon_{mi} = \nu\varepsilon_{mi}^{+} = 0.16\left[r_o \ln(1+\lambda\eta\xi^{\frac{1}{2}})^{\frac{1}{2}}\right]^2 \left\{1-\exp\left(-\dfrac{u_\infty Re_x^{-\frac{1}{4}} f_w''^{\frac{1}{2}} r_o \ln(1+\lambda\eta\xi^{\frac{1}{2}})^{\frac{1}{2}}}{26\ \nu}\right)\right\}^2 \\ \qquad (1+\gamma\eta\xi^{\frac{1}{2}})^{0.5}\ u_\infty^2 f'' Re_x^{-\frac{1}{2}} \gamma_{tr} \\ \varepsilon_{mo} = \nu\varepsilon_{mo}^{+} = 0.0168\ Re_x^{\frac{1}{2}}\ \nu r_o\left[\int_0^\infty (1-f')/\sqrt{r_o + \dfrac{2r_o L\eta}{(Re_L/\xi)^{\frac{1}{2}}}}\, d\eta\right]\gamma_{tr} \end{cases} \qquad (6\text{-}2\text{-}21)$$

(6-2-22)

We choose the turbulent Prandtl expression of Jischa and Rieke [34] , which is

$$Prt + \varepsilon_m/\varepsilon_h = a + b(Pr + 1)/Pr \qquad (6\text{-}2\text{-}23)$$

is used with experiment giveng a=0.825 and b=0.0309, a result fitting data for air (Pr=0.7) quite well.

Results and Discussion

The numerical procedure of solving the boundary layer equations and the heat conduction equation are identical to that in Ref. [39]. The dimensionless overall rate of heat transfer Q from the pin can be expressed as

$$\frac{Q}{r_o k(T_o-T_\infty)Re_L^{\frac{1}{2}}} = \frac{2\pi}{N_c}\left.\frac{d\theta_f}{d\xi}\right|_{\xi=1} \qquad (6\text{-}2\text{-}24)$$

or

$$\frac{Q}{r_o k(T_o-T_\infty)Re_L^{\frac{1}{2}}} = 2\pi\int_0^1 \left(-\frac{\partial\theta}{\partial\eta}/\ \xi^{\frac{1}{2}}\right)_{\eta=0} d\xi \qquad (6\text{-}2\text{-}25)$$

The overall heat transfer rate of the pin in the pure laminar flow and the mixed laminar and turbulent flow are show in Fig.(6-2-1) It is observed from Fig.(6-2-1) that an increase in N_c yields a decrease in the corresponding overall heat transfer rate. Fig.(6-2-1) also shows that the overall heat transfer rate of the pin in the turbulent flow is higher than that of the pin in the laminar flow. This behavior is due to the action of turbulent eddies which increase the lodal heat transfer rate at the wall.

Fig.(6-2-2) illustrate the local heat transfer coefficient along the pin surface for various values of N_c. The local heat transfer coefficients can be written as, in dimensionless form

$$\frac{hL}{kRe_L^{\frac{1}{2}}} = -\theta'(\xi,\ 0)/\ (\theta_f\xi^{\frac{1}{2}}) \qquad (6\text{-}2\text{-}26)$$

As seen from the figure, the distribution of the local heat transfer coefficient $\hat{h}$ decreases monotonically before the

transition zone along the streamwise direction, but the $\hat{h}$ becomes irregular in the transition zone due to the occurance of the random spots of turbulence. This figure also shows that the large values of N_c give rise to larger value of $\hat{h}$. It is observed from Fig.(6-2-2) that the turbulent-affected local heat transfer coefficient is higher than $\hat{h}$ of the pin surface in pure laminar flow.

Fig. (6-2-3) presents pin temperature distributions in turbulent forced convective flow. The figure illustrates that the larger values of N_c give rise to larger variations of pin temperature distributions. The phenomenon of this behavior is the same as the forced convective laminar flow over a circular pin [39]. Fig.(6-2-3) also shows the temperature distributions of the pin in the turbulent flow give a larger variation than those of the pin in the laminar flow ($\varepsilon_m, \varepsilon_h = 0$). This behavior is attributed to enhanced surface heat transfer rate associated with an increase in the random spots of turbulence along the streamwise direction.

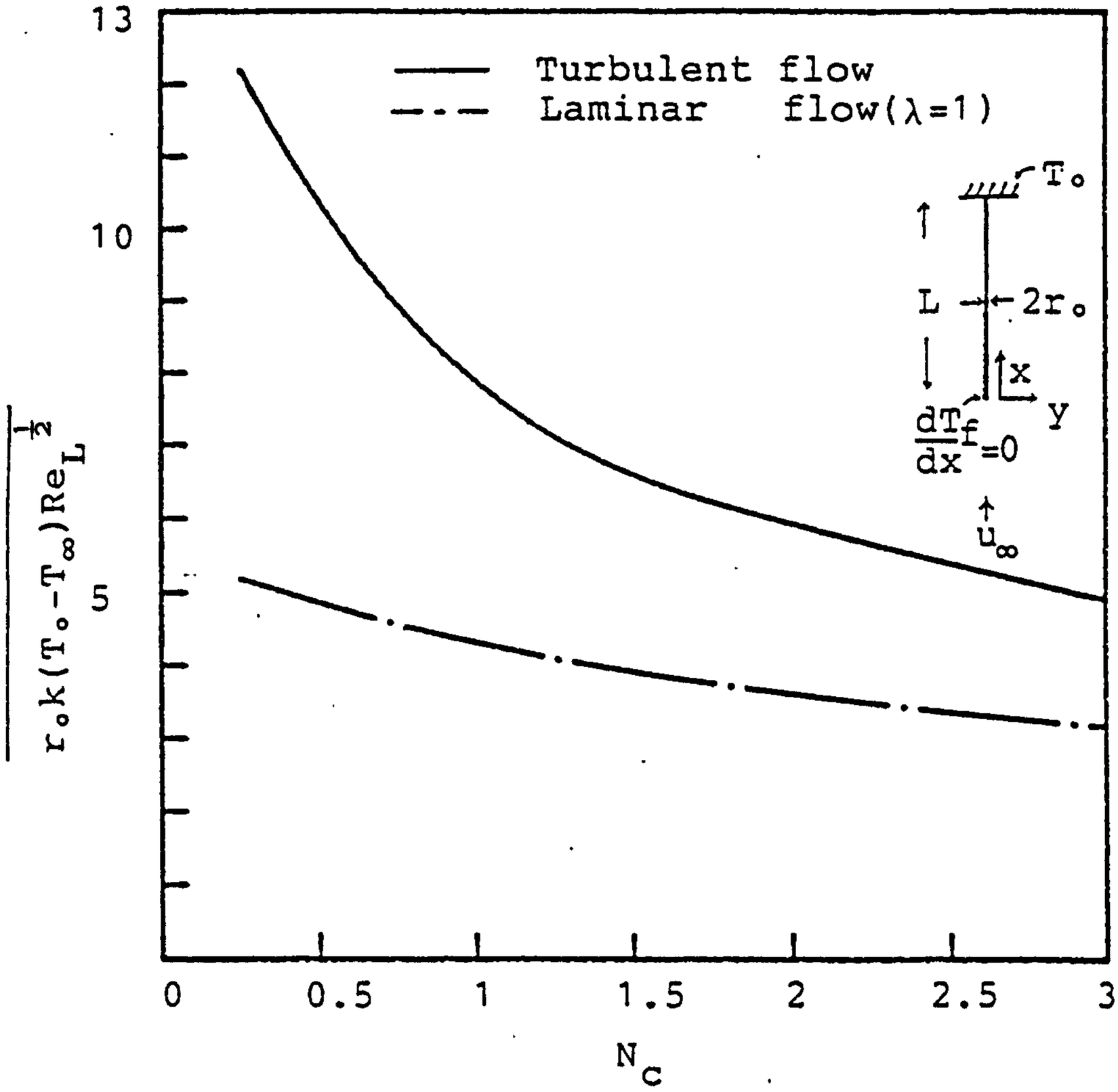

Fig.6-2-1 Total heat transfer rate for Pr=0.7 ,Prt=0.9, ξ_{tr}=0.75 and λ=0.049.

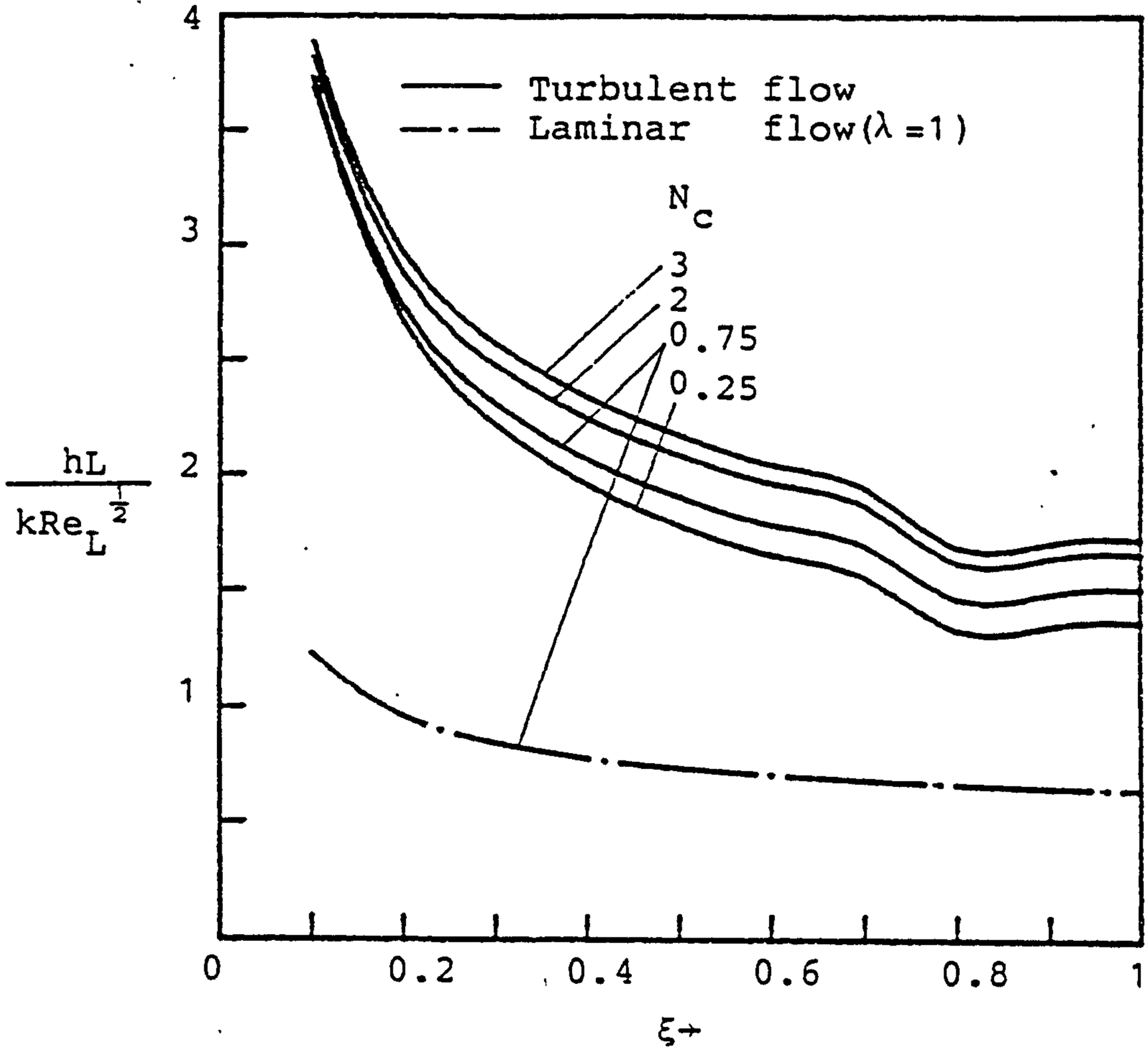

Fig.6-2-2 The local heat transfer coefficient along the circular pin for Pr=0.7 and Prt =0.9, ξ_{tr}=0.75, λ=0.049 and various values of N_c.

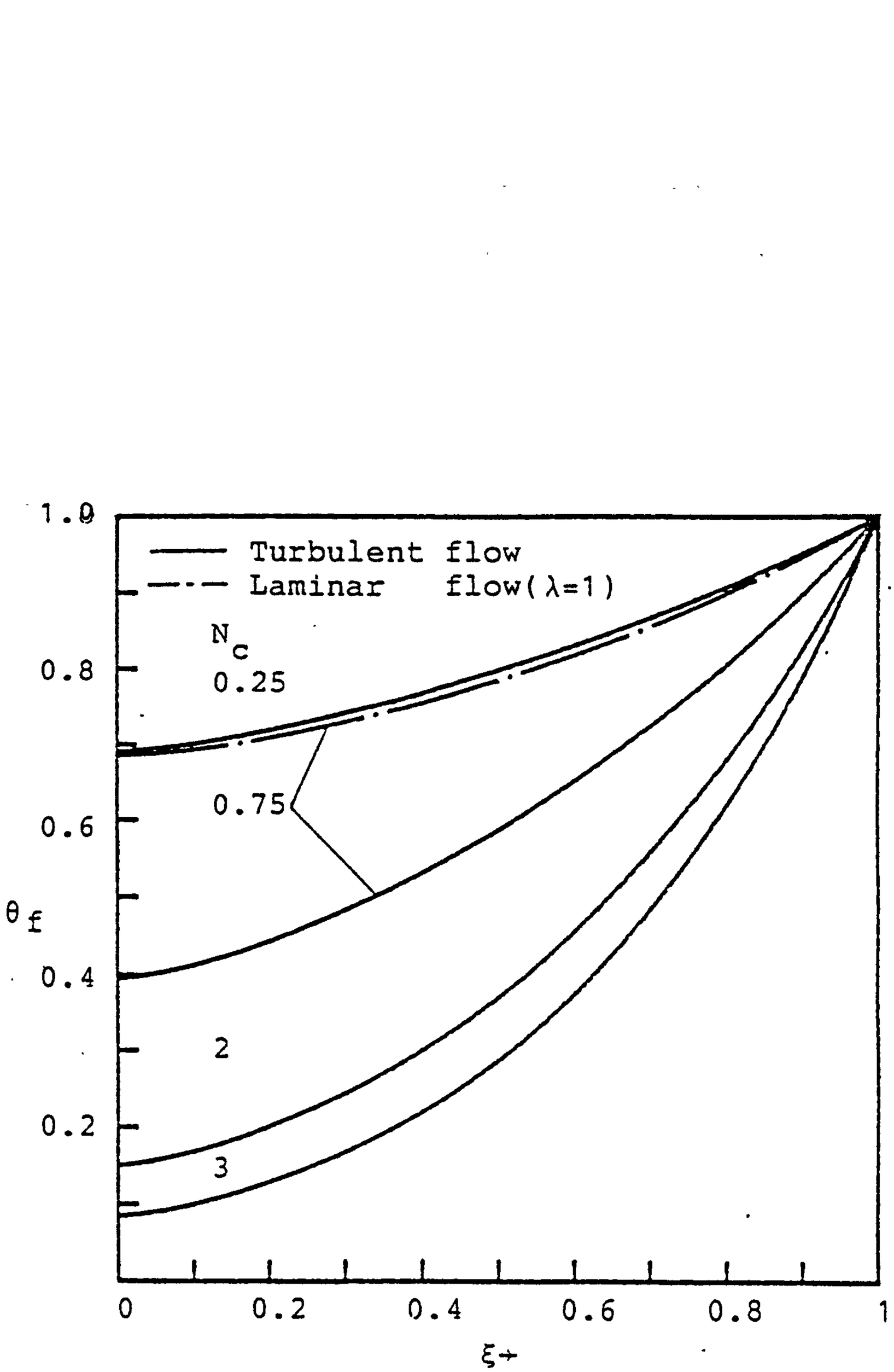

Fig.6-2-3 The temperature distributions along the circular pin for Pr=0.7,Prt=0.9, ξ_{tr} =0.75, λ =0.049 and various values of N_c.

VII. CONCLUSIONS

The efficient implicit finite difference method proposed in this dissertation is demonstrated to be a very useful method for wide class of conjugated convection-conduction heat transfer problems of boundary layer type. The following problems are studied in detail with a view to illustrating this method.

(1) Radiative Effect on the Vertical Plate Fin in Conjugated Natural Convection-Conduction Flow.

(2) Radiative Effect of the Vertical Plate Fin in Conjugated Forced Convection-Conduction Flow.

(3) Radiative Effect on the Vertical Plate Fin in Conjugated Mixed Convection-Conduction Flow with Temperature Dependent Viscosity.

(4) Radiative Effect and Viscosity Variations on Conjugated Natural Convection-Conduction Analysis of Heat Transfer in a Vertical Circular Pin.

(5) Radiative Effect on the Vertical Circular Pin in Conjugated Forced Convection-Conduction Flow with Temperature Dependent Viscosity.

(6) Radiative Effect and the Viscosity Variation on the Conjugated Mixed Convection-Conduction Analysis of Heat Transfer in a Vertical Circular Pin.

(7) Vertical Flate Fin with Conjugated Forced Convection-Conduction Turbulent Flow.

(8) Vertical Circular Pin with Conjugated Forced Convection-Conduction Turbulent Flow.

The above problems can be classified into two groups:
(i) the first six cases are steady laminar flow with convection-conduction heat transfer problems and (ii) the others are steady turbulent flow with convection-conduction heat transfer problems.

The analysis of the steady laminar flow convection-conduction cases have yielded the results of heated vertical fin (or pin) for convective thermal boundary layer flow with radiative effect. The optically thick limit approximation for the radiative heat flux is assumed. Although the range of the validity of the optically thick limit approximation is small in the boundary layer flow, it possesses the advantage of simplicity in the analysis because the governing energy equation can be transformed into an ordinary differential equation by the conventional similarity transformation. The exact solutions of the fin surface temperature should lie between those for the nonradiating gas case and the optically thick limit approximation.

The agreement of the results for the special case (i.e. fin or pin without radiation and viscosity variation) with the previous works are very satisfactory.

The analysis of the steady turbulent flow convection-conduction cases over a vertical plate fin (or pin) has been studied. The local heat transfer coefficient along the fin (or pin) is simultaneously solved for the turbulent forced convective boundary layer equations of the fluid and the con-

duction equation of the fin. The results for the special case (i.e. fin or pin in the laminar flow) are also in good agreement with previous works.

VIII. SUGGESTIONS

The successful applications of the efficient implicit finite difference method on the steady conjugated laminar convection-conduction analysis of heat transfer in a vertical fin (or pin) and the steady conjugated turbulent forced convection-conduction analysis of heat transfer in a vertical fin (or pin) in this dissertation suggest that the extension of this method should be available to the following problems:

1) unsteady conjugated laminar convection-conduction analysis of heat transfer in a vertical fin (or pin)
2) steady conjugated turbulent natural convection-conduction analysis of heat transfer in a vertical fin (or pin)
3) unsteady conjugated turbulent convection-conduction analysis of heat transfer in a vertical fin (or pin)
4) steady conjugated laminar convection-conduction non-Newtonian power law fluids of heat transfer in a vertical fin (or pin)
5) unsteady non-Darcian effects on convective heat transfer in porous midium.
6) extension to other steady and unsteady turbulent heat and mass transfer problems of boundary layer type.

IX REFERENCES

1) Kern, D. Q. and Kraus, A. D., Extended Surface Heat Transfer, McGraw-Hill, New York, 1972.

2) Arpaci, V. S., Conduction Heat Transfer Addison-Wesley Publishing Company, Inc., Reading. Mase., 1966.

3) Holman, J. P., Heat Transfer, Second ed., McGraw-Hill, New York, 1968.

4) Chapman, A. J., Heat Transfer, Second ed., Macmillan, New York, 1969.

5) Jacob, M., Heat Transfer, John Wiley & Son, New York, 1949.

6) Harper, D. R. and Brown, W. B., "Mathematical Equations for Heat Conduction in the Fins of Air Cooled Engines, "N. A. C. A. Rept, pp.158, 1922.

7) Gardner, D. A., "Efficiency of Extended Surface," Trans. ASME, Vol.67, pp.621, 1945.

8) Gate, R., Heat Transfer and Pressure Loss in Extended Surface Heat Exchangers Operating under Frosting Condition, "ASHRAE, Trans., 73, 1967.

9) Chapman, A. J., "Transient Heat Conduction in Annular Fins of Uniform Thickness, "Chemical Engineering Symposium, Vol. 55, No.29, pp.195, 1959.

10) Hung, H. M., "Heat Transfer of thin Fins with Stochastic Root," Trans. ASME, J. Heat Transfer, C, Vol.91, pp.129-134, 1969.

11) Yang, J. W., "Periodic Heat Transfer in Straight Fins, "Trans. ASME, J. Heat Transfer, C. Vol.94 pp.310-314, 1972.

12) Suryanarayana, N. V., "Transient Response of Straight Fins," Trans. ASME., J. Heat Transfer, C, Vol.97, pp. 417-423, 1975.

13) Azia, A. and Na, T. Y. "Perildic Heat Transfer in Fins with Variable Thermal parameters", Int. J. Heat Transfer, Vol.24, No.8, pp.1397-1404, 1981.

14) Heggs, P. J., Ingham, D. B., and Manzoor, M. "The Effect of Non-uniform Heat Transfer from an Annular Fin of Triangular Profile", Trans. ASME, Vol.103, Feb., pp.184-185, 1983.

15) Sparrow, E. M. and Acharya, S., "A Natural convection Fin with a Solution-Determined Nonmonotonically Varying Heat Transfer coefficient," Trans. ASME., J. Heat Transfer Vol. 103, pp.218-225, 1981.

16) Sparrow, E. M. and Chyu, M. K., "Conjugate Forced Convection-Conduction Analysis of Heat Transfer in a Plate Fin," Trans. ASME., J. Heat Transfer, Vol.104, pp.204-206, 1982.

17) Karvinen, R., "Natural and Forced Convection Heat Transfer From a Flate Fin," Int. J. Heat Mass Transfer, Vol.24, pp.881-885, 1981.

18) Karvinen, R., "Efficiency of straight fins cooled by Natural or Forced convection," int. J. Heat Mass Transfer, Vol.26, pp.635-638, 1983.

19) Cebeci, T. and Bradshow, P. "Momentum Transfer In Boundary Layer" Hemisphere publishing corp., washington, D. C. (1977).

20) Carier and Anderson "Resistance to Heat Flow Through

Finned Tubing" , ASHRAE Tran, Vol.50, 1944.

21) Sparrow, E. M., Baliga, B. R., and Patankar, S. V., "Forced Convection Heat Transfer from a Shrouded Fin Array with and without Tip Clearance", ASME J. of Heat Transfer, Vol. 100, pp.572-579 (1978).

22) Stachiewicz, J. W. "Effect of Variation of Local Film Coefficients on Fin Performance", ASME J. Heat Transfer, Vol. 91, pp.21-26 (1969)

23) Lock, G. S. H. and Gunn, J. C., "Laminar Free Convection from a Downward-Projecting Fin", ASME J. of Heat Transfer, Vol.90, pp.63-70 (1968).

24) Huang, M. J. and Chen, C. K. "Vertical Circular Pin with Conjugated Natural Convection-Conduction Flow", ASME J., of Heat Transfer, Vol. 107, No.1, pp. 242-245 (1985).

25) Chu, H. S. "analysis on the Transient Heat Transfer of Two Dimensional STraight Fins", Master Thesis, Cheng Kung Unv., 1977.

26) Aziz, A., "Periodis Heat Transfer in Annular Fins", Trans. ASME, J. Heat Transfer, Vol. 97, pp.302-303, 1975.

27) Eslinger, R. G. and Chung, B. T. F., "Peiodic Heat Transfer in Radiating and Convecting Fins or Fin Arrays", AIAA, Vol. 17, pp.1134-1140, 1979.

28) Cebeci, T., Bradshaw, P. and Whitelaw, J. H., "Engineering Calculation Methods for Turbulent Flow", pp.43-44(1981)

29) Cebeci, T. and Smith, A. M. O., "Analysis of Turbulent Boundary Layers", Appl. Mech. 15, pp.249-251 (1974).

30) Cebeci, T., "Calculation Method for Compressible Turbulent Boundary layers with Heat and Mass Transfer", AIAA J. 9, pp.1091-1097 (1971).

31) Klebanoff, P. S., "Characteristics of Turbulence in a Boundary Layer with Zero Pressure Gradient", NACA Technical Note, No.3178 (1954).

32) Maise, G. and McDonald, H., "Mixing length and Kinematic eddy viscosity in a compressible boundary layer", AIAA J. 7, pp.305-311 (1969).

33) Cebeci, T., Smith, A. M. O. and Mosinskis, G., "Solution of the Incompressible Turbulent Boundary-layer Equations with Heat Transfer", ASME J. Heat Transfer, Vol. 92, pp.133-143 (1970).

34) Muller, W., Rosener, K. G. and Schmidt, B., Eds., "Recent Developements in Theoretical and Experimental Fluid Mechanics", Springer, Berlin (1979).

35) Ali, M. M., Chen, T. S. and Armaly, B. F., " Natural Convection-Radiation Interaction in Boundary-Layer Flow over Horizontal Surface", AIAA J. Vol.22, pp.1797-1803 (1984).

36) Novotny, J. L. and Yang, K. T. "The Interaction of Thermal Radiation in Optically Thick Boundary Layer", ASME paper No. 67-HT-9 (1967).

37) Kim K. H., Ozisik, M. N. and Mulligan, J. C., "Radiation Effections in an Optically Thick Non-Newtonian Boundary Layer with Injection" Conference, Paris, Vol.3, section

R2-4, pp.1-10 (1970).

38) Jang, J. Y. "The Stability of a Vertical Natural Convection Boundary Layer with Temperature Dependent Viscosity", Ph. D. Thesis, SUNY at Buffalo, U.S.A. (1983).

39) Huang, M. J. and Chen, C. K. "Vertical circular Fin with Conjugated Forced Convection-Conduction Flow", ASME. J. of Heat Transfer Vol.106, pp.658-661 (1984)

40) Minkowycz, W. J. and Sparrow, E. M. "Local Nonsimilar Solutions for Natural Convection on a Vertical Cylinder" ASME J. of Heat Transfer, Vol.96, pp.178-183 (1978).

41) Cebeci, T. "Laminar-Free-Convection Heat Transfer from the Outer Surface of Vertical Slender Circular Cylinder" Proc. Fifth Intl. Heat Transfer Conference, paper Vol. 4 pp. 15-19 (1974).

42) Huang, M. J. and Chen, C. K. "Conjugated Mixed Convection and Conduction Heat Transfer Along a Vertical Circular Pin", Int. J. Heat and Mass Transfer, Vol. 28, No.3, pp. 523-529 (1985).

43) Lien, F. S., Chen, C. K. and Cleaver, J. W. "Vertical Plate Fin with Conjugated Forced Convection-Conduction Turbulent Flow", ASME Winter Annual Meeting in New Orleans (1984)

X. APPENDIX

APPENDIX A THE TRANSFORMED GOVERNING EQUATION

(i) Combined convection and forced convection in a vertical plate fin.

Under the boundary layer theorey and Boussinesq assumption, the governing equation can be written as follows:

Continuity equation: $$\frac{\partial u}{\partial x} + \frac{\partial v}{\partial y} = 0 \qquad \text{(A-1)}$$

Momentum equation: $$u\frac{\partial u}{\partial x} + v\frac{\partial u}{\partial y} = \frac{\partial}{\partial y}\left[(\nu + \varepsilon m)\frac{\partial u}{\partial y}\right] + g\beta(T-T\infty) \qquad \text{(A-2)}$$

Energy equation: $$u\frac{\partial T}{\partial x} + v\frac{\partial T}{\partial y} = \frac{\partial}{\partial y}\left[(\alpha + \varepsilon h)\frac{\partial T}{\partial y}\right] - \frac{1}{\rho C_p}\frac{\partial q^r}{\partial y} \qquad \text{(A-3)}$$

where εm = eddy viscosity

εh = eddy diffusion coefficient

C_p = constant pressure heat capacity

q^r = heat radiation flux

The boundary conditions are

$$\left.\begin{aligned} &\text{at } y = 0, \quad u = v = 0, \quad T = T_w(x) \\ &\text{at } y \to \infty, \quad u \to u_\infty, \quad T \to T_\infty \end{aligned}\right\} \qquad \text{(A-4)}$$

(a) With a constant kinematic viscosity

The dimensionless transformation formula are defined as follows:

$$\left.\begin{aligned} &\xi = \frac{x}{L}, \quad \eta = \frac{yRe_L^{\frac{1}{2}}}{L\xi^{\frac{1}{2}}}, \quad f(\xi,\eta) = \frac{\psi(x,y)}{\sqrt{u_\infty \nu L\xi}}, \\ &\theta = \frac{T(x,y) - T_\infty}{T_0 - T_\infty}, \qquad \theta_f = \frac{T_f(x) - T_\infty}{T_0 - T_\infty} \end{aligned}\right\} \qquad \text{(A-5)}$$

where $Re_L = \frac{u_\infty L}{\nu}$, $u = \frac{\partial \psi}{\partial y}$ and $v = -\frac{\partial \psi}{\partial x}$

After substituting equation (A-4) into equations (A-2) and (A-3), the transformed momentum and energy equations are

$$[f''(1+\varepsilon_m^+)]' + \tfrac{1}{2}ff'' + \xi\Omega\theta = \varepsilon\left[f'\frac{\partial f'}{\partial \xi} - f''\frac{\partial f}{\partial \xi}\right] \qquad \text{(A-6)}$$

$$[(Pr^{-1}+\varepsilon h^+)\theta']' + \tfrac{1}{2}f\theta' + \frac{4[(\theta+C_T)^3\theta]'}{3NPr} = \xi\left[f'\frac{\partial \theta}{\partial \xi}\theta' - \frac{\partial f}{\partial \xi}\right] \qquad \text{(A-7)}$$

where

$$\varepsilon m^+ = \varepsilon m/\nu, \quad \varepsilon h^+ = \varepsilon h/\nu, \quad N = \frac{k\beta^*}{4\sigma(T_0 - T_\infty)^3}, \quad C_T = \frac{T_\infty}{T_0 - T_\infty}$$

$$Pr = \nu/\alpha, \quad \Omega = \frac{Gr_L}{Re_L^2} = \frac{g\beta(T_0-T_\infty)L^3}{\nu^2} \Big/ \left(\frac{u_\infty L}{\nu}\right)^2$$

"'" denotes the partial differential of η.

The transformed boundary condition are

$$\begin{aligned} &\text{at } \eta = 0, \quad f = f' = 0, \quad \theta = \theta_w(\xi) \\ &\text{at } \eta \to \infty, \quad f' \to 1, \qquad\quad \theta \to 0 \end{aligned} \qquad \text{(A-8)}$$

(b) With a temperature-dependent kinematic viscosity

The temperature-dependent viscosity can be expressed as

$$\nu = \nu_\infty[1 + a_1\theta + a_2\theta^2] \qquad \text{(A-9)}$$

where a_1 and a_2 are determined by the curve fitting of experimental data.

The demensionless transformation formula are redefined as follows:

$$\xi = \frac{x}{L}, \quad \eta = \frac{yRe_{L\infty}^{\frac{1}{2}}}{L\xi^{\frac{1}{2}}}, \quad f(\xi,\eta) = \frac{\psi(x,y)}{\sqrt{u_\infty \nu_\infty L\xi}}$$

$$\theta = \frac{T(x,y) - T_\infty}{T_0 - T\infty}, \qquad \theta_f = \frac{T_f(x) - T_\infty}{T_0 - T_\infty} \qquad \text{(A-10)}$$

where $Re_{L\infty} = \frac{u_\infty L}{\nu_\infty}$, ν_∞ is the kinematic viscosity of the fluid outside the boundary layer.

After substituting equation (A-10) into equations (A-2) and

(A-3), the transformed momentum and energy equations become

$$[f''(1 + \varepsilon m_\infty^+ + a_1\theta + a_2\theta^2)]' + \tfrac{1}{2}ff'' + \xi\Omega_\infty\theta = \xi\left[f'\frac{\partial f}{\partial \xi} - f''\frac{\partial f}{\partial \xi}\right] \quad \text{(A-11)}$$

$$[(Pr_\infty^{-1} + \varepsilon h_\infty^+)\theta']' + \tfrac{1}{2}f\theta' + \frac{4[(\theta + C_T)^3\theta']'}{3Pr_\infty N} = \xi\left[f'\frac{\partial \theta}{\partial \xi} - \theta'\frac{\partial f}{\partial \xi}\right] \quad \text{(A-12)}$$

where $\varepsilon m_\infty^+ = \varepsilon m/\nu_\infty$,

$\varepsilon h_\infty^+ = \varepsilon h/\nu_\infty$, $Pr_\infty = \nu_\infty/\alpha$, $\Omega_\infty = \dfrac{Gr_{L\infty}}{Re_{L\infty}^2} =$

$$\frac{g\beta(T_0 - T_\infty)L^3}{\nu_\infty^2} \Big/ \left(\frac{u_\infty L}{\nu_\infty}\right)^2$$

(ii) Natural Convection

Under the boundary layer theorey and Boussinesq assumption, the governing equations can be written as follows:

$$\frac{\partial u}{\partial x} + \frac{\partial v}{\partial y} = 0 \quad \text{(A-13)}$$

$$u\frac{\partial u}{\partial x} + v\frac{\partial u}{\partial y} = \frac{\partial}{\partial y}\left(\nu\frac{\partial u}{\partial y}\right) + g\beta(T - T_\infty) \quad \text{(A-14)}$$

$$u\frac{\partial T}{\partial x} + v\frac{\partial T}{\partial y} = \alpha\frac{\partial^2 T}{\partial y^2} - \frac{1}{\rho C_p}\frac{\partial q^r}{\partial y} \quad \text{(A-15)}$$

The boundary conditions are

$$\left.\begin{array}{lll} \text{at } y = 0 , & u = v = 0 , & T = T_w(x) \\ \text{at } y \to \infty , & u \to 0 , & T = T_\infty \end{array}\right\} \quad \text{(A-16)}$$

(a) With a constant kinematic viscosity

The dimensionless transformation formula can be defined as follows:

$$\left.\begin{array}{l} \xi = \dfrac{x}{L} , \quad \eta = \dfrac{y}{L\xi^{\frac{1}{4}}}\,(Gr_L/4)^{\frac{1}{4}} \\ \psi(x,y) = f(\xi,\eta)[4\nu(Gr_L/4)^{\frac{1}{4}}]\xi 3/4 \end{array}\right\}$$

$$\left.\begin{aligned} \theta = \frac{T(x,v) - T_\infty}{T_0 - T_\infty} \quad , \qquad \theta_f = \frac{T_f(x) - T_\infty}{T_0 - T_\infty} \end{aligned}\right\} \tag{A-17}$$

After substituting equation (A-17) into equations (A-14) and (A-15), the transformed momentum and energy equations become

$$f'''' + 3ff'' - 2(f')^2 + \theta = 4\xi\left[f'\frac{\partial f'}{\partial \xi} - f''\frac{\partial f}{\partial \xi}\right] \tag{A-18}$$

$$Pr^{-1}\theta'' + 3f\theta' + \frac{4\left[(\theta+C_T)^3\theta'\right]'}{3PrN} = 4\xi\left[f'\frac{\partial \theta}{\partial \xi} - \theta'\frac{\partial f}{\partial \xi}\right] \tag{A-19}$$

(b) With a temperature-dependent kinematic viscosity

The dimensionless transformation formula can be redefined as follows:

$$\xi = \frac{x}{L} \quad , \quad \eta = \frac{y}{L\xi^{\frac{1}{4}}}\left(Gr_{L_\infty}/4\right)^{\frac{1}{4}}$$

$$\psi(x,y) = f(\xi,\eta)\left[4\nu_\infty\left(Gr_{L_\infty}/4\right)^{\frac{1}{4}}\right]\xi^{3/4} \tag{A-20}$$

$$\left.\begin{aligned} \theta = \frac{T(x,y) - T_\infty}{T_0 - T_\infty} \quad , \qquad \theta_f = \frac{T_f(x) - T_\infty}{T_0 - T_\infty} \end{aligned}\right.$$

After substituting equation (A-20) into equations (A-14) and (A-19), the transformed momentum and energy equations become

$$\left[f''(1+a_1\theta+a_2\theta^2)\right]' + 3ff'' - 2(f')^2 + \theta = 4\xi\left[f'\frac{\partial f'}{\partial \xi} - f''\frac{\partial f}{\partial \xi}\right] \tag{A-21}$$

$$Pr_\infty^{-1}\theta'' + 3f\theta' + \frac{4\left[(\theta+C_T)^3\theta'\right]'}{3Pr_\infty N} = 4\xi\left[f'\frac{\partial \theta}{\partial \xi} - \theta'\frac{\partial f}{\partial \xi}\right] \tag{A-22}$$

where $Gr_L = \dfrac{g\beta(T_0-T_\infty)L^3}{\nu^2}$, $Gr_{L\infty} = \dfrac{g\beta(T_0-T_\infty)L^3}{\nu_\infty^2}$

The transformed boundary conditions can be obtained by substituting the transformation formula (A-17) or (A-20) into equation (A-16).

$$\left.\begin{aligned} &\text{at } \eta = 0, \quad f = f' = 0, \quad \theta = \theta_w(\xi) \\ &\text{at } \eta \to \infty, \quad f' = 0, \quad \theta = 0 \end{aligned}\right\} \tag{A-23}$$

(iii) The transformed heat conduction equation of the fin

The heat conduction equation of the fin is

$$\frac{d^2T_f(x)}{dx^2} = \frac{h^*(x)}{k_f\delta}[T_f(x) - T_\infty] \qquad (A-24)$$

Where T_f is the temperature distribution, K_f is the heat conductivity of the fin, h* is the modified heat transfer coefficient. The boundary conditions are

$$x = 0 , \quad \frac{dT_f}{dx} = 0$$
$$x = L , \quad T_f = T_0 \qquad (A-25)$$

The constraint conditions are

$$T_f(x) = T_w(x)$$
when y=0, and $0 \leq x \leq L$ (A-26)
$$h^*(T_f - T_\infty) = -k\frac{\partial T}{\partial y} + q^r$$

Where q^r is the heat radiation flux under the assumption of "Optically Thick Limit Approximation". It can be expressed as

$$q^r = \frac{-4\sigma}{3\beta^*}\frac{\partial T^4}{\partial y} \qquad (A-27)$$

where σ is Stefan-Boltzmann constant, and β^* is extinction coefficient.

After substituting equation (A-5) (transformation formula) into equation (A-24), we obtained the transformed heat conduction equation with a constant kinematic viscosity as follows:

$$\frac{d^2\theta_f}{d\xi^2} = N_c\hat{h}^*\theta_f(\xi) \qquad (A-28)$$

And after substituting equation (A-10) into equation (A-24) we also obtained the transformed heat conduction equation with a non-constant kinematic viscosity as follows:

$$\frac{d^2\theta_f}{d\xi^2} = N_{c\infty}\hat{h}^*_{\infty}\theta_f(\xi) \qquad \text{(A-29)}$$

where $\hat{h}^*$ and $\hat{h}^*_{\infty}$ are dimensionless modified heat transfer coefficient, N_c and $N_{c\infty}$ are heat-conduction-convection parameters. The definition are

$$\hat{h}^* = \frac{h^*L}{kRe_L^{\frac{1}{2}}}, \quad \hat{h}^*_{\infty} = \frac{h^*L}{kRe_{L\infty}^{\frac{1}{2}}}$$
$$N_c = \frac{kLRe_L^{\frac{1}{2}}}{k_f\delta}, \quad N_{c\infty} = \frac{kLRe_{L\infty}^{\frac{1}{2}}}{k_f\delta} \qquad \text{(A-30)}$$

where k and k_f and the heat conductivities of the fluid and the fin respectively.

The transformed boundary conditions transformed by equation (A-5) or (A-10) become

$$\frac{d\theta}{d\xi} = 0 \quad \text{at} \quad \xi = 0$$
$$\theta = 1 \quad \text{at} \quad \xi = 1 \qquad \text{(A-31)}$$

APPENDIX B NUMERICAL METHOD

(I) The use of Box method to solve the problem of boundary layer:

(i) The equation for calculating $\hat{h}^*$ under combined, or forced or natural convection:

In order to reduce the number of iteration, the temperature distribution of the entire fin may be assumed to be a boundary condition of the thermal boundary layer as follow:

$$\theta_f(\xi) = \cosh(\xi)/\cosh(1.0)$$

Then we can get the temperature gradient of the boundary layer on the surface of the fin by solving the (thermal) boundary layer equation. Moreover, we can use the following equations (B-1) and (B-2) to obtain the $\hat{h}^*$.

(a) Under the situation of combined or forced convection:

$$-\left[1+\frac{4(\theta+C_T)^3}{3N}\right]\frac{\partial\theta}{\partial\eta}\Big/\left[\theta_f\,\xi^{\frac{1}{2}}\right] \quad , \qquad \eta = 0$$

$$\hat{h}^* = \quad \text{(with heat radiation)} \tag{B-1}$$

$$-\frac{\partial\theta}{\partial\eta}\Big/\left[\theta_f\,\xi^{\frac{1}{2}}\right] \quad , \quad \eta = 0 \text{ (with heat radiation)}$$

(b) Under the situation of natural convection:

$$-\left[1+\frac{4(\theta+C_T)^3}{3N}\right]\frac{\partial\theta}{\partial\eta}\Big/\left[\theta_f(4\xi)^{\frac{1}{4}}\right] \, ,$$

$$\hat{h}^* = \qquad \eta = 0 \text{ (with heat radiation)} \tag{B-2}$$

$$-\frac{\partial\theta}{\partial\eta}\Big/\left[\theta_f(4\xi)^{\frac{1}{4}}\right] \, , \; \eta = 0 \text{ (with no heat radiation)}$$

We can obtain the new temperature distributions by substituting the values of h* into the heat conduction equation of the

fin. Besides, the equations (A-6), (A-7), (A-11), (A-12), (A-18), (A-19), (A-21) and (A-22) themselves are the non-similar equations. In order to solve these problems, the implicit finite difference method introduced by Cebeci and Bradshaw (19) in the present study.

According to the above method, the unknown function of the derivative of η has to be introduced first. Then the governing equations of boundary layer can be written as five first order conjugated equations. The centered finite difference approximation is applied to get the average value at the middle of the grid point to approach the derivative and function of the first order equations. The tolerance (accuracy) can be achieved as $(\Delta\xi)^2$ and $(\Delta\eta)^2$. And the Newton's method are used to solve these non-linear difference equations and their coorespondent values of boundary condition. This method is more simpler, effective and with higher accuracy than the other numerical method such as local nonsimilar method for solving this problem. Significantly, the numerical solutions are very stable and it is permitted to calculate the very close value approaching the location of flow separation. The detailed procedure will be described in the next section.

(ii) The difference equation of combined convection

Under the situation of combined convection and with non-constant kinematic viscosity, the new functions

$\bar{u}(\xi,\eta)$, $\bar{v}(\xi,\eta)$, $w(\xi,\eta)$ are introduced as

$$\frac{\partial f}{\partial \eta} = \bar{u} \ , \quad \frac{\partial \bar{u}}{\partial \eta} = \bar{v} \ , \quad \frac{\partial \theta}{\partial \eta} = w \qquad \text{(B-3)}$$

then equations (A-11) and (A-12) can be written as

$$[\bar{v}(b+a_1\theta+a_2\theta^2)]' + \tfrac{1}{2}f\bar{v} + \xi\Omega\theta = \xi[\,\bar{u}\frac{\partial\bar{u}}{\partial\xi} - \bar{v}\frac{\partial f}{\partial\xi}\,] \qquad \text{(B-4)}$$

$$(Pr_\infty^{-1} - Prt^{-1})w' + Prt^{-1}[bw]' + \tfrac{1}{2}fw + \frac{4[(\theta+C_T)^3 w]'}{3Pr_\infty N}$$

$$= \xi[\,\bar{u}\frac{\partial\theta}{\partial\xi} - w\frac{\partial f}{\partial\xi}\,] \qquad \text{(B-5)}$$

where $b = (1+\varepsilon m^+)$

The grid is now considered as Fig. B-1. The grid points can be expressed as:

$$\xi_0 = 0\ ,\quad \xi_n = \xi_{n-1}+k_n\ ,\quad n = 1,2,3.....N$$

$$\eta_0 = 0\ ,\quad \eta_j = \eta_{j-1}+h_j\ ,\quad j = 1,2,3.....J \qquad \text{(B-6)}$$

$$\eta_J = \eta_\infty$$

The values of $(f,\ \bar{u},\ \bar{v},\ \theta\ ,\ w)$ at point $(\xi_n,\ \eta_j)$ can be expressed by the grid point functions $(f_j^n,\ \bar{u}_j^n,\ \bar{v}_j^n,\ \theta_j^n,\ w_j^n)$

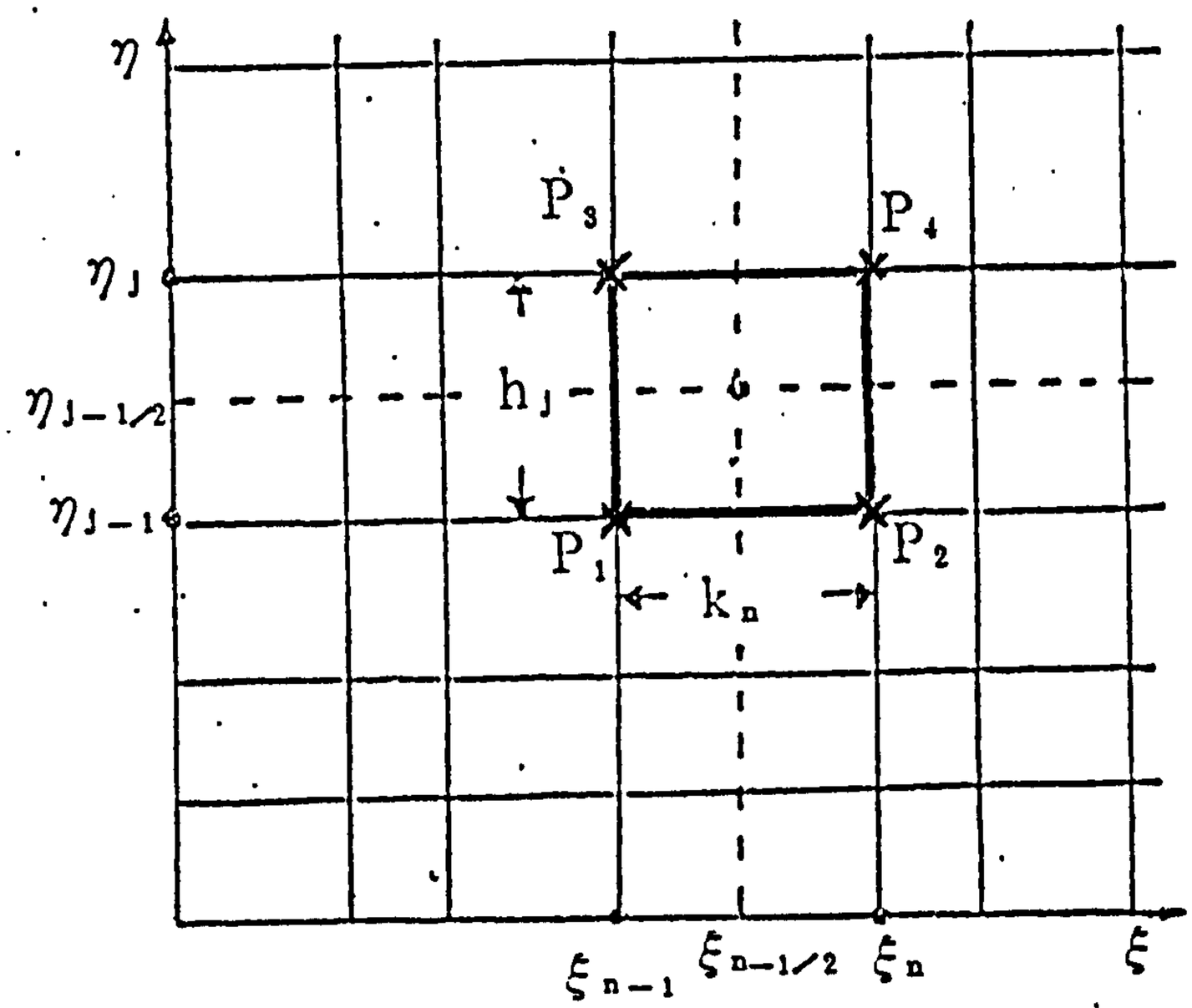

Fig. B-1 The grid point of boundary layer

The functions at the middle of arbitrary grid point with the function m_j^n are

$$\xi_{n-\frac{1}{2}} = \tfrac{1}{2}(\xi_n + \xi_{n-1}),\ \eta_{j-\frac{1}{2}} = \tfrac{1}{2}(\eta_j + \eta_{j-1})$$
$$m_j^{n-\frac{1}{2}} = \tfrac{1}{2}(m_j^n + m_j^{n-1}),\ m_{j-\frac{1}{2}}^n = \tfrac{1}{2}(m_j^n + m_{j-1}^n) \qquad \text{(B-7)}$$

The centered difference method is applied at $(\xi_n, \eta_{j-\frac{1}{2}})$ and the average value is gotten. Then equation (B-3) can be written as:

$$(f_j^n - f_{j-1}^n)h_j^{-1} = \bar{u}_{j-\frac{1}{2}}^n$$
$$(\bar{u}_j^n - \bar{u}_{j-1}^n)h_j^{-1} = \bar{v}_{j-\frac{1}{2}}^n \qquad \text{(B-8)}$$
$$(\theta_j^n - \theta_{j-1}^n)h_j^{-1} = w_{j-\frac{1}{2}}^n$$

Similarly, the centered different method is applied to equations (B-4), (B-5) with respect to $(\xi_{n-\frac{1}{2}}, \eta_{j-\frac{1}{2}})$,

$$\left(\frac{b_j\bar{v}_j - b_{j-1}\bar{v}_{j-1}}{h_j}\right)^n + (\tfrac{1}{2}+\alpha_n)(f\bar{v})_{j-\frac{1}{2}}^n - \alpha_n(\bar{u}^2)_{j-\frac{1}{2}}^n$$
$$+ \xi_{\Omega}^n\theta_{j-\frac{1}{2}}^n + \alpha_n(\bar{v}_{j-\frac{1}{2}}^{n-1}f_{j-\frac{1}{2}}^n - f_{j-\frac{1}{2}}^{n-1}\bar{v}_{j-\frac{1}{2}}^n) + [a_1\theta_{j-\frac{1}{2}}^n +$$
$$a_2(\theta^2)_{j-\frac{1}{2}}^n]\left(\frac{\bar{v}_j^n - \bar{v}_{j-\frac{1}{2}}^n}{h_j}\right) + [a_1 w_{j-\frac{1}{2}}^n + 2a_2\theta_{j-\frac{1}{2}}^n w_{j-\frac{1}{2}}^n]\ \bar{v}_{j-\frac{1}{2}}^n$$
$$= R_{j-\frac{1}{2}}^{n-1} \qquad \text{(B-9)}$$

$$(Pr_\infty^{-1} - Prt^{-1})\left(\frac{w_j - w_{j-1}}{h_j}\right)^n + Prt^{-1}\left[\frac{b_j w_j - b_{j-1}w_{j-1}}{h_j}\right]^n +$$
$$(\tfrac{1}{2}+\alpha_n)(fw)_{j-\frac{1}{2}}^n + \alpha_n(-(\bar{u}\theta)^n - \bar{u}^{n-1}\theta^n + \bar{u}^n\theta^{n-1} + w^{n-1}f^n$$
$$- w^n f^{n-1})_{j-\frac{1}{2}} + \frac{4}{3Pr_\infty N}\left[(\theta_{j-\frac{1}{2}}^n + C_T)^3\left(\frac{w_j^n - w_{j-1}^n}{h_j}\right) +\right.$$

$$3(\theta^{n}_{j-\frac{1}{2}} + C_T)^2(w^2)^{n}_{j-\frac{1}{2}}] = Y^{n-1}_{j-\frac{1}{2}} \qquad \text{(B-10)}$$

where $$\alpha_n = \xi^{n-\frac{1}{2}}/k_n \qquad \text{(B-11)}$$

$$R^{n-1}_{j-\frac{1}{2}} = \alpha_n[(f\bar{V})^{n-1}_{j-\frac{1}{2}} - (\bar{u}^2)^{n-1}_{j-\frac{1}{2}}] - \{(\frac{b_j\bar{v}_j - b_{j-1}\bar{v}_{j-1}}{h_j})^{n-1}$$

$$+ [a_1\theta^{n-1}_{j-\frac{1}{2}} + a_2(\theta^2)^{n-1}_{j-\frac{1}{2}}](\frac{v_j - v_{j-1}}{h_j})^{n-1} + [a_1 w^{n-1}_{j-\frac{1}{2}} +$$

$$2a_2\theta^{n-1}_{j-\frac{1}{2}} w^{n-1}_{j-\frac{1}{2}}]\bar{v}^{n-1}_{j-\frac{1}{2}} + \frac{1}{2}(f\bar{v})^{n-1}_{j-\frac{1}{2}} + \xi^{n-1}\Omega\theta^{n-1}_{j-\frac{1}{2}}\} \qquad \text{(B-12)}$$

$$Y^{n-1}_{j-\frac{1}{2}} = \alpha_n[(wf)^{n-1}_{j-\frac{1}{2}} - (\bar{u}\theta)^{n-1}_{j-\frac{1}{2}}] - \{(Pr_\infty^{-1} - Prt^{-1})$$

$$(\frac{w_j - w_{j-1}}{h_j})^{n-1} + Prt^{-1}(\frac{b_j w_j - b_{j-1}}{h_j})^{n-1} + \frac{1}{2}(fw)^{n-1}_{j-\frac{1}{2}} + \frac{4}{3Pr_\infty N}$$

$$[(\theta^{n-1}_{j-\frac{1}{2}} + C_T)^3(\frac{w_j - w_{j-1}}{h_j})^{n-1} + 3(\theta^{n-1}_{j-\frac{1}{2}} + C_T)^2(w^2)^{n-1}_{j-\frac{1}{2}}]\} \qquad \text{(B-13)}$$

The transformed boundary conditions (equation (A-8) become

$$f^n_0 = 0\ ,\quad \bar{u}^n_0 = 0\ ,\quad \bar{u}^n_J = 1\ ,\quad \theta^n_0 = \theta_w\ ,\quad \theta^n_J = 0 \qquad \text{(B-14)}$$

(iii) The difference equation of natural convection

Under the situation of natural convection with a non-constant kinematic viscosity, the new functions $\bar{u}(\xi,\eta)$, $\bar{v}(\xi,\eta)$, $w(\xi,\eta)$ with the same definition as equation (B-3) are introduced. Thus, equations (A-21) and (A-2) can be written as

$$[\bar{v}(1 + a_1\theta + a_2\theta^2)]' + 3fv - 2(\bar{u})^2 + \theta = 4\xi[\bar{u}\frac{\partial\bar{u}}{\partial\xi} - \bar{v}\frac{\partial f}{\partial\xi}] \qquad \text{(B-15)}$$

$$Pr_\infty^{-1}w' + 3fw + \frac{4}{3Pr_\infty N}[(\theta+C_T)^3 w]' = 4\xi[\bar{u}\frac{\partial\theta}{\partial\xi} - w\frac{\partial f}{\partial\xi}] \qquad \text{(B-16)}$$

The same difference rule used in the above combined convection

is applied. Then equations (B-3), (B-15) and (B-16) can be written as follows:

$$(f_j^n - f_{j-1}^n) = \bar{u}_{j-\frac{1}{2}}^n$$

$$(\bar{u}_j^n - \bar{u}_{j-1}^n)h_j^{-1} = \bar{v}_{j-\frac{1}{2}}^n \qquad \text{(B-17)}$$

$$(\theta_j^n - \theta_{j-1}^n)h_j^{-1} = w_{j-\frac{1}{2}}^n$$

$$\left(\frac{\bar{v}_j^n - \bar{v}_{j-1}^n}{h_j}\right) + \left[a_1\theta_{j-\frac{1}{2}}^n + a_2(\theta^2)_{j-\frac{1}{2}}^n\right]\left(\frac{\bar{v}_j^n - \bar{v}_{j-1}^n}{h_j}\right) + \left[a_1 w_{j-\frac{1}{2}}^n + 2a_2\theta_{j-\frac{1}{2}}^n w_{j-\frac{1}{2}}^n\right]\bar{v}_{j-\frac{1}{2}}^n + (3+\alpha_n)(f\bar{v})_{j-\frac{1}{2}}^n -$$

$$(2+\alpha_n)(\bar{u}^2)_{j-\frac{1}{2}}^n + \theta_{j-\frac{1}{2}}^n + \alpha_n(\bar{v}_{j-\frac{1}{2}}^{n-1} f_{j-\frac{1}{2}}^n - f_{j-\frac{1}{2}}^{n-1}\bar{v}_{j-\frac{1}{2}}^n)$$

$$= R_{j-\frac{1}{2}}^{n-1} \qquad \text{(B-18)}$$

$$Pr^{-1}\left(\frac{w_j - w_{j-1}}{h_j}\right)^n + (3+\alpha_n)(fw)_{j-\frac{1}{2}}^n + \alpha_n(-(\bar{u}\theta)^n -$$

$$\bar{u}^{n-1}\theta^n + \bar{u}^n\theta^{n-1} + w^{n-1}f^n - w^n f^{n-1})_{j-\frac{1}{2}} + \frac{4}{3Pr_\infty N}\left[(\theta_{j-\frac{1}{2}}^n + C_T)^3\right.$$

$$\left.\left(\frac{w_j - w_{j-1}}{h_j}\right) + 3(\theta_{j-\frac{1}{2}}^n + C_T)^2(w^2)_{j-\frac{1}{2}}^n\right] = Y_{j-\frac{1}{2}}^{n-1} \qquad \text{(B-19)}$$

where $\alpha_n = 4\xi^{n-\frac{1}{2}} / k_n$ (B-20)

$$R_{j-\frac{1}{2}}^{n-1} = \alpha_n\left[(f\bar{v})_{j-\frac{1}{2}}^{n-1} - (\bar{u}^2)_{j-\frac{1}{2}}^{n-1}\right] - \left\{\left(\frac{\bar{v}_j - \bar{v}_{j-1}}{h_j}\right)^{n-1} +\right.$$

$$\left[a_1\theta_{j-\frac{1}{2}}^{n-1} + a_2(\theta^2)_{j-\frac{1}{2}}^{n-1}\right]\left(\frac{\bar{v}_j - \bar{v}_{j-1}}{h_j}\right)^{n-1} + \left[a_1 w_{j-\frac{1}{2}}^{n-1} +\right.$$

$$\left.\left.2a_2\theta_{j-\frac{1}{2}}^{n-1} w_{j-\frac{1}{2}}^{n-1}\right]\bar{v}_{j-\frac{1}{2}}^{n-1} + 3(f\bar{v})_{j-\frac{1}{2}}^{n-1} - 2(\bar{u}^2)_{j-\frac{1}{2}}^{n-1} + \theta_{j-\frac{1}{2}}^{n-1}\right\} \qquad \text{(B-21)}$$

$$Y_{j-\frac{1}{2}}^{n-1} = \alpha_n[(wf)_{j-\frac{1}{2}}^{n-1} - (\bar{u}\theta)_{j-\frac{1}{2}}^{n-1}] - \{Pr_\infty^{-1}(\frac{w_j - w_{j-1}}{h_j})^{n-1}$$

$$+ 3(fw)_{j-\frac{1}{2}}^{n-1} + \frac{4}{3Pr_\infty N}[(\theta_{j-\frac{1}{2}}^{n-1}+C_T)^3(\frac{w_j - w_{j-1}}{h_j})^{n-1} +$$

$$3(\theta_{j-\frac{1}{2}}^{n-1}+C_T)^2(w^2)_{j-\frac{1}{2}}^{n-1}]\} \qquad (B-22)$$

The transformed boundary conditions equation (A-23) become $f_0^n = 0$,

$\bar{u}_0^n = 0$, $\bar{u}_j^n = 0$, $\theta_0^n = \theta_w^n$ and $\theta_j^n = 0$ (B-23)

If we assume $(f_j^{n-1}, \bar{u}_j^{n-1}, \bar{v}_j^{n-1}, \theta_j^{n-1}, w_j^{n-1})$ to be known for

$0 \leq j \leq J$, then equations (B-8) - (B-10) and boundary condition (B-14) or equations (B-17) - (B-19) and boundary condition (B-23) are a system of 5J+5 non-linear algebraic equations for the solution of 5J+5 unknows $(f_j^n, \bar{u}_j^n, \bar{v}_j^n, \theta_j^n, w_j^n)$, $j = 0, 1, \ldots, J$. To solve this nonlinear system, we use the Newton's method.

(iv) Newton's Method

Let $f_j^{(i+1)} = f_j^{(i)} + \delta f_j^{(i)}$, $\bar{u}^{(i+1)} = \bar{u}_j^{(i)} + \delta\bar{u}_j^{(i)}$

$\bar{v}_j^{(i+1)} = \bar{v}_j^{(i)} + \delta\bar{v}_j^{(i)}$, $\theta_j^{(i+1)} = \theta_j^{(i)} + \delta\theta_j^{(i)}$ (B-24)

$w_j^{(i+1)} = w_j^{(i)} + \delta w_j^{(i)}$

where i denotes the numbers of iteration.

When i = 0 (the initial guess value), we may use the previous station value as the initial guess value.

(a) Under the situation of combined or forced convection:

$f_0^{(0)}=0$, $\bar{u}_0^{(0)}=0$, $\bar{v}_0^{(0)}=\bar{v}_0^{n-1}$, $\theta_0^{(0)}=\theta_w(\xi_n)$, $w_0^{(0)}=w_0^{n-1}$

$f_j^{(0)}=f_j^{n-1}$, $\bar{u}_j^{(0)}=\bar{u}_j^{n-1}$, $\bar{v}_j^{(0)}=\bar{v}_j^{n-1}$, $\theta_j^{(0)}=\theta_j^{n-1}$

$$w_j^{(0)}=w_j^{n-1} \quad , \quad 1 \leq j \leq J-1$$

$$f_J^{(0)}=f_J^{n-1} \quad , \quad \bar{u}_J^{(0)}=1 \quad , \quad \bar{v}_J^{(0)}=\bar{v}_J^{n-1} \quad , \quad \theta_J^{(0)}=0 \quad , \quad w_J^{(0)}=w_J^{n-1}$$

(b) Under the situation of natural convection:

$$f_0=0 \quad , \quad \bar{u}_0^{(0)}=0 \quad , \quad \bar{v}_0^{(0)}=\bar{v}_0^{n-1} \quad , \quad \theta_0^{(0)}=\theta_w(\xi_n) \quad , \quad w_0^{(0)}=w_0^{n-1}$$

$$f_j^{(0)}=f_j^{n-1} \quad , \quad \bar{u}_j^{(0)}=\bar{u}_j^{n-1} \quad , \quad \bar{v}_j^{(0)}=\bar{v}_j^{n-1} \quad , \quad \theta_j^{(0)}=\theta_j^{n-1} \quad ,$$

$$w_j^{(0)}=w_j^{n-1} \quad , \quad 1 \leq j \leq J-1$$

$$f_J^{(0)}=f_J^{n-1} \quad , \quad \bar{u}_J^{(0)}=0 \quad , \quad \bar{v}_J^{(0)}=\bar{v}_J^{n-1} \quad , \quad \theta_J^{(0)}=0 \quad , \quad w_J^{(0)}=w_J^{n-1}$$

The process with respect to the non-linear terms is:

$$\begin{Bmatrix} f_j^{(i)} + \delta f_j^{(i)} \\ \bar{u}_j^{(i)} + \delta \bar{u}_j^{(i)} \\ \bar{v}_j^{(i)} + \delta \bar{v}_j^{(i)} \\ \theta_j^{(i)} + \delta \theta_j^{(i)} \\ w_j^{(i)} + \delta w_j^{(i)} \end{Bmatrix} \times \begin{Bmatrix} f_j^{(i)} + \delta f_j^{(i)} \\ \bar{u}_j^{(i)} + \delta \bar{u}_j^{(i)} \\ \bar{v}_j^{(i)} + \delta \bar{v}_j^{(i)} \\ \theta_j^{(i)} + \delta \theta_j^{(i)} \\ w_j^{(i)} + \delta w_j^{(i)} \end{Bmatrix}$$

knows unknowns knows unknowns

We may neglect the product of any two terms of ($\delta f_j^{(i)}$, $\delta \bar{u}_j^{(i)}$, $\delta \bar{v}_j^{(i)}$, $\delta \theta_j^{(i)}$; $\delta w_j^{(i)}$), then equations (B-8)-(B-10) or (B-17)-(B-19) can be linearized. The "block elimination method" can be applied to solve the unknowns ($\delta f_j^{(i)}$, $\delta \bar{u}_j^{(i)}$, $\delta \bar{v}_j^{(i)}$, $\delta \theta_j^{(i)}$, $\delta w_j^{(i)}$). Then using equation (B-24) to solve the knowns of next iteration. Keeping on the iteration until $|\delta \bar{v}_0| \leq 10^{-5}$ (when flow is laminar) or $\delta \bar{v}_0/(fw''+0.5\delta \bar{v}_0)| \leq 0.02$ (when flow is turbulent).

The above process can be shown in Fig. B-2.

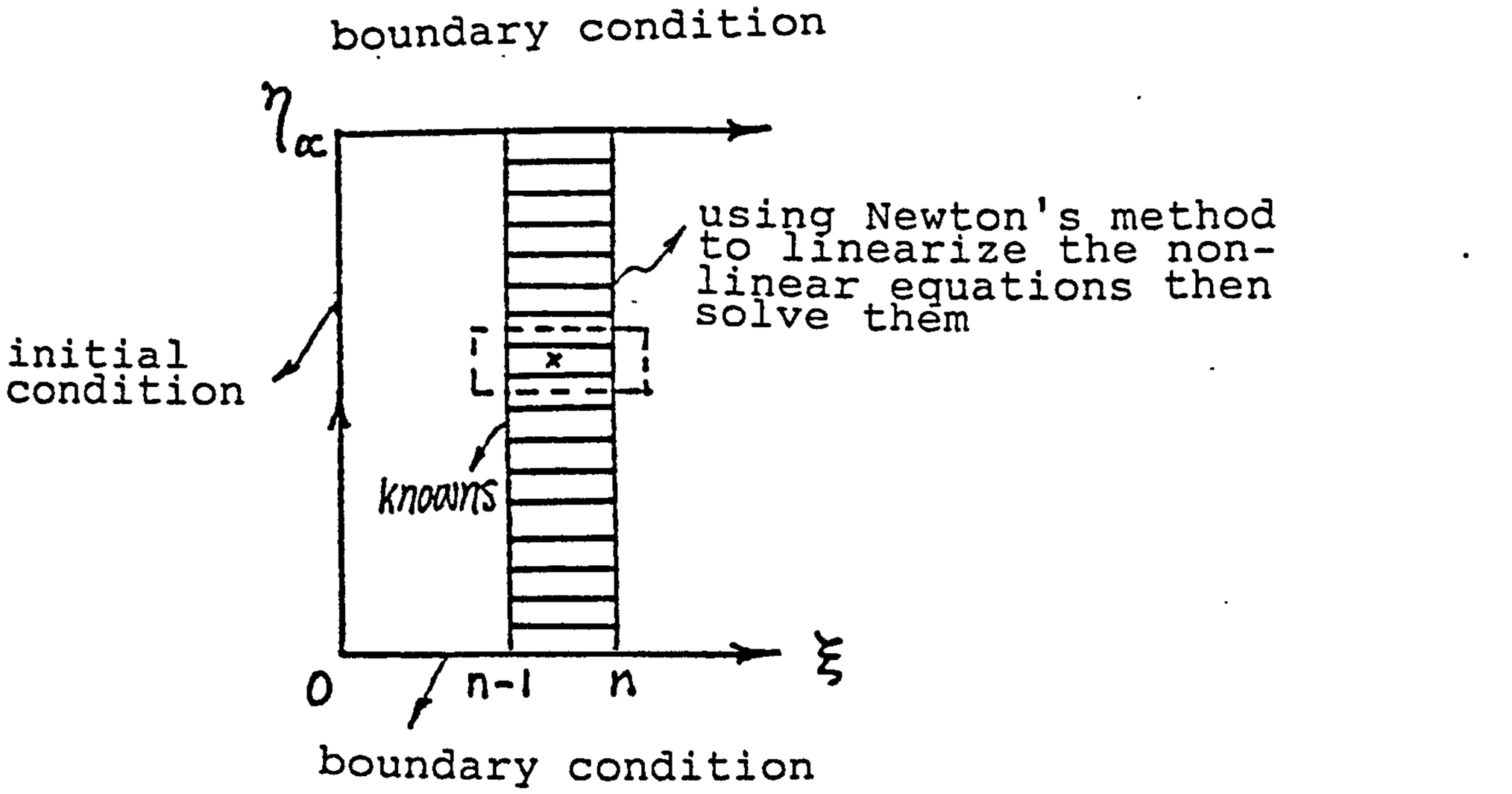

Fig. B-2

With regards to most laminar flow, the transformed thickness η_∞ of the boundary layer is about 4-8. After the flow leaves from the transition zone to the turbulent zone, the value of η_∞ increases as ξ increases owing to the eddy viscosity (see Fig. B-3).

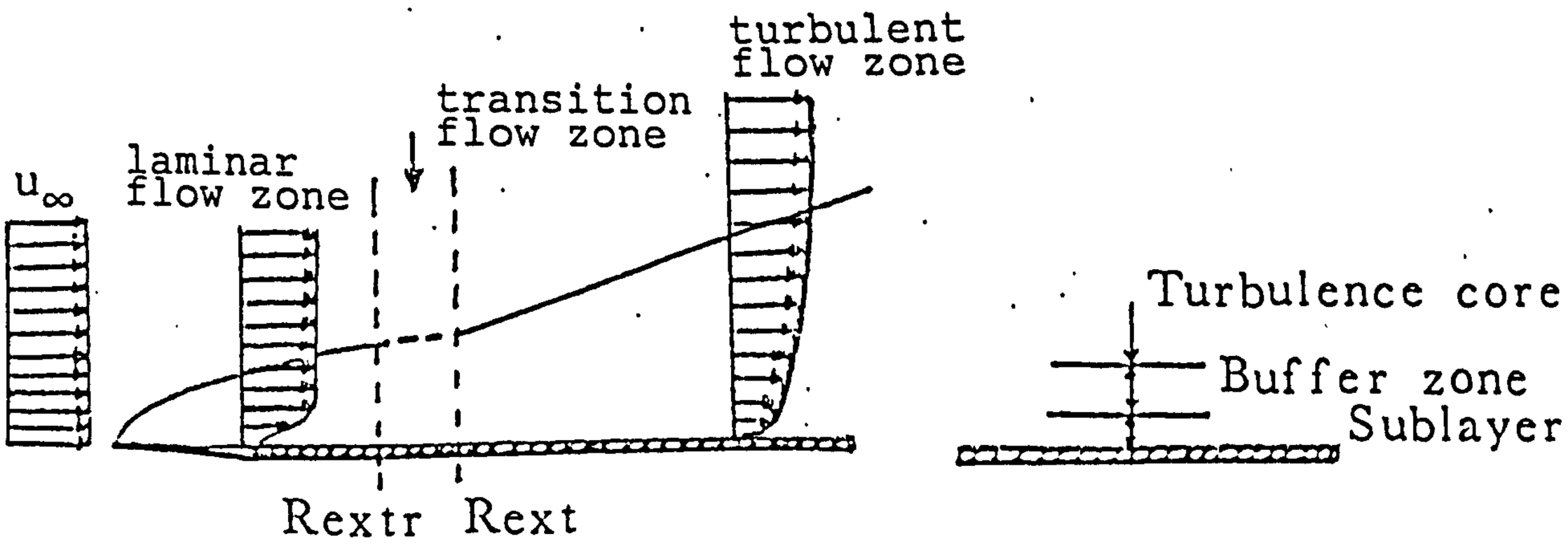

Fig. B-3 Laminar and turbulent boundary layer on flate plate

In order to sustain the accuracy of calculation, we may take the irregular grid points at the direction of η. The way to get the grid points can be calculated by the following formula:

$$h_j = Rh_{j-1}$$

$$\eta_j = h_1 \frac{R^{j-1}}{R-1}, \quad j = 1, 2, 3...., J, \quad R \geq 1 \qquad \text{(B-25)}$$

where R is a constant ratio of two continuous intervals. It has to be assumed first. And the number of grid point at η-direction, J, can be obtained by the following formula

$$J = \frac{\ln[1 + (R-1)\eta_\infty/h_1]}{\ln R} \qquad \text{(B-26)}$$

where h_1 is the interval of the first $\Delta\eta$.

In the present study, $h_1 = 0.1$ and R=1 are taken for the laminar flow and $h_1 = 0.01$ and R=1.1 are taken for the turbulent flow. Besides, when the pre-assumed value of η_∞ is not great enough, the computer program applied in the present study can increase the number of grid point automatically.

(II) The use of inverse matrix to solve the heat conduction equation:

To consider the heat conduction equation of the fin, the entire length of the fin is dirived into 44 control volumes. Each control volume i is with a axial length $\Delta\xi_i$ and the thickness of fin. The surface of control volume just locate at the middle of two neighboring grid points. Thus, if the coordinates of three neighboring grid point are ξ_{i-1}, ξ_i and ξ_{i+1} respectively, then the coordinates of the two surfaces for control

volume are $(\xi_{i-1} + \xi_i)/2$ and $(\xi_i + \xi_{i+1})/2$, the axial length is $\Delta\xi_i = (\xi_{i+1} - \xi_{i-1})/2$. The relation is shown as Fig. B-4.

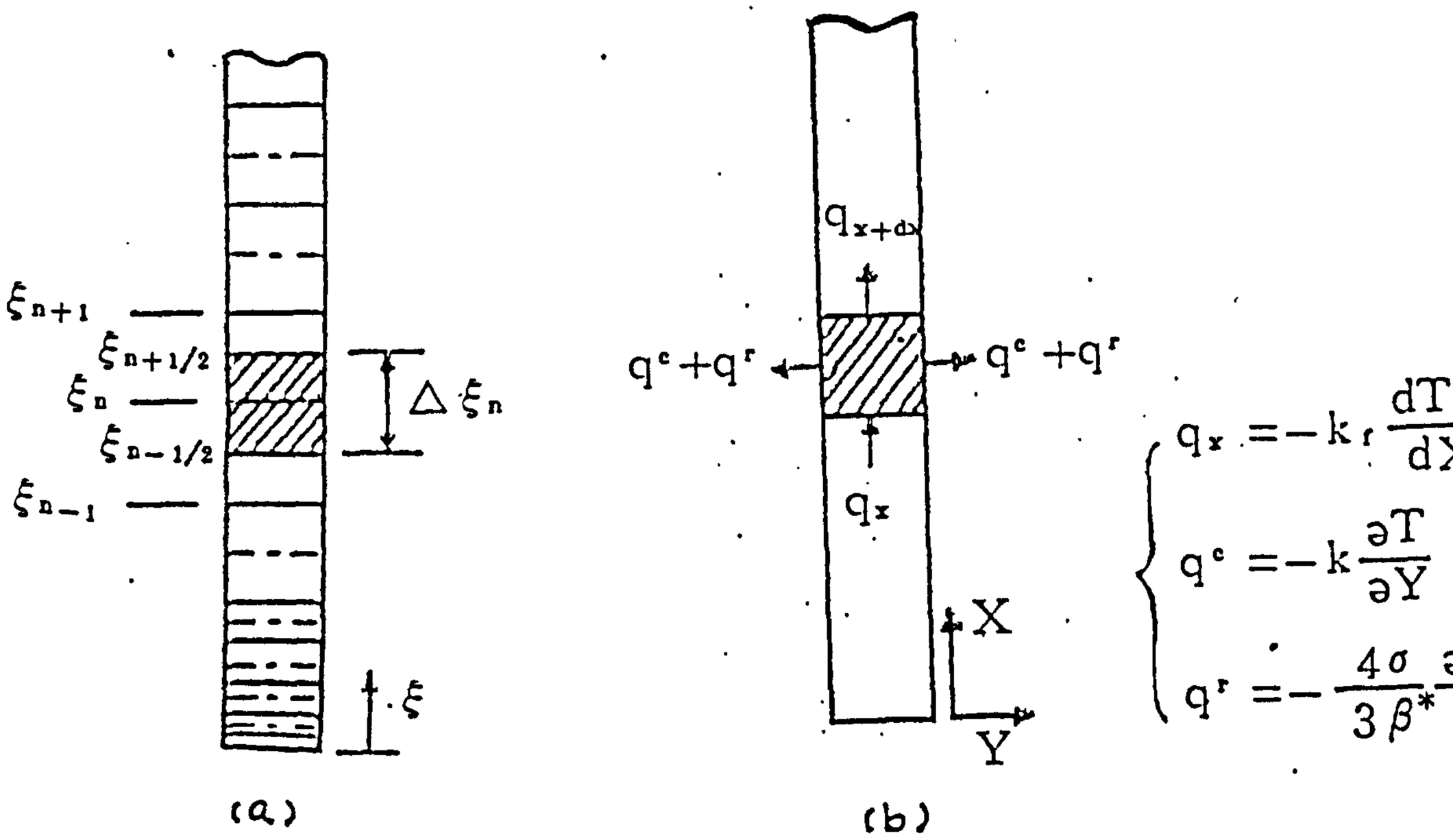

$$\begin{cases} q_x = -k_f \dfrac{dT_f}{dX} \\ q^c = -k \dfrac{\partial T}{\partial Y} \\ q^r = -\dfrac{4\sigma}{3\beta^*} \dfrac{\partial T^4}{\partial Y} \end{cases}$$

Fig. B-4 (a) The difference grid points of the fin
(b) The energy balance of the control volume in the fin

Using the middle difference for equation (A-28) or (A-29), we can get:

$$A_i \theta_i = B_i \theta_{i+1} + C_i \theta_{i-1}, \quad 2 \leq i < 44 \tag{B-27}$$

where,
$$A_i = (\xi_{i+1} - \xi_i)^{-1} + (\xi_i - \xi_{i-1})^{-1} + \hat{h}_i * Nc \; (\xi_{i+1} - \xi_i)/2$$

or,
$$A_i = (\xi_{i+1} - \xi_i)^{-1} + (\xi_i - \xi_{i-1})^{-1} + \hat{h}^*_{i\infty} Nc_\infty \; (\xi_{i+1} - \xi_i)/2 \tag{B-28}$$

$$B_i = (\xi_{i+1} - \xi_i)^{-1}, \quad C_i = (\xi_i - \xi_{i-1})^{-1}$$

equations (B-27) and (B-28) can be expressed as the form of matrix as follows,

$$\begin{bmatrix} -A_1 & B_1 & & & \\ C_2 & -A_2 & B_2 & & \\ & C_3 & -A_3 & B_3 & \\ & & \ddots & \ddots & \ddots \\ & & & C_{45} & -A_{45} \end{bmatrix} \begin{bmatrix} \theta_1 \\ \theta_2 \\ \theta_3 \\ \vdots \\ \theta_{45} \end{bmatrix} = \begin{bmatrix} 0 \\ 0 \\ 0 \\ \vdots \\ 1 \end{bmatrix} \qquad \text{(B-29)}$$

From boundary condition (A-31), we can get $A_1=B_1=1$, $C_{45}=0$, $A_{45}=-1$. Because $\xi=0$ is a singular point, let the temperature of this point equal to the temperature of the neighbor $\xi=10^{-10}$. In order to correspond to the solution of the thermal boundary layer, we take a dense division of control volume near the end of fin. To solve this algebraic system, we assume $\hat{h}^*$ to be the last previous result of the iteration for the boundary layer. The temperature distribution of entire the fin can be directly obtained from the inverse of the matrix. The result of temperature distribution is taken as the boundary condition of thermal boundary layer for the next iteration.

VITA

Cha'o-Kuang Chen was born in Taiwan. Republic of China, on October 17, 1934.

His academic background includes:

B.S. degree (1958) in Mechanical Engineering from National Cheng Kung University, Tainan, Taiwan, Republic of China.

M.S. Degree (1969) in Mechanical Engineering from Georgia Institute of Technology. U.S.A.